

**Advanced Modelling and Visualisation  
of Liquid-Liquid Separations  
of Complex Sample Components,  
with Variable Phase Distribution and Mode of Operation**

A thesis submitted for the degree of Doctor of Philosophy

By

Jozefus Johannes Martinus (Joost) de Folter

Brunel Institute for Bioengineering, Brunel University

October 2012

# Abstract

This research is about liquid-liquid chromatography modelling. While the main focus was on liquid-liquid chromatography, where the stationary and mobile phases are both liquid, theory of different types of chromatography, including the currently most used techniques, were considered as well. The main goal of this research was to develop a versatile liquid-liquid separation model, able to model all potential operating scenarios and modes of operation. A second goal was to create effective and usable interfaces to such a model, implying primarily information visualisation, and secondarily educative visualisation. The first model developed was a model based on Counter-Current Distribution. Next a new more elemental model was developed, the probabilistic model, which better models continuous liquid-liquid chromatography techniques. Finally, a more traditional model was developed using transport theory. These models were used and compared to experimental data taken from literature. The models were demonstrated to model all main liquid-liquid chromatography techniques, incorporated the different modes of operation, and were able to accurately model many sample components and complex sample injections. A model interface was developed, permitting functional and effective model configuration, exploration and analysis using visualisation and interactivity. Different versions of the interface were then evaluated using questionnaires, group interviews and Insight Evaluation. The visualisation and interactivity enhancements have proven to contribute understanding and insight of the underlying chromatography process. This also proved the value of the Insight Evaluation method, providing valuable qualitative evaluation results desired for this model interface evaluation. A prototype of a new graphical user interface developed, and showed great potential for combining model parameter input and exploring the liquid-liquid chromatography processes. Additionally, a new visualisation method was developed that can accurately visualise different modes of operation. This was used to create animations, which were also evaluated. The results of this evaluation show the new visualisation helps understanding of the liquid-liquid chromatography process amongst CCC novices. The model software will be a valuable tool for industry for predicting, evaluating and validating experimental separations and production processes. While effective models already existed, the use of interactive visualisation permits users to explore the relationship between parameters and performances in a simpler yet more powerful way. It will also be a valuable tool for academia for teaching & training, both staff and students, on how to use the technology. Prior to this work no such tool existed or existing tools were limited in their accessibility and educational value.

## Keywords

liquid-liquid chromatography, modelling, computer model, simulation, probabilistic, ProMISE, visualisation, interactivity, model previews, insight evaluation

# Table of Contents

Abstract .....	2
Table of Contents.....	3
List of Tables.....	6
List of Figures .....	7
Acknowledgements .....	13
Abbreviations .....	14
Symbols.....	15
List of author's internal reports.....	16
List of author's publications .....	16
1 Introduction .....	18
2 Literature review.....	20
2.1 Chromatography history.....	20
2.2 Chromatography theory .....	32
2.3 Modelling .....	36
2.3.1 Transport models .....	37
2.3.2 Plate model.....	38
2.3.3 Cell model.....	38
2.3.4 Predictive model.....	39
2.4 Chromatogram deconstruction .....	40
2.5 Modelling summary .....	40
2.6 Visualisation history in chromatography.....	40
2.7 Educative visualisation.....	43
2.8 Information visualisation and interactivity.....	46
2.8.1 Dynamic querying.....	47
2.8.2 Query previews .....	50
2.8.3 Influence explorer.....	50
2.9 Implementation and Evaluation .....	52
2.9.1 Formative and summative evaluation.....	54
2.9.2 Insight evaluation .....	54
2.10 Visualisation summary .....	55
3 Modelling.....	57
3.1 Model based on CCD.....	57
3.2 Model based on probabilistic theory (ProMISE) .....	69
3.3 Model based on transport theory .....	73
3.4 Simplified model for interactivity .....	75
3.5 From model to simulation.....	77
3.6 Implementing advanced operations.....	78

3.7	Computer implementation .....	80
3.7.1	Model-View-Controller flow.....	82
3.7.2	Data flow.....	84
3.7.3	Coding .....	84
3.8	Modelling experimental data.....	87
3.8.1	Modelling using CCD model .....	88
3.8.2	Modelling using probabilistic model .....	88
3.8.3	Modelling using transport model .....	88
4	Modelling results and verification .....	89
4.1	Elution .....	89
4.1.1	CCD.....	89
4.1.2	CPC.....	91
4.1.3	CCC.....	93
4.1.4	Droplet CCC.....	103
4.1.5	Vortex CCC.....	105
4.1.6	Toroidal CCC .....	106
4.1.7	Controlled-cycle pulsed liquid-liquid chromatography .....	108
4.2	Sample injection .....	109
4.3	Efficiency .....	112
5	Visualisation design.....	113
5.1	Design of the initial prototype .....	113
5.2	Initial evaluation.....	115
5.2.1	Requirements.....	115
5.2.2	Data collection.....	115
5.2.3	Evaluation results.....	116
5.3	Revised requirements .....	117
5.4	Improved Interface.....	117
5.4.1	Chromatogram view .....	118
5.4.2	Time mode chromatogram view.....	118
5.4.3	3D time trace view.....	119
5.4.4	Model parameter setup.....	120
5.4.5	The interactive configuration explorer (ICE) .....	120
6	Insight Evaluation .....	123
6.1	Experimental design and procedure .....	123
6.2	Evaluation results and discussion.....	125
7	Final Proposed Interface.....	127
7.1	Latest model interface.....	127
7.2	Prototype graphical user interface .....	130
7.3	Prototype graphical user interface feedback .....	133
8	Educative visualisation .....	135



8.1	Improved visualisation tool .....	135
8.2	Evaluation.....	138
8.3	Evaluation results.....	138
8.4	Improvements to visualisation .....	140
9	Discussion.....	141
9.1	Modelling .....	141
9.1.1	Elution.....	141
9.1.2	Sample injection.....	146
9.1.3	Efficiency .....	146
9.1.4	Models in general.....	147
9.2	Software implementation.....	149
9.3	Visualisation .....	150
9.3.1	Visualisation techniques .....	150
9.3.2	Insight evaluation .....	150
9.3.3	Prototype graphical user interface .....	152
9.3.4	Improved visualisation tool .....	152
9.4	Integration.....	153
10	Conclusion.....	154
10.1	Modelling .....	154
10.2	Visualisation .....	155
10.3	Future work.....	156
10.4	Closing remarks.....	157
	References .....	158
Appendix A	: Software model user manual .....	168
Appendix B	: Software versions.....	185
Appendix C	: Model user feedback questionnaire .....	198
Appendix D	: Visual Walkthrough .....	200
Appendix E	: New graphical user interface group interview.....	202
Appendix F	: New visualisation feedback questionnaire.....	204
Appendix G	: New visualisation group interview .....	206

# List of Tables

Table 3.1 C++ code of model loop function.....	87
Table 4.1 CCD experimental and model results (first 4 peaks retained in columns shown in red) (with error) .....	90
Table 4.2 CPC experimental and model values (with error) - case 1 .....	91
Table 4.3 CPC experimental and model values (with error) - case 2 .....	92
Table 4.4 CCC experimental, theoretical and model values (with error) for conventional flow mode.....	94
Table 4.5 CCC experimental, theoretical and model values (with error) for co-current flow mode .....	97
Table 4.6 CCC experimental, theoretical and model values (with error) for dual flow mode case 1 .....	99
Table 4.7 Droplet CCC experimental and model values (with error) .....	104
Table 4.8 Vortex CCC experimental and model values (with error).....	105
Table 4.9 CCC Toroidal coil experimental and model values (with error).....	107
Table 4.10 Controlled-cycle pulsed liquid-liquid chromatography (CPLC) experimental and model values.....	108
Table 4.11 CCC sample injection concentration comparing experimental and model values ..	110
Table 4.12 System efficiency values for different apparati / operation modes .....	112
Table 5.1 Numerical results including weighing.....	116
Table 6.1 Template for recorded data for each insight .....	123
Table 6.2 Total number of insights for version and enhanced version of model .....	125
Table 6.3 Insights for each visual element .....	125
Table 6.4 Description of most important insights.....	126
Table 8.1 Feedback results .....	138
Table 9.1 Continuous model comparison.....	148

# List of Figures

Figure 2.1 Plant extract separated using thin layer chromatography [ <a href="http://en.wikipedia.org/wiki/Thin_layer_chromatography">http://en.wikipedia.org/wiki/Thin_layer_chromatography</a> (Accessed 22 July 2011)], showing separation of different coloured components. Tswett's original experiment would have been very similar to this. ....	21
Figure 2.2 Thin Layer Chromatography diagram: A: Plate with sample on it is introduced into mobile phase; B: Mobile phase moving through absorbent material on plate separating sample; C: Final separated sample. [ <a href="http://www.chemguide.co.uk/analysis/chromatography/thinlayer.html">http://www.chemguide.co.uk/analysis/chromatography/thinlayer.html</a> (Accessed 22 July 2011)] .....	22
Figure 2.3 Craig CCD apparatus allowing simple manual operation [Craig 1944]. Phases can be mixed by shaking the device. After each distribution phase, the top phase is transferred by rotating part 'B'.....	24
Figure 2.4 Manual version of Craig's CCD machine designed by Erich Hecker [Hecker 1955]..	24
Figure 2.5 Schematic diagram of helical CCC coil in planetary motion showing distribution of heavy phase (dark) and light phase (light) and mixing waves [Conway 1990].....	25
Figure 2.6 Photo of helical CCC column showing phase mixing using dyed phases [Sutherland et al. 1985].....	26
Figure 2.7 Schematic view of Toroidal coil illustrating the phase distribution [Sutherland and Ito 1978].....	26
Figure 2.8 Droplet CCC: A: Apparatus; B: Close-up view and C: Schematic diagram showing droplets of mobile phase moving through stationary phase [Tanimura et al. 1970] .....	28
Figure 2.9 Light micrograph of HPLC packing [ <a href="http://www.sciencephoto.com/media/359391/view">http://www.sciencephoto.com/media/359391/view</a> (Accessed 22 July 2011)] .....	29
Figure 2.10 HPLC schematic diagram of mobile phase flow through packed column: 1. Sample inserted with mobile phase. 2. Component is moving with mobile phase through column. 3. Different components move at different speeds due to affinity to phases. 4. Components are separated and start eluting from column. ....	30
Figure 2.11 CPC disc showing partitioned column [Roullier et al. 2009] .....	30
Figure 2.12 Vortex CCC: A. Vortex column; B. Column design [Ito et al. 2011a].....	31
Figure 2.13 Controlled-cycle pulsed liquid-liquid chromatography schematic [Kostanyan et al. 2011].....	31

Figure 2.14 Counter-Current extraction system with a stationary lower and mobile upper phase. Sample component distribution for two mixing & settling ('D') and transfer ('T') steps. A light coloured component (squares) has a K value of 2, and a dark coloured component (triangles) has a K value of 0.5, where K for each component is defined as the concentration in the upper phase divided by the concentration in the lower phase [de Folter and Sutherland 2009].....	33
Figure 2.15 A single CCC coil (circle with solid line) (left) describing planetary motion (right) [Wood 2006].....	34
Figure 2.16 Phase mixing in: A: Sun motion (I-type); B: Planetary motion (J-type) [Sutherland et al. 1987].....	34
Figure 2.17 Two completely separated components (A and B) eluting from the chromatography column. $t_A$ and $t_B$ are the retention times, and $V_A$ and $V_B$ the respective volumes of components A and B. In this illustration components A and B have K values of 1 and 2, respectively. Other parameters: Total column volume = 200 ml, stationary phase retention = 0.5 (50%) (therefore $V_M = 100$ ml and $V_S = 100$ ml), mobile phase flow rate = 10 ml / min. ....	35
Figure 2.18 Determining width and resolution of two chromatography peaks [Conway 1990]....	36
Figure 2.19 First chromatogram plotted [James and Martin 1952]; A (bottom): accumulative detector circuit output signal; B (top): tangent of accumulative output .....	41
Figure 2.20 Enhancements made to chromatogram type visualisation [Berthod et al. 2003], showing component concentrations of two components in upper (solid line above horizontal axis) and lower phase (dotted line below horizontal axis), inside the column (grey background) and eluting out of the column (white background). (W relates to the width of the peak.) .....	42
Figure 2.21 Interactive visualisation of liquid-chromatography/mass-spectrometry data [Linsen et al. 2005].....	43
Figure 2.22 CCD separation animation with yellow upper mobile phase and green lower stationary phase showing separation of sample components $K=0.5$ (red circles) and $K=2$ (blue triangles); A: mixing/settling stage; B: Just after mixing/settling stage, preceding a transfer stage [CCC Animations, de Folter 1998b] .....	44
Figure 2.23 CCC separation animation with yellow upper mobile phase and green lower stationary phase; A: Just after transfer stage, before mixing/settling stage; B: Just after mixing/settling stage [CCC Animations, de Folter 1998b] .....	45
Figure 2.24 CCC planetary motion animation: A: Mechanics and acceleration field; B: Phase distribution and mixing waves [CCC Animations, de Folter 1998b] .....	45
Figure 2.25 Interactive exploration of classical periodic table of elements [Ahlberg et al. 1992]. Moving the controls at the bottom of the screen interactively updates the highlighted elements in the main area of the screen. ....	47

Figure 2.26 HomeFinder: Interactive exploration of data set [Williamson and Shneiderman 1992]. Selection criteria on the right hand side of the screen interactively highlight homes in the main map view. ....	48
Figure 2.27 SpotFire [Ahlberg 1996]: query/statistical results visualised (in main area of the screen) in accordance to selected criteria (on the right hand side of the screen and yellow slider controls).....	49
Figure 2.28 Iterative process (p1 and p2 are parameters): following dashed arrows requires human expertise [Spence et al. 1995].....	51
Figure 2.29 Data from an engineering model is displayed in the forms of histograms; performances on the left, parameters on the right. A selection is being made on the 'Working Life' scale, and corresponding values are highlighted (in white) on each of the other scale. [Tweedie et al. 1996]. ....	51
Figure 2.30 Simple interaction design lifecycle model [Sharp et al. 2007]. ....	53
Figure 2.31 The information visualisation reference model [Card et al. 1999] .....	53
Figure 2.32 Model of visualisation [Keim et al. 2008]. Visualised data is perceived by a user, resulting in gaining an insight (from top left to right). Based on the insight, the user forms a hypothesis, evaluates this by further exploration and analysis which are fed back into the visualisation (bottom right to left). ....	55
Figure 3.1 CCD system with a stationary lower and mobile upper phase. Sample component distribution for two mixing & settling ('D') and transfer ('T') steps. A light coloured component (squares) has a K value of 2, and a dark coloured component (triangles) has a K value of 0.5, where K for each component is defined as the concentration in the upper phase divided by the concentration in the lower phase [de Folter and Sutherland 2009] .....	58
Figure 3.2 CCD system in co-current operation. Sample component distribution for two mixing/settling and transfer steps. The upper phase moves twice as fast than the lower phase. This is shown here by moving both phases in one step and only moving the upper phase for the next step [de Folter and Sutherland 2009] .....	59
Figure 3.3 CCD system in dual flow operation mode. Sample component distribution for two mixing/settling and transfer steps. The upper and lower phase move in opposite direction [de Folter and Sutherland 2009] .....	60
Figure 3.4 CCD system in intermittent flow operation mode. Sample component distribution for two mixing/settling and transfer steps. The upper and lower phase move (in opposite direction) alternatively.....	62
Figure 3.5 Showing how cells are created as the model progresses (in conventional flow mode). The numbers represent the index of each cell. Cells with a higher number have been created later. ....	64

Figure 3.6 Showing how cells are created as the model progresses (in co-current flow). Lower phase flow is half that of upper phase flow.....	65
Figure 3.7 Showing how cells are synchronised (in co-current flow). Lower phase flow is half that of upper phase flow. ....	66
Figure 3.8 A: Comparing the model mixing / settling efficiency (f) and resulting efficiency effect (f'). B: The relationship between the f and f' found using curve-fitting: $R^2 = 0.998$ and standard deviation = 0.0174.....	72
Figure 3.9 Simplified object model: Model (blue - right), View (green - left), Controller (orange - top), and the main parameters (yellow).....	81
Figure 3.10 Model-View-Controller flow diagram (simplified). Functions are displayed chronologically in vertical direction.....	83
Figure 3.11 Data flow from model output to screen rendering format.....	84
Figure 3.12 Summary report on Source Lines Of Code (SLOC) .....	85
Figure 3.13 Simplified diagram of main model loop.....	86
Figure 4.1 Experimental and theoretical CCD curves [Craig 1950] .....	90
Figure 4.2 Showing separate peaks with composite sum superimposed .....	90
Figure 4.3 CCD Model results for co-current flow compared to experimental data [de Folter and Sutherland 2009].....	96
Figure 4.4 Probabilistic model results for co-current flow compared to experimental data [de Folter and Sutherland 2011]. ....	96
Figure 4.5 CCC Dual flow case 2 comparing: A: experimental [Ignatova et al. 2011] to: B: CCD model, C: Probabilistic model, D: Transport model.....	100
Figure 4.6 CCC Intermittent flow mode comparing: A: Experimental (normalised) [Hewitson et al. 2011], B: CCD model (accumulated), C: Probabilistic model (accumulated) (components: Caffeine (C), Aspirin (A), Coumarin (M), Salicylic Acid (Z), Carvone (O), Ionone (I), Salicin (H), Biphenyl (BP). A, M, Z, O, I, and BP largely overlap in the upper phase in all graphs.) .....	102
Figure 4.7 CCC Batch sample injection comparing: A: experimental [Sutherland et al. 2009] (normalised) to: B: CCD model, C: Probabilistic model, D: Transport model.....	111
Figure 5.1 User interface for model input parameters.....	113
Figure 5.2 Chromatogram view graphically showing model result .....	114
Figure 5.3 Preview using traditional dynamic query controls .....	114
Figure 5.4 Improved chromatogram view including more customisation .....	118

Figure 5.5 Time mode chromatogram view .....	119
Figure 5.6 3D time trace view with annotated labels, showing different sample components represented by different colours .....	119
Figure 5.7 Screenshot of model input parameter setup interface.....	120
Figure 5.8 Screenshot of model: Real time interactive configuration explorer; with interactive controls (top), where the far left control is being rotated using the mouse causing its value to increase; chromatogram view (centre); key numerical results (bottom).....	122
Figure 7.1 Interface accommodating an increased number of input parameters. Sample components can be entered and modified directly using a grid view (bottom right). .....	127
Figure 7.2 Screenshot of model: Real time interactive configuration explorer; with interactive controls relevant for currently selected model (top); chromatogram view (centre); key numerical results (bottom). .....	128
Figure 7.3 Chromatogram view, showing upper phase component in the upper half, and lower phase component in the lower half, visualising probabilistic units at the very top. ....	128
Figure 7.4 Superimposed screenshots of model: A: Time mode chromatogram where different views are shown in different opacity in this figure, illustrating the view at different points in time of the simulation process (at different positions of the slider control); B: The probabilistic units showing time from start to end (top to bottom). ....	129
Figure 7.5 Prototype of combined graphical user interface; from top to bottom: general parameters, graphical representation of system according to profile, model input parameters for selected element (right), preview chromatogram, main chromatogram peak values. As the main input parameters are changed, the graphical representation dynamically visualises these changes. ....	131
Figure 7.6 Visual representations of chromatography systems used in new graphical user interface A: CCC, B: CCD, C: CPC; The mobile phase arrows, phase distribution, point of injection etc. are visually represented, and change real-time as model parameters are changed. ....	132
Figure 7.7 Prototype chromatogram view. Numerical values displayed by hovering over a peak, and main peak values displayed by selecting a peak. ....	133
Figure 8.1 Visualisation tool illustrating chromatography process: A. Sample components to be inserted (top left) are inserted into the first cell of the chromatography column representation. The column is represented by test tubes with the upper half showing the upper phase, and the lower half, the lower phase. Component mass is represented by coloured circles, and component concentration by the background colour of each cell; B. further showing component eluting from the column. Each horizontal column line represents a different point (in time) in the separation process. ....	136

Figure 8.2 Visualisation tool screenshot showing slider control manipulation to advance animation .....	137
---	-----



# Acknowledgements

I would like to thank my first supervisor, Ian Sutherland, for enabling me to do this PhD by helping me find funding, and helping me stay on track and in my chromatography research. I would also like to thank my second supervisor, Timothy Cribbin, for helping me putting things into context and all his help with visualisation techniques and evaluation methods research.

I would like to thank everyone from the Brunel Institute for Bioengineering, and in particular from the CCC team, for their help during the entire period of my research.

I would like to thank Alain Berthod and Nazim Mekaoui, Guido Pauli, Artak Kostanyan, Matthias Gläfke for their valuable input.

I would like to thank Brunel University for supporting me by not charging study fees being a member of staff, and awarding me a Vice Chancellor Travel Prize. I would also like to thank the Royal Academy of Engineering for awarding me an International Travel Grant twice.

I would like to thank my wife Veronica Silva Cano for her understanding as I spent a significant amount of time at home on my research.

Finally I would like to thank God who made all things possible, giving me support and inspiration during my research that could only have come from Him.

## Abbreviations

ATPS	Aqueous Two-Phase System
C++	name of common higher level programming language
CCC	Counter-Current Chromatography
CCD	Counter-Current Distribution
CFD	Computational Fluid Dynamics
CFL	Courant–Friedrichs–Lewy (constant)
CLR	Common Language Runtime (computer programming)
CPC	Centrifugal Partition Chromatography
CPLC	Controlled-Cycle Pulsed liquid-liquid Chromatography
DCCC	Droplet Counter-Current Chromatography
DQ	Dynamic Queries
GUESS(mix)	Generally Useful Estimate of Solvent Systems (sample component mixture)
HEMWat	Hexane / Ethyl acetate / Methanol / Water solvent system
HPLC	High Performance Liquid Chromatography
ICE	Interactive Chromatogram Explorer
ICcE	Intermittent Counter-current Extraction
id	inner diameter
MDM	Multiple Dual Mode (intermittent CCC operation mode)
MSIL	Microsoft Intermediate Language (computer programming)
.NET	Microsoft software framework including a large library of functions
OO	Object Oriented (programming technique)
PDE	Partial Differential Equation
PFA	Poly-Fluoro-Alkoxy (tubing material)
PTFE	Poly-Tetra-Fluoro-Ethylene (tubing material)
ProMISE	Probabilistic Model for Immiscible phase Separations and Extractions
SLOC	Source Lines Of Code (computer programming)
TCC	Toroidal Coil Chromatography

# Symbols

$a$	specific interfacial area [ $\text{m}^2/\text{m}^3 = 1/\text{m}$ ]
$C$	dimensionless constant
$C_{L/U}$	sample concentration in lower / upper phase
$f$	efficiency factor
$f'$	resulting efficiency effect factor
$F_{L/U}$	flow rate of lower / upper phase
$i$	unit index
$k_0$	overall mass-transfer coefficient [ $\text{m/s}$ ]
$k_0a$	overall volumetric mass transfer coefficient [ $1/\text{s}$ ]
$K$	K value, or distribution coefficient
$L$	length of column
$L_F$	lower phase volume ratio (analogue to terminology $S_F$ )
$m$	weight in probability theory
$m_{i/\text{tot}}$	weight in probability theory, at index $i$ / total weight
$n$	number of units, number of steps, or trails in probability theory
$N$	number of CCD steps or cells
$N_R$	retention time (analogue to terminology $t_R$ ) [steps]
$O$	number of computational iterations (Landau notation)
$p$	probability in probability theory
$r$	number of steps, or successes in probability theory
$S_F$	classical stationary phase retention factor
$t_R$	retention time [min]
$T_M$	mobile phase elution time
$U_F$	upper phase volume ratio (analogue to terminology $S_F$ )
$v$	linear velocity of the mobile phase flow
$V_R$	retention volume (analogue to terminology $t_R$ ) [ml]
$W$	peak width
$x$	position value
$X$	phase distribution ratio
$X_{FL/FU}$	normalised flow rate of lower / upper phase
$X_{F\text{max}}$	maximum normalised phase flow rate
$z$	dimensionless position variable
$\mu$	(Greek mu) average value as chromatographic peak parameter
$\sigma$	(Greek sigma) standard deviation as chromatographic peak parameter
$\tau$	(Greek tau) dimensionless time variable
$\omega$	(Greek omega) rotational speed in centrifugal CCC system [ $1/\text{min}$ ]

## List of author's internal reports

**de Folter, J.** (1998) *Countercurrent Chromatography Practical and Theoretical models*. Uxbridge, UK: Brunel Institute for Bioengineering, internal publication.

Contribution: 95% (acknowledging support from supervisor: Ian Sutherland)

## List of author's publications

### Before this research

Sutherland, I. A., **de Folter, J.**, Wood, P. (2003) *Modelling CCC using an eluting countercurrent distribution model*. Journal of Liquid Chromatography and Related Technologies, 26, 1449-1474.

Contribution: 40%

Citations: 25

### From this research

**de Folter, J.**, Sutherland, I. A. (2009) *Universal counter-current chromatography modelling based on counter-current distribution*. Journal of Chromatography A, 1216, 4218-4224.

Contribution: 95%

Citations: 10

**de Folter, J.**, Sutherland, I. A. (2011) *Probabilistic model for immiscible separations and extractions (ProMISE)*. Journal of Chromatography A, 1218, 6009-6014.

Contribution: 95%

Sutherland, I., Hewitson, P., **de Folter, J.** (2011) *Toroidal coil chromatography: The effect of scale-up and "g" field on stage efficiency*. Journal of Chromatography A, 1218, 6144-6147.

Contribution: 25%

**de Folter, J.**, Cribbin, T. (2012) *Facilitating insight into a simulation model using visualization and dynamic model previews*. Journal of Visual Languages and Computing, 23, 344-353.

Contribution: 75%

The following works were presented at conferences.

**de Folter, J.**, Sutherland, I. A. (2008) *Advanced modelling of counter-current chromatography with variable phase distribution and movement*, 5th International Conference on Countercurrent Chromatography (CCC2008). (oral presentation)

**de Folter, J.**, Sutherland, I. A., Cribbin, T. (2008) *Introducing interactive visualisation to counter-current chromatography modelling*, 5th International Conference on Countercurrent Chromatography (CCC2008). (poster presentation)

**de Folter, J.**, Sutherland, I. A. (2010) *Modelling advanced Counter-Current Chromatography modes*, 6th International Symposium on Countercurrent Chromatography (CCC2010). (oral presentation)

**de Folter, J.**, Sutherland, I. A. (2010) *Counter-current chromatography units model*, 6th International Symposium on Countercurrent Chromatography (CCC2010). (poster presentation)

**de Folter, J.**, Sutherland, I. A. (2010) *Accurate chromatogram peak fitting*, 6th International Symposium on Countercurrent Chromatography (CCC2010). (poster presentation)

# 1 Introduction

While the main focus of this research is on liquid-liquid chromatography, where the stationary and mobile phases are both liquid, theory of different types of chromatography, including the currently most widely used techniques such as thin layer chromatography, liquid chromatography, and high performance liquid chromatography, are covered in the literature review as well.

This research continues from previous work done in the Brunel Institute for Bioengineering Counter-Current Chromatography (CCC) group, where a basic discrete model was developed with the aim of predicting larger scale separations at a time when CCC instruments were just in the process of being scaled up [de Folter 1998a, Sutherland et al. 2003]. However, this initial research was very restricted, mainly using non chromatography related input parameters, a very limited range of operation and accuracy, and also did not provide an acceptable user interface. The current work takes into account all research relating to liquid-liquid chromatography modelling to date.

The research problem addressed here is twofold:

Firstly, there is a need in the development of new drugs to predictably model and scale up processes from analysis to process & manufacturing. The research challenge will be in being able to model all potential operating scenarios and modes of operation. In addition, new and innovative methods of visualising the technology are urgently required in order to educate a traditionally conservative pharmaceutical industry to take on this exciting new technology.

Secondly, and the main goal of this research, is to develop a versatile liquid-liquid separations model. Since models were first created in the 1950s [Glueckauf 1955, van Deemter 1956], they traditionally describe a final state, relying on mathematical approximations resulting in a set of equations that could in turn be evaluated. Traditional models are also more mathematical in nature using many model parameters that have no direct relationship to conditions of the experimental setup. However, today there is a strong need for a model that is very accessible and readily usable by separation scientists. With the use of computers it is possible to make versatile and accurate model software, enabled by current computing performance, and to create effective and usable interfaces for such a model, enabled by currently available development tools and supported by modern operating systems.

Complementary to this goal there is a need to create effective and usable interfaces to such a model. This would imply primarily information visualisation, and secondarily educative visualisation.

The scope of this research is modelling of liquid-liquid chromatography; to be able to predict elution as a pragmatic tool, independent of material properties, solvent systems, complex fluid dynamics, pH and any chemical or biological reactions. The scope of the information visualisation will be where this provides a useful interface to the model, and the educative visualisation to illustrate the basic principles of the liquid-liquid chromatography model.

The research in this thesis does not cover other types of chromatography such as solid-liquid chromatography, generally referred to as liquid chromatography (LC) or more recently high performance liquid chromatography (HPLC), or liquid-gas chromatography. Also it does not cover complex phase distribution and fluid dynamics. Finally, it does not look at chemical or biological reactions, and assumes linear behaviour of the way compounds distribute between the phase systems (K values) as described in the theory section (2.2).

The objectives of this research were to:

1. develop a readily usable liquid-liquid chromatography computer model, able to model all main liquid-liquid chromatography techniques known to date.
2. incorporate into this model different modes of operation.
3. be able to accurately model many sample components and complex sample injections.
4. model the different states in time, enabling appreciation of the entire chromatography process from injection to elution (i.e. not just model the final eluted result).
5. find a more elemental model that better describes continuous liquid-liquid chromatography techniques, as opposed to discrete models currently used.
6. develop a model interface that permits functional and effective model configuration, exploration and analysis using visualisation and interactivity.
7. design a visual representation to better support understanding of the liquid-liquid chromatography process for CCC novices.

The literature review (chapter 2) gives a general background on chromatography, look at different chromatography techniques and, of course, chromatography modelling. Furthermore it looks at computer visualisation techniques and how these have evolved over time, and more importantly how these could be functional to this research. The modelling chapter (chapter 3) looks at how the modelling theory was applied and realised, from concept to implementation. It describes the different liquid-liquid chromatography models in detail, including the computer implementation. Chapter 4 subsequently compares the results of the developed models to experimental results. Chapter 5, entitled *Visualisation Design*, describes how the user interface of the computer model evolved, following a *User Centred Design* approach. The *Insight Evaluation* (chapter 6) is the logical continuation of the design process, looking at a more in-depth evaluation. The *Final Interface* (chapter 7) in turn describes the continued visualisation development. Chapter 8 details the development of an improved visualisation tool. The Discussion (chapter 9) discusses the results presented in the results chapter for both, modelling and visualisation, and puts these into context. The final chapter is the conclusion chapter (chapter 10), describing how the set objectives are met, ending with recommendations for future research.

## 2 Literature review

This chapter will give a general background on chromatography, look at different chromatography techniques and, of course, chromatography modelling. Furthermore it will look at computer visualisation techniques and how these have evolved over time, and more importantly, how these could be functional to this research. The first section on chromatography history (2.1) starts with a brief history of chromatography generally leading up to the current situation with liquid-liquid chromatography and is then followed by a basic theory section (2.2). The next section (2.3) is the main literature study on modelling, followed by a short section on chromatogram deconstruction (2.4), concluding with a summary on what the focus on modelling will be (2.5). Then follow three sections on visualisation: the visualisation history in chromatography (2.6), educative visualisation (2.7) and information visualisation (2.8). The next section (2.9) will be looking at suitable evaluation methods. Finally, the literature review is concluded with a summary on visualisation and evaluation (2.10). In this chapter the context for this project will be established.

### 2.1 Chromatography history

Chromatography was first developed as a technique by the Russian botanist Mikhail Semyonovich Tswett in 1906 [Berezkin 1990]. He applied the technique on a plant leaf extract and found the components (or pigments) separated as coloured bands (Figure 2.1). This is how the name chroma ('colour') and graphein ('to write') (from the Greek language) was created, and now applies to separation techniques in general. The technique Tswett used is now known as thin layer chromatography (TLC) (Figure 2.2). TLC uses a sheet of material such as glass, plastic or aluminium foil which is coated with a thin layer of absorbent material, usually silica gel, aluminium oxide or cellulose (blotting paper). Tswett used calcium carbonate for the absorbent, which is known as the stationary phase. The technique proceeds by the sample being placed on the plate, and a solvent or solvent mixture being drawn up the plate via capillary action. As solvent Tswett used petrol ether / ethanol mixtures. This moving phase is known as the mobile phase. As different components in the sample mixture travel at different speeds up the plate, separation is achieved. Thin layer chromatography is used to identify the number of components in a mixture, to determine their purity and to separate them. An illustration showing separated dyes from a plant extract is given in Figure 2.1.



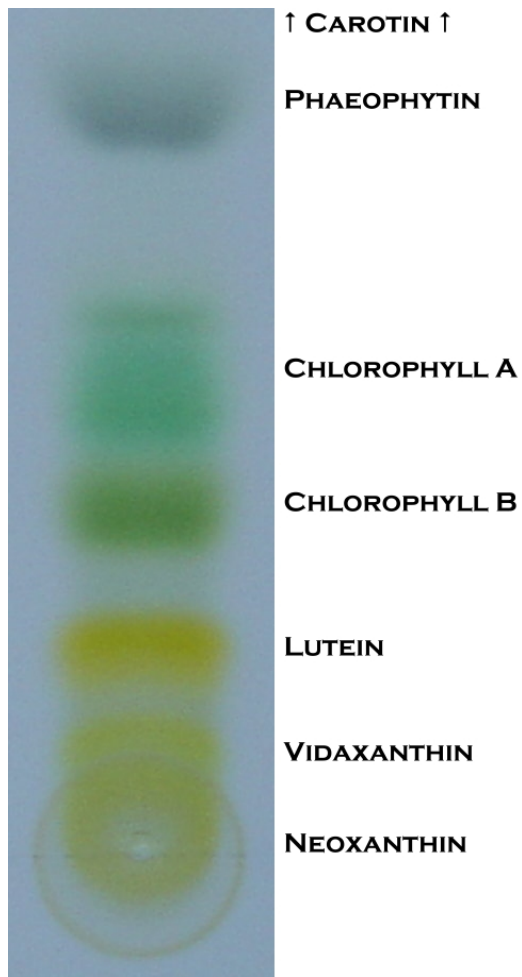
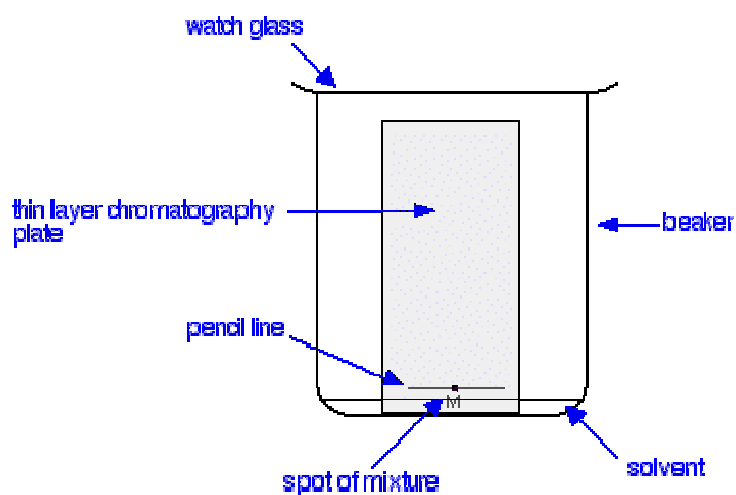
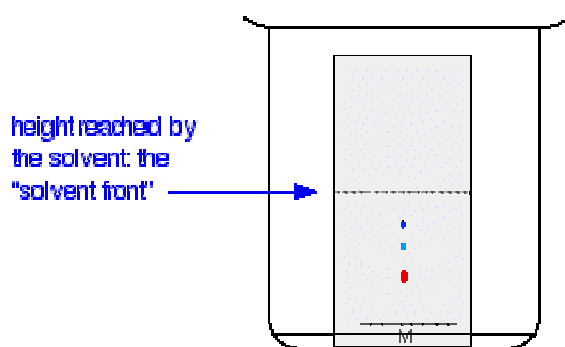


*Figure 2.1 Plant extract separated using thin layer chromatography [http://en.wikipedia.org/wiki/Thin\_layer\_chromatography (Accessed 22 July 2011)], showing separation of different coloured components. Tswett's original experiment would have been very similar to this.*

A



B



C

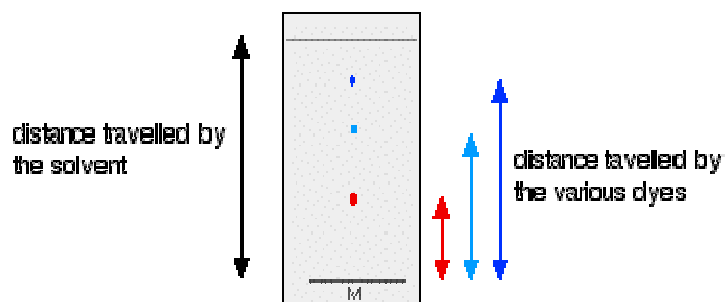


Figure 2.2 Thin Layer Chromatography diagram: A: Plate with sample on it is introduced into mobile phase; B: Mobile phase moving through absorbent material on plate separating sample; C: Final separated sample.

[<http://www.chemguide.co.uk/analysis/chromatography/thinlayer.html> (Accessed 22 July 2011)]

In general separation techniques use two different phases that are in direct contact with each other. This can be a solid phase and a liquid phase, two immiscible liquid phases or a liquid phase and a gaseous phase. The phases are moved at different relative velocities. Commonly one phase is stationary and the other phase is mobile. Separation of different components is obtained by their difference in affinity to the phases. If a component has a larger affinity to the mobile phase, it will travel faster than a component with a larger affinity to the stationary phase.

Chromatography was developed further by Martin and Synge [1941] who developed partition chromatography techniques and created various 'counter-current liquid-liquid extraction' apparati. These mostly consisted of a number of glass tubes connected in series, separating by performing step wise transfers each with perfect component distribution (see section 2.2 on theory). This technique was mainly applied to separation of amino acids. Their research contributed greatly to chromatography, setting in motion development of paper chromatography, gas chromatography and what would later become high performance liquid chromatography. In 1952 they were awarded the Chemistry Nobel Prize "*for their invention of partition chromatography*" [[http://www.nobelprize.org/nobel\\_prizes/chemistry/laureates/1952/](http://www.nobelprize.org/nobel_prizes/chemistry/laureates/1952/)] (*Accessed 22 July 2011*) [Martin 1964, Synge 1964]. In the same period, Craig and Post developed similar devices (Figure 2.3, Figure 2.4) [Craig 1944] and called the technique Counter-current Distribution (CCD) [Craig and Post 1949]. CCD instruments with as many as 100 to 400 test tubes were constructed. More detail on CCD is provided in section 2.2.

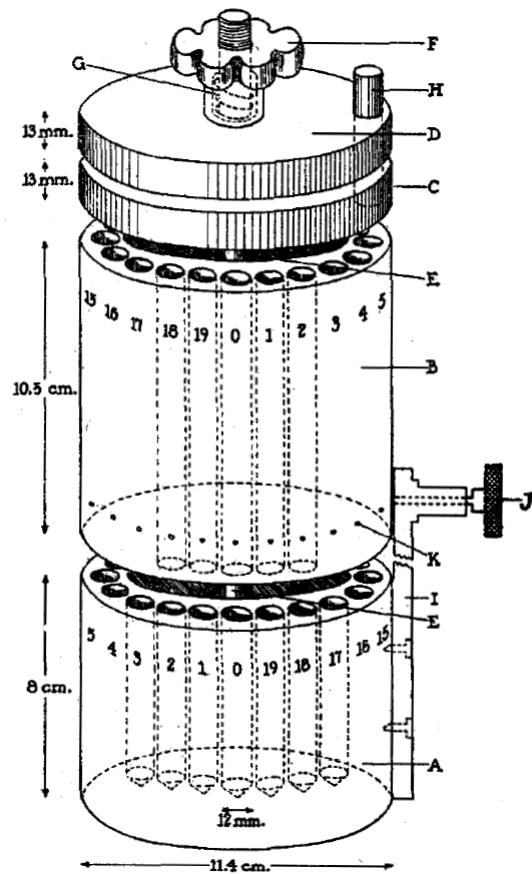


Figure 2.3 Craig CCD apparatus allowing simple manual operation [Craig 1944]. Phases can be mixed by shaking the device. After each distribution phase, the top phase is transferred by rotating part 'B'.

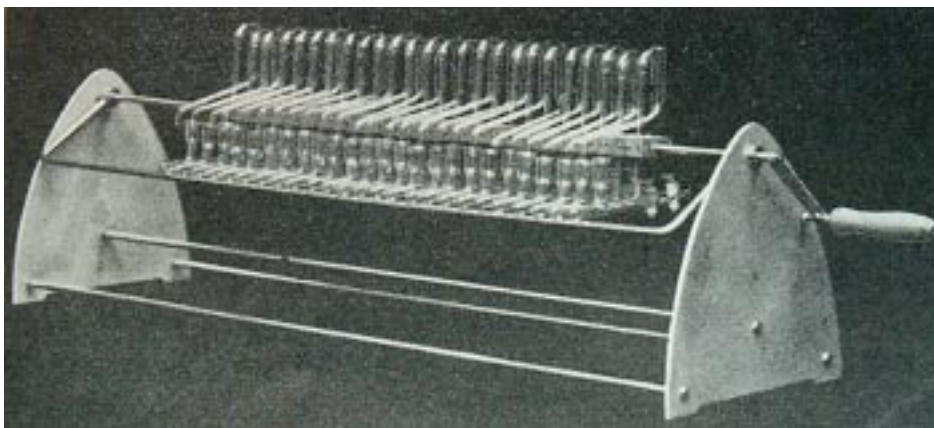


Figure 2.4 Manual version of Craig's CCD machine designed by Erich Hecker [Hecker 1955]

Based on CCD, Counter-current Chromatography (CCC) is a liquid–liquid chromatography technique first introduced by Ito et al [1966]. Like CCD, the process is based on two immiscible phases; traditionally a stationary phase and a mobile phase. However, in CCC the phases flow freely in continuous tubing (Figure 2.5, Figure 2.6). One of the phases is maintained stationary in the tubing due to a combination of hydrodynamic and hydrostatic forces, while the mobile phase is pumped through the system. The geometry of the column is highly variable. The tubing can be wound on bobbins in a number of different configurations, and the bobbins (usually two) are centrifuged in different ways resulting in a variable, high g-field [van den Heuvel and König 2011]. The theory section will go into more detail on this.

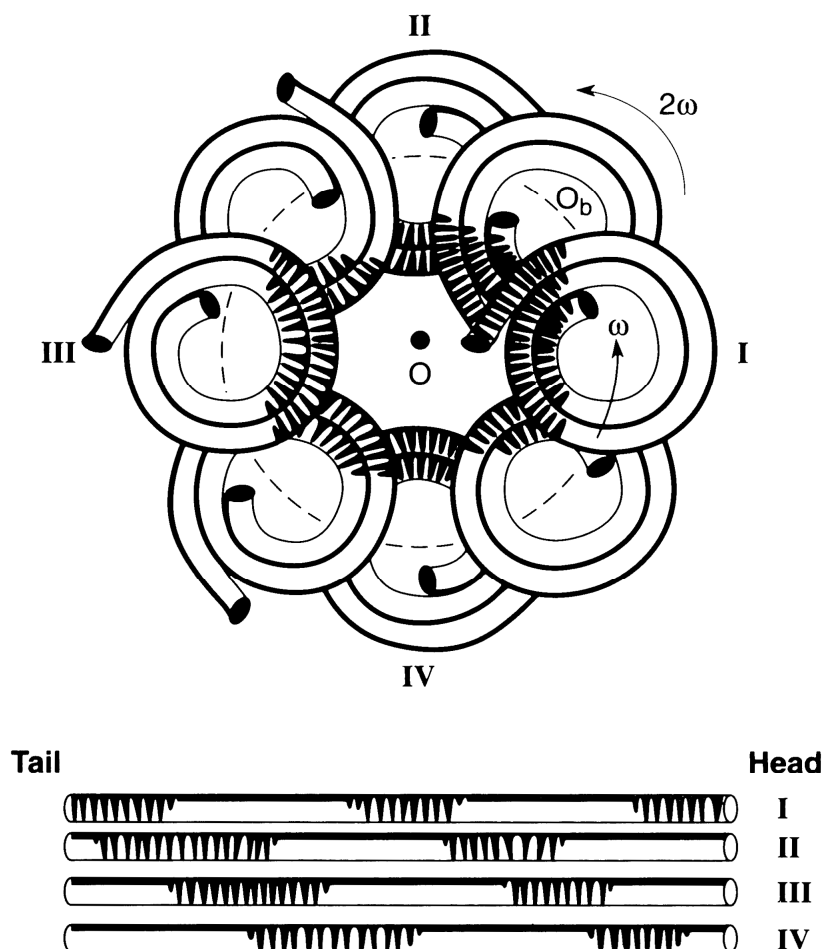


Figure 2.5 Schematic diagram of helical CCC coil in planetary motion showing distribution of heavy phase (dark) and light phase (light) and mixing waves [Conway 1990].

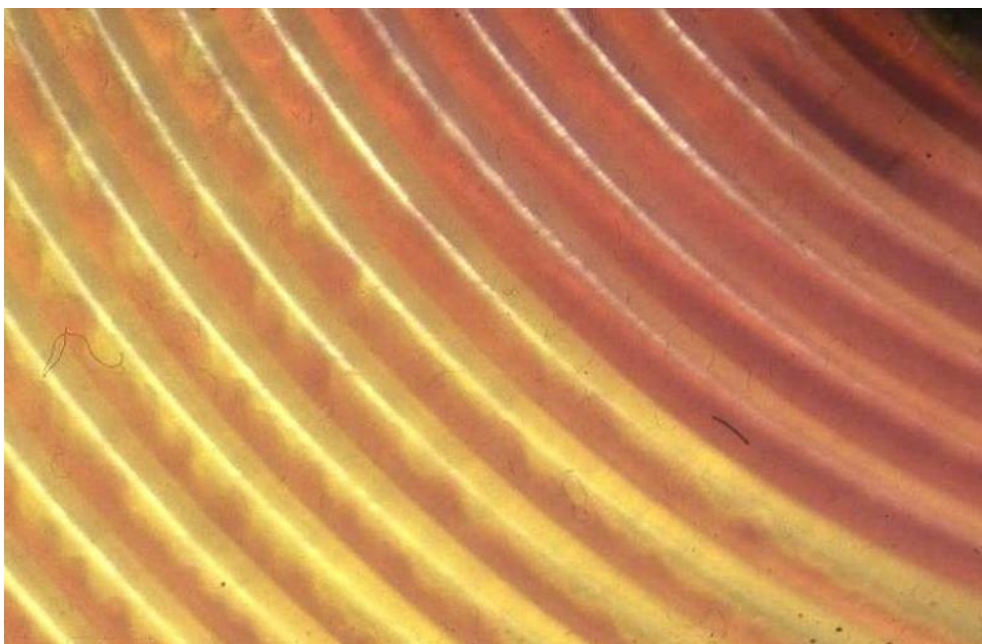


Figure 2.6 Photo of helical CCC column showing phase mixing using dyed phases [Sutherland et al. 1985]

A variation on CCC using a helical coil, is a technique called Toroidal Coil Chromatography (TCC) [Sutherland and Ito 1978], also referred to as Toroidal CCC. In TCC, a helical coil is arranged around the circumference of a rotating disk (Figure 2.7).

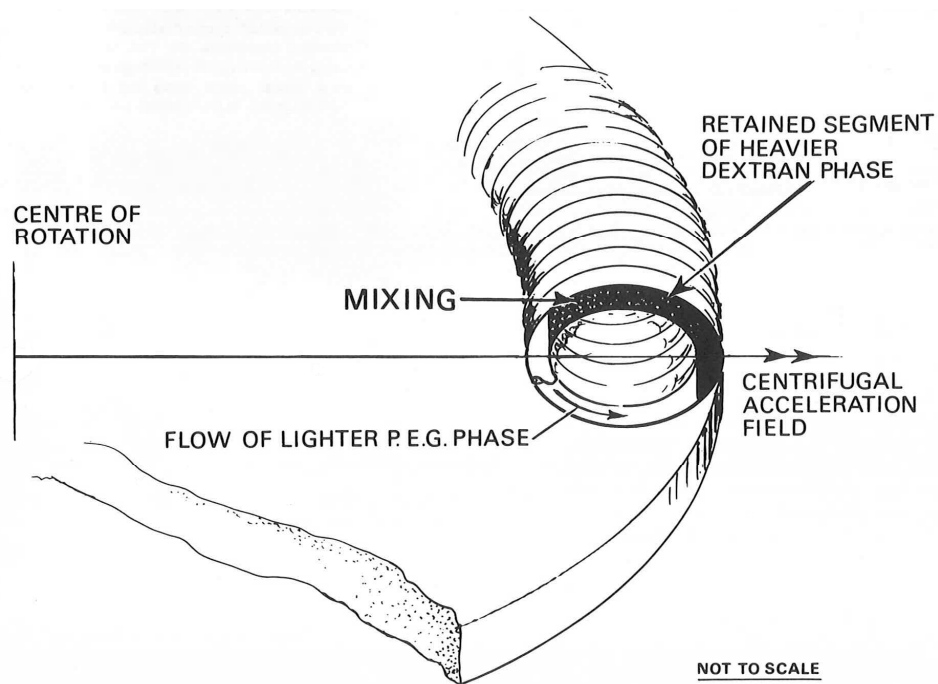


Figure 2.7 Schematic view of Toroidal coil illustrating the phase distribution [Sutherland and Ito 1978]

Another important development in liquid-liquid separation is a technique called Droplet Counter-current Chromatography (DCCC) developed by Ito and colleagues in 1970 [Tanimura et al. 1970] (Figure 2.8), which was applied to separate amino acids. In DCCC most of the column is occupied by stationary phase and mobile phase is slowly pumped through the column forming droplets. Either a lighter mobile phase is pumped through a heavier stationary phase via the bottom of the column, or a heavier mobile phase is pumped through a lighter stationary phase via the top of the column. This form of CCC uses simple gravity (1 g) as opposed to higher g forces in CCC.

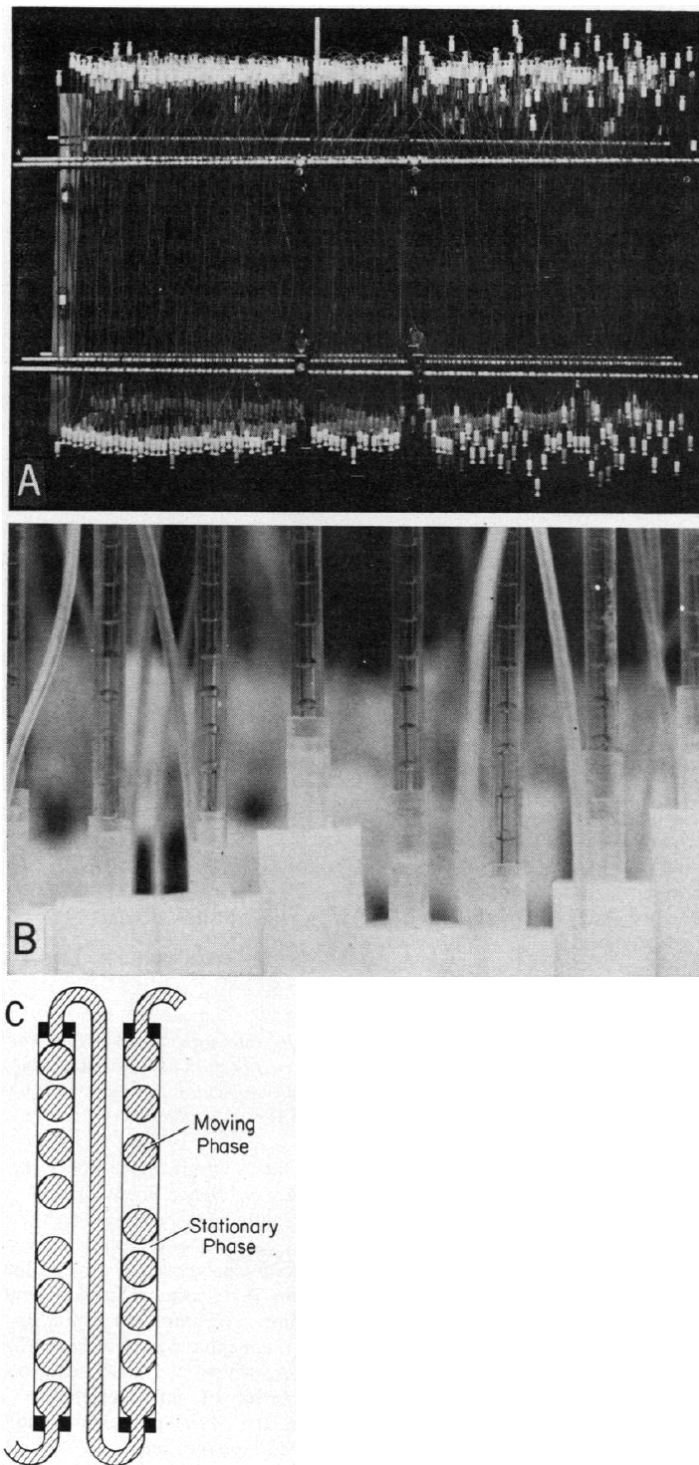


Figure 2.8 Droplet CCC: A: Apparatus; B: Close-up view and C: Schematic diagram showing droplets of mobile phase moving through stationary phase [Tanimura et al. 1970]



Liquid chromatography, which is a separation technique using a liquid mobile phase and a solid stationary phase, has many variants [Snyder et al. 2010]. One of the currently most known ones, called High Performance Liquid Chromatography (HPLC), arose around the late 1960s. HPLC (sometimes also referred to as High Pressure Liquid Chromatography) columns can be packed with various types of materials, in many cases densely packed small spherical particles creating a porous structure (Figure 2.9). Under pressure, the liquid mobile phase is then forced through the packing inside the column (Figure 2.10). This type of chromatography has a more complex interaction between sample mixture and phases, in particular the solid stationary phase. The most important interaction is that the sample can be adsorbed and temporarily retained in the solid phase. There are many variations of liquid chromatography (LC) under a number of different names, such as Column Chromatography, Displacement Chromatography, Normal Phase Liquid Chromatography (NPLC), Reversed Phase Liquid Chromatography (RPLC), Simulated Moving Bed Chromatography (SMB), Affinity Chromatography, Ion Exchange Chromatography, and Size-Exclusion Chromatography (SEC).

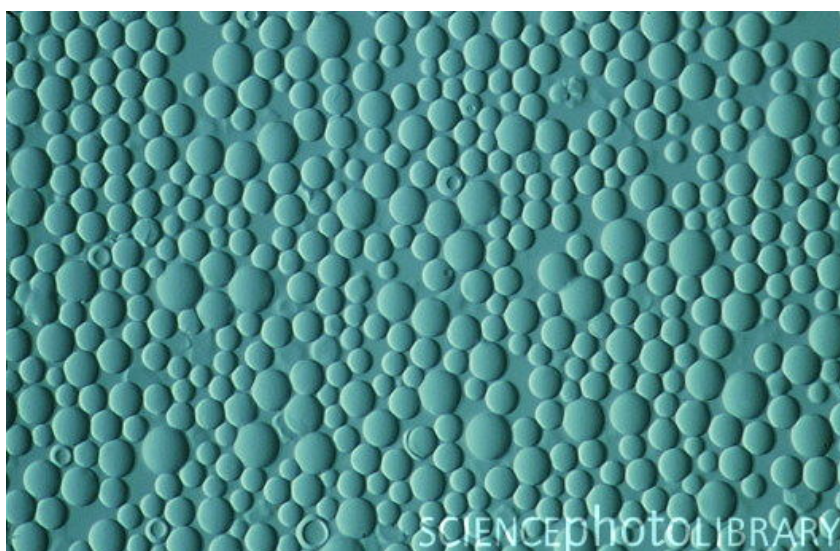


Figure 2.9 Light micrograph of HPLC packing [<http://www.sciencephoto.com/media/359391/view> (Accessed 22 July 2011)]

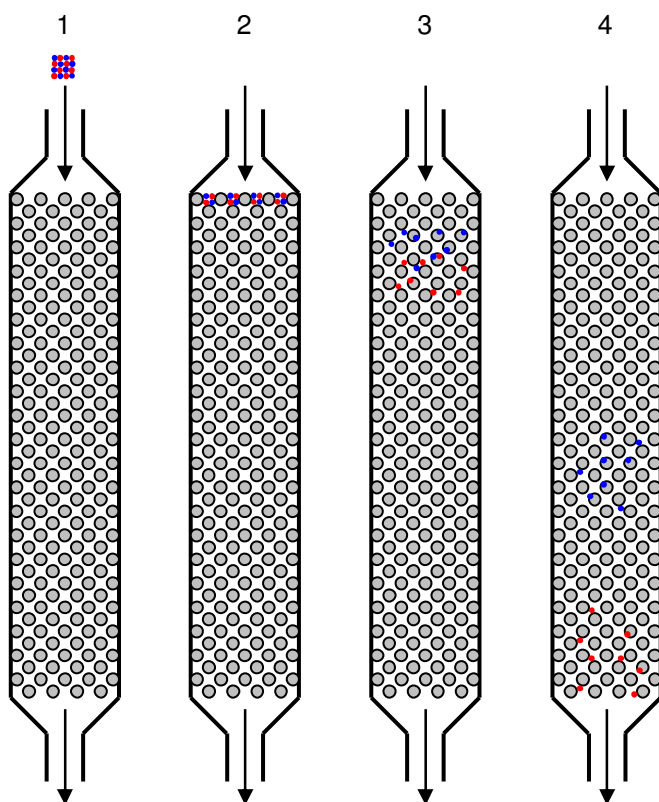


Figure 2.10 HPLC schematic diagram of mobile phase flow through packed column: 1. Sample inserted with mobile phase. 2. Component is moving with mobile phase through column. 3. Different components move at different speeds due to affinity to phases. 4. Components are separated and start eluting from column.

Centrifugal Partition Chromatography (CPC) was introduced by a Japanese company called Sanki Eng in 1982. The column consists of a number of discs, each one having many mixing chambers with connecting channels (Figure 2.11). Like CCC, CPC uses centrifugal force, although it is usually a static  $g$  field obtained using conventional centrifugal motion.



Figure 2.11 CPC disc showing partitioned column [Roullier et al. 2009]

A technique called Vortex CCC was developed recently [Ito et al. 2011a], mounting a *Vortex* column on a planet motion centrifuge, applying the same motion as in CCC (Figure 2.12).

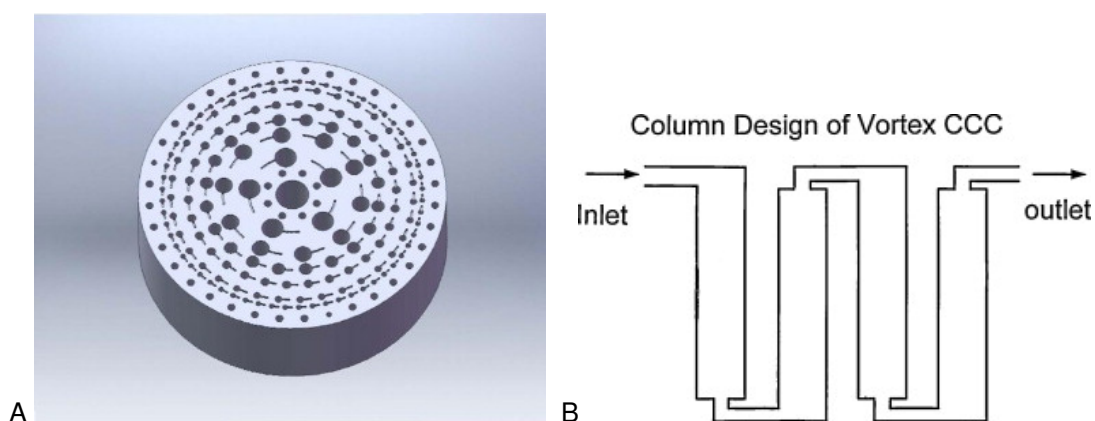


Figure 2.12 Vortex CCC: A. Vortex column; B. Column design [Ito et al. 2011a]

Very recently an experimental technique called Controlled-cycle pulsed liquid-liquid chromatography (CPLC) was developed by Kostanyan and colleagues [Kostanyan et al. 2011]. This technique uses vertical columns, where each column is divided into discrete stages by equally spaced horizontal perforated plates at regular intervals (Figure 2.13).

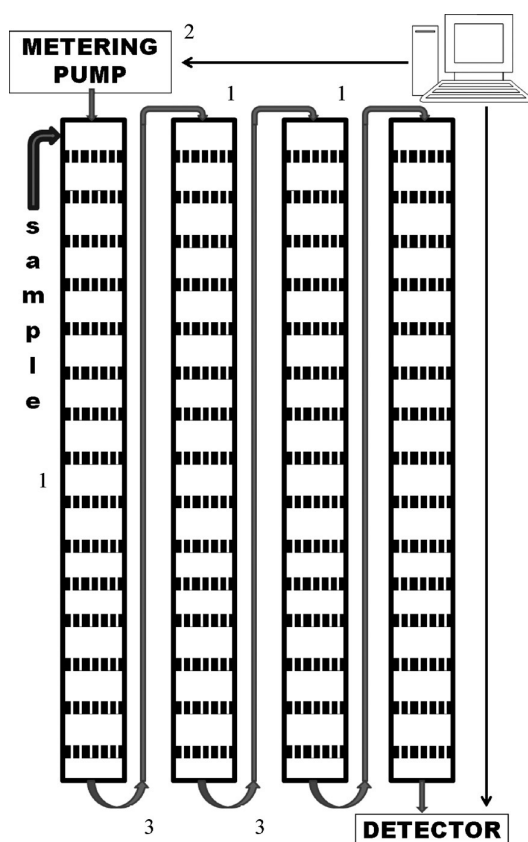


Figure 2.13 Controlled-cycle pulsed liquid-liquid chromatography schematic [Kostanyan et al. 2011].

## 2.2 Chromatography theory

The affinity of a component to the phases is called the distribution coefficient, or simply called 'K value', which is traditionally defined as the concentration (of a component) in the stationary phase divided by the concentration in the mobile phase [Conway 1990]. The K value is the basis of liquid-liquid chromatography theory and is a normalised value, independent of the flow rate, phase distribution, and physical column properties. In Counter-Current Distribution (CCD) the distribution coefficient is defined as the concentration of the upper phases divided by the concentration of the lower phase, where the upper phase is the mobile phase. This is illustrated using CCD (Figure 2.14). In CCD there is a (re)distribution or mixing phase, where the phases mix and subsequently settle, so the components distribute according to their K value. The mobile phase is moved by moving the top content of the test tubes (the upper phase) into the next tube. The stationary phase (the bottom phase) is not moved. A (re)distribution / mixing phase is applied between each transfer phase.

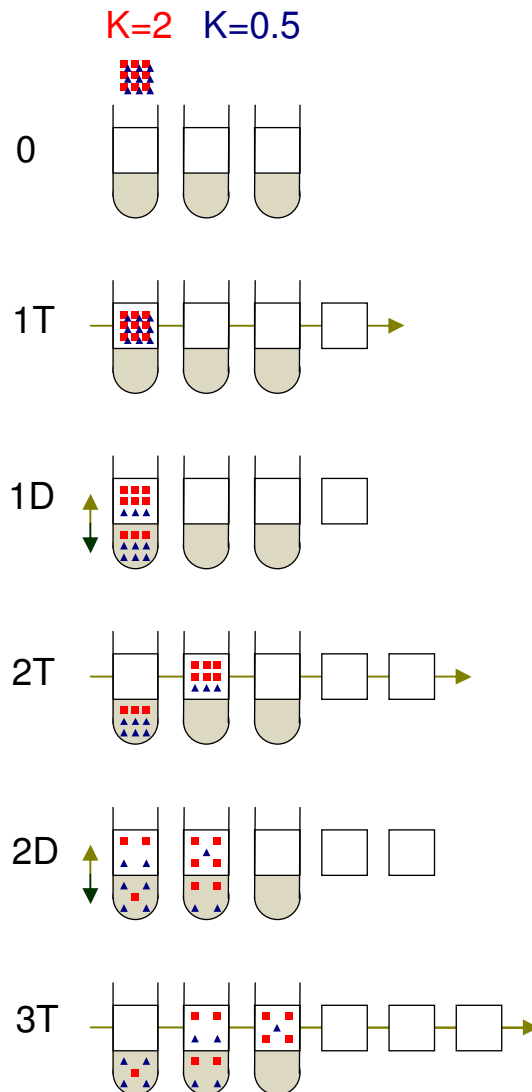


Figure 2.14 Counter-Current extraction system with a stationary lower and mobile upper phase. Sample component distribution for two mixing & settling ('D') and transfer ('T') steps. A light coloured component (squares) has a  $K$  value of 2, and a dark coloured component (triangles) has a  $K$  value of 0.5, where  $K$  for each component is defined as the concentration in the upper phase divided by the concentration in the lower phase [de Folter and Sutherland 2009]

To promote distribution of sample components between the phases, in CCC, mixing and settling is stimulated by the varying g-force. The column is formed by coils of continuous tubing in a helical configuration. To maintain the distribution of the two liquid phases, in particular the stationary phase, the coils are rotated at high velocity, usually in a planetary motion (Figure 2.15). The mixing of the phases depends on the g-forces applied to the column, which depends on the coil orientation and movement [Conway 1990] [van den Heuvel and König 2011]. CCC coils can be rotated in simple centrifugal motion, also referred to as I-type (Figure 2.16A) or the previously described planetary motion also called J-type (Figure 2.16B), or a variable ratio of rotation referred to as 'non-sync' [Ignatova et al. 2010].

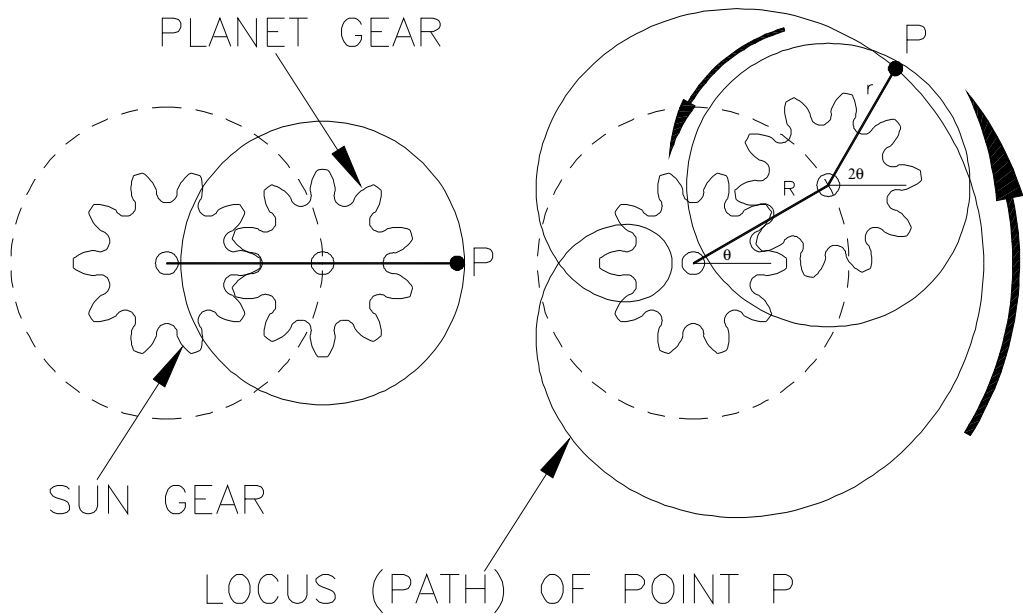
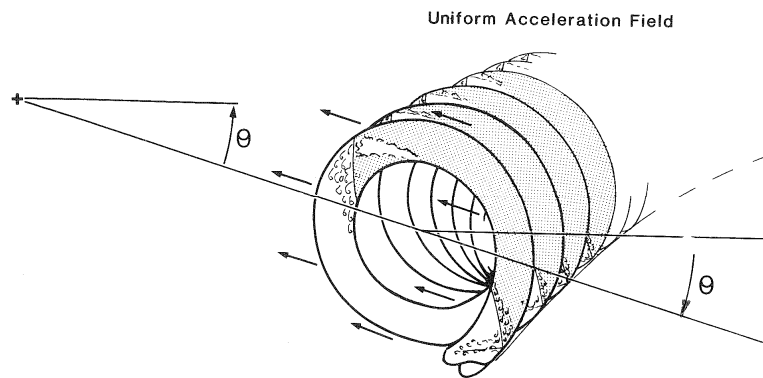


Figure 2.15 A single CCC coil (circle with solid line) (left) describing planetary motion (right) [Wood 2006]

A



B

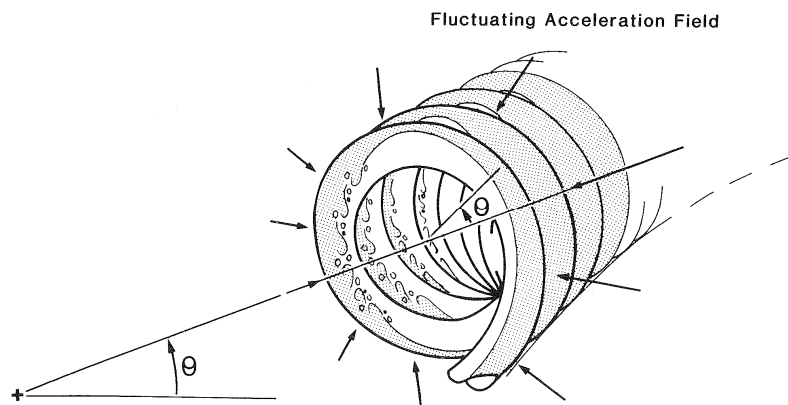


Figure 2.16 Phase mixing in: A: Sun motion (I-type); B: Planetary motion (J-type) [Sutherland et al. 1987]

If there is sufficient transfer between the phases, the components will distribute between the phases according to their K value [Conway 1990] (as illustrated in Figure 2.14).

$$K = \frac{C_S}{C_M} \quad (2.1)$$

where  $C_S$  and  $C_M$  are the concentration of the component in the stationary and mobile phase, respectively. Note that this equation implies linear K value behaviour. Using the current definition the time required for the component to elute, called the retention time, is subsequently calculated as follows [Conway 1990]:

$$t_R = \frac{V_M + KV_S}{F_M} \quad (2.2)$$

where  $V_M$  and  $V_S$  are the volumes of the mobile and stationary phase, and  $F_M$  the volumetric flow rate of the mobile phase. This can be considered a very basic model as it predicts the elution time for any component.

Ideally the components elute from the chromatography column completely separated, illustrating this theory [Conway 1990] in Figure 2.17.

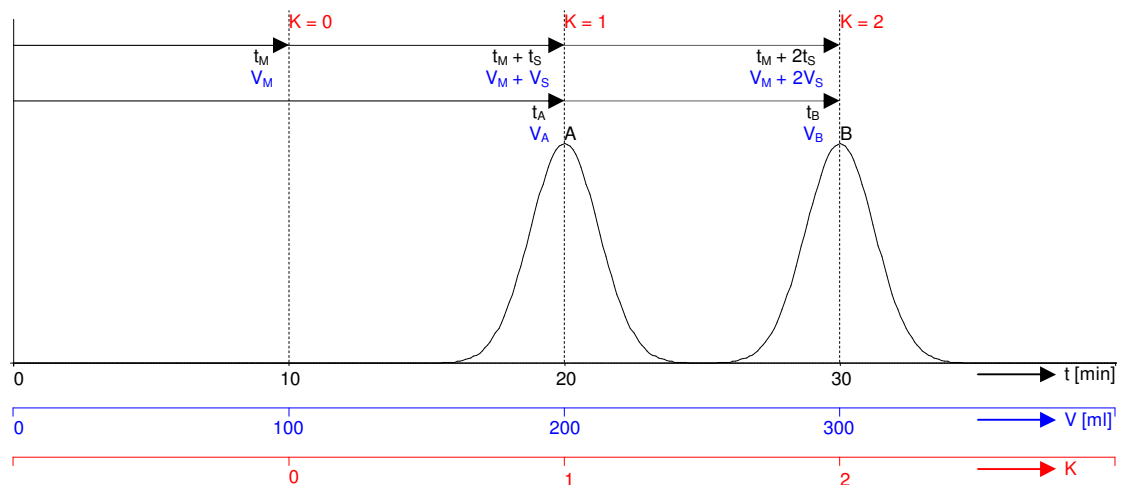


Figure 2.17 Two completely separated components (A and B) eluting from the chromatography column.  $t_A$  and  $t_B$  are the retention times, and  $V_A$  and  $V_B$  the respective volumes of components A and B. In this illustration components A and B have K values of 1 and 2, respectively. Other parameters: Total column volume = 200 ml, stationary phase retention = 0.5 (50%) (therefore  $V_M = 100$  ml and  $V_S = 100$  ml), mobile phase flow rate = 10 ml / min.

Traditionally the peak position or retention time is defined by the maximum peak value. However, the peak position can also be determined by the (statistical) average value of the peak area of a single component. Note that with an asymmetric peak, the peak average would most likely not coincide with the peak maximum. The peak width can be determined in various ways as well. The peak width ( $W$ ) at the base of the peak is defined equal to 4 times the variance sigma ( $\sigma$ ), considering the peak as a normal distribution or Gaussian function. The width of the base of the peak is traditionally determined by tangents passing through the points of inflection of the peak on both sides of the peak maximum (Figure 2.18). The peak width is the distance between where the tangents intersect the base line. Another method is measuring the points where the peak is 0.6065 times the peak height. The position of these points coincides with the variance  $\sigma$  on both sides of the peak maximum, so the position difference of these points is multiplied by 2 to obtain the peak width.

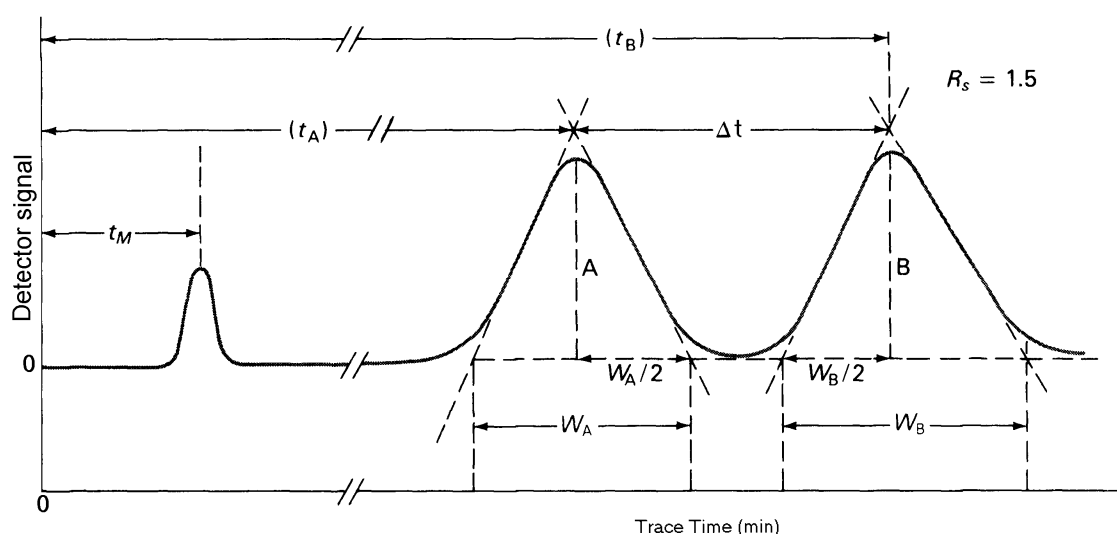


Figure 2.18 Determining width and resolution of two chromatography peaks [Conway 1990].

The resolution of two peaks gives an ideal measure of how well they are separated (Figure 2.18). The resolution is defined as the position difference of the peaks divided by their average width [Conway 1990]:

$$R_s = \frac{\Delta t}{(W_A + W_B)/2} = \frac{2|t_A - t_B|}{W_A + W_B} \quad (2.3)$$

## 2.3 Modelling

The main purpose of modelling is to predict, improve and verify lab and industrial experiments and processes. Modelling allows numerous scenarios to be considered that would require significant resources and would not be feasible, or even impossible, to realise as chromatography experiments.



The subsequent section focuses on chromatography modelling, looking at the various models in the field of liquid chromatography and liquid-liquid chromatography.

### 2.3.1 Transport models

The most commonly used theory to model chromatography is diffusion theory. Diffusion (also referred to as dispersion) is the process of movement of molecules from high concentration areas to low concentration areas, independently from convection (liquid flow). Transport models usually consist of a set of partial differential equations (PDE), describing the concentration profile as a function of position and time, with a basic mass transfer component and diffusion component(s). The set of PDEs can then be solved (possibly numerically) into a final solution. The theory particularly applies to liquid chromatography (solid-liquid chromatography), and chromatography in general.

One of the most historic articles where diffusion theory is applied to chromatography [Glueckauf 1955], shows choosing a temporal equation for the concentration profile. Then Van Deemter published a very thorough analysis considering chromatography partitioning stages [van Deemter 1956], applying the Rate theory, creating what now is known as the classic Van Deemter equations.

The '**Rate Model**' is based on diffusion theory, taking various effects into account: eddy diffusion, longitudinal diffusion, resistance to mass transfer, creating an equation with a constant for each of these components.

Giddings [1965] studied diffusion and mass transfer theory applied to different chromatography techniques in depth, looking at each of the elements in detail.

Morris and Morris [1976] presented diffusion and also general chromatography theory. Later Said [1981] and Ruthven [1984] presented good explanations on general diffusion principles and Rate theory.

In 1995 Gu specifically looked at chromatography modelling and scale up, comparing and combining techniques including computer simulation of the rate model [Gu 1995].

Guiochon and his group started publishing on mass transfer theory applied to liquid chromatography around 1988 [Golshan-Shirazi and Guiochon 1988; 1989; Guiochon et al. 1994], applying the '**Ideal Model**' where effects of axial dispersion and kinetics of mass transfer are ignored. From the need for creating a more realistic model, Guiochon later developed the '**Equilibrium Dispersive Model**' which takes axial dispersion and mass transfer resistances into account.

More recently Guiochon and his group have applied these theories to other types of chromatography as well [Staerk et al. 1996; Miyabe and Guiochon 2000; 2002]. Reviews giving a thorough overview on diffusion theory in liquid chromatography have been presented by Bellot and Condoret [1991], Golshan-Shirazi and Guiochon [1994] and Kolev [1995].

In 1997 Van Buel and his group applied a transport model to Centrifugal Partition Chromatography (CPC) assuming a plug flow model [van Buel et al. 1997a; 1997b].

More recently, Kostanyan and his fellow researchers started applying diffusion theory to Counter-current Chromatography (CCC) [Kostanian 2002; Kostanian et al. 2004; Kostanyan et al. 2007], taking the continuous nature of CCC into account. It is important to note here that between the main molecular transport mechanisms, molecular diffusion is especially applicable to transfer in solids, in techniques such as solid liquid chromatography. More detail on this will be revealed in the modelling chapters. As mentioned before, most transport models are based on a final solution of the transport equations in the form of PDEs, resulting in an approximate solution. In 2010 Guiochon and colleagues have developed an iterative computer model based on transport theory [Horváth et al. 2010]. The clear advantage of iterating the partial solution is that the transport equation can be implemented accurately as opposed to using an approximate final solution.

### 2.3.2 Plate model

The theoretical plate theory originates from separation techniques such as distillation columns having a number of discrete plates or trays. To compare separation columns, the total number of (equivalent) theoretical plates then provides a measure of efficiency of the column.

This model divides a continuous column up into theoretical plates, each plate having a perfect equilibrium of sample components over the phases.

Van Deemter applied the plate theory to liquid chromatography [van Deemter et al. 1956], extending it to incorporate more realistic sample injection. Later Guiochon also incorporates plate theory into his mass transfer models [Miyabe and Guiochon 2000].

### 2.3.3 Cell model

The first model applied to liquid-liquid chromatography, using discrete plates (or cells) was presented by Martin and Synge [1941]. This is sometimes also referred to as the **Martin-Synge Model** or **Distribution** (MSD).

This chromatography technique was later named Counter-current Distribution (CCD), and therefore the model is sometimes also referred to as the '**CCD model**'.

Williamson and Craig [1947] used a binomial expansion, creating a more generalised equation using a simplified transfer equation.

The technique was expanded for dual mode CCD, where both phases move on in counter current direction, (called double distribution or CDCD) by Post and Craig [1963]. In this mode both phases are mobile, flowing in counter-current direction.

This model is further described by Hynninen [1976], Morris and Morris [1976], and Treffry et al [1985].

Kostanyan and his group more recently applied this method to CCC [Kostanian 2002; Kostanian et al. 2004; Kostanyan 2006; Kostanyan et al. 2007]. Previous to the present research, an iterative simulation model was created within the author's research group and published in 2003 [Sutherland et al. 2003]. One great advantage of this simulation model is that the chromatography profile can be viewed both inside and outside the column as the components elute over time.

After publishing the first model as part of the current research [de Folter and Sutherland 2009], Guzlek and colleagues published research on a cell model as well [Guzlek et al. 2010], incorporating physical properties of the CCC apparatus and column into the model.

### **2.3.4 Predictive model**

Inherent to the principles of the distribution coefficient (or K value), a simple equation describes the parameters, mainly the retention, of the eluted components. These were first described by Craig and Craig in 1956 [1956], and later by Morris and Morris in 1976 [1976]. These same principles were applied to CCC by Conway [1990] and Ito and Conway [1995].

Taking this further, Berthod and colleagues developed equations to predict the peak retention and peak width, for components inside and outside the column, furthermore taking recent CCC flow modes into account as well [Berthod and Billardello 2000; Berthod 2002; 2006; Berthod and Hassoun 2006; Berthod et al. 2007]. Using the distribution coefficient theory, a chromatogram normalisation method was developed by Friesen and Pauli, plotting the chromatogram against a logarithmic distribution coefficient scale on the x-axis [2007].

## 2.4 Chromatogram deconstruction

To study model performance, comparing this to experimental data, it is also useful to deconstruct an experimental chromatogram determining its main peak properties, such as peak position, width and resolutions. If peaks are overlapping, accurately determining the peak position and width can become impossible without the use of a computer tool. It should be noted that although such computer tools do exist, they are not readily accessible for researchers. Torres-Lapasio and colleagues studied and evaluated existing methods creating a new, more comprehensive method [Vivó-Truyols et al. 2005a; 2005b]. In their two-part publication, they first look at peak detection, using the Savitsky–Golay method to obtain smoothed derivatives. Next they considered peak shapes which best describe chromatography peaks, and finally applied curve fitting to obtain accurate deconvoluted peak properties.

## 2.5 Modelling summary

After reviewing current literature on chromatography modelling it can be concluded there is a wide range of chromatography models published, however the majority of these best apply to liquid solid chromatography. The initial liquid-liquid chromatography models are designed for discrete types of chromatography like CCD. Later, liquid-liquid chromatography models in general use an approximation for the final solution and do not provide an evaluation over time from the start of injection to final elution. From a practical point of view it is clearly desirable to have a final solution that can be quickly evaluated, but is not required from a research point of view. More importantly an approximation does not provide an evaluation of the process over time and is inflexible considering more accurate modelling effects such as gradual sample injection and dynamic phase flow modes. So creating a model that accurately simulates the chromatography concept iteratively would provide an accurate solution, making this important evaluation over time possible, modelling the various liquid-liquid chromatography techniques currently applied and, furthermore, adding flexibility to expand to more complex flow modes.

As the model would be implemented as a readily usable computer application, it is important to consider how visualisation could be used within an interface to facilitate understanding as well as interacting with the model. These aspects are described in the following sections.

## 2.6 Visualisation history in chromatography

One of the main goals of this research is to implement visualisation and interactivity; primarily information visualisation and secondarily educative visualisation. Before addressing this, the history of visualisation in chromatography will be explored.

A chromatogram is the visual output of the chromatograph. In the case of a successful separation, different peaks or patterns on the chromatogram correspond to different components of the separated mixture after the chromatography process. The first example of a chromatogram was presented in 1906 by Tswett [Berezkin 1990], where the process itself formed a direct visual output (Figure 2.1).

In 1952, James and Martin [1952] developed what we now know as the common chromatogram. They produced an experimental graphic plotter that created an accumulative graph of the detected eluting compounds (Figure 2.19). The tangent of this graph was then taken to show the compounds concentration as function of the elution time. Here the chromatogram is the recorded plot of the eluting component concentration.

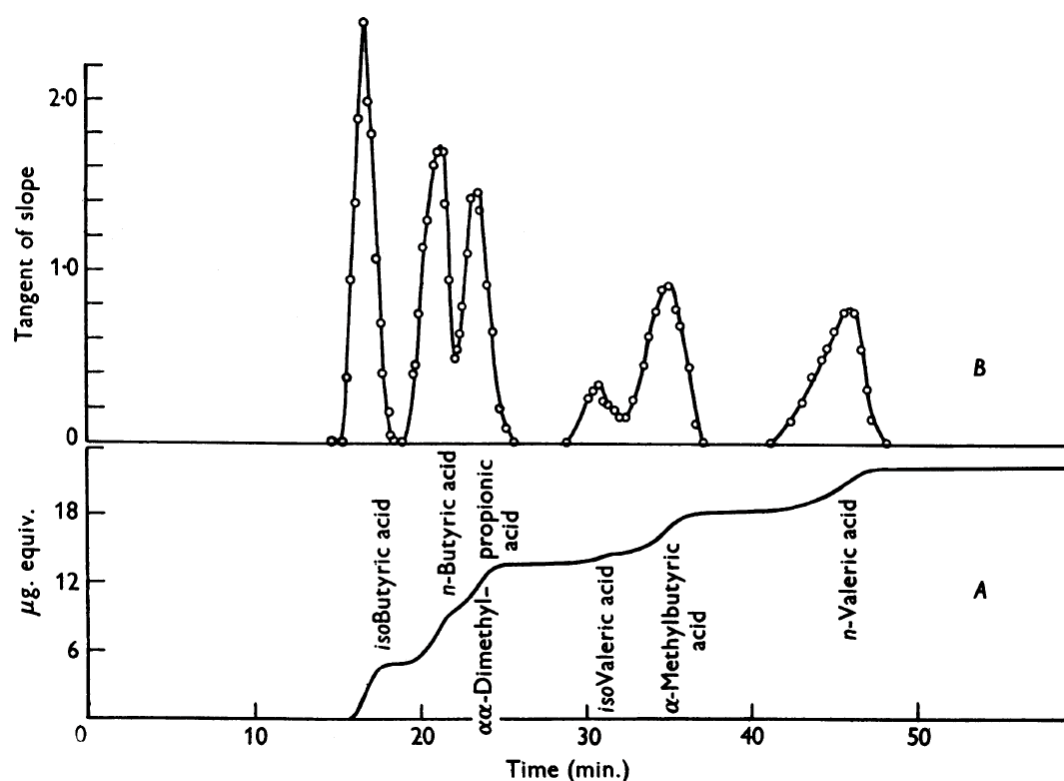


Figure 2.19 First chromatogram plotted [James and Martin 1952]; A (bottom): accumulative detector circuit output signal; B (top): tangent of accumulative output

As computers are being used more commonly to record the detector output, with data being stored digitally, one could say plotting a chromatogram then becomes non-essential. However, even without further processing of this raw data, the basic chromatogram gives essential information about the component concentration, with the peak profiles providing key elution parameters such as retention time and peak width. Although these parameters can be calculated obtaining a numerical result, the chromatogram still provides valuable detail on peak shapes, impurities, stationary phase eluting and other information of an unpredictable nature.

Berthod and colleagues relatively recently made a visualisation improvement [Berthod et al. 2003], by displaying compound concentrations inside the separation column, and in each phase separately (Figure 2.20). This visualisation clearly illustrates how the different phases interact with the components. Most importantly it visualises how each component partitions over the two phases, directly showing the components' affinity to the phases. This type of enhancement is important to consider in current research, and will be looked at in the Visualisation Design chapter.

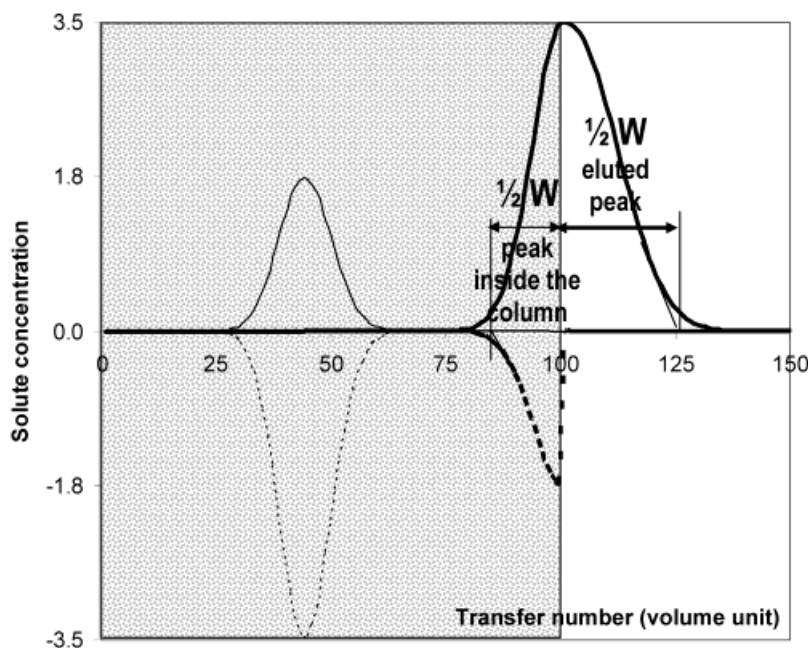
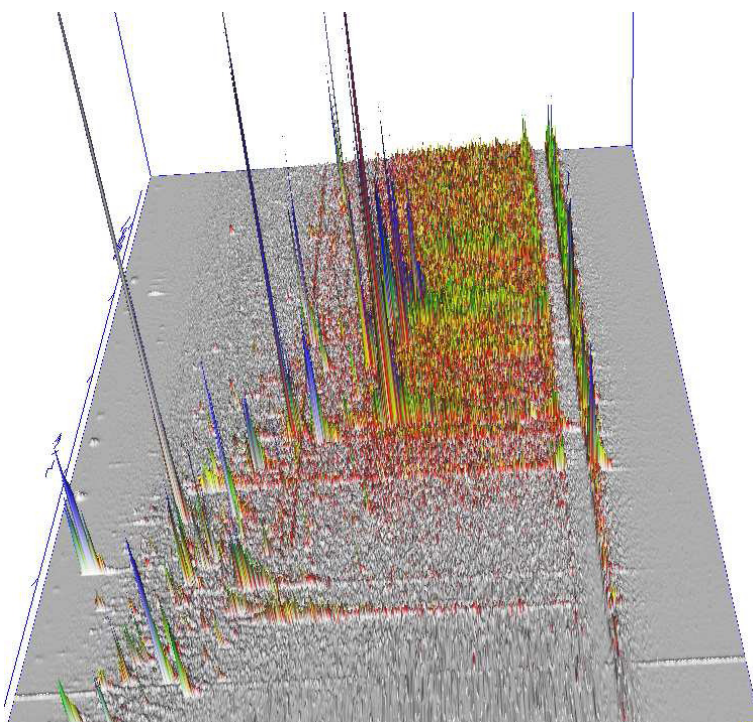


Figure 2.20 Enhancements made to chromatogram type visualisation [Berthod et al. 2003], showing component concentrations of two components in upper (solid line above horizontal axis) and lower phase (dotted line below horizontal axis), inside the column (grey background) and eluting out of the column (white background). ( $W$  relates to the width of the peak.)

To better view liquid chromatography / mass spectroscopy data in its entirety and to perform detailed analysis, an interactive 3D visual exploration and quantification tool was developed by Linsen et al. [2005]. (Mass spectroscopy is a common analysis technique to determine different compounds in a mixture discriminated by molecular weight.) The visualisation was used to help identification of particular patterns in result data sets. This tool plots retention time against a mass spectrogram, with the depth axis showing the signal strength (Figure 2.21). In this 3D chromatogram various colouring schemes were used to improve compound identification. Although this application of visualisation was developed with particular objectives in mind, it "... provides an intuitive understanding of the data on a global scale and allows for detailed data exploration." [Linsen et al. 2005].



*Figure 2.21 Interactive visualisation of liquid-chromatography/mass-spectrometry data [Linsen et al. 2005].*

Currently the basic two dimensional chromatogram still appears to be most commonly used. Westerman and Cribbin have shown that the additional information conveyed by 3D can be outweighed by the additional cognitive demands, associated with assimilating the additional dimension [Westerman and Cribbin 2000]. Note that this depends on the degree and type of additional information afforded by the third dimension. When using the third dimension to add a distinct variable that is critical to a particular analysis, it may be that this outweighs the cognitive demands. This will be taken into consideration in the current research for model visualisation, in chapter 5.

So the chromatogram has evolved from physically being the experimental result (thin layer chromatography: Figure 2.1), to the recorded result (first plotted chromatogram: Figure 2.19), to currently being an optional, customisable visual output.

## **2.7 Educative visualisation**

One of the reasons for including visualisation in this research was to improve the understanding of the chromatography process. Visualisation has been widely used to explain scientific processes, where scientific visualisation promotes insight into these processes [Spence 2001].

Prior to this research, in 1998b, work on educative scientific visualisation was performed in this research group by creating animations [CCC Animations, de Folter 1998b]. These animations showed how two components behaved in CCD (Figure 2.22) and CCC (Figure 2.23), visualising the mixing / settling phases <sup>1</sup>.

The CCD animation used discrete test tubes where they were all shaken to mix the upper mobile phase and lower stationary phase (Figure 2.22A), illustrating separation of two sample components, with  $K$  values of 0.5 (red circles) and 2 (blue triangles). When the shaking stops, the phases settle and the sample components redistribute (Figure 2.22B). After this the mobile phase (yellow) parts are transferred to the next tube, and the sequence is repeated.

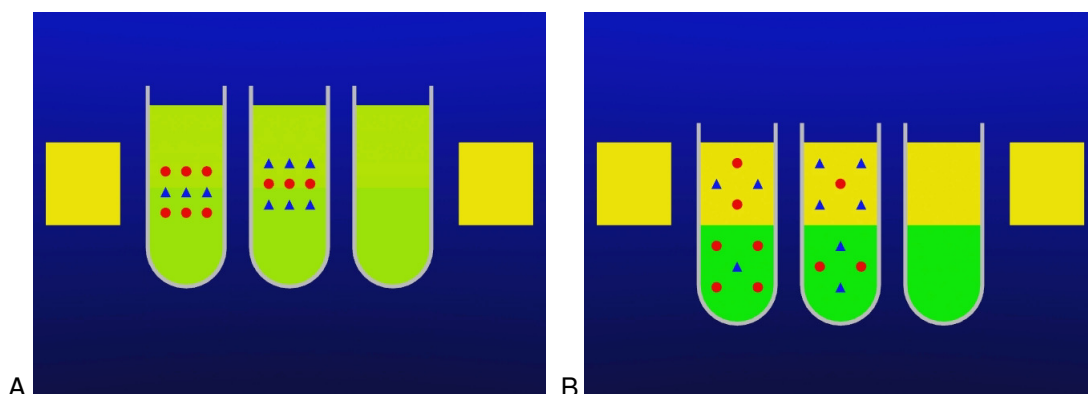


Figure 2.22 CCD separation animation with yellow upper mobile phase and green lower stationary phase showing separation of sample components  $K=0.5$  (red circles) and  $K=2$  (blue triangles); A: mixing/settling stage; B: Just after mixing/settling stage, preceding a transfer stage [CCC Animations, de Folter 1998b]

The CCC animation used the same phase system and sample components as the CCD animation. Here a short length of tubing of the CCC column is shown. Waves of mixing (Figure 2.23A) and settling (Figure 2.23B) travel along the tubing and distribute the sample components between the mobile and stationary phases.

---

<sup>1</sup> <http://vimeo.com/joostdefolter/albums>



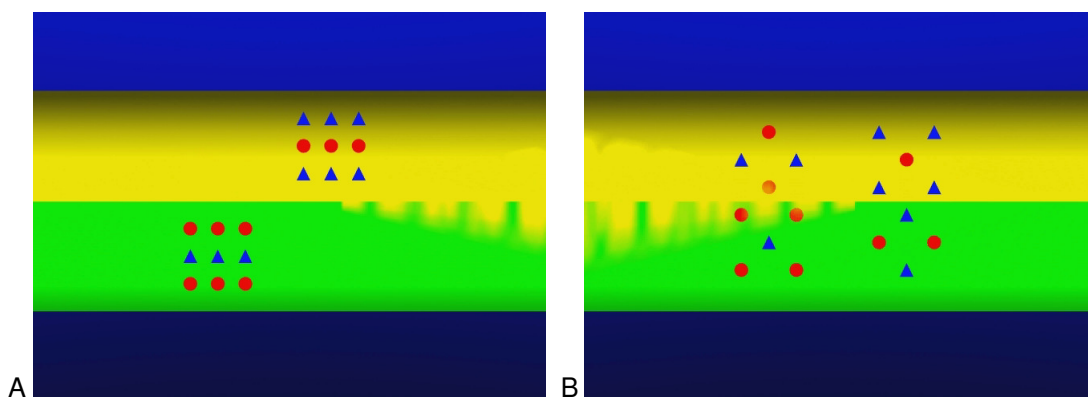


Figure 2.23 CCC separation animation with yellow upper mobile phase and green lower stationary phase; A: Just after transfer stage, before mixing/settling stage; B: Just after mixing/settling stage [CCC Animations, de Folter 1998b]

Another animations then showed the planetary motion (and the mechanics behind it) including the acceleration field applied on the column (Figure 2.24A), fading into the chromatography process inside the coil (Figure 2.24B) showing how the mixing waves travel through the column.

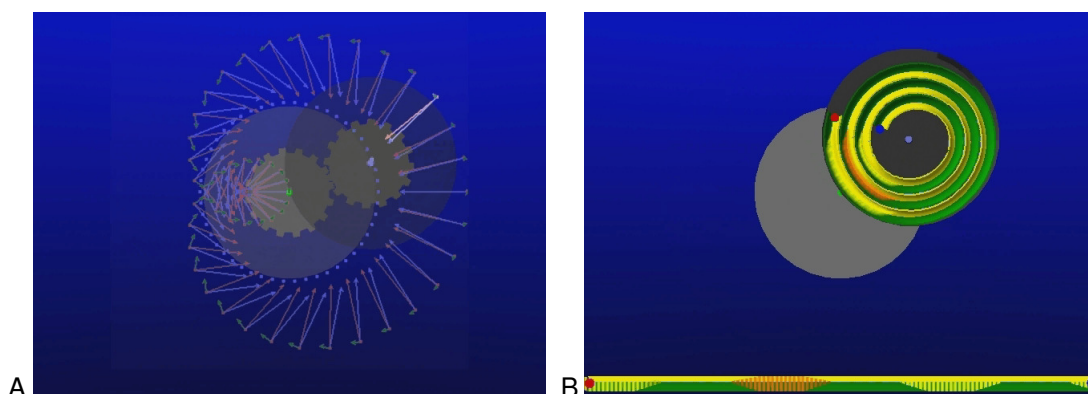


Figure 2.24 CCC planetary motion animation: A: Mechanics and acceleration field; B: Phase distribution and mixing waves [CCC Animations, de Folter 1998b]

This educational visualisation in the form of an animation has been widely used in the current research group, and beyond. The test tube type visualisation as shown in Figure 2.14 or very similar has been used in many publications since 1998 [de Folter 1998a] to illustrate the CCC process and showing different types of phase movements [de Folter and Sutherland 2009] proving this visualisation to be a valuable and effective educational tool. Visualisation performed in the area of molecular and cellular biology [McClean et al. 2004], with the purpose of enhancing education by visualisation, demonstrated the contribution of animation as educational tool.

## 2.8 Information visualisation and interactivity

Whilst the original motivation was for educative visualisation, a greater need for (analytical) information visualisation has become apparent during the course of this project. Whilst the aim for educative visualisation is communicating the physical process of liquid-liquid chromatography, the aim of information visualisation and interactivity is to provide a useful and effective interface for the model, allowing configuration, exploration and analysis.

Information visualisation is defined [Card et al. 1999] as: “*The use of computer-supported, interactive, visual representations of abstract data to amplify cognition.*” So information visualisation is about representing abstract information, affirmed by the following. In information visualisation “... *the physical ‘thing’ is not so important ... [but is] ... more concerned with abstract concepts ...*” [Spence 2001].

Visualisation is essential to reveal patterns; finding the optimal visualisation and relying on the human ability to recognise complex patterns not easily detected otherwise [Card et al. 1999]. Tswett’s original chromatogram (Figure 2.1) is an example of precisely this.

Where the result of the simulation could be visualised with a classic chromatogram, information visualisation techniques can again be implemented to enhance the understanding of the process and its result. Information visualisation is about presenting data or information in a logical and clear way that exploits perceptual strengths (e.g. our ability to see patterns in structures formed by proximity/similarity), leading to an easy and intuitive understanding of that information. Information visualisation should be functional. Spence and Tweedie and colleagues developed the Influence Explorer [Tweedie et al. 1995] [Spence et al. 1995], which aids design by visualisation. Section 2.8.3 will go into more detail on the Influence Explorer’s relevance to simulation modelling. This really demonstrates the significance and contribution of information visualisation. In 2005 Seo and Shneiderman published research demonstrating understanding of data (in particular multidimensional data) can be enhanced by interactive visualisation and exploration [Seo and Shneiderman 2005]. Van Wijk pointed out that there is a general gap between the visualisation researcher and domain expert, and that cooperation between these two is important, further describing a number of methods to achieve this [van Wijk 2006]. In the current work this gap is intended to be bridged.

Visualisation has also been applied to simulation specifically, as Herrod and Bosch et al show in their work, looking at performance analysis of complete machine simulation (simulating a computer’s hardware and software), and conclude “... *visualization can be used to realize the full power of simulation ...*” [Herrod 1998] [Bosch et al. 2000].

The chromatography model is highly parameterised and though the resulting separation is a direct result of the parameters used in the model, there is not always an obvious direct relationship between them. This is where the combination with interactivity has an important role.

In this research the following interactive visualisation techniques have been identified to be very applicable to effectively enhance the model interface.

### 2.8.1 Dynamic querying

As mentioned before, the chromatography model is highly parameterised.

To enable interaction with multiple parameters in the user interface, the well known technique of dynamic querying (DQ) was used. This technique was first proposed by Ahlberg and colleagues [Ahlberg et al. 1992] as a means of filtering records in a property database such as the table of elements (Figure 2.25). It has since been incorporated into tools supporting a wide range of visual analytical tasks, i.e. HomeFinder [Williamson and Shneiderman 1992], FilmFinder [Ahlberg and Truvé 1995], Hierarchical Clustering Explorer [Seo and Shneiderman 2005], and later developed into the commercial tool SpotFire [Ahlberg 1996].

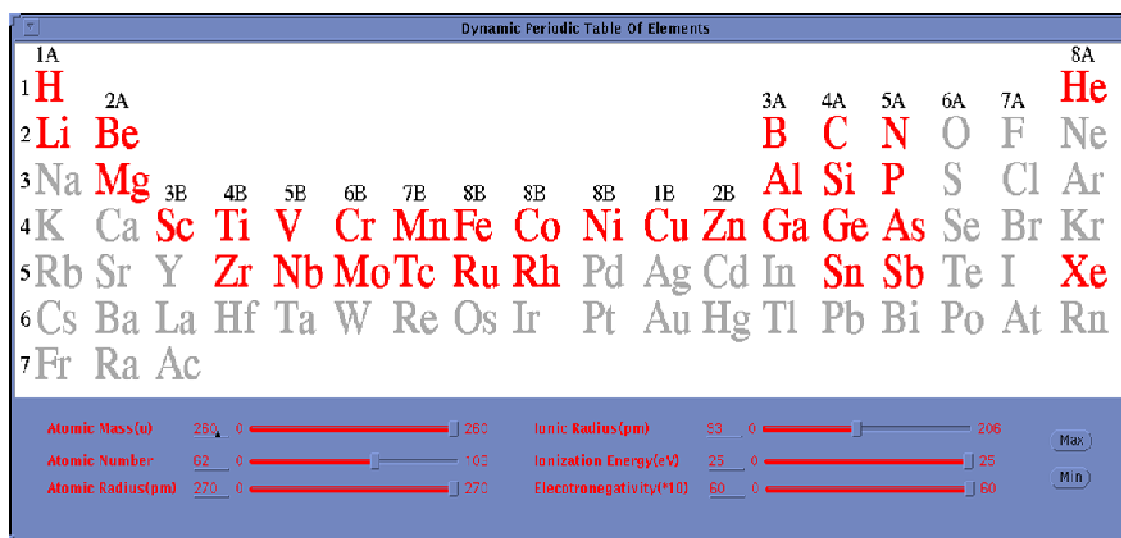


Figure 2.25 Interactive exploration of classical periodic table of elements [Ahlberg et al. 1992]. Moving the controls at the bottom of the screen interactively updates the highlighted elements in the main area of the screen.

In dynamic querying, a number of graphical widgets, such as sliders, allow the user to query a database with the search criteria set by these widgets. Both, the database and search result are graphically represented. This concept was further developed in a different application called HomeFinder which allows finding homes corresponding to particular criteria set by a combination of parameters, displaying a visual representation of the resulting data [Williamson and Shneiderman 1992] (Figure 2.26). This publication also included a detailed evaluation of dynamic querying versus alternative querying methods, concluding the former to have a clear benefit for complex searches and finding trends in the underlying data. Later this concept was expanded into a more generic, to be widely used application, called SpotFire [Ahlberg 1996] (Figure 2.27). SpotFire is a data analysis tool using predictive and complex statistics in the analysis, and is currently used in a variety of industries, including: Life Sciences, Energy, Financial Services, and the Defence and Government [<http://spotfire.tibco.com> (accessed 25 February 2012)].

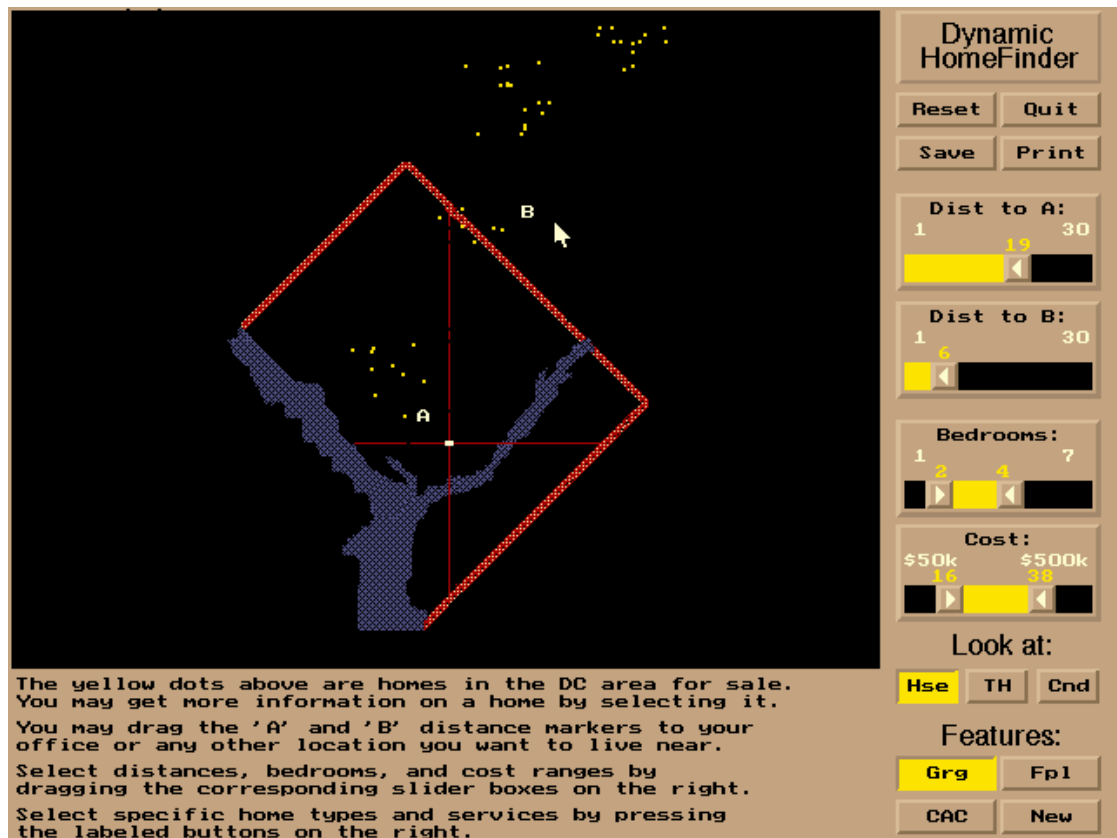


Figure 2.26 HomeFinder: Interactive exploration of data set [Williamson and Shneiderman 1992]. Selection criteria on the right hand side of the screen interactively highlight homes in the main map view.

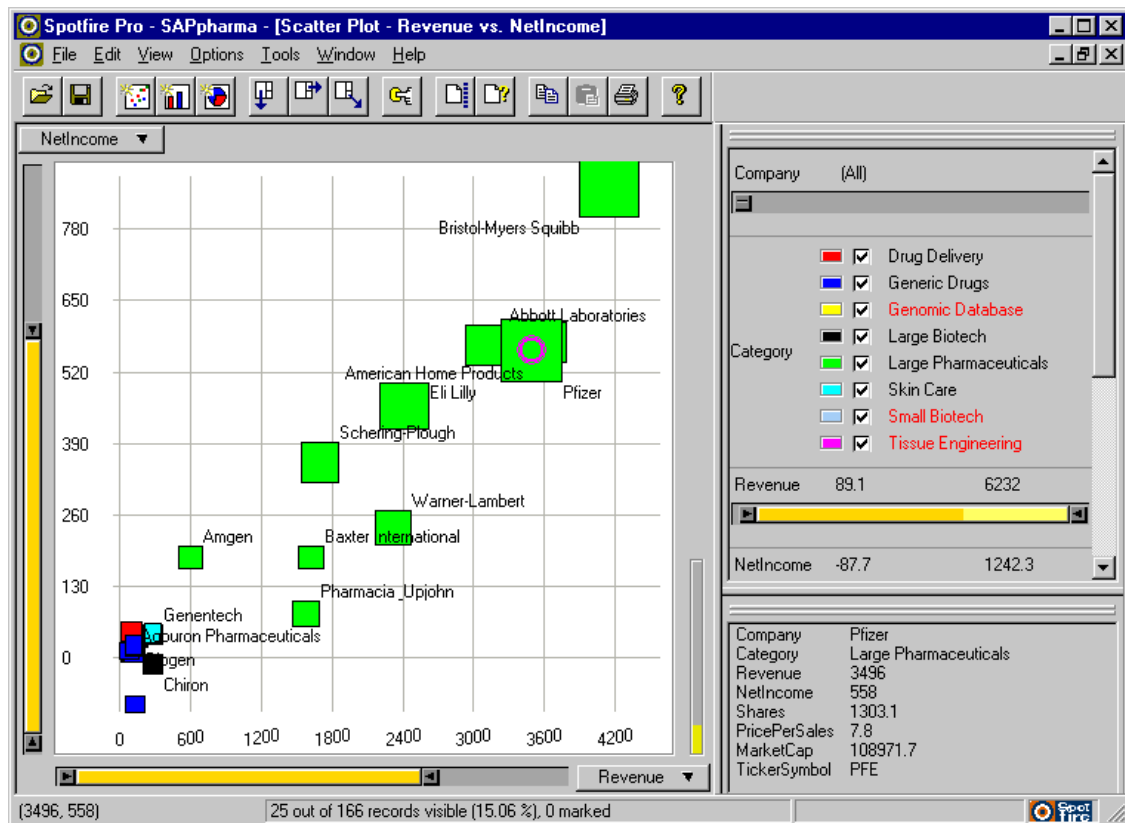


Figure 2.27 SpotFire [Ahlberg 1996]: query/statistical results visualised (in main area of the screen) in accordance to selected criteria (on the right hand side of the screen and yellow slider controls).

Tight coupling between interactive query widgets (sliders, check boxes etc.) and a visual representation of the resulting data allows the user to dynamically experiment with different levels and combinations of variables. Key to the method are real-time updates as the query changes. To enable model configuration with real-time feedback, is relevant to the current research as well. Shneiderman suggests that real-time means less than 100 msec [Shneiderman 1994].

### 2.8.2 Query previews

The technique, called *query previews*, has been combined previously with *dynamic queries* [Plaisant et al. 1999; Tanin et al. 2000], and has been used in context of database queries. Instead of retrieving a large data set, a simpler fast query is performed, to give a rough idea (or preview) of the result of the actual, full query. This was particularly relevant at a time where bandwidth and computational power were limited. However, in the current research, using a complex and iterative model, similarly, a performance problem is expected. The concept of *query previews* could also be applied to computational heavy calculations, by instead doing a much lighter simplified calculation resulting in a quick estimation. More on this simplification will be described in section 3.4 of the modelling chapter. In the context of the current project, the techniques *dynamic querying* and *query previews* could be combined, into a single concept of *model previews*.

### 2.8.3 Influence explorer

Like the model to be developed here, many visualisation tasks involve the manipulation of mathematical models that have multiple, co-dependent parameters of influence creating very large spaces of potential states or configuration. The Influence Explorer [Tweedie et al. 1995; Spence et al. 1995], was an interface originally designed to support the task of finding an optimal electronic circuit design according to customer-specified performance criteria. It uses a basic cause-effect approach implementation, interactively showing performances resulting from changes in parameters (Figure 2.28, Figure 2.29). This appears quite relevant to the current research as it presents an overall solution for models in general.

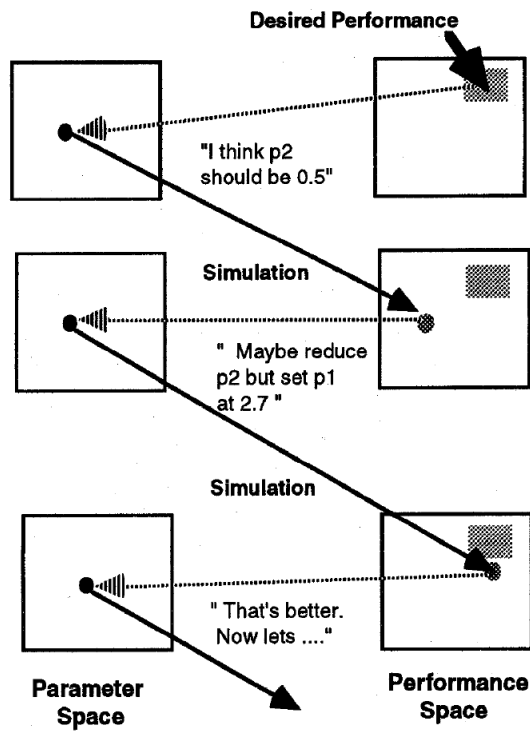


Figure 2.28 Iterative process ( $p_1$  and  $p_2$  are parameters): following dashed arrows requires human expertise [Spence et al. 1995].

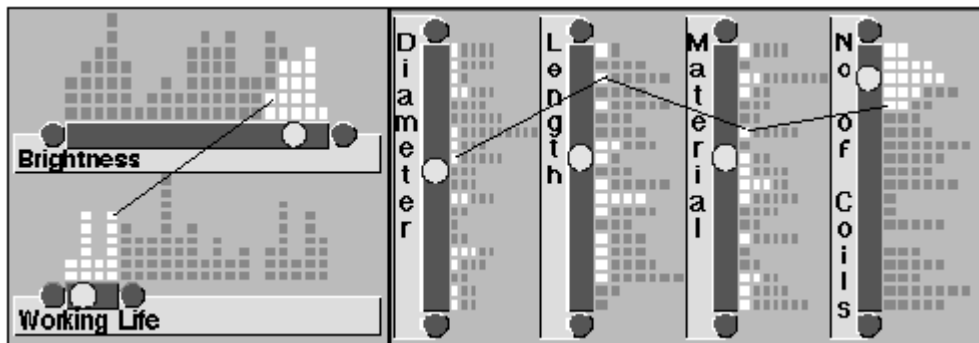


Figure 2.29 Data from an engineering model is displayed in the forms of histograms; performances on the left, parameters on the right. A selection is being made on the 'Working Life' scale, and corresponding values are highlighted (in white) on each of the other scale. [Tweedie et al. 1996].

A logical solution to the problem of implementing a dynamic query in a simulation environment is to pre-compute a database of simulation results. Influence Explorer indeed exemplifies this. However, when a model is defined by multiple, continuous performance variables it is not practical to pre-compute all possible scenarios. Influence Explorer solves the problem by sampling a random distribution of points (usually a few hundred) within a user-specified region of the parameter space. Dix and Ellis [2002] explain how random sampling can provide a solution to a large variety of hard problems, including those relating to visualisation of large spaces. Simulations are then run using each of these configurations. The resulting database of parameter-performance relationships can then be queried in real-time. Perhaps most valuable, from a designer's perspective, is that this approach makes it possible to formulate performance queries and instantly see the parameter configurations that meet these constraints. This form of two-way, dynamic interaction was shown to be effective, not only for circuit design, but also for a number of task domains including financial design [Tweedie 1997] and structural design [Su et al. 1996].

Using the concept of the influence explorer, a set of conditions can be changed interactively, where the result complying with those conditions is shown in real time. As the visualised data is abstract, this technique can potentially be applied to any type of data set. A limitation of the influence explorer concept is the requirement of a pre-computed data set. Therefore, if a pre-computed data set is not available, it may not be readily applicable in the current project. In that case, at least the concept of the iterative behaviour should be taken into account in the design process.

The interactive visualisation techniques described in section 2.8 have been identified to be highly applicable to effectively enhance the model interface. Next a suitable method needs to be identified to evaluate visualisation techniques used to enhance the model interface.

## **2.9 Implementation and Evaluation**

Evaluation is an essential part of the construction of the software model, as a User Centred Design (UCD) approach [Sharp et al. 2007] will be followed integrating user feedback into the interface design (Figure 2.30). An Evolutionary Prototyping [Sharp et al. 2007] approach will be adopted, which is the process of designing the software and, at each redesign stage, adapting or evolving the software until the final version is reached. Note that this process can lead to revision of requirements.



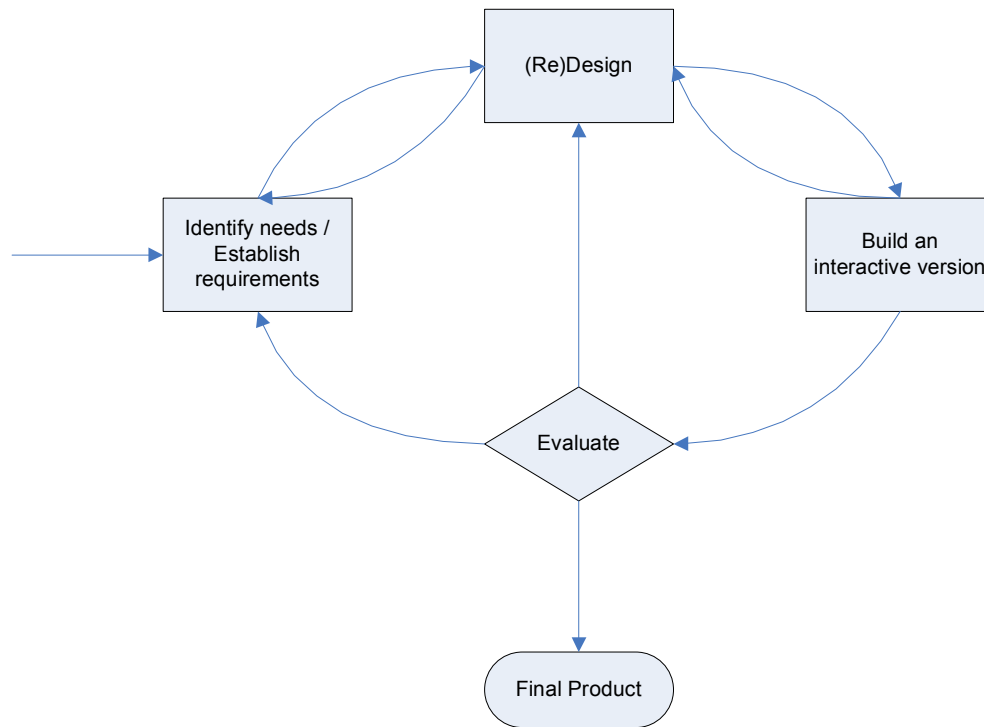


Figure 2.30 Simple interaction design lifecycle model [Sharp et al. 2007].

For the computer implementation of visual components, the well known framework called the information visualisation reference model is commonly used [Card et al. 1999] (Figure 2.31). Source data is mapped into data tables that back a visualisation. These backing data tables are then used to construct a visual abstraction of the data, encoding data variable to visual properties such as position, colour, and geometry. The visual abstraction is then used to create interactive views of the data, for example, the user could be selecting a user interface control, resulting in the views in need of updating. The user interaction potentially affects change at any level of the framework, in an iterative process.

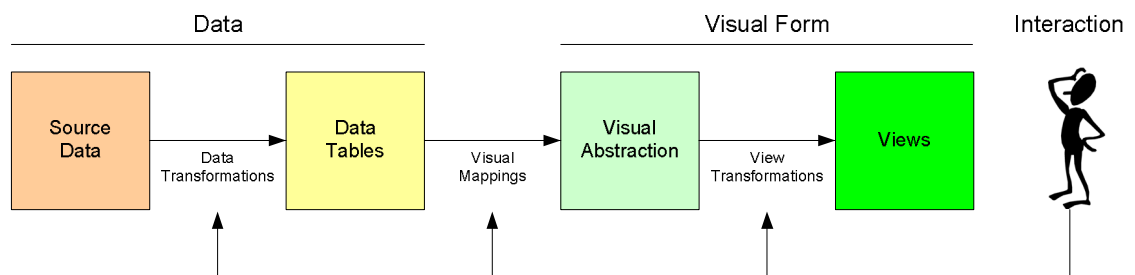


Figure 2.31 The information visualisation reference model [Card et al. 1999]

Once an interactive / visualisation technique has been implemented as a functional prototype, it would need to be objectively evaluated.

### 2.9.1 Formative and summative evaluation

As Sharp's lifecycle model shows, a software interface is usually evaluated many times, both on a formative and a summative basis. A formative evaluation (sometimes referred to as internal) is a method for judging the worth of a program while the program activities are forming (in progress). This part of the evaluation focuses on the process. A summative evaluation (sometimes referred to as external) is a method of judging the worth of a program at the end of the program activities (summation). The focus is on the outcome [Scriven 1991]. Both evaluation methods traditionally apply to user interfaces, having a set of tasks evaluating usability and correctness of the user interface. However, these quantitative methods do not appear the most suitable for measuring the qualitative contribution of visual elements.

Around the mid 00s, with accelerating uses of information visualisation, and visualisations being exploratory and complex in nature, weaknesses of the evaluation methods were becoming apparent. The commonly used evaluation metrics such as task time completion and number of errors appeared insufficient to quantify the quality of an information visualisation system. To address the shortcomings of existing evaluation methods, the workshop 'Beyond Time and Errors' [<http://www.beliv.org> (Accessed 1 October 2012)] was created, exploring new evaluation methods more suitable to evaluate surging information visualisations. In a recent study, North and colleagues demonstrated suitability of various evaluation methods, comparing task and insight evaluation methods [North et al. 2011].

### 2.9.2 Insight evaluation

*Insight evaluation* [North 2006] is a relatively new, very qualitative method, measuring *insights*. North argues that *insight* is the key outcome to any exploratory analysis task and is far more meaningful than traditional measures such as speed or errors gathered from controlled task performance.

"Insight: The capacity to discern the true nature of a situation; The act or outcome of grasping the inward or hidden nature of things or of perceiving in an intuitive manner." [North 2006]

A more specific definition within the context of information visualisation based on North's findings is given as: insight is "a nontrivial discovery about the data or as a complex, deep, qualitative, unexpected, and relevant assertion" [Plaisant et al. 2008].

A basic definition of how data visualisation can provide relevant insight is illustrated in Figure 2.32, showing the various stages, from a new insight being formed, to exploring a new hypothesis and further analysis in turn making this an iterative cycle.

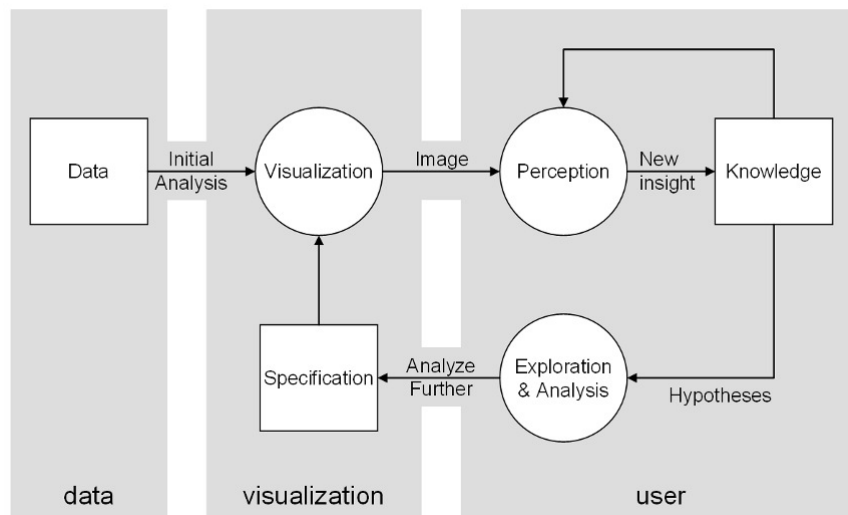


*Figure 2.32 Model of visualisation [Keim et al. 2008]. Visualised data is perceived by a user, resulting in gaining an insight (from top left to right). Based on the insight, the user forms a hypothesis, evaluates this by further exploration and analysis which are fed back into the visualisation (bottom right to left).*

As North defines, this is an open method. It's not so much using an exact controlled protocol, but open tasks defined by simple guidelines. North found that traditional evaluation methods, using detailed controlled tasks, inhibit insights. Instead, North suggested using an open-ended protocol, a qualitative analysis rather than a quantitative one and an emphasis on domain relevance. North suggested insights can be qualitatively measured by their complexity, depth, quality, unexpectedness and relevance. Furthermore insights can be categorised [Saraiya et al. 2004] into: overview, patterns, groups and details. In the latter, insight evaluation was applied to evaluate bioinformatics visualisation. The data recorded in this study was taken from a number of subjects and insights were presented in a quantitative way. The conclusion of this study was that the visualisation tool used clearly influences understanding and insight. In 2006 insight evaluation was again applied in a longitudinal study [Saraiya et al. 2006]. Here visualisation in a bioinformatics area was tested, where subjects recorded insights themselves, for later analyses. The results were presented in qualitative form, evaluating each insight on its own. This allowed subjects to work in a natural way which resulted in a successful study.

The insight evaluation method appears to be the most suitable method to evaluate the model interface to be developed in this research, as it is able to measure the contribution of the visual elements in an optimal, qualitative way.

## 2.10 Visualisation summary

Reviewing current information visualisation literature, a number of aspects have become clear. The general design should follow a User Centred Design, iterating the development using Evolutionary Prototyping.

It is evident that different types of visualisation are applicable to this domain. The primary contribution would be gained from information visualisation, where a number of interactive visualisation techniques have been identified to be very applicable to effectively enhance the model interface. The methods *dynamic queries* and *query previews*, originally used for database queries could be combined into *model previews*, proposed to be applied to effectively enhance the simulation model. To realise this, some simplification of the model would be required enabling such previews. It appears the predictive model described in section 2.3.4 would be very suitable for this. More on this will be described in section 3.4 of the modelling chapter.

Using the concept of the influence explorer, a set of conditions can be changed interactively, where the result complying with those conditions is shown in real time. A question here is whether a pre-calculated data set is feasible for the chromatography model. As it is abstract data that is visualised, the concept can be adapted and applied to the model. An important question arising here is how information visualisation can be applied in a useful and effective way to the computer model. User interface design can contribute to the model configuration and interactive visualisation can provide an additional tool for the modelling process. These techniques are to be implemented into the model.

A secondary contribution could be gained from educative visualisation, as is already proven by widely used visualisation techniques used throughout the CCC field.

To evaluate the usability of the different interfaces to be developed here, traditional quantitative evaluation methods could be used. However, to evaluate advanced visualisation and interactive interfaces, a more qualitative method is desired. Previous research shows *insight evaluation* to be the optimal method for qualitative evaluation of the visualisations to be developed.

## 3 Modelling

This chapter looks at how the modelling theory was applied and realised, from concept to implementation. It will describe the different liquid-liquid chromatography models in detail (sections 3.1, 3.2, 3.3, 3.4), the process from model to simulation (section 3.5) and finally the computer implementation (section 3.7). A user manual of the software model can be found in Appendix A. The software model itself can be freely downloaded <sup>2</sup>.

### 3.1 Model based on CCD

This section has been published in similar form [de Folter and Sutherland 2009].

The first liquid-liquid separation technique chosen for modelling was counter-current chromatography (CCC). Although this is a continuous column, a discrete CCD model was first chosen to model CCC, because of its nature and its relatively ease to be converted into a computer model.

---

<sup>2</sup> <http://theliquidphase.org/index.php?title=Modeling>

### Conventional mode

In CCC traditionally there is a stationary phase and mobile phase. In CCD this means that the mobile phase of each tube is transferred to the next tube. This is followed by mixing of the entire contents of each tube, and a settling into upper and lower phase again, in order to promote distribution of the components over the phases according to their  $K$  value [Conway 1990]

(Figure 3.1 – same as Figure 2.14 – repeated here for completeness).

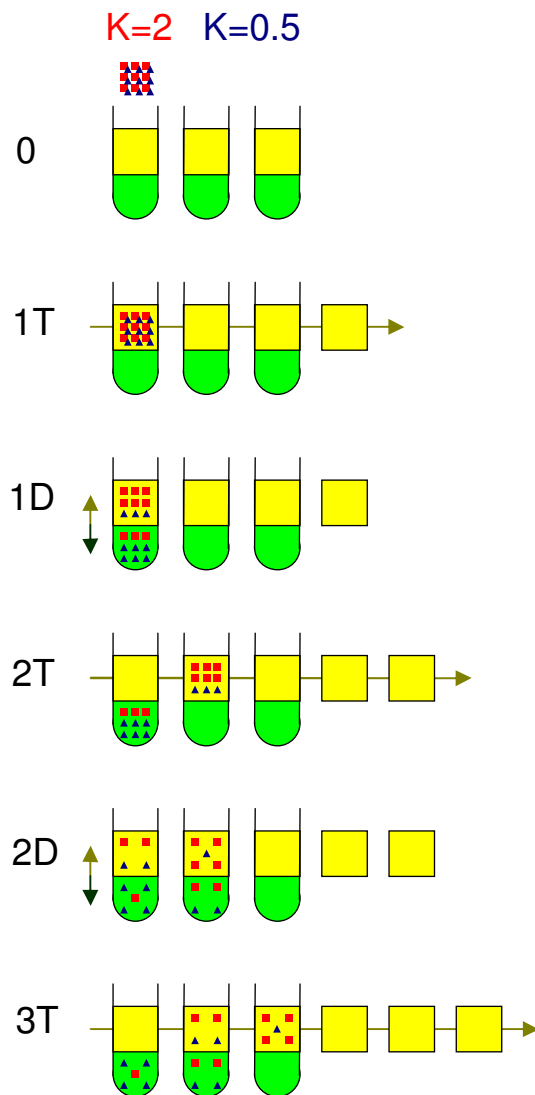


Figure 3.1 CCD system with a stationary lower and mobile upper phase. Sample component distribution for two mixing & settling ('D') and transfer ('T') steps. A light coloured component (squares) has a  $K$  value of 2, and a dark coloured component (triangles) has a  $K$  value of 0.5, where  $K$  for each component is defined as the concentration in the upper phase divided by the concentration in the lower phase [de Folter and Sutherland 2009]

## Co-current flow

In co-current flow the phases move in the same direction, but at different speeds (Figure 3.2). This mode of operation, also called co-current CCC, was first introduced by Sutherland and colleagues [Sutherland et al. 1984] and further developed by Berthod [Berthod and Hassoun 2006]. Note that in this mode, one of the two phases flows slower than the other, so in order to calculate the total sample component concentration for eluted components at any point in time, the scales of the phases need to be normalised in time. This will be described in more detail a bit later on in this section.

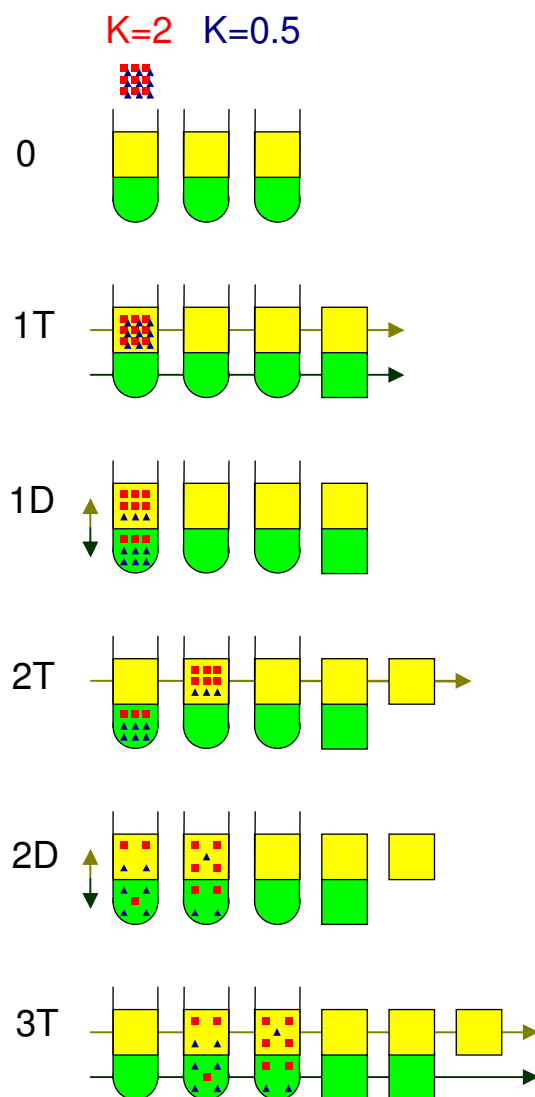


Figure 3.2 CCD system in co-current operation. Sample component distribution for two mixing/settling and transfer steps. The upper phase moves twice as fast than the lower phase. This is shown here by moving both phases in one step and only moving the upper phase for the next step [de Folter and Sutherland 2009]

## Dual flow

In dual flow (also labelled Dual Counter-Current or Dual Flow Counter-Current Chromatography), the phases move in opposite direction [Ito 1985]. Therefore, there is no stationary phase in this mode, as both phases are mobile (Figure 3.3).

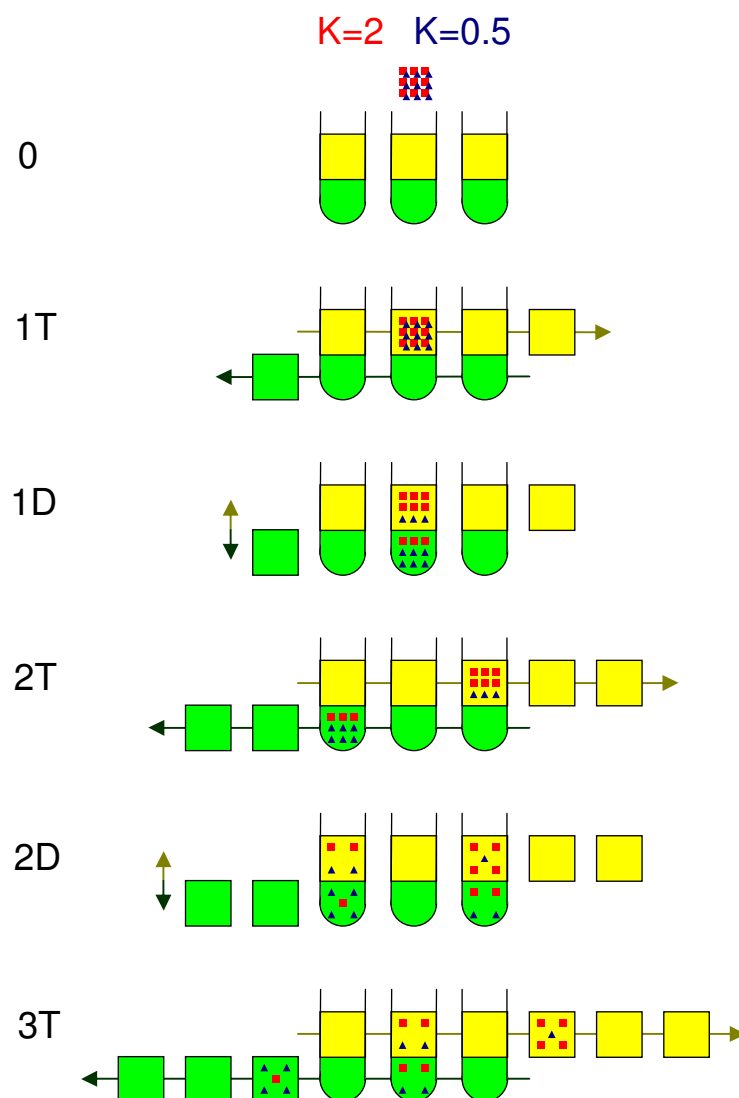


Figure 3.3 CCD system in dual flow operation mode. Sample component distribution for two mixing/settling and transfer steps. The upper and lower phase move in opposite direction [de Folter and Sutherland 2009]



### **Intermittent flow**

Intermittent Counter-current Extraction (ICcE) was developed as a new operational scenario for hydrodynamic CCC in 2009 [Hewitson et al. 2009]. In ICcE, after injection in the centre of the column, the phases are pumped alternating between the upper and lower phase for a fixed amount of time or volume. In practice this is realised using a system with two separate bobbins, with a sample inlet where the bobbins are joined. The alternate phases are pumped into alternate ends of the column, effectively the external inlets of the alternative bobbins.

Multiple Dual Mode (MDM) was developed in 2006 as an alternative technique for the preparative separation of structurally similar compounds [Delannay et al. 2006]. In MDM, after injecting at the start of the column, the phases are pumped as in the intermittent mode. The switching time can be adjusted so that sample components are retained within the column for an optimum period.

Both these modes function similarly, moving phases alternatively (Figure 3.4).

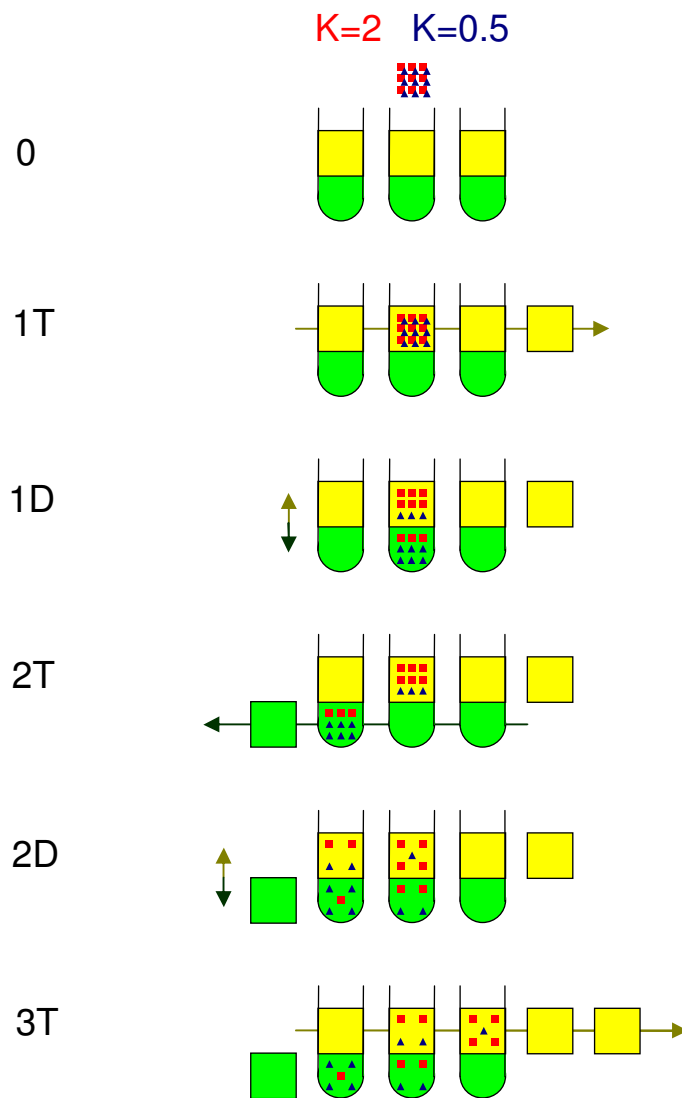


Figure 3.4 CCD system in intermittent flow operation mode. Sample component distribution for two mixing/settling and transfer steps. The upper and lower phase move (in opposite direction) alternatively.

## Model

The CCD model developed here is in fact a simulation of the CCD process, iterating through the transfer and distribution steps. The model simulates a number of imaginary test tubes, also called cells. The cells in the model consist of arrays of numbers representing the mass concentrations of sample components. This way the arrays can be made any length dynamically, allowing for a greater flexibility and optimisation of available computer memory. Since the cells for the lower and upper phase (like the top and bottom part of each test tube in the CCD process) are always changing position, they are each created and moved independently (Figure 3.5). Between each movement step, there is a (re)distribution. This is where the components' mass is distributed over the phases according to the distribution coefficient of each component, like in the CCD process. The transfer of component is obtained as [Craig 1944]:

$$\frac{1}{KX + 1} \quad \text{or} \quad \frac{KX}{KX + 1} \quad (3.1a,b)$$

depending in which phase the unit is, where  $K$  is the distribution coefficient:

$$K = \frac{C_U}{C_L} \quad (3.2)$$

(with  $C_U$  and  $C_L$  being the sample concentrations of the upper and lower phase, respectively), and for the current definition of  $K$  (eq. (3.2))  $X$  is defined as the phase distribution ratio:

$$X = \frac{U_F}{L_F} = \frac{V_U}{V_L} \quad (3.3)$$

where  $U_F$  is the proportion of the column volume occupied by the upper phase and  $L_F$  is the proportion of the column occupied by the lower phase:

$$U_F = \frac{V_U}{V_C} \quad \text{and} \quad L_F = \frac{V_L}{V_C} \quad (3.4a,b)$$

where  $V_U$  and  $V_L$  are the volumes of the upper phase and lower phase, respectively, together making up the total volume of the column  $V_C$ .

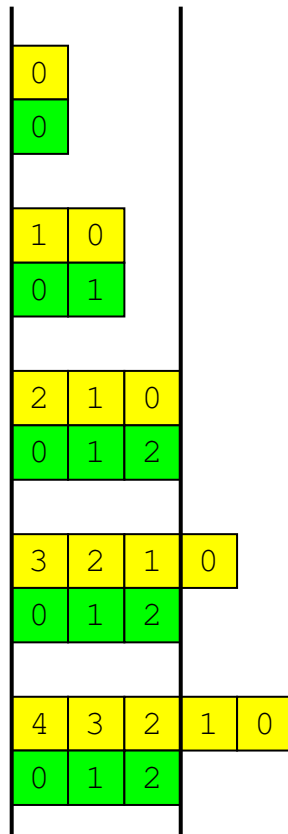


*Figure 3.5 Showing how cells are created as the model progresses (in conventional flow mode). The numbers represent the index of each cell. Cells with a higher number have been created later.*

The cell movement depends on the flow rates of each phase and the flow mode (Figure 3.6). At each step, the 'fastest' phase will move 1 cell, and the other phase will either, move 1 cell per step as well, move periodically but not every step, or not move at all.



If  $X_{Fx}$  has a value of 1, the entire content of the cell (for the respective phase) will be moved each model step, which is the same as a normal CCD step. A value lower than 1, results in the entire phase cell content being moved once every  $1 / X_{Fx}$  steps. In the model it is fundamental that the entire content of any cell is moved. If only a part of the content were to be moved to the next cell, resulting in a part staying behind, the concentration for each component would become the average, so to speak, of the different concentrations. This would then result in a blending of the concentration over the cells depending on the value of  $X_{Fx}$ , resulting in an undesired peak broadening. The introduction of such an effect is clearly unwanted, and avoided by only moving the entire contents of a cell as described before.

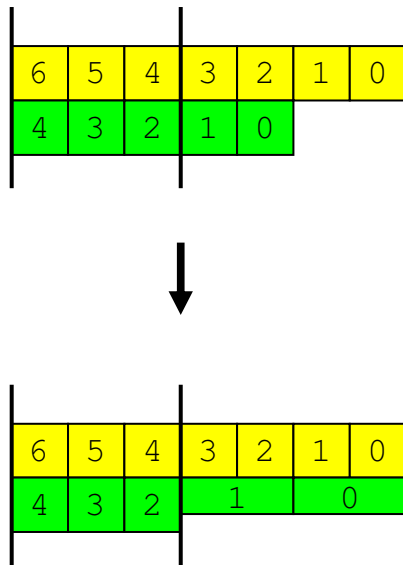


Figure 3.7 Showing how cells are synchronised (in co-current flow). Lower phase flow is half that of upper phase flow.

If one of the two phases flows slower than the other, the scales of the phases need to be normalised in time in order to obtain the total sample component concentration at any point past elution (Figure 3.7). This means that the part of the slower phase that has flown out of the column will be stretched over the flown out part of the faster phase. The mass concentration will be reduced proportionally to the amount of stretching to keep the total mass concentration of each component correct. In a physical experiment, for example in co-current flow, both phases will join in a single flow after elution, resulting in the effect that the model simulates here.

The equation for the retention time is [Berthod and Hassoun 2006]:

$$t_R = \frac{V_R}{F} = \frac{V_M + KV_S}{F_M + KF_S} \quad (3.9)$$

This equation can be generalised:

$$t_R = \frac{V_L + KV_U}{F_L + KF_U} \quad (3.10)$$

where  $V_U$ ,  $V_L$  and  $F_U$ ,  $F_L$  are the volumes and flow rates of the upper and lower phase, respectively, and  $K$  is defined as before. For the CCD process, using cell model theory [Kostanian 2002], this is translated into:

$$N_R = (N-1) \frac{L_F + KU_F}{L_F X_{FL} + KU_F X_{FU}} \quad (3.11)$$

where  $N_R$  is the retention in cells,  $N$  is the number of system cells, and  $X_{FU}$  and  $X_{FL}$  are the normalised flow rates as defined previously. Although this theory has only been applied to conventional and co-current CCC flow values to date, it seems logical that the method should also apply to dual flow.

A chromatography peak can be characterised by its position, which is the retention time, and its width. For conventional CCC mode, the following relationship was established [Sutherland et al. 2003]:

$$W = 4\sqrt{t_R KX} \quad (3.12)$$

By studying the different flow modes using the built model it was found empirically that for conventional and co-current flow:

$$W = \frac{4\sqrt{t_R KX}}{X_{FL} + KXX_{FU}} \quad (3.13)$$

And for dual flow:

$$W = \frac{4\sqrt{t_R KX}}{L_F X_{FL} + KU_F X_{FU}} \quad (3.14)$$

In a standard planetary motion CCC column, the number of mixing/settling steps for a component is determined as:

$$N_R = \omega t_R \quad (3.15)$$

where  $\omega$  is the number of rotations per unit time [1/min] and  $t_R$  is the retention time [min] for the component. This makes  $N_R$  dimensionless.

Substituting  $t_R$  for eq. (3.10) gives:

$$N_R = \omega \frac{V_L + KV_U}{F_L + KF_U} \quad (3.16)$$

In the CCD model, the number of steps it takes the component to elute is equal to the number of mixing/settling steps (as in eq. (3.11)):

$$N_R = (N-1) \frac{L_F + KU_F}{L_F X_{FL} + KU_F X_{FU}} \quad (3.17)$$

where N is the number of system cells. Substituting  $N_R$  for eq. (3.16) gives:

$$(N-1) \frac{L_F + KU_F}{L_F X_{FL} + KU_F X_{FU}} = \omega \frac{V_C (L_F + KU_F)}{F_L + KF_U} \quad (3.18)$$

For large values of N, N-1 can be substituted for N. Isolating the column size in steps N gives:

$$N = \omega \frac{V_C (L_F X_{FL} + KU_F X_{FU})}{F_L + KF_U} \quad (3.19)$$

Since this is the equivalent number of steps for the mobile volume to emerge, the mobile phase is represented by K equals 1, resulting in:

$$N = \omega \frac{V_C (L_F X_{FL} + U_F X_{FU})}{F_L + F_U} \quad (3.20)$$

This is the number of mixing/settling steps that occur in a CCC column for a component with  $K=1$ , or standard number of mixing/settling steps.

## Filtering

Under certain conditions, for example in dual flow (Figure 3.3), component concentration can distribute non-homogeneously over the discrete cells. This is considered to be an effect caused by the nature of the model, and not an accurate representation of continuous chromatography techniques. To correct for this, filtering is applied to the sample concentrations when they are stored in preparation to be displayed on the screen. The filtering used here is Gaussian filtering, which is adjusted dynamically according to the model output. This is done by taking the sum of the absolute values of the differences between each cell component concentration, and subsequently dividing this sum by two times the peak height. In a smooth peak this value should be 1. To keep filtering minimal, it is adaptively applied when this value is larger than a certain threshold. This process is iterated, increasing the strength of the Gaussian filtering as needed to meet the threshold condition. Good results were obtained using a threshold value of 2.5% above the ideal (smooth peak) value.



## Efficiency

A basic efficiency was implemented by simply multiplying the ideal concentration after (re)distribution by an efficiency factor:

$$C = fC_{ideal} + (1 - f)C_0 \quad (3.21)$$

where  $C_{ideal}$  is the ideal concentration according to the (re)distribution,  $C_0$  is the concentration before (re)distribution and  $f$  is the efficiency factor.

## 3.2 Model based on probabilistic theory (ProMISE)

This section has been published in similar form [de Folter and Sutherland 2011].

The model labelled ProMISE stands for Probabilistic Model for Immiscible phase Separations and Extractions. This model was developed for the need of an iterative model that better describes continuous liquid-liquid chromatography processes, providing a better model by finding a more elemental solution.

Martin and Synge [1941] showed that the CCD process can be described using a binomial solution. This is also known as the probability mass function which describes the probability of getting exactly  $r$  successes in  $n$  trials:

$$\binom{n}{r} p^r (1 - p)^{n-r} \quad (3.22)$$

$p$  is the probability of each trial (being 0 or 1), and  $r = 0, 1, 2, \dots, n$ , where the binomial coefficient is defined as

$$\binom{n}{r} = \frac{n!}{r!(n-r)!} \quad (3.23)$$

The probability mass function is based on Bayes' theorem, which shows the relation between two conditional probabilities which are the reverse of each other [Bayes and Price 1763]. Using a more elemental approach, a new model can be developed as follows.

Considering a molecule of a particular compound in a two phase system, assuming it is located somewhere in either phase, its behaviour can be described by the probability of it moving to the other phase. This probability is then simply as described in equations (3.1a,b).

Furthermore an efficiency factor is introduced here by simply multiplying the resulting term by the efficiency factor for the final probability value.

This behaviour is followed regardless of other molecules of the same compound, e.g. (local) compound concentration in the phases. The model consists of simulating many of these representative units, following the probabilistic rules described here, where each unit represents a very small amount of sample compound. Each unit is then moved according to the movement of the phase it is located in.

Because the model is based on compound units, a density function with an adaptive Gaussian filter is used to convert the separate unit values into a chromatogram. The nature of this model allows its internal values to be volume or time.

## Output

The model output consists of a number of units, each having a position value. The main peak values can be directly obtained from the model output. The peak position is equal to the mathematical average of the weighted units:

$$\mu = \frac{1}{m_{tot}} \sum_{i=0}^n m_i x_i \quad (3.24)$$

where  $x_i$  is the position value of each unit index  $i$ , out of  $n$  total units.  $m_i$  represents the (relative) weight of each unit, and  $m_{tot}$  the total weight of all units. Note that the peak average does not necessarily coincide with the peak maximum (in case of asymmetrical peaks).

The peak width is subsequently obtained by taking the standard deviation from the units:

$$\sigma = \sqrt{\frac{1}{m_{tot}} \sum_{i=0}^n m_i (x_i - \mu)^2} \quad (3.25)$$

Using this theory, the compounds naturally distribute according to their  $K$  value.

The retention times can therefore be predicted using standard theory. It was found the peak width for (normal flow mode) can be calculated by adapting eq. (3.12) to take the rotational speed into account:

$$\sigma = \sqrt{t_R \frac{KX}{\omega}} \quad (3.26)$$

where  $\omega$  is the rotational speed giving the number of mixing/settling steps per unit time, and  $t_R$  the retention time. The peak width is equal to  $4\sigma$ .

The mixing/settling efficiency is taken into account in the model by multiplying the probabilities with the efficiency factor  $f$ . Accordingly, the peak width can be calculated by modifying equation (3.26):

$$\sigma = \sqrt{t_R \frac{KX}{\omega f'}} \quad (3.27)$$

where  $f'$  represents the efficiency effect.

However, in reality this is a simplified equation for normal flow mode. In the same way, a more general equation incorporating different flow modes can be expanded (eq. (3.13)):

$$\sigma = \frac{\sqrt{t_R \frac{KX}{\omega f'}}}{X_{FL} + KX_{FU}} \quad (3.28)$$

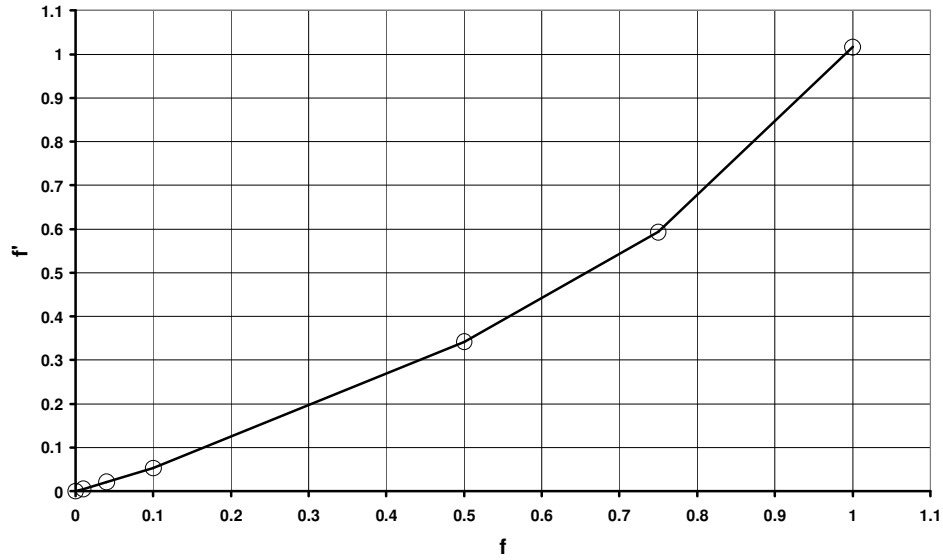
where  $X_{FU}$  and  $X_{FL}$  are the normalised upper and lower phase flow rates as defined in eq. (3.7a,b).

This set of equations for peak width appears to work well in most cases, though a general equation that perfectly satisfies all flow modes correctly has not yet been found.

### Efficiency

The efficiency of the mixing / settling in the model is determined by an efficiency factor  $f$ . However, it was found that this efficiency factor was not equal to the efficiency as in the equations for the peak shape (eq. (3.27)). The relationship between the model mixing / settling efficiency and resulting efficiency effect was obtained by using equation (3.27) to determine  $f'$  (Figure 3.8A).

A



B

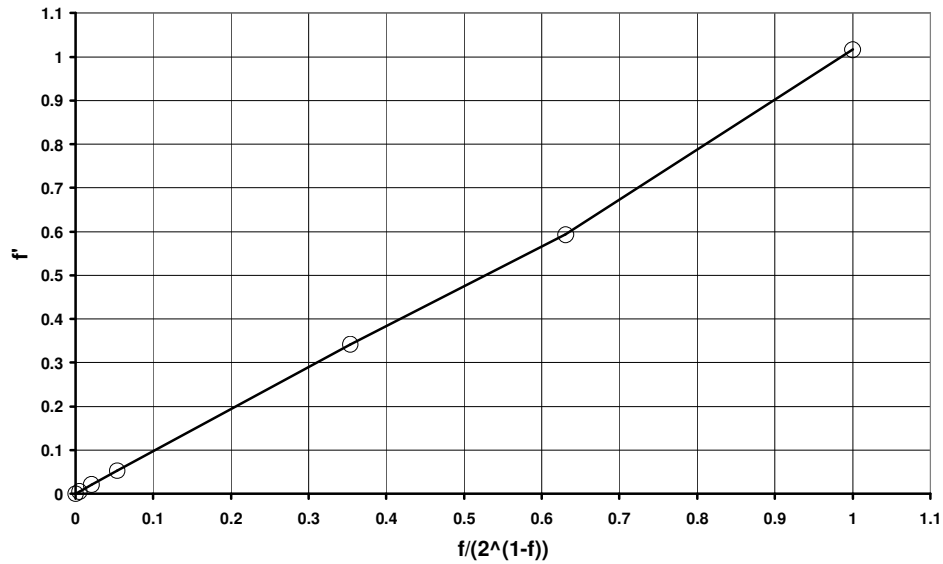


Figure 3.8 A: Comparing the model mixing / settling efficiency ( $f$ ) and resulting efficiency effect ( $f'$ ). B: The relationship between the  $f$  and  $f'$  found using curve-fitting:  $R^2 = 0.998$  and standard deviation = 0.0174.

Using curve fitting techniques, the relationship between the initial efficiency factor  $f$  and the resulting efficiency effect  $f'$  was empirically found to approximate (Figure 3.8B) as follows:

$$f' = \frac{f}{2^{1-f}} \quad (3.29)$$

This efficiency factor actually represents a composite factor, not only for the mixing / settling efficiency, but for the CCC system in general.

### 3.3 Model based on transport theory

Transport theory, commonly known in heat and mass transfer theory, has been used extensively in solid liquid chromatography, and include molecular diffusion or dispersion.

From general transport theory [Patankar 1980] [Cussler 2007] and its application in liquid-liquid chromatography [van Buel 1997] [Zhao 2009], it can be concluded that convection flow is the main (longitudinal or axial) propagation mechanism in liquid-liquid chromatography, and diffusion does not significantly contribute to this. Diffusion is therefore neglected in this model.

Based on Van Buel [1997] the partial differential equations for liquid-liquid chromatography, for mobile and stationary phases are:

$$\frac{\partial C_M}{\partial t} = -v \frac{\partial C_M}{\partial x} - \frac{k_0 a}{1 - S_F} (K C_M - C_S) \quad (3.30)$$

$$\frac{\partial C_S}{\partial t} = \frac{k_0 a}{S_F} (K C_M - C_S) \quad (3.31)$$

Where  $C_M$  and  $C_S$  are the concentrations of a component in the mobile and stationary phase,  $t$  represents time,  $x$  represents distance,  $v$  is the linear velocity of the mobile phase flow,  $K$  is the  $K$  value of the component,  $S_F$  is the stationary phase retention,  $a$  is *the specific interfacial area* defined as *the total interfacial area* divided by the total column volume, and  $k_0$  is *the overall mass-transfer coefficient* which is defined as:

$$\frac{1}{k_0} = \frac{K}{k_M} + \frac{1}{k_S} \quad (3.32)$$

Using the following substitutions:

$$\tau = \frac{t}{T_M} \quad (3.33)$$

where  $T_M$  is the time it takes for the mobile phase volume to flow through the column; and:

$$z = \frac{x}{L} \quad (3.34)$$

where  $L$  is the total length of the column; applied to equations (3.30) and (3.31) the following partially dimensionless forms are obtained:

$$\frac{\partial C_M}{\partial \tau} = -\frac{\partial C_M}{\partial z} - T_M \frac{k_0 a}{1 - S_F} (K C_M - C_S) \quad (3.35)$$

$$\frac{\partial C_S}{\partial \tau} = T_M \frac{k_0 a}{S_F} (KC_M - C_S) \quad (3.36)$$

The original equations were based on a single phase being mobile. The model is made more generically here by substituting mobile and stationary phase with lower and upper phase, respectively. Generalising for variable phase movement, where K is defined as upper phase over lower phase concentration, these new equations are obtained:

$$\frac{\partial C_L}{\partial \tau} = -\frac{T_M}{T_{ML}} \frac{\partial C_L}{\partial z} - \frac{T_M k_0 a}{L_F} (KC_L - C_U) \quad (3.37)$$

$$\frac{\partial C_U}{\partial \tau} = -\frac{T_M}{T_{MU}} \frac{\partial C_U}{\partial z} + \frac{T_M k_0 a}{U_F} (KC_L - C_U) \quad (3.38)$$

where  $T_M$  is the time it takes for the mobile phase volume to flow through the column;  $T_{MU}$  for the upper phase and  $T_{ML}$  for the lower phase. Note that  $T_M$  cannot be replaced by the specific mobile phase elution time, as this is a conversion constant defining the size of  $\partial \tau$  (or rather it's finite version  $\Delta \tau$ ), which needs to be the same for both phases. In general the following can be used:

$$T_M = \text{MAX}\{T_{MU}, T_{ML}\} \quad (3.39)$$

In the partial differential equations, the first component after the equal signs (for the lower phase):

$$-\frac{T_M}{T_{ML}} \frac{\partial C_L}{\partial z}$$

represents the (mobile) phase movement, and the second component (for the lower phase):

$$-\frac{T_M k_0 a}{L_F} (KC_L - C_U)$$

represents the transfer between the phases. The model consists of the iterative evaluation of these partial differential equations, using small (finite) differences in time and distance.

The model needs to take a number of conditions into account to ensure stability. The first is known in Computational Fluid Dynamics (CFD) simulation as the Courant–Friedrichs–Lewy (CFL) condition, which defines the relationship between the step size of the iterations in time and in distance [Courant et al. 1976]:

$$\frac{\Delta \tau}{\Delta z} \leq C \quad (3.40)$$

where C is the dimensionless Courant constant.

It was empirically found the model shows good stability with  $C = 0.1$

This first condition is derived from the first component in the partial differential equation (the phase movement component). Analogue to the CFL condition, a second condition can be derived from the second component in the partial differential equation (the transfer between the phases):

$$\frac{T_M k_0 a K}{U_F} \Delta \tau \leq C_2 \quad (3.41)$$

$$\frac{T_M k_0 a K}{L_F} \Delta \tau \leq C_2 \quad (3.42)$$

where  $T_M$  is the mobile elution time. The model is stable for  $C_2 = 1$ .

These conditions are simply expressing that the concentration increments (the first and second components in the partial differential equations) must be small enough; smaller than the total integral concentration value of the system.

The initial model implemented, iterated through the mass transfer equations through the entire system, including the eluted component. To more accurately model the eluted component, a modified mass transport model was implemented. Here the mass transfer equations are only applied to the component 'inside' the chromatography column, the same way the CCD and probabilistic models operate.

### 3.4 Simplified model for interactivity

To be able to implement dynamic model previews as proposed in section 2.10, and described later in chapter 5 in detail, there was a need for a simplified model. To enable real-time feedback, the requirement is that it takes less than 100 ms to complete on a currently readily available computer system.

As reducing the complexity of the model would directly affect a key model parameter and would therefore not result in a representative model, a different approach had to be used. Instead, the predictive equations previously mentioned were chosen to represent a simplified model.

For 'eluted' components equations (3.10) and (3.27) are used:

$$t_R = \frac{V_L + KV_U}{F_L + KF_U}$$

$$\sigma = \sqrt{t_R \frac{KX}{\omega f'}}$$

For components not eluted out of the column, it was found that the position can be calculated by inverting equation (3.10):

$$V_{Pos} = t_x \frac{F_L + KF_U}{L_F + KU_F} \quad (3.43)$$

where  $t_x$  is the run time. The corresponding peak width (or sigma) can be calculated based on [Berthod et al. 2007]:

$$\sigma_{Col} = \sigma \frac{V_C}{V_R} \sqrt{\frac{V_{Pos}}{V_C}} \quad (3.44)$$

where  $\sigma$  represents the eluted peak width.

It is proven that the normal distribution is very similar to the chromatography peak inside the chromatography column [Nichols 1950] [Williamson and Craig 1949], as well as eluted out [Kostanian 2002]. The normal distribution graph is well known as:

$$Y = \frac{1}{\sigma\sqrt{2\pi}} e^{-\frac{(x-\mu)^2}{2\sigma^2}} \quad (3.45)$$

where  $\mu$  is substituted for the peak retention or position. The chromatogram is then obtained by simply plotting this function as  $Y = f(x)$ .

This simplified model does not iterate through component movement and redistribution. A comparison between the complexity of the original model and simplified model using Landau notation (also known as 'Big O notation') follows here.

CCD model complexity:  $O(CNT)$

Where C is the number of input components in a mixture (in the order of  $10^{0...1}$ ), N is the number of chromatography system cells (in the order of  $10^{2...3}$ ), and T is the total number of iterative steps to separate the components out of the chromatography system (in the order of  $10^{2...4}$ ). The total estimated complexity for the CCD model is therefore in the order of  $10^{4...8}$ .

Probabilistic model complexity:  $O(CUT)$

Where C is the same as before, U is the number of probabilistic units (in the order of  $10^{3...4}$ ) and T is the total number of iterative steps to separate the components out of the chromatography system (in the order of  $10^{4...6}$ ). The total estimated complexity for the probabilistic model is in the order of  $10^{7...11}$ . However due to the nature of the probabilistic model, there is a reduction of model computations typically in the order of  $10^{1...2}$ , resulting in a final estimated complexity in the order of  $10^{6...9}$ .



Transport model complexity:  $O(CT^2)$

Modified transport model complexity:  $O(CNT)$

Where C is the same as before, N is the number of chromatography system cells (in the order of  $10^{2...3}$ ) and T is the total number of iterative steps to separate the components out of the chromatography system (in the order of  $10^{3...5}$ ). The total estimated complexity of the transport model is in the order of  $10^{6...11}$ , and the modified transport model  $10^{5...9}$ . It needs to be noted that the calculations performed for this model are significantly more complex than the CCD and probabilistic models, further impacting computational performance.

Simplified model complexity:  $O(C)$

Where C is the same as before, resulting in a total estimated complexity in the order of  $10^{0...1}$ . As the simplified model removes most of the iterations, it is therefore not only much faster, it also removes most of the variability of the calculation times the full models have. This enables real-time interaction, as it typically only takes 1 to 10 ms (<sup>3</sup>) to complete.

For the purpose of completeness, employment of random sampling to enable the technique as described by the Influence Explorer (section 2.8.3) could be considered. This would require sampling over at least 9 independent input parameters considering a single sample component, using a single model in a single sample flow mode. Using very rough (exponentially scaled) sampling, this would require an order of  $10^9$  full simulations to be performed. Even using an extremely optimistic average model run time of 1 second, it is clear that this method is not feasible.

It is important to note though, that the simplified model is an approximation, and cannot substitute the full models. Further limitations of the simplified model are that it does not take sample injection details into account, nor does it show concentration distribution over the phases.

### 3.5 From model to simulation

In the previous sections of this chapter, a number of models have been described, each consisting of a number of equations. However, to make the models applicable, the theory has to be converted to a readily usable form. To appreciate how modelled components progress through the 'column' in time, instead of a final solution, the model is implemented by iterating more fundamental equations as previously described. Clearly these equations cannot be evaluated manually due to their iterative nature, and therefore a computer implementation is required, resulting in a computer model that closely simulates the chromatography process.

---

<sup>3</sup> On a PC with a 3GHz Intel Core 2 Duo CPU

During this simulation, the component concentrations are stored in dynamic arrays, allowing the number of storage elements to increase as the simulated components progress through and beyond the 'column'. For the CCD and Transport model, the chromatogram is simply obtained by plotting the concentration of these elements. However, the probabilistic model consists of a number of representative units and their position. Here the chromatogram is obtained histographically, determining the density of the representative units over a fixed number of discrete intervals.

When implementing these models, the model's 'native' units have to be taken into account. The units of the CCD model are the number of steps (representing volume), the probabilistic model uses volumetric units, and the transport model's units are the number of steps (representing time). The model's variables have to be converted from their native units to units such as time or volume.

### **3.6 Implementing advanced operations**

The different models are implemented in a very flexible way, allowing advanced operations to be integrated in each of them.

#### **Determining peak results**

As important as the graphical results, are the numerical results such as the peak position and peak width, if not even more so. Together these are used to obtain another key numerical result: the resolution between peaks. As described in section 2.2, there are various methods to obtain the peak position and peak width. The peak position is obtained in two ways: the position at the maximum peak value, and the (statistical) average value of the peak area. The computer model uses both these methods, displaying these separately. Note that contrary to the other models, for the probabilistic model the statistical average value is the value first obtained from the original model output, and the peak maximum obtained from the processed histographical results.

The peak width is another key model output. Again different methods are used to obtain this. For the CCD and the transfer model. The first one is the width at fixed peak height (0.6065 times the peak height), and the second is using the tangents to obtain the width at the base of the peak. The two methods are combined in a single result, by taking their average, with the exception that the results for both methods are expected to be similar values (within 10% of each other). If this is not the case, only the smallest of the results is used. For the probabilistic model, only the statistical deviation ( $\sigma$ ) is calculated. The peak width is then obtained using the definition that the width at the base of the peak is equal to 4 times the variance ( $\sigma$ ).

## **Sample injection**

In most current models, sample components are treated as injected instantly, as if they were injected in an infinitely small amount of time. This is also the case for traditional models informing of a set of equations representing an approximation of the final result. In practice, though sample mixtures are injected over a period of time, in some cases even a long period of time relative to the elution time. The way this feature is implemented is by calculating the amount of component that is introduced into the column for each iteration. This amount is introduced until the total mass for the component has been injected into the column.

Multiple components are implemented by modelling each component separately, holding a computer buffer for the intermediate states of each of the components.

## **Dead volume**

Chromatography columns in general have tubing between a sample injection point, the actual column, and the detector / fraction collector. Although this tubing is normally very small compared to the column, and can be compensated for experimentally, it is also implemented into the models. In the different models the column length is extended by the dead volume. This consists out of the dead volume after the sample loop, at the intake of the column, the dead volume at the outlet of the column between the column and the detector, and the dead volume in case the total column comprises the physical columns or coils where the sample is injected in between them. In the model, dead volume areas are considered where sample component is not distributing over the phases, simply maintaining it in its current phase.

## **Elusion Extrusion**

Elusion extrusion is a relatively new technique [Berthod et al. 2007] where the mobile phase flow is discontinued at some point, before all sample components have eluted, and then the entire column contents is directly pumped out. This is implemented into the different models by iterating the model up to a certain point, and then displacing the components inside the column by the column volume (or the model column length equivalent).

## **Intermittent flow mode**

Intermittent mode CCC is implemented into the different models as follows. First the model is run for a certain amount of iterations in isocratic mode where the mobile phase is the intermittent mode start phase. Next the model is run for a certain amount of iterations where the alternate phase is mobile. The numbers of iterations are calculated from the amount of time (or volume) each intermittent switch is to run for.

### Partial transfer

Partial transfer mode is implemented into the CCD model only. This is to attempt to model a technique such as CPC in a more accurate way with the CCD model. Instead of transferring the entire cell content each iteration, only a part of the cell content is transferred. The partial transfer parameter is a factor, representing how much of the cell content is transferred in each model iteration, where a value of 1 means the entire cell content is transferred.

## 3.7 Computer implementation

The computer model was realised in the software development package Microsoft Visual Studio. This package was chosen to be able to develop a completely customised interface, including customised user controls. The programming language C++ .NET was chosen as it offers a high level of control, flexibility and efficient management of computer resource, while at the same time providing a library of tools that can be deployed to decrease development efforts. Section 3.7.3 will concentrate on the programming environment. As the software development would likely be a continuous work in progress, choosing the right architecture of the software with emphasis on maintainability was very important. For this reason the software was developed using Object Oriented Design and Design Patterns [Gamma et al. 1994]. The design patterns used were the *Abstract Factory* pattern, *Composition*, the *Observer* pattern, *Chain-of-responsibility* and the *Model-View-Controller* combination (Figure 3.9). In this triangularly linked system, the View represents the visual elements of the software, and the user interface. The user interface connects to the Controller where actions are decided for each interaction. This in turn drives the Model, which in this case is the chromatography model. The View is updated with the model results when the Model notifies the View that it has completed. An illustration of the Model-View-Controller flow is described in the next section. Object types (also called Classes) were defined for different elements such as view elements like windows and controls for the user interface, the chromatography model itself, and the sub elements the different chromatography models are composed of. The entire C++ project comprised a total of 56 Classes.



The programming language mainly used for the model is C++, and for the arrays a dynamic storage type is used called a vector. Variations of these storage types were used for the different chromatography models as most appropriate for each model. See section 3.7.2 for more detail on how these storage types are processed. Additionally, the internal model and output parameters, as displayed (Figure 3.9) were also stored for different instants, during the chromatography model process, to be displayed in the time mode chromatogram. The .NET version of the programming language was subsequently used to reduce development efforts. The .NET namespaces provide an extensive set of tools and controls, simplifying the implementation especially of the user interface and graphical views.

### 3.7.1 Model-View-Controller flow

The software application was designed using the *Model-View-Controller* principle. To illustrate the control flow using this design, a simplified diagram is shown here (Figure 3.10). The *View* is basically the user interface. Subsequently the *Controller* controls the user interface behaviour. Finally the *Model* is the 'business logic', managing the different chromatogram models. In this illustration the entry point is an interaction of the user interface. In this case the view is changed from the model input parameter screen to the model results screen. The user interface interaction is passed to the *Controller*, where the appropriate action is decided. The *Model* is called, which generates an *instance* of the CCD model. Next a new processor thread is created to execute the CCD model and subsequent processing. This new thread then runs the model and processes the model output, as described in more detail in the next section. Finally the *View* is activated, showing the chromatogram on the screen. The creation of a new processor thread enables multiple *instances* of the CCD (or other) model to be executed at the same time.

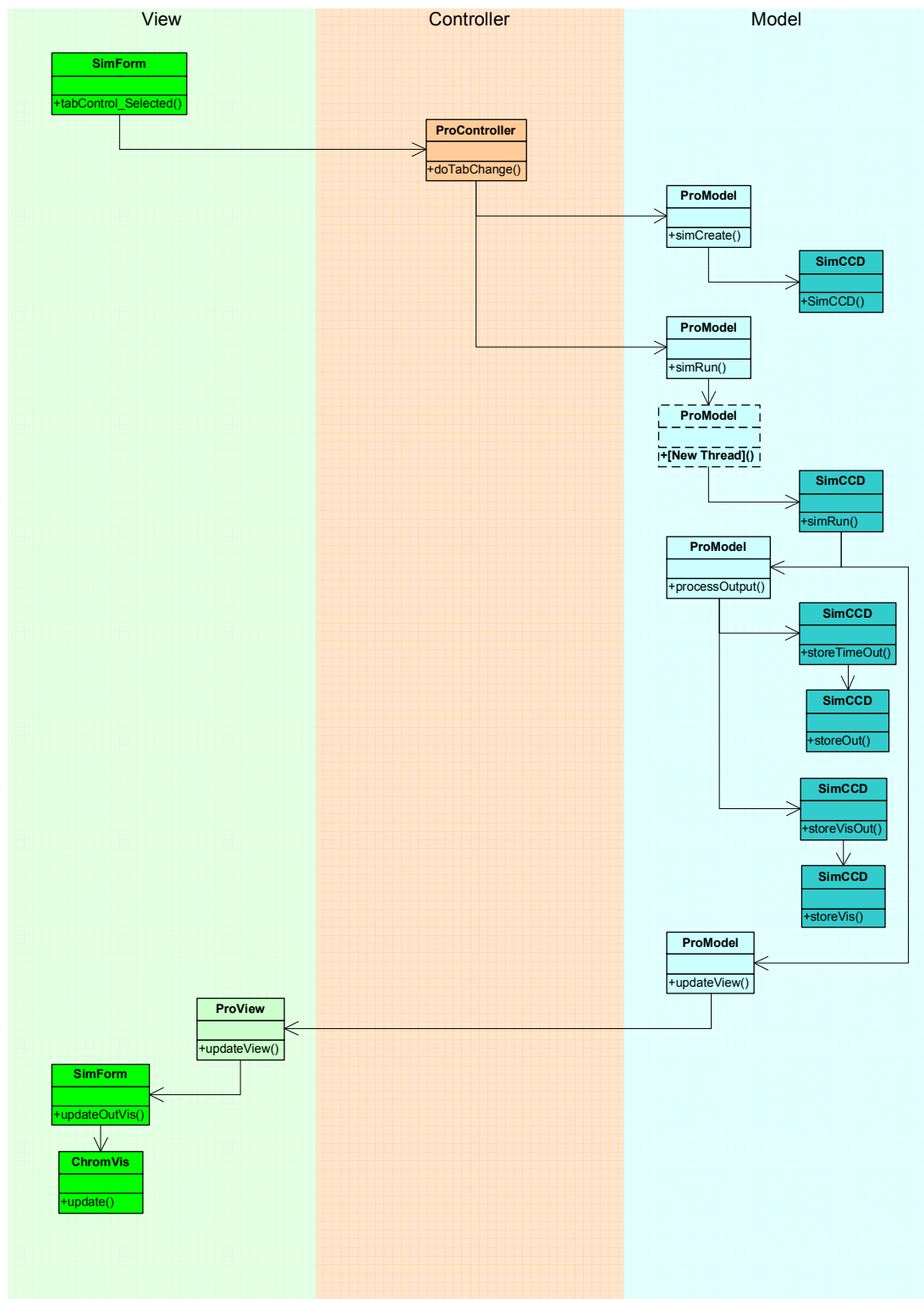


Figure 3.10 Model-View-Controller flow diagram (simplified). Functions are displayed chronologically in vertical direction.

### 3.7.2 Data flow

After the simulation model completes, its internal raw data is the main model output. The data processing, from model to view - optimising for efficiency - is based on the reference model described in section 2.9 (Figure 3.11). First the internal raw data is converted to a generalised format. This format is highly compatible with a basic spreadsheet format, and at this point can be saved to a file for processing in a spreadsheet program like Microsoft Excel. Next, the data is normalised into a vector format and is bound to a visualisation component. This enables the component to render to screen very efficiently, rapidly handling any update (such as resizing and zooming in/out).

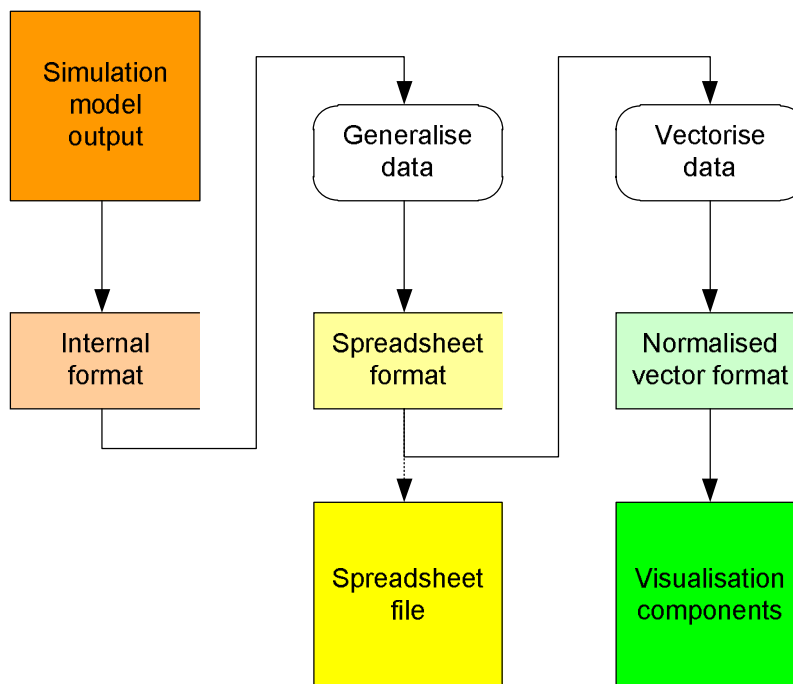


Figure 3.11 Data flow from model output to screen rendering format

### 3.7.3 Coding

The computer model was realised (or coded) as follows. From the initial version to the final version incorporating all the models, the C++ project was coded by the researcher. A summary report of the code can be seen in Figure 3.12, showing the total number of lines of code.



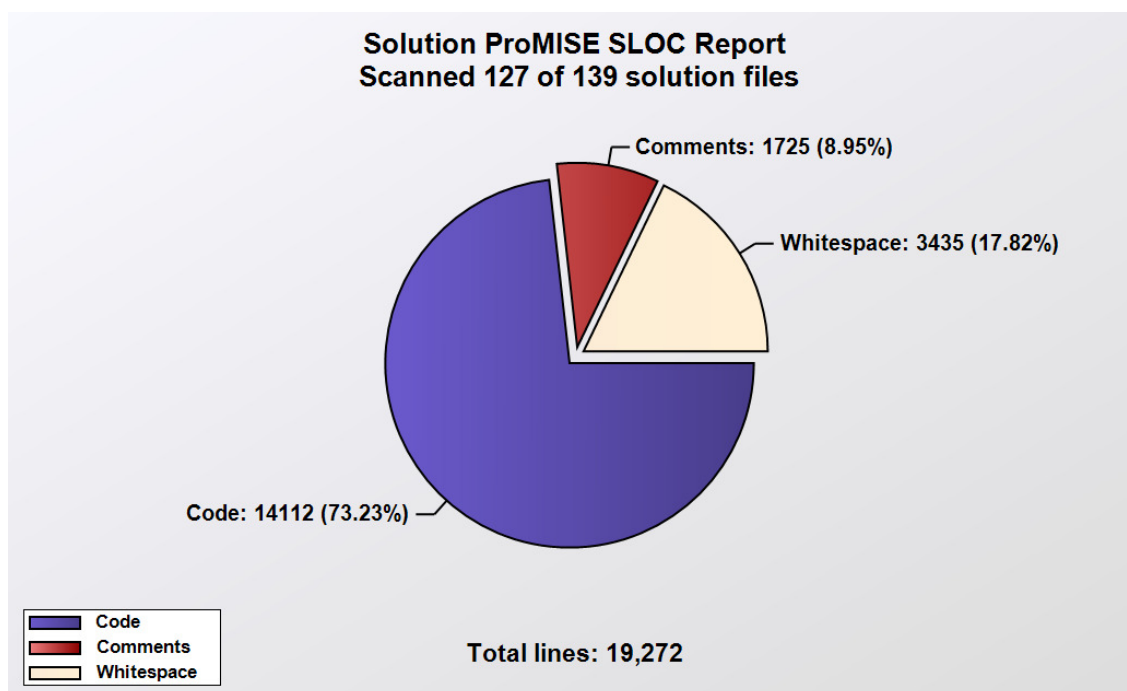


Figure 3.12 Summary report on Source Lines Of Code (SLOC)

The programming environment used for the coding was Microsoft Visual Studio. The project type was Common Language Runtime (CLR) / Safe Microsoft Intermediate Language (MSIL) / Windows Forms Application, including .NET framework support. The programming language used was C++. Two components were realised as separate Windows Forms Controls as part of the C++ project. The first of these was the main Chromatogram Visualisation component, used to visualise the model results in different views as described in sections section 5.4.1 and 5.4.2. The second component was the Jog-wheel control which will be described in detail in section 5.4.5. The entire C++ project comprised a total of 56 Classes. To print out the entire source code would require about 300 pages (using small print).

The main model loop is similarly implemented for all models. As illustration this is presented as a diagram (Figure 3.13) and shown as C++ code (Table 3.1) for comparison. As can be seen here, transfer and distribute steps are iterated until the completion conditions are met, and the model is 'done'. After this the model results are processed and displayed on the screen (using the Chromatogram Visualisation component).

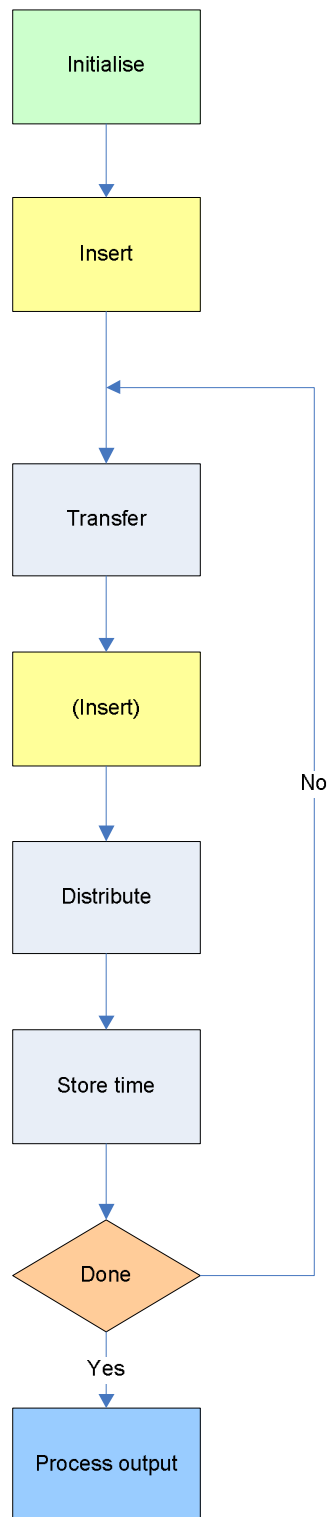


Figure 3.13 Simplified diagram of main model loop

*Table 3.1 C++ code of model loop function*

```
void SimCCD::simRun(ViewParams^ viewparams) {
    int estit;
    float storestep;
    float storeit = 0;

    it = 0;

    model->updateProgress(0);
    model->stats.start();
    estit = simInit();
    storestep = (float)estit / optionparams->timeStores;
    simCreate();
    simInsert(); // Initial sample insert
    storeTime();
    simDist(); // Initial distribute
    storeTime();
    it++;
    storeit++;
    while (!isSimDone()) {
        simMove(); // Transfer
        simInsert(); // (Insert)
        simDist(); // Distribute
        if (storeit >= storestep) {
            storeTime(); // Store time
            storeit -= storestep;
        }
        model->updateProgress((float)it/estit);
        it++;
        storeit++;
    }
    storeTime();
    if (inparams->eeMode != EEMode::None) {
        simEE();
        storeTime();
    }
    model->stats.storeSimtime();
    model->clearProgress();

    model->processOutput(viewparams); // Process Output
    model->updateView();
}
```

## 3.8 Modelling experimental data

This section explains how experimental data is modelled using the different models (sections 3.1, 3.2, and 3.3). The common input parameters for the model are the column volume, the phase retention (or distribution), the phase flow rate(s), and the K values of the modelled components. Each model has specific input parameters which will be described in the following sub sections. To subsequently compare the model results to experimental results, the peak positions and peak widths of the experimental data are used.

### 3.8.1 Modelling using CCD model

The main input parameter specific to the CCD model is the number of CCD steps or cells. This is the number of discrete cells representing the column. Additional CCD model parameters are the mixing efficiency and partial transfer. After the common model parameters have been set, normally the mixing efficiency is left to the default value (100% mixing efficiency), and only the number of CCD steps is adjusted, such that the model peak width matches the experimental value. This value is by default set to 100 steps which seems a reasonable starting point. The obtained value for the number of CCD steps can then be used for other experiments using the same experimental conditions. However, in other more discrete modelling scenarios, like CPC for example, the number of model cells can be set to the number of CPC cells. The mixing efficiency is then subsequently adjusted so peak width matches experimental values.

### 3.8.2 Modelling using probabilistic model

The probabilistic model does not have a number of discrete cells like the CCD model, but does have a mixing efficiency as parameter specific for this model. Additionally it uses the mixing speed, which is normally set to the rotational velocity for a CCC scenario. There are two other, less consequential model parameters. The number of probabilistic units, representing each sample component, is by default set to 10000. The higher this value is, the less noisy and more reliable the resulting peaks will be. A value of 10000 is recommended for reliable results with minimal noise effect. Using smaller values does result in faster computation, although a value lower than 1000 is not recommended. Finally there is the number of histographical bins, by default set to 200. This is the number of bins representative to the column volume only, and will be increased dependent to the total eluted volume. Then the mixing efficiency is adjusted so the model peak width matches the experimental value. This obtained mixing efficiency value can subsequently be used for the same experimental conditions.

### 3.8.3 Modelling using transport model

The transport model has the most model specific parameters. There is the number of cells representing the column, somewhat similar to the CCD model. Next, the overall volumetric mass transfer coefficient ( $k_0a$ ) represents how easy the component is transported from a higher concentration area to a lower concentration area. Although this model should be independent to the number of discrete steps, the step size should be very small. Of course in practice this step size cannot be made infinitely small, which would result in an infinite number of discrete steps. The default value for the number of steps is 100, but good results are obtained with a higher value of 1000 steps. In practice this value is limited mainly by computing power, and higher values would possibly give even more accurate results. The overall volumetric mass transfer coefficient is then adjusted so the model peak width matches the experimental value.

## 4 Modelling results and verification

This chapter compares the results of the developed models to experimental data. The sections are separated by elution (section 4.1), sample injection (4.2) and ends with an efficiency study (section 4.3).

### 4.1 Elution

The experimental setup of the elution data the model was compared to, and subsequent suitable input parameters that were used for the model(s) are described here. These comparisons include the peak position (retention), the peak width, and the shape of the peaks. This is done for different liquid-liquid separation methods and modes of operation.

#### 4.1.1 CCD

##### Experimental setup

The set up was a specially produced CCD apparatus containing 220 equilibration cells, realised by glass tubes. The system was made by equilibrating an equal volume of 5% hydrochloric acid with n-butyl alcohol. The mixture chosen contained 300 mg. of each amino acid: Glycine, Alanine,  $\alpha$ -amino butyric, Valine, Methionine, Tyrosine, Leucine, Isoleucine, Phenylalanine, Tryptophane. The K values of these components are 0.095, 0.135, 0.207, 0.342, 0.397, 0.563, 0.740, 0.825, 0.99, and 2, respectively. At the start the sample was dissolved in a mixture of 80 ml of each phase, sufficient to fill the first 8 cells. After each transfer stage, 15 mixing strokes were applied, and 30 seconds were required for the phases to separate. The apparatus was permitted to operate until 780 transfers had been applied, approximately 20 hours [Craig 1950; Craig et al. 1951]. The experimental results are displayed in Figure 4.1.

##### Model setup

The CCD model was set up to match the CCD experimental set up, with 220 CCD cells. The model results are compared to the experimental (Table 4.1). Here the experimental peak position (or retention) and width were graphically extrapolated from publication [Craig 1950]. The chromatographic model results are shown in Figure 4.2.

Table 4.1 CCD experimental and model results (first 4 peaks retained in columns shown in red) (with error)

K	Experimental		Model			
	Retention [steps]	Width [steps]	Retention (max) [steps]	Retention Error [%]	Width [steps]	Width Error [%]
0.095	70.1	25.4	67	-4%	31.46	24%
0.135	96.4	34.8	92	-5%	36.18	4%
0.207	137.0	41.6	133	-3%	42.12	1%
0.342	198.9	48.6	198	0%	47.42	-2%
0.397	758.4	182.6	771	2%	176.25	-3%
0.563	599.8	142.0	608	1%	131.47	-7%
0.740	509.2	113.3	515	1%	105.54	-7%
0.825	479.1	104.7	485	1%	96.94	-7%
0.99	437.7	81.7	441	1%	84.36	3%
2	325.5	58.0	329	1%	51.27	-12%

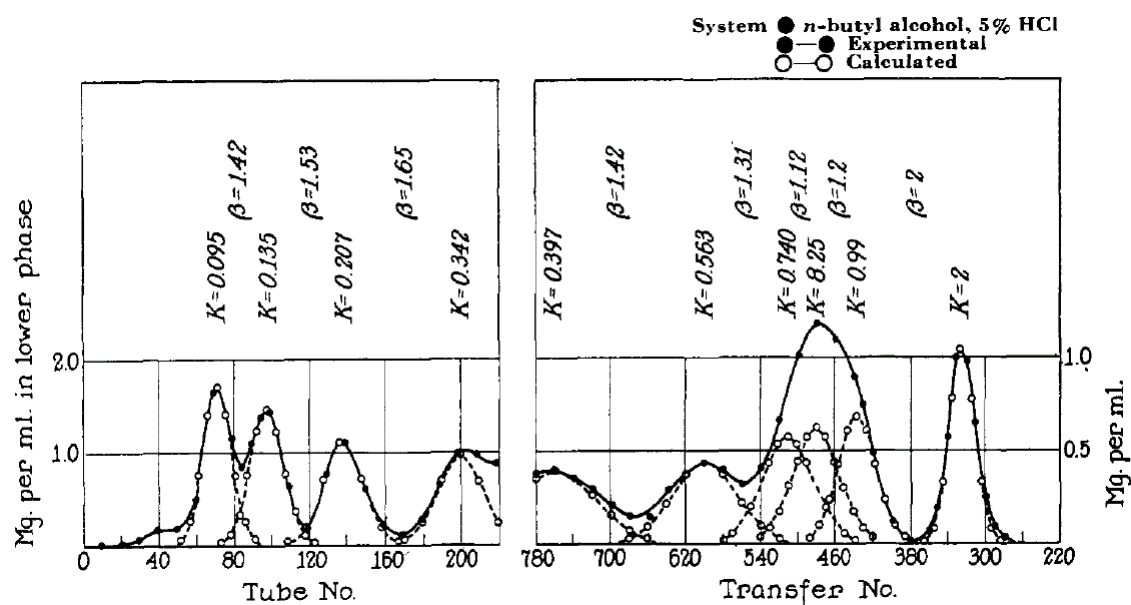


Figure 4.1 Experimental and theoretical CCD curves [Craig 1950]

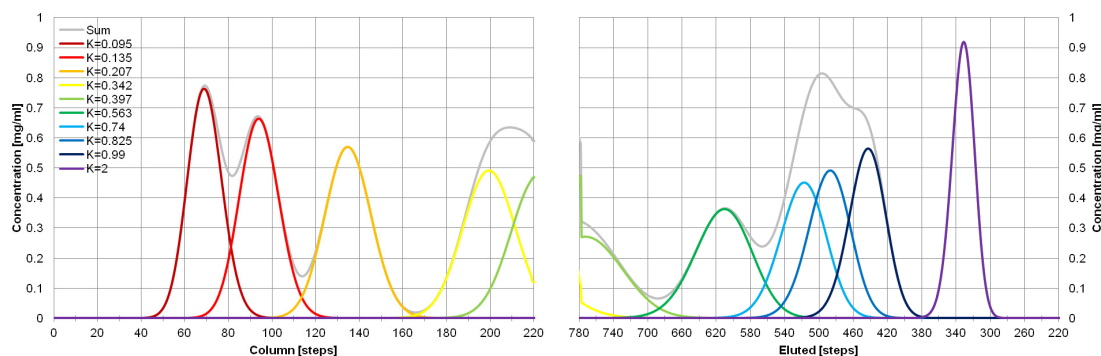


Figure 4.2 Showing separate peaks with composite sum superimposed

## 4.1.2 CPC

### *CPC case 1*

#### **Experimental setup**

The device used was an Armen CPC apparatus. The system was made up out of 1008 cells (42 discs of 24 cells each), with a total volume of 500 ml of which 71 ml was the total volume of the ducts between cells. The solvent system used was a PEG 1000 11/11% ammonium sulphate system. The system had a stationary phase retention of 53% using a mobile phase flow rate of 5 ml/min. A sample of 1 mg/ml of Immunoglobulin G ( $K = 0.43$ ) was used [Fernando 2011].

#### **Model setup**

The CCD model was chosen as the CPC device has discrete chambers. The number of system cells was set to 1008, and the total system volume was set to 500ml. A dead volume of 71 ml was used to simulate the connecting ducts in the experimental system. Finally, a mixing / settling efficiency of 0.4 (40%) obtained best results (Table 4.2).

*Table 4.2 CPC experimental and model values (with error) - case 1*

<b>Experimental</b>		<b>CCD Model</b>			
<b><math>t_R</math> [min]</b>	<b>Width [min]</b>	<b><math>t_R</math> [min]</b>	<b>Error <math>t_R</math> [%]</b>	<b>Width [min]</b>	<b>Error width [%]</b>
64.05	8.93	66.3	3.5%	8.6	-3.7%

### *CPC case 2*

#### **Experimental setup**

A study on scaling up from a 500 ml laboratory scale centrifugal partition chromatography (CPC) column to a 6.25 litre pilot scale column was performed by Sutherland et al. [2008]. In the latter, the used model was the same CCD model that is presented in the current research. A similar model comparison is performed here.

The laboratory scale instrument is equipped with two 500 ml rotors each containing 42 stacked discs with a total of 1008 cells (chambers) or 24 per disc. Each chamber has a volume of 0.424 ml (total active volume 429 ml). The volume of the interconnecting passages between the chambers is 71 ml. This is the same instrument used in CPC case 1 described earlier in this section. The pilot scale instrument is equipped with two 6.25 litre rotors each containing 24 stacked discs with a total of 528 cells (chambers) or 22 per disc. Each chamber has a volume of 8.93 ml (total active volume 4.715 litre). The volume of the interconnecting passages between the chambers is 1.535 litre.

For the experiments a 12.5% (w/w) PEG-1000:12.5% (w/w)  $K_2HPO_4$  ATPS solvent system was used. The sample components here were Myoglobin ( $K = 0.59$ ) and Lysozyme ( $K = 1.91$ ). The laboratory scale instrument used a sample loading volume of 40 ml (10% of the total column volume), had a mobile phase flow rate of 10 ml/min and had a rotor speed of 2000 rpm. The pilot scale instrument used a sample loading volume of 500 ml (10% of the total column volume), had a mobile phase flow rate of 125 ml/min and had a rotor speed of 1293 rpm.

### Model setup

The CCD model was used and compared against the available experimental results. Contrary to the model configuration reported in [Sutherland et al. 2008], the model was configured matching the number of model cells to the number of chambers of each instrument. The model mixing / settling efficiency was then adjusted to match the experimental data. The experiment was also modelled more accurately compared to the previous publication here, using a dead volume (made up by the connecting ducts between the CPC chambers) equal to each instrument, and using an accurate sample injection set up similarly to the sample injection in the actual experiments. A comparison of the model results to experimental data for both CPC instruments is presented in Table 4.3. The average errors (labelled |AVG|) were calculated by taking the average of the absolute values of the individual errors.

Table 4.3 CPC experimental and model values (with error) - case 2

		Experimental		CCD model				
Component	K	t <sub>R</sub> [min]	Width [min]	S <sub>F</sub> [%]	t <sub>R</sub> [min]	Error t <sub>R</sub> [%]	Width [min]	Error Width [%]
V = 500 ml, F = 10 ml/min, N = 1008				Efficiency = 0.135 (13.5%)				
Myoglobin	0.59	41.6	9.6	40.0%	42	1.0%	10.3	7.3%
Lysozyme	1.91	57.9	15.4	19.5%	57.9	0.0%	14.1	-8.4%
AVG						0.5%	AVG	7.9%
V = 6.25 l, F = 125 ml/min, N = 528				Efficiency = 0.2 (20%)				
Myoglobin	0.59	38.9	11.1	52.5%	37.1	-4.6%	10.8	-2.7%
Lysozyme	1.91	63.7	15.2	24.2%	56.8	-10.8%	15.4	1.3%
AVG						7.7%	AVG	2.0%



### 4.1.3 CCC

#### *Conventional flow*

#### **Experimental setup**

The CCC experiments are from a SFCC 2000 (Societe Francaise Chromato Colonnes, Paris, France) hydrodynamic type J coil planet centrifuge CCC machine, with a spiral coil using 73 m of 1.65 mm id PTFE tubing with a total volume of 156 ml. A heptane–methanol–water system with sample components toluene ( $K = 0.33$ ) and hexylbenzene ( $K = 0.064$ ) were used. The machine was running at a rotational speed of 600 rpm with mobile phase flow rates of 1, 2, 3 and 4 ml/min, with stationary phase retentions of 0.85, 0.71, 0.65 and 0.49, respectively [Berthod and Billardello 2000].

#### **Model setup**

The experimental data was compared against theoretical equations, the CCD, probabilistic, and transport models (Table 4.4), including specific peak error, the average error and the standard deviation of the error (labelled  $\sigma$ ). For the retention time (or peak position), both the peak maximum (max) and peak average ( $\mu$ ) are reported. The theoretical equations used were eq. (3.10) and (3.27), with rotational speed  $\omega = 600$  and efficiency = 0.02 (2%). In the CCD model the number of CCD cells used was  $N = 143$ . The probabilistic model parameters were  $\omega = 600$  and efficiency = 0.02 (2%). Finally the transport model parameters used were a number of cells  $N = 1000$  and an overall volumetric mass transfer coefficient  $k_0a = 0.1$  [1/s].

Table 4.4 CCC experimental, theoretical and model values (with error) for conventional flow mode

[illegible]

### ***Co-current flow***

#### **Experimental setup**

The CCC experiments are from a SFCC 2000 (Societe Francaise Chromato Colonnes, Paris, France) three-coil planet CCC centrifuge, with a 26 m multi-layer coil of 1.6 mm id PTFE tubing with a total volume of 53 ml. A water/methanol/ethyl acetate/heptane system with ratio 6/5/6/5 (v/v) also called Arizona System M was used, with steroid sample components prednisone ( $K = 0.12$ ), prednisolone acetate ( $K = 0.56$ ), testosterone ( $K = 1.4$ ), estrone ( $K = 4.6$ ) and cholesterol ( $K = 40$ ). It was run at a rotational speed of 800 rpm with an upper phase flow rate of 2 ml/min and lower phase flow rates of 0, 0.5 and 1.5 ml/min, with a lower phase ratio of 0.66, 0.68 and 0.71, respectively. Both phases were pumped in the same direction [Berthod and Hassoun 2006].

#### **Model setup**

The experimental data was compared against theoretical equations, the CCD, probabilistic, and transport models (Table 4.5) (Figure 4.3, Figure 4.4). The theoretical equations were used with rotational speed  $\omega = 800$  and efficiency = 0.03 (3%). In the CCD model,  $N = 100$  was used. The probabilistic model parameters were  $\omega = 800$  and efficiency = 0.03 (3%). Finally, the transport model parameters used were a number of cells  $N = 1000$  and an overall volumetric mass transfer coefficient  $k_0a = 0.1$  [1/s].

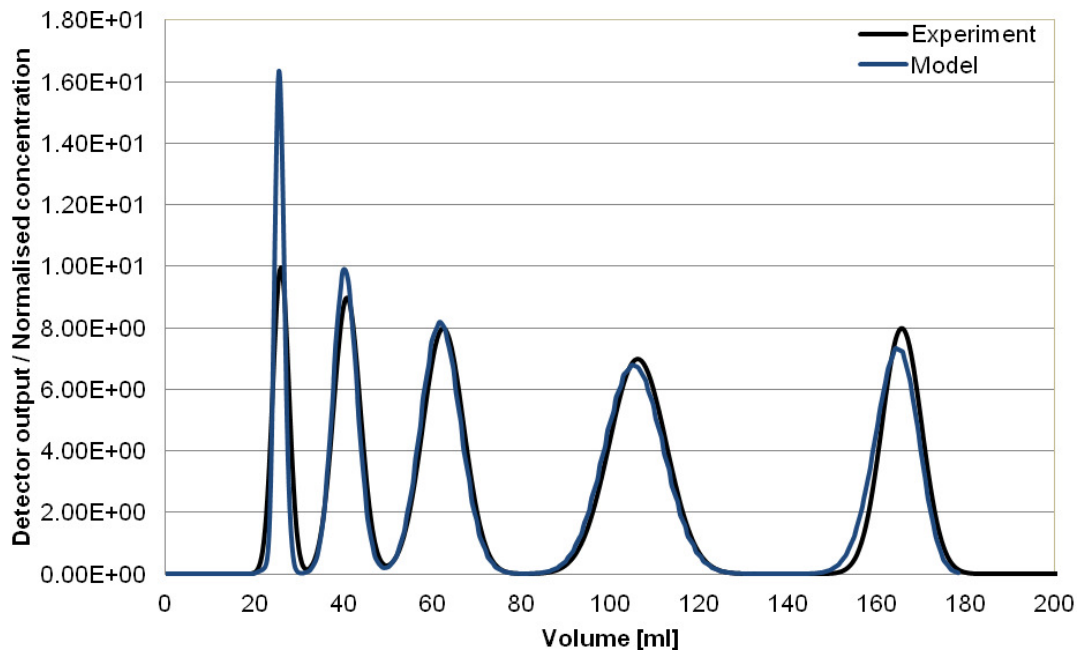


Figure 4.3 CCD Model results for co-current flow compared to experimental data [de Folter and Sutherland 2009].

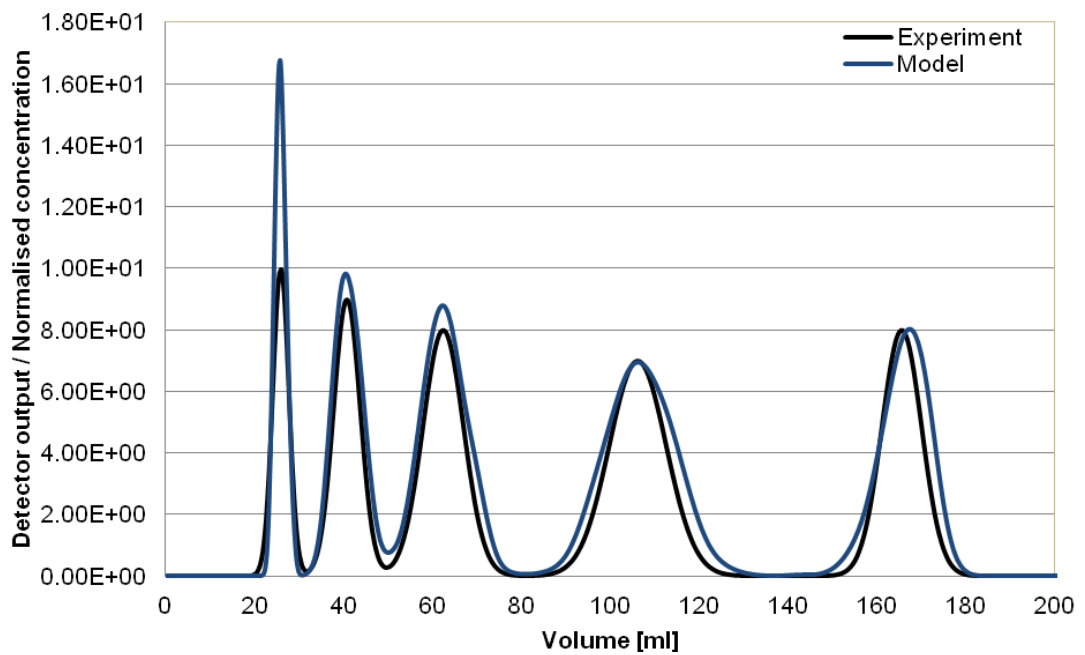


Figure 4.4 Probabilistic model results for co-current flow compared to experimental data [de Folter and Sutherland 2011].



### **Dual flow case 1**

#### **Experimental setup**

A special dual flow planet coil centrifuge CCC instrument with a multilayer helical coil made of 35 m of 5 mm id tubing with a total of 561 ml total volume was run at a rotational speed of 1000 rpm. A heptane/ethyl acetate/methanol/water system with sample components benzyl alcohol ( $K = 1.46$ ) and para-cresol ( $K = 0.69$ ) were used. The phases were pumped in opposite direction at 35 ml/min. Experiments were performed with a lower phase ratio of 0.3 and 0.5. [Ignatova and Hewitson 2008].

#### **Model setup**

The experimental values were compared to model results (Table 4.6). The theoretical equations were used with rotational speed  $\omega = 1000$  rpm and efficiency = 0.15 (15%). In the CCD model,  $N = 500$  was used. The probabilistic model parameters were  $\omega = 1000$  rpm and efficiency = 0.15 (15%). Finally the transport model parameters used were a number of cells  $N = 1000$  and an overall volumetric mass transfer coefficient  $k_0a = 0.5$  [1/s].

### **Dual flow case 2**

#### **Experimental setup**

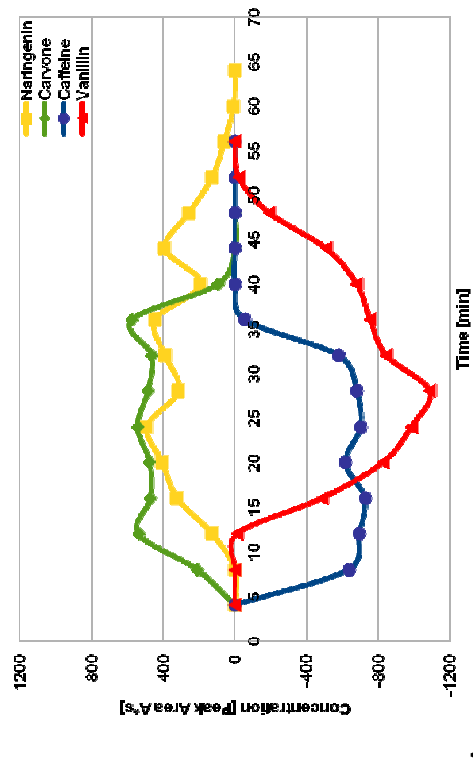
The instrument used was a Midi-CCC equipped with a specially designed preparative bobbin (supplied by Dynamic Extractions, Slough, UK). The column has a 5 mm bore and a total volume of 561 ml. The instrument was rotated at 1000 rpm and the back pressure regulators were set on the periphery and centre outlets. Sample was loaded through the mid-point inlet over a time of 30 minutes. The back pressure on the centre outlet was manually adjusted throughout the runs to keep the flow of eluant equal to the upper phase inlet flow. A Hexane / Ethyl acetate / Methanol / Water 4:6:4:6 (HEMWat15) solvent system was used. Four compounds from the G.U.E.S.S. mix [Friesen and Pauli 2005] were used: Caffeine ( $K = 0.14$ ), Vanillin ( $K = 1.21$ ), Naringenin ( $K = 3.82$ ) and Carvone ( $K = 14.8$ ). Results were achieved with 40% UP / 60% LP as the initial ratio, which gave 45% / 55% phase ratio at the end, with a back pressure of 72 psi set on the centre outlet and 54 psi set on the periphery outlet. However, even with manual pressure control, the phase retention drifted over time. The upper phase was flowed at 20 ml/min, and the lower phase at 50 ml/min [Ignatova et al. 2011].

#### **Model setup**

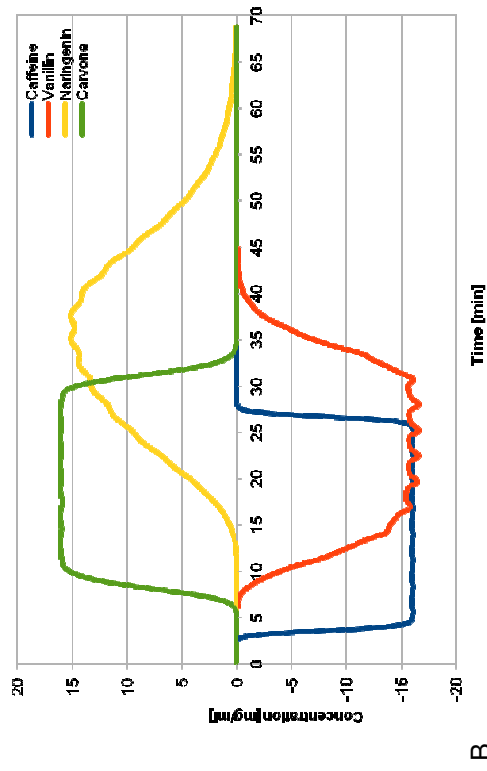
The model was set up to match experimental parameters as closely as possible, where the phase ratio was set to the final experimental value. As the sample was inserted gradually, instead of numerical values, the graphical values of the experimental and model data were compared (Figure 4.5). CCD model:  $N = 100$  cells, Probabilistic model: Efficiency = 0.1 (10%), Transport model:  $N = 100$ ,  $k_0a = 0.09$  [1/s].

*Table 4.6 CCC experimental, theoretical and model values (with error) for dual flow mode case 1*

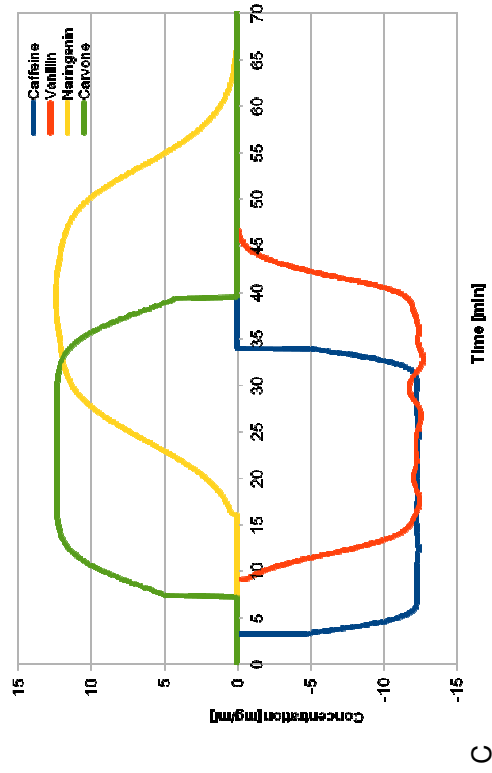
Experimental			Theoretical			CCD model			Probabilistic model			Transport model				
K	V <sub>R</sub> [ml]	Width [ml]	V <sub>R</sub> [ml]	Error V <sub>R</sub> [%]	Width [ml]	Error Width [%]	V <sub>R</sub> (μ) [ml]	V <sub>R</sub> (max) [ml]	Error V <sub>R</sub> [%]	Width [ml]	Error Width [%]	V <sub>R</sub> (μ) [ml]	V <sub>R</sub> (max) [ml]	Error V <sub>R</sub> [%]	Width [ml]	Error Width [%]
Lf=0.3																
1.46	600.6	323.4	693.9	15.5%	548.4	69.6%	693.2	674.9	12.4%	358.3	10.8%	696.1	678.4	13.0%	397.5	22.9%
0.69	585.2	450.45	820.7	40.2%	608.4	35.1%	824.7	804.1	37.4%	401.7	-10.8%	824.5	801.8	37.0%	441.7	-1.9%
Lf=0.5																
1.46	626.15	431.9	750	19.8%	373.2	-13.6%	750	726.5	16.0%	416.3	-3.6%	750.2	731.8	16.9%	374.9	-13.2%
0.69	667.1	430.85	764.6	14.6%	384.4	-10.8%	768.2	743.3	11.4%	429.4	-0.3%	766.8	748.6	12.2%	390.6	-9.3%
			AVG  ± σ		AVG  ± σ		AVG  ± σ		AVG  ± σ		AVG  ± σ		AVG  ± σ		AVG  ± σ	
			22.5% ± 12.0%		32.3% ± 39.9%		19.3% ± 12.2%		19.8% ± 11.7%		11.8% ± 16.2%		17.5% ± 11.3%		21.8% ± 10.3%	



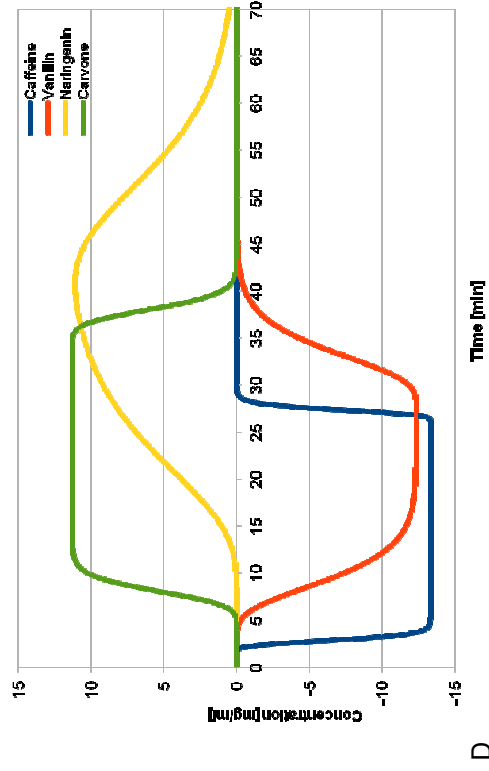
A



B



C



D

Figure 4.5 CCC Dual flow case 2 comparing: A: experimental [Ignatova et al. 2011] to B: CCD model, C: Probabilistic model, D: Transport model



## ***Intermittent mode***

### **Experimental setup**

A high performance Midi CCC instrument (Dynamic Extractions, Slough, UK) fitted with 4 mm id preparative columns made of polyfluoroalkoxy tubing (PFA) with a total volume of 912.5 ml was used to perform the intermittent counter-current extraction (ICcE) [Hewitson et al. 2011]. The mobile phase was pumped alternately, first in normal phase (upper phase mobile, from tail-periphery to head-centre) and then in opposite reversed phase direction (lower phase mobile, from head-centre to tail-periphery). The flow direction was switched between normal and reversed phase, every 4 minutes (in a single direction), using a flow rate of 40 ml/min for both phases. A rotational speed of 1400 rpm was used. A Hexane / Ethyl acetate / Methanol / Water 1:4:1:4 (HEMWat 11) solvent system was used to separate eight compounds from a modified G.U.E.S.S. mix [Friesen and Pauli 2005]. The sample mix contained Caffeine ( $K = 1.7$ ), Aspirin ( $K = 0.111$ ), Coumarin ( $K = 0.026$ ), Salicylic Acid ( $K = 0.025$ ), Carvone ( $K = 0.01$ ) and Ionone ( $K = 0.01$ ) at 10 mg/ml, and Salicin ( $K = 100$ ) and Biphenyl ( $K = 0.01$ ) at 5 mg/ml.

### **Model setup**

Results from the CCD model and probabilistic model were graphically compared to experimental results (Figure 4.6). The models were configured to match experimental condition, including the dead volumes and inlet, outlet and between the bobbins. The CCD model was configured with  $N = 100$  cells, and the probabilistic model was set up with efficiency = 0.01 (1%).

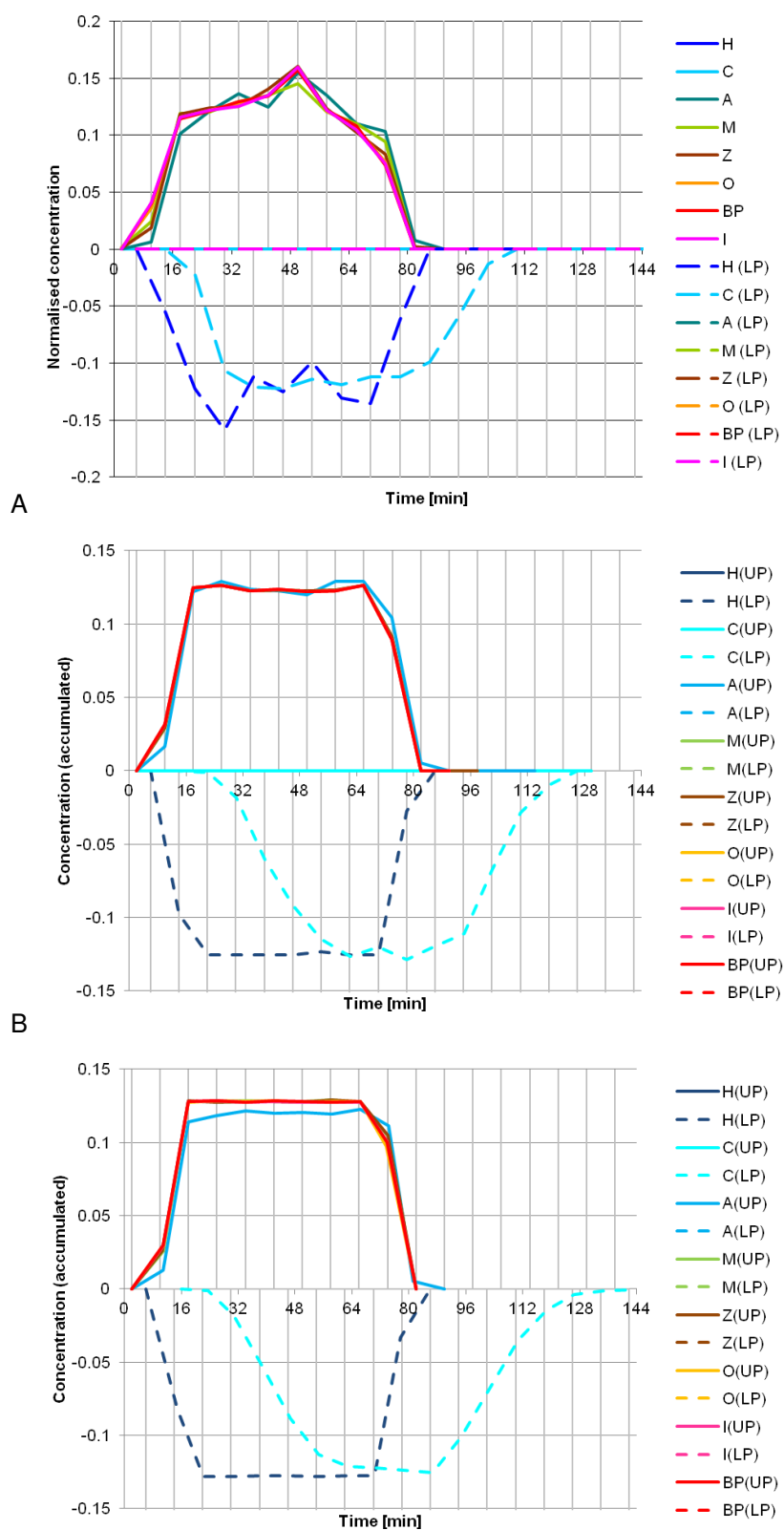


Figure 4.6 CCC Intermittent flow mode comparing: A: Experimental (normalised) [Hewitson et al. 2011], B: CCD model (accumulated), C: Probabilistic model (accumulated) (components: Caffeine (C), Aspirin (A), Coumarin (M), Salicylic Acid (Z), Carvone (O), Ionone (I), Salicin (H), Biphenyl (BP). A, M, Z, O, I, and BP largely overlap in the upper phase in all graphs.)

#### 4.1.4 Droplet CCC

##### Experimental setup

The apparatus for droplet counter-current chromatography consists of 300 silylated glass columns each 60 cm long having a 1.8 mm internal diameter. The total system capacity is about 460 ml, excluding a total of 80 ml of interconnecting tubing. A Chloroform / Acetic acid / 0.1N HCl 2:2:1 solvent system was used. The sample components were Dinitrophenyl (DNP) amino acids: Dinitrophenyl-L-ornithine ( $K > 100$ ), L-serine ( $K = 3.8$ ), Dinitrophenyl-L-threonine ( $K = 2.4$ ), *N,N'*-di(dinitrophenyl)cystine ( $K = 0.94$ ), di-nitrophenyl- $\beta$ -alanine ( $K = 0.71$ ), dinitrophenyl-L-alanine ( $K = 0.56$ ) and dinitrophenyl-L-proline ( $K = 0.45$ ). The heavier mobile phase was pumped through the lighter stationary phase at 16 ml/hour [Tanimura et al. 1970].

##### Model setup

The experiment is compared to three model set ups (table 4.6). The stationary phase retention was empirically approximately as 0.92 (92%). The dead volume was set to 80 ml in all set ups matching the experimental setup. First the CCD model was used to model this experiment, setting the number of steps to the number of columns in the experimental setup ( $N = 300$ ). Next, the CCD model was used again with  $N = 300$ , but this time using the partial transfer mode. The partial transfer fraction was calculated by calculating the tube fraction of one mobile phase droplet (as can be seen in Figure 2.8). A single droplet occupies every 164<sup>th</sup> part of a tube approximately, so the partial transfer fraction was set to  $1/164 = 0.006$ . Finally, the probabilistic model was used, using a mixing speed of 143 [1/min] and an efficiency of 0.1 (10%). The mixing speed represents the time for each droplet to pass, effectively generating a 'mixing wave'. This was calculated from the time it takes for a single droplet to be formed.

Table 4.7 Droplet CCC experimental and model values (with error)

K	Experimental				CCD model (normal)				CCD model (partial transfer)				Probabilistic model			
	V <sub>R</sub> [ml]	Width [ml]	V <sub>R</sub> (μ) [ml]	V <sub>R</sub> (max) [ml]	Error V <sub>R</sub> [%]	Width [ml]	Error Width [%]	V <sub>R</sub> (max) [ml]	Error V <sub>R</sub> [%]	Width [ml]	Error Width [%]	V <sub>R</sub> (μ) [ml]	V <sub>R</sub> (max) [ml]	Error V <sub>R</sub> [%]	Width [ml]	Error Width [%]
3.8	271.5	25.8	154.4	153.9	-43.3%	29.62	14.8%	153.8	-43.4%	34.10	32.2%	154.3	153.7	-43.4%	16.13	-37.5%
2.4	328.8	29.1	219.4	218.7	-33.5%	44.70	53.6%	218.0	-33.7%	48.82	67.8%	220.3	218.4	-33.6%	24.28	-16.6%
0.94	527.1	59.1	493.3	491.6	-6.7%	107.97	82.7%	502.7	-4.6%	114.05	93.0%	498.2	496.1	-5.9%	59.05	-0.1%
0.71	669.9	69.0	639.1	637.0	-4.9%	141.61	105.2%	637.5	-4.8%	142.51	106.5%	644.9	644.5	-3.8%	75.76	9.8%
0.56	796.8	87.9	798.8	796.2	-0.1%	178.44	103.0%	792.9	-0.5%	178.39	102.9%	803.8	800.8	0.5%	96.08	9.3%
0.45	980.4	96.3	938.5	980.4	0.0%	257.93	167.8%	972.7	-0.8%	220.07	128.5%	988.9	986.9	0.7%	118.39	22.9%
			AVG  ± σ		14.8% ± 18.8%	AVG  ± σ	87.9% ± 51.9%	AVG  ± σ	14.6% ± 18.9%	AVG  ± σ	88.5% ± 33.9%		AVG  ± σ	14.7% ± 19.2%	AVG  ± σ	16.0% ± 21.7%

### 4.1.5 Vortex CCC

#### Experimental setup

The type-I coil planet centrifuge and the vortex CCC column were fabricated at the NIH Machine Shop. As mentioned, in the type-I motion, the column counter-rotates about its own axis once during every revolution cycle. The column is made of a high-density polyethylene disk (16 cm diameter and 5 cm high) with multiple holes (966) of 3 mm diameter connected in series with a total capacity of 364 ml. The solvent system used was Hexane / Ethyl acetate / Methanol / 0.1M HCl (1:1:1:1). The sample compounds were Dinitrophenyl (DNP) amino acids: DNP-lys, asp, glu, beta-ala, ala, and leu at a concentration of 1 mg/ml. The mobile phase flow rate was 3.0 ml/min, the revolution 1000 rpm, and the stationary phase retention 35% [Ito et al. 2011b].

#### Model setup

The CCD model was used, matching the number of CCD cells to the experimental setup ( $N = 966$ ), and using an efficiency of 0.8 (80%). Model results were compared to experimental values (Table 4.8).

Table 4.8 Vortex CCC experimental and model values (with error).

Compound	K (up/lp)	K (lp/up)	Experimental		CCD model			
			$t_R$ [min]	Width [min]	$t_R$ [min]	Error $t_R$ [%]	Width [min]	Error Width [%]
DNP-lysine	0.005	1181	90	6	78.9	-12%	0.6	-90%
DNP-aspartic acid	0.3	3.33	90	6	91.4	2%	5.4	-10%
DNP-glutamic acid	0.47	2.13	101.3	11.4	98.6	-3%	7.0	-39%
DNP-beta-alanine	1.09	0.92	123.8	12.1	124.9	1%	12.0	-1%
DNP-alanine	1.97	0.51	150.3	18.1	162.2	8%	18.4	1%
DNP-Leucine	7.8	0.13	298.5	56.1	409.5	37%	58.1	4%
					<b> AVG </b>	<b>10%</b>	<b> AVG </b>	<b>24%</b>
					<b><math>\pm \sigma</math></b>	<b><math>\pm 17\%</math></b>	<b><math>\pm \sigma</math></b>	<b><math>\pm 37\%</math></b>

#### 4.1.6 Toroidal CCC

##### Experimental setup

Stainless steel (SS316) tubing with 5mm ID and 6mm OD (Aalco, Aylesbury, UK) was wound to create two helixes containing 404 close-packed turns each. The helical coiled tubing was wound onto two paired bobbins of a standard high performance Midi rotor (Dynamic Extractions, Slough, UK). A single bobbin with a column volume of 333 ml was used. An Aqueous two-phase system (ATPS) was used made up by 14% (w/w) PEG-1000: 14% (w/w). The rotational speed used was 800 rpm, and the mobile (lower) phase flow rate was 10 ml/min (against the rotation of the bobbin). The sample components were Myoglobin ( $K = 0.47$ ) at 2.2 mg/ml and Lysozyme ( $K = 2.46$ ) at 2.2 mg/ml, and were injected using a 5 ml sample loop. The stationary phase retention was 34% [van den Heuvel et al. 2010].

##### Model setup

Results from two modelling approaches were compared to experimental results (Table 4.9). The first was representing each coil turn as a discrete mixing / settling cell. The model used for this was the CCD model, setting the number of model steps  $N = 404$ , simulating the coil turns by using a partial transfer of 0.015. This was calculated using the cell volume ( $V_c/N$ ) and the volume transferred each cycle ( $F/\omega$ ). Next the CCD model with the same number of steps was used with normal discrete transfers and using a mixing efficiency value of 0.22 (22%).

Table 4.9 CCC Toroidal coil experimental and model values (with error).

Component	Experimental			CCD model (partial transfer)				CCD model			
	K	t <sub>R</sub> [min]	Width [min]	t <sub>R</sub> (μ) [min]	t <sub>R</sub> (max) [min]	Error t <sub>R</sub> [%]	Width [min]	Error Width [%]	t <sub>R</sub> (μ) [min]	t <sub>R</sub> (max) [min]	Error t <sub>R</sub> [%]
Myoglobin	0.47	27.3	6.1	27.6	27.5	0.7%	5.29	-13.3%	27.6	27.1	-0.7%
Lysozyme	2.46	49.8	23	50.2	50.1	0.6%	11.26	-51.0%	50.1	49.4	-0.8%
				AVG		0.7%	AVG	32.2%	AVG		0.8%
											9.4%

#### 4.1.7 Controlled-cycle pulsed liquid-liquid chromatography

##### Experimental setup

Controlled-cycle pulsed liquid-liquid chromatography is a very recent experimental technique developed by Kostanyan and colleagues [Kostanyan et al. 2011]. Each unit presented a column divided into 26 stages by equally spaced horizontal perforated plates at 35 mm intervals (stage volume 1.1ml). The columns were of 6.4 mm internal diameter FEP tubing; the perforated plates were fabricated from PTFE sheet, 3 mm thick and contained 130.25 mm diameter holes.

Additional conditions of considered experimental results were stationary phase retention of 0.76, and mobile phase flow rate of 1.1 ml/min. 2 column units were used resulting in a total of 52 stages. The sample components were Acetic acid ( $K = 0.15$ ), Propionic acid ( $K = 0.17$ ), Butyric acid ( $K = 0.24$ ) and Valeric acid ( $K = 0.51$ ).

##### Model setup

The experimental data was compared to modelled results (Table 4.10). First the CCD model was used with the number of cells equal to the number of stages of the experimental setup (52), and efficiency = 1 (100%). The model results closely matched the experimental values for the retention but not for the peak width. Therefore, subsequently the model efficiency was adjusted so the width values matched the experimental data values for each component.

Table 4.10 Controlled-cycle pulsed liquid-liquid chromatography (CPLC) experimental and model values

K	Experimental		CCD Model (Efficiency = 1)			CCD Model (Efficiency varying)			
	Retention [steps]	Width [steps]	Retention ( $\mu$ ) [steps]	Retention (max) [steps]	Width [steps]	Efficiency [%]	Retention ( $\mu$ ) [steps]	Retention (max) [steps]	Width [steps]
0.15	75.8	36.2	75.7	75	23.93	59 %	75.7	73.0	36.3
0.17	77.2	43.2	79.0	78	26.00	51 %	79.0	76.0	43.4
0.24	86.9	78.8	90.5	89	33.06	28 %	90.5	82.0	78.8
0.51	129.1	143.9	135.0	133	58.72	27 %	135.0	122.0	143.6



## 4.2 Sample injection

This section compares modelled results to experimental data, in particular looking at sample injection.

### Experimental setup

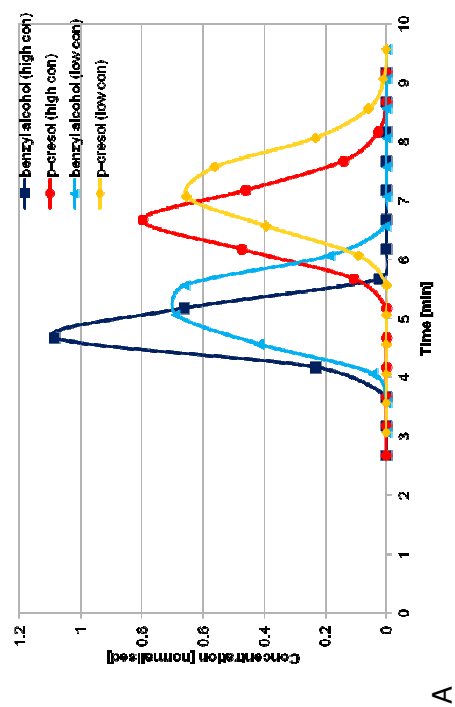
A Maxi-CCC centrifuge supplied by Dynamic Extractions (Slough, UK) was used. This centrifuge has a rotor radius of 300 mm, bobbins with 10 mm bore tubing and a capacity of 4.6 litre and was operated at a rotational speed of 600 rpm and a flow rate of 850 ml/min. The sample components used were benzyl alcohol ( $K = 0.3$ ) and p-cresol ( $K = 1.1$ ). Low concentration / high volume loading (12.8 mg/ml benzyl alcohol + 6.1 mg/ml p-cresol in 960 ml) is compared to the high concentration / low volume loading (42 mg/ml benzyl alcohol + 20 mg/ml p-cresol in 290 ml). The stationary phase retention before the injection was 80.0%, and after separation was 40.8% [Sutherland et al. 2009].

### Model setup

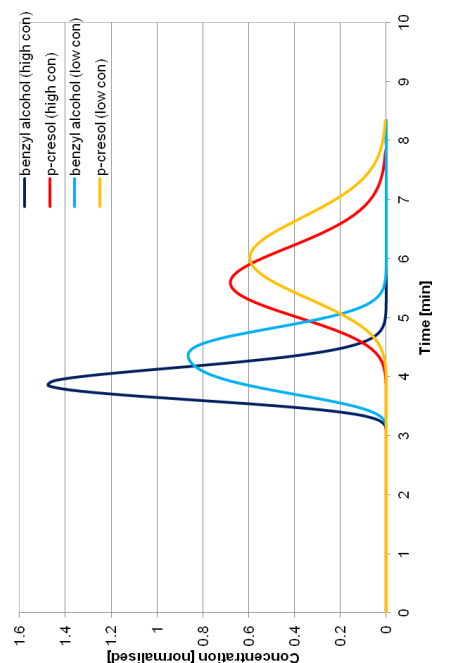
The different models were set up with parameters matching the experimental setup, using the same specific model parameters for high and low concentration set ups. The model results were compared to the experimental data. See Table 4.11 for numerical results, and Figure 4.7 for graphical peak shape comparisons. To compensate for specific detector sensitivity, all graphs were normalised to the peak area to allow for a better comparison. Additionally the original data was corrected for a time offset that was originally applied to the experimental data (as mentioned by I. Sutherland in a personal conversation on 4<sup>th</sup> December 2012). The stationary phase retention was set to 40.8%. Specific model parameters used were  $N = 40$  for the CCD model, efficiency = 0.04 (4%) for the probabilistic model, and  $N = 1000$  and  $k_0a = 0.1$  [1/s] for the transport model.

Table 4.11 CCC sample injection concentration comparing experimental and model values

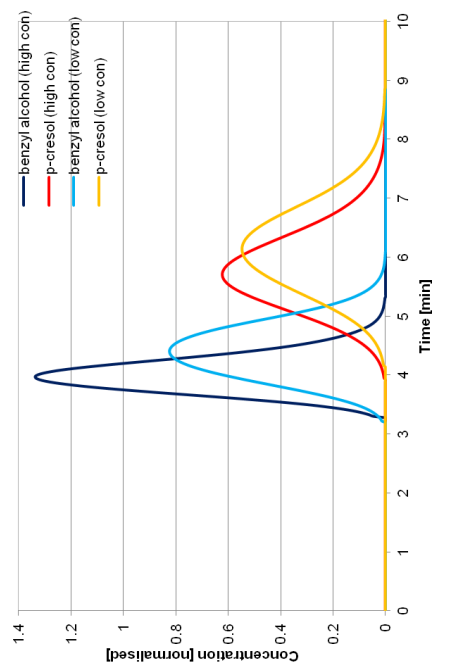
Compound	Experimental			CCD model			Probabilistic model				Transport model			
	K	t <sub>R</sub> [min]	Width [min]	t <sub>R</sub> (μ) [min]	t <sub>R</sub> (max) [min]	Error t <sub>R</sub> [%]	Width [min]	Error Width [%]	t <sub>R</sub> (μ) [min]	t <sub>R</sub> (max) [min]	Error t <sub>R</sub> [%]	Width [min]	Error Width [%]	
(high concentration low volume)														
benzyl alcohol	0.3	4.7	1.6	3.9	3.8	-19%	1.08	-33%	4.0	4.0	-15%	1.10	-31%	-19%
p-cresol	1.1	6.7	2.1	5.7	5.6	-16%	2.35	12%	5.8	5.7	-15%	2.39	14%	14%
(low concentration high volume)														
benzyl alcohol	0.3	5.2	2.4	4.3	4.3	-17%	1.89	-21%	4.4	4.4	-15%	1.65	-31%	-18%
p-cresol	1.1	7.1	2.5	6.1	6.0	-15%	2.70	8%	6.2	6.2	-14%	2.66	6%	10%
					AVG  ± σ	17% ± 2%	AVG  ± σ	18% ± 22%			15% ± 1%	AVG  ± σ	21% ± 24%	15% ± 17%
											15% ± 1%			± σ
														± σ
														± σ
														± σ



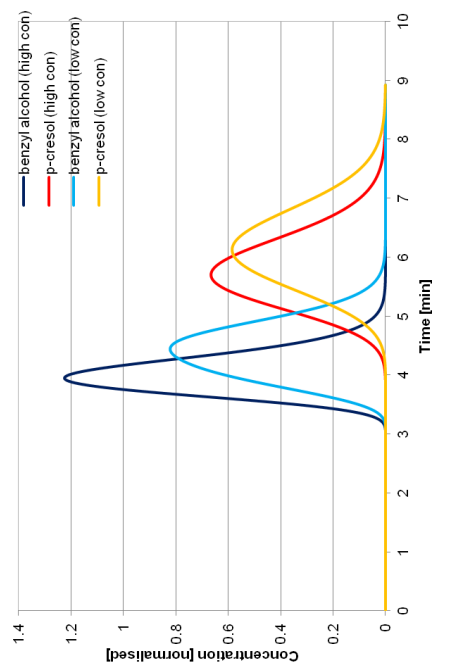
A



B



C



D

Figure 4.7 CCC Batch sample injection comparing: A: experimental [Sutherland et al. 2009] (normalised) to: B: CCD model, C: Probabilistic model, D: Transport model

### 4.3 Efficiency

Sutherland and colleagues recently performed research on stage efficiency using the CCD model [Sutherland et al. 2011]. In the latter, each toroidal loop is considered a separate mixing chamber, calculating a mixing / settling efficiency for these toroidal loops.

A different type of efficiency study is performed here, considering continuous chromatography techniques. The CCD and the probabilistic model were used to obtain efficiency values. The models were calibrated to match experimental separation values: finding the best number of model cells  $N$  for the CCD model, and for the probabilistic model, directly the model efficiency value. Respective efficiency values were obtained for both models (Table 4.12). For the CCD mode, the nominal number of mixing/settling steps (' $N$  mixing') were calculated using equation (3.20),  $f'$  is subsequently calculated by dividing the number of model steps by the nominal number of steps, and equation (3.29) is finally used to calculate the efficiency  $f$  ('Efficiency').

Table 4.12 System efficiency values for different apparati / operation modes

Apparatus (mode)	Source	Volume [ml]	Flow [ml/min]	Speed [RPM]	$S_F$ ( $L_F$ ) [%]	CCD model				Probabilistic model
						$N$ mix/settle	$N$ model	$f'$ [%]	Efficiency [%]	Efficiency [%]
CCC	1	156	1	600	85.0%	14040	130	0.93%	1.85%	1.80%
CCC	1	156	2	600	71.0%	13572	115	0.85%	1.69%	1.65%
CCC	1	156	3	600	65.0%	10920	155	1.42%	2.84%	2.60%
CCC	1	156	4	600	49.0%	11934	170	1.42%	2.85%	2.60%
CCC (co)	2	53	2	800	66.0%	7208	100	1.39%	2.77%	3.00%
CCC (co)	2	53	2.5	800	68.0%	8310	90	1.08%	2.17%	2.50%
CCC (co)	2	53	3.5	800	71.0%	9964	90	0.90%	1.81%	2.00%
CCC (dual)	3	561	35	1000	30.0%	8014	500	6.24%	12.48%	17.00%
CCC (dual)	3	561	35	1000	50.0%	8014	500	6.24%	12.48%	12.00%

#### Sources

1. [Berthod and Billardello 2000]
2. [Berthod and Hassoun 2006]
3. [Ignatova and Hewitson 2008]

## 5 Visualisation design

In the following, the user interface of the computer model evolution is described, following a User Centred Design approach. Section 5.1 describes how this process initially started, followed by the initial evaluation (section 5.2). The requirements obtained from this evaluation are described in section 5.3. The next section (5.4) describes the improved interface which implements said requirements.

### 5.1 Design of the initial prototype

A User Centred Design (UCD) approach was followed (Figure 2.30), as shown throughout the current chapter. Furthermore, an Evolutionary Prototyping [Sharp et al. 2007] approach was adopted. This means that after each evaluation stage, instead of starting again from 'scratch', the current software is adapted, until the final version is reached. What follows is a discussion of how the user interfaces were developed into the final solution. See Appendix B for a complete list of different builds of the model software. This section explores the first version that was evaluated.

A basic user interface was designed for the configuration of the input parameters of the model (Figure 5.1). After the model was run, the graphical model result was displayed in the form of a chromatogram view (Figure 5.2). Additional prototype result views were developed in the form of a time mode chromatogram view, and a 3D time trace view. More developed versions of these views are shown in section 5.4 (Figure 5.5 and Figure 5.6 respectively).

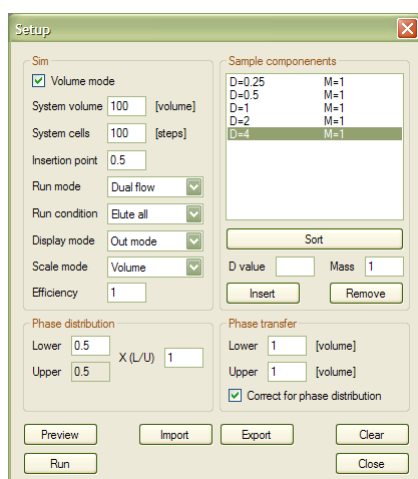


Figure 5.1 User interface for model input parameters

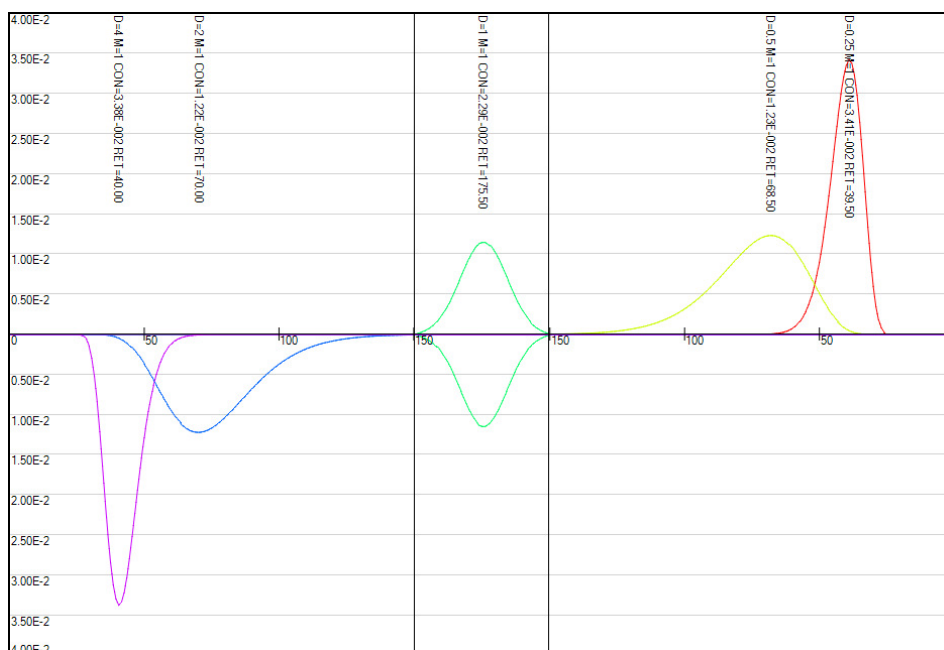


Figure 5.2 Chromatogram view graphically showing model result

As the aim was to improve users' understanding of the chromatography process, given that the model is highly parameterised, and that though the resulting separation is a direct result of the parameters used in the model, there is not always an obvious direct relationship between them. So IV techniques (section 2.8) were applied to aid finding the optimal configuration. This was realised in the form of Model Previews.

After setting input parameters, a new screen with traditional dynamic querying style controls for a reduced number of input parameters was shown (Figure 5.3). Additionally, this view showed a chromatogram 'preview' with graphical and numerical data, based on the simplified model described in section 3.4.



Figure 5.3 Preview using traditional dynamic query controls

## **5.2 Initial evaluation**

Following the principles of User Centred Design (UCD), a formative evaluation study was conducted.

Initially feedback was informally collected from individual users. The main requirement here was that these had to be domain experts. The computer model was made available, and potential users were able to see it demonstrated. As feedback was collected from experts in the CCC field, this feedback was weighed according to the number of years they reported to have been active in the field. This feedback was collected in two tiers. Initially, only summary feedback was collected in the form of a questionnaire (Appendix C). The main questions were: the number of years of experience in the CCC field, how useful each of the visual aspects of the interface were, and then additional comments like: what did the user like / dislike most, and if there was anything else the user would like to see. A second phase of feedback was collected using a visual walkthrough (Appendix D). Here the user was guided through the different aspects of the interface, capturing user feedback on each of these in detail. This method allowed the user interface to evolve over a number of iterations.

At a later stage, feedback was collected from the BIB CCC team (see chapter 6 for feedback results), again by demonstrating the model and collecting summary feedback.

Addressing a common need that had previously been identified, a prototype of a more graphical user interface was developed. Summary feedback was collected using a focus group, using an unstructured group interview. A prototype of this new graphical user interface was demonstrated, where the group interview was guided by a number of key questions (Appendix E).

### **5.2.1 Requirements**

At this stage the only requirement concerning the evaluation method, was that the model interface would be evaluated by potential users, which would be domain experts.

### **5.2.2 Data collection**

Feedback was gathered at the major biennial conference in the CCC field in mid 2008 (CCC2008, Rio de Janeiro, Brazil). At this conference the model application was demonstrated to potential users, and their feedback subsequently captured using questionnaires.

The first question was, how useful the different elements of the user interface were considered, which was converted into numerical values as follows: not very useful: 0, somewhat useful: 1, and very useful: 2.

Considering the requirement that the potential users of the model would be experts in the CCC field, a weight was associated to each subject, according to the number of years experience they had in the CCC field. The weight value applied was: For no experience or less than two years: 1, for two to five years: 2, and for more than five years: 3.

### 5.2.3 Evaluation results

The results were calculated using the weight, and finally averaged over the total (Table 5.1).

*Table 5.1 Numerical results including weighing*

Subject	Non-weighted						Weighted				
	Preview	Chrom	Time	3D	General	Weight	Preview	Chrom	Time	3D	General
1	2	2	1	0	2	1	2	2	1	0	2
2	2	2	2		2	1	2	2	2		2
3	2	2	2	2	2	2	4	4	4	4	4
4	2	2	2	2	2	3	6	6	6	6	6
5	2	2	2	2	2	3	6	6	6	6	6
6	2	2	2	0	2	3	6	6	6	0	6
7	2	1	0	0	2	2	4	2	0	0	4
8	2	2	2	1	2	2	4	4	4	2	4
<b>Average:</b>	<b>2.0</b>	<b>1.9</b>	<b>1.6</b>	<b>0.9</b>	<b>2.0</b>	<b>2.1</b>	<b>2.0</b>	<b>1.9</b>	<b>1.7</b>	<b>1.1</b>	<b>2.0</b>

So the average values (except for the weight column) can be evaluated using the same numerical scale used for the usefulness (not very useful: 0, somewhat useful: 1, and very useful: 2). The weighted results were considered in the analysis.

The numerical results of the user feedback questionnaires showed that the initial chromatogram preview was considered the most useful (score: very useful), and the 3D mode view the least (score: somewhat useful). The chromatogram and time mode also showed a high level of usefulness. This was taken into account by further developing the visual elements according on how each of the interface elements scored in the evaluation, and subsequently performing a deeper evaluation, using the insights method.

The other questions on the questionnaire, more qualitative in nature were also analysed, looking for commonalities. The visual walkthrough revealed a number of areas where the interface appeared not intuitive or logical, identifying 3 main areas.

Firstly, the general work flow, navigating between the model input parameters screen (Figure 5.1), the preview screen (Figure 5.3), and the chromatogram view showing model results (Figure 5.2) was not intuitive. It was difficult for the users to grasp how, or when to change between the different interface screens. Also some of the interface screens required at certain stages, were not found.



Secondly, many of the input parameters appeared confusing, the user either misinterpreting their meaning, resulting in undesired modification of parameters, or missing an essential parameter during model setup. In general it was unclear which the main parameters to be set were. Users also reported the way some parameters were modified was inconvenient.

Finally, the preview mode, although generally intuitively understood, controls appeared too sensitive.

These results were used to compile requirements for the model interface.

### **5.3 Revised requirements**

The user feedback was analysed, identifying issues to be addressed into the model interface. The visual walkthrough revealed a number of areas where the interface behaviour was not intuitive.

The first important area for improvement was the general flow. There should be a clear starting point, and subsequent natural flow leading from model input parameters to desired model results.

The second issue was the model input parameters. An important requirement for any system, as identified at the biennial international CCC conference, was 'to keep it simple', a motto that had been taken on by the CCC community [Berthod 2009]. A contribution to the model interface would be to have a beginner's mode, leaving options to a minimum, where only the main model input parameters were accessible. Some controls should be removed entirely to avoid confusion. Furthermore, most common, default values should be pre-set in the interface.

The final issue was the high sensitivity of the controls of the preview screen. This could be addressed with variable sensitivity scale.

It was essential to make the user interface as intuitive as possible, and to resolve all the issues raised. This resulted in the new interface, which is described in the next section.

### **5.4 Improved Interface**

The improved interface was developed according to the requirements described previously. The following sections focus on each of the elements of this interface in detail.

### 5.4.1 Chromatogram view

Recall that the main basic visual output of any chromatography process is the chromatogram. The results of the model are displayed in a chromatogram style view (Figure 5.4). It is also possible to show only the total components over both phases. This view is highly customisable, including the units (model steps, volume or time) and zoom level on the horizontal axis and the scaling on the vertical axis can be changed.

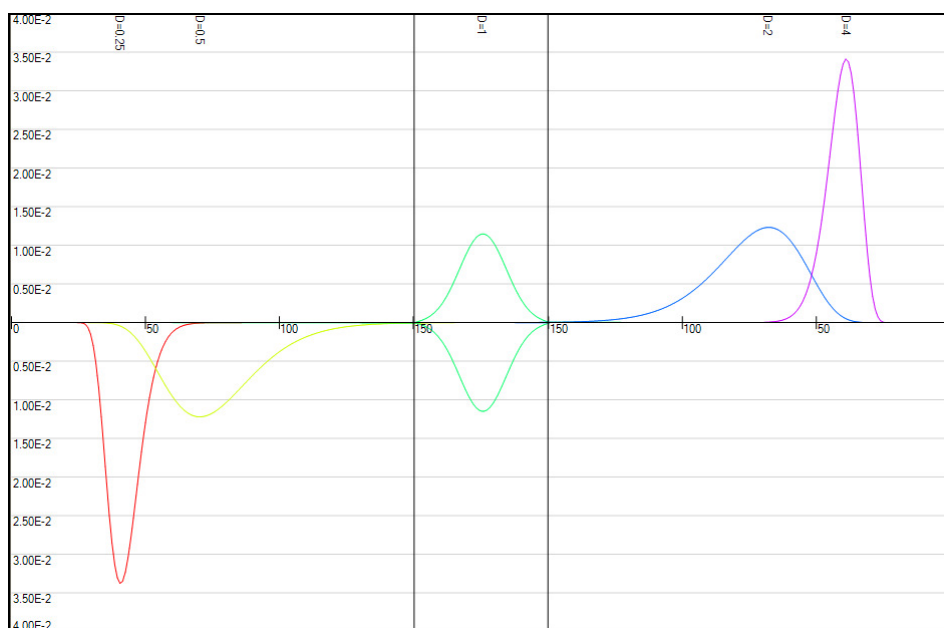


Figure 5.4 Improved chromatogram view including more customisation

### 5.4.2 Time mode chromatogram view

A way to show how the CCC process develops over time was realized by adding time as a parameter to the chromatogram view (Figure 5.5). A slider control allows interactively moving to any point in time in the CCC process. Gradually moving the slider control shows how the chromatographic peaks develop as the process continues.

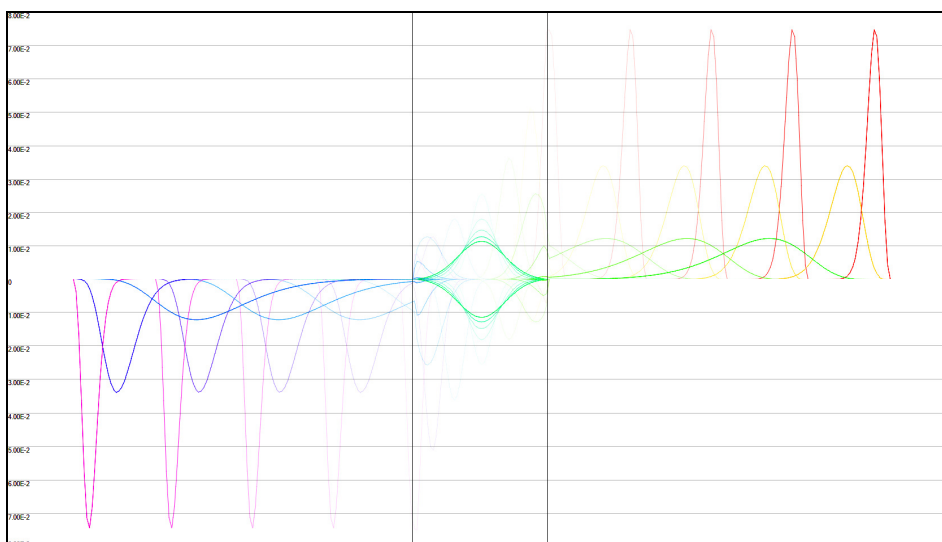


Figure 5.5 Time mode chromatogram view

### 5.4.3 3D time trace view

Having developed the time mode chromatogram, it seemed interesting to attempt to display the time profile in a single representation, resulting in a 3D view. This was realised resulting in an interactive OpenGL graphics interface, where the view can be rotated and zoomed (Figure 5.6).

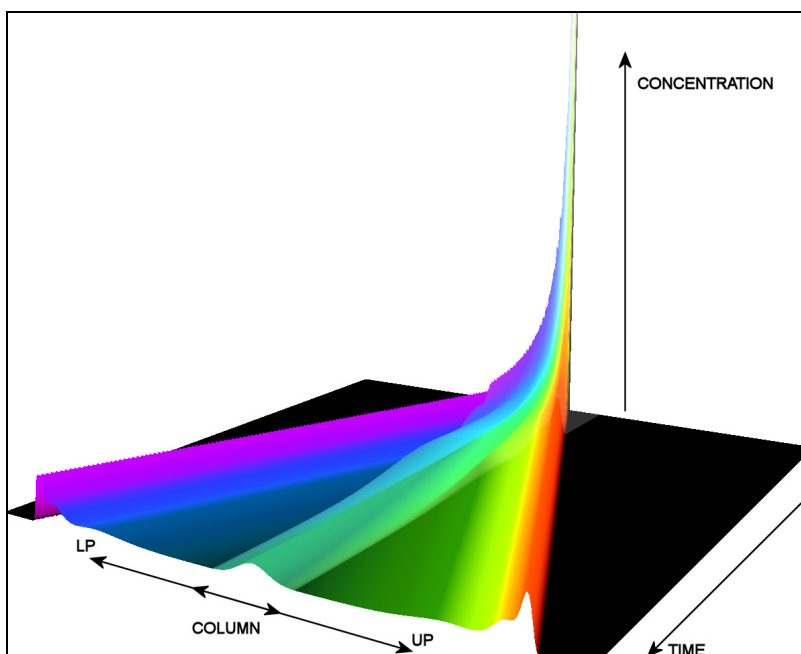


Figure 5.6 3D time trace view with annotated labels, showing different sample components represented by different colours

### 5.4.4 Model parameter setup

As requirements were incorporated into the user interface, and also as model development proceeded enabling increased flow modes, this required the user interface to be adapted accordingly (Figure 5.7). The Setup and Preview windows are integrated into a single tab control, addressing the first main requirement regarding the work flow, making moving between the different views more intuitive. The second main requirement regarding the input parameters, was implementing a beginner's mode. This was done by adding an 'Advanced options' control, disabled by default, allowing only the most essential model input parameters to be modified. Further all the input parameters were initially set with suitable default values.

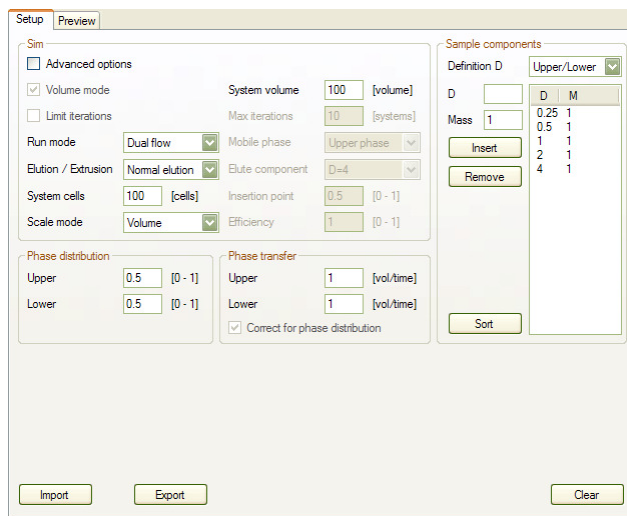


Figure 5.7 Screenshot of model input parameter setup interface

### 5.4.5 The interactive configuration explorer (ICE)

The motivation for the interactive configuration explorer (ICE) was to allow users to explore these interactions in real-time. ICE makes the query-output process more interactive by applying an established IV interaction technique known as dynamic querying. A dynamic query interface employs graphical 'widgets' (such as check-boxes and sliders) that allow the user to continuously manipulate the constraints of the query, whilst the output is presented visually with updates occurring in virtually real-time (less than 100 ms [Shneiderman 1994]). To improve the understanding of how the model responds to each parameter, the dynamic queries and query previews were combined into the interface of the computer model, where the dynamic queries provide the interactive parameter selection, and the query previews enable the real-time updates of the model. This will be referred to as model previewing or model previews.

The interactive configuration explorer shows the output of the simplified model in a chromatogram view, which is updated real-time when the input parameters are changed (fig. 3.3). Traditionally, slider controls are used to manipulate each input parameter. Though the sliders controls visually provide the parameter range and indicate their absolute value, it is difficult to allow for finer adjustments or non-linear scales. This was one of the issues reported in the initial evaluation, requiring the controls to have a variable sensitivity. Many of the model parameters require a logarithmic adjustment and are furthermore very sensitive to small changes. To meet these requirements, a new type of control was designed, allowing for relative changes. The visual interface of this control is a springed 'jog' wheel, allowing increments and decrements, ranging from very coarse to very fine changes (Figure 5.8). Furthermore, manual numerical input was integrated into the current parameter value, allowing a specific value to be set directly. As the wheel is selected and 'dragged' towards the right of its normal position, the value is increased, and as it is turned towards the left, the value is decreased. The further the wheel is turned from its normal position, the more the value is changed. The equation for the factor that the value is multiplied with is:

$$factor = 10^{\frac{jogpos}{10}}$$

where *jogpos* is the position of the jog wheel ranging from the centre to its maximum towards the right: 0, 0.25, 0.5, 0.75, 1; and ranging from the centre to its maximum towards the left: 0, -0.25, -0.5, -0.75, -1. This corresponds to a value increase of approximately 6%, 12%, 19%, 26%, and a decrease of approximately 6%, 11%, 16%, 21% respectively. Due to this scaling, after any number of varied increases and decreases using the control, the value that was started with can easily be reached again using the jog wheel only. The result is shown using a chromatogram view (in the centre of the screen), following each parameter change in real time. Key numerical results at the bottom of the screen are updated in real time as well.

As described earlier in the computer implementation (section 3.7), a custom Windows Forms Control was used to implement this component into the model interface (section 3.7.3). It is also included in the simplified object model (Figure 3.9) as the class labelled 'ValueScroll' in the View category.

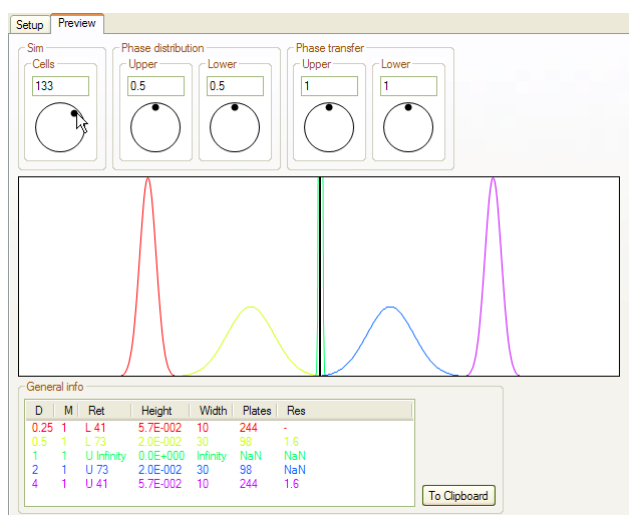


Figure 5.8 Screenshot of model: Real time interactive configuration explorer; with interactive controls (top), where the far left control is being rotated using the mouse causing its value to increase; chromatogram view (centre); key numerical results (bottom).

This improved interface implemented all identified requirements stated in the revised requirements section (5.3). This new interface was subsequently evaluated more in depth with the insight evaluation method described in the next chapter.

## 6 Insight Evaluation

This chapter has been submitted for publication in similar form [de Folter and Cribbin 2012].

North suggested that traditional evaluation methods, using detailed controlled tasks, potentially inhibit the generation (or at least recording) of insights [North 2006]. In contrast, an open-ended protocol, resulting in a qualitative analysis rather than a quantitative, allows greater domain relevance and therefore a higher likelihood of inducing and recording the occurrence of insight.

As mentioned before in section 2.9.2, insight evaluation was originally proposed to deal with shortcomings in the traditional empirical method. Unlike traditional evaluation protocols, both formative and summative [Scriven 1991], insight evaluation do not rely on a set of predefined tasks. Instead users (generally domain experts) are left reasonably free to explore the system, relying on their own knowledge and interests to drive their activity. Insight evaluation has been applied successfully in a number of contexts [Saraiya et al. 2004, 2006, Plaisant et al. 2008].

It was felt that insight evaluation was ideally suited for measuring the effect of the added interactivity and visualisation in the user interface.

### 6.1 Experimental design and procedure

This study was performed at the end of 2009, with the subjects available according to the requirements for the participants.

Five subjects took part in the experiment. All were experts in the CCC field, rather than usability experts. The goal was to determine the potential for insight generation, rather than usability per se, and thus required users with strong domain knowledge. The use of a user-centered, evolutionary design process meant that major usability issues had already been addressed by this stage. A *think-aloud* protocol was used, where subjects were invited to provide a narrative on their experience and, in particular, mention insights as they occurred. As insights occurred, subjects paused their activity to allow the experimenter to record the details. The format for the recording sheet is shown in Table 6.1. Note that data collection was carried out by the primary author. Whilst this may have introduced some risk of experimenter bias, this was minimized by instructing subjects to explore the model according to their own interests and all reported insights were recorded and included in the analysis.

Table 6.1 Template for recorded data for each insight

Visual element	Insight	Category			Domain value	Complexity / Depth	Time Short/Med/Long			Errors
		Dif	New	Idea			S	M	L	
					1 2 3 4 5	1 2 3 4 5				

The procedure for recording insights was as follows. First the visual element (e.g. Chromatogram, Timeline, ICE) of the interface where the insight occurred was recorded. Then a short description of the insight was recorded. The insight was then streamed into one of the three categories. The first category was: different from expectation ('Dif'), where a (model) behavior different from the subject's expectation was observed. The second category was: a new discovery ('New'). The third category: the creation of a new hypothesis ('Idea') meant (model) behavior was observed, resulting in the subject to form a new hypothesis that could subsequently be investigated. Then domain value, or importance of the insight was marked in a range from 1 (low) to 5 (high). The same scale was used for the insight complexity or depth. A rough indication of the time it took the subject from using a particular element to having the insight was marked as short, medium or long. And finally a note was made in case an insight was actually erroneous, or incorrectly interpreted. The subjects were also recorded, using a webcam, recording sound in case necessary to later verify any comments the subject made, and the subjects' face in case any additional information was provided by the facial expression indicating an insight or unexpected behavior of the interface.

To quantify the contribution of the visual enhancements, a basic version of the CCC computer model that included just the non-interactive chromatogram, was used as a control. An open task scenario was used which allowed subjects to 'explore' the model, rather than simply completing set tasks. Two simple data sets of input parameters were initially loaded into the computer model. The working of the computer model, its interface, its features and the loaded parameters were then explained to the subject. The subject was then encouraged to freely use the computer application and explore the behavior of the model while changing parameters.

Although subjects were free to move to any of the elements of the interface, the general sequence of use was as follows. First a simple data set would be loaded with some basic model parameters displaying a plain form with numerical input values. These could then be modified, and using the basic version, subjects could then proceed to run the model with set parameters to obtain the model result. In the enhanced version, subjects would first move from the parameter input to the ICE interface. The subject could then dynamically manipulate the interface and see the preview results as described in previous sections, and then continue to run the model to obtain final model results. However, in the enhanced version, subjects would likely spend more time using the ICE interface.

Using the *think-aloud* method, the subject indicated when gaining an insight (as previously defined). At that time, details about the insights were recorded by the experimenter. The basic version of the CCC computer model, the control condition, was evaluated first. This version of the model did not include any of the visual enhancements described earlier, but only had a simple user interface with a basic chromatogram output showing units in model steps on the horizontal axis. After the subject satisfactory finished exploring the two data sets, the subject was asked to switch to the enhanced version of the model. In this way only new insights gained by the enhanced version were recorded, excluding any insight already gained using the basic version.



## 6.2 Evaluation results and discussion

Table 6.2, Table 6.3 and Table 6.4 summarize the main results of the study. Table 6.2 shows the total insights accrued by each subject using both the basic and enhanced interfaces. It can be seen that the proposed visualisations resulted in a relative increase in insights of 6.5 times over the basic chromatogram view.

*Table 6.2 Total number of insights for version and enhanced version of model*

Subject	Basic	Enhanced
1		5
2	1	1
3		1
4		1
5	1	5
<b>Total</b>	<b>2</b>	<b>13</b>

Table 6.3 goes into more detail, showing the number of insights accrued for each visual element of the enhanced interface. Whilst the time-mode view accounted for some of this increase, it can be seen that the ICE mode accounted for the majority (77%) of all significant insights achieved, with the time-mode view accounting for 15% and the basic chromatogram accounting for the remaining 8%. The 3D time trace view did not account for any insights.

*Table 6.3 Insights for each visual element*

Subject	ICE	Chromatogram	Time-mode	3D
1	5			
2		1		
3	1			
4			1	
5	4		1	
<b>Total</b>	<b>10</b>	<b>1</b>	<b>2</b>	<b>0</b>
	<b>77%</b>	<b>8%</b>	<b>15%</b>	<b>0%</b>

Table 6.4 describes the most important insights (as defined by domain value) and the visual element with which they were achieved. The ICE mode generated five out of total six most important insights. It is apparent that most of these insights relate to what effect the input parameters have on the separation results.

*Table 6.4 Description of most important insights*

<b>Insight</b>	<b>Visual Element</b>
Determine critical amount of phase distribution for good resolution	ICE
Resolution not directly dependant on retention	ICE
Number off system cells big impact on resolution; New hypothesis	ICE
Hypothesis: Physical experiment must have very inefficient mixing	ICE
Flow rates critical effect on separation	ICE
Most of separation occurs at the start	Time-mode

Each subject showed unique insights, as well as insights that subjects had in common. The most common insight was that particular input parameters critically influenced the quality of the result of the model. Furthermore, the most important insights (with the highest domain value) occurred using the ICE mode. A relationship between the time before the insight occurred, and the complexity of the insight was also seen. In general the more complex insights were recorded after a longer time. Subject 1 had no insights using the basic version of the model, and five using the enhanced version (all in the ICE mode). Three of these triggered the formation of a new hypothesis, which the subject subsequently tested. Most insights were of high domain value. Subject 2 had one insight using the basic version, of a low complexity and domain value, and one insight using the enhanced version (in the Chromatogram mode), also of low domain value. Subject 3 had one insight of high domain value using the enhanced version (in the ICE mode). Subject 4 had one insight using the enhanced version (in the Time mode) with a high domain value. Subject 5 had one insight using the basic version of a low complexity, and five insights with high domain value using the enhanced version (four in the ICE mode and one in the Time mode).

The insight classification and scaled values (complexity and domain value) proved adequate for this study, and provided good detail and relevance. Although the general insight evaluation method was followed, subjects still seemed reluctant to be explorative. Subjects possibly had an objective oriented mindset and/or had set a time limit in the context of the study. Another problem encountered was that some subjects tended to focus on the interface and its usability rather than the model itself, in spite of efforts made to encourage focusing on the behavior of the model. This was a problem with subject 3 in particular. Overall, the number of recorded insights, whilst not as high as initially expected, was still sufficient to identify clear differences in the efficacy of each visual element.

## 7 Final Proposed Interface

This chapter describes the subsequent continued visualisation development. Section 7.1 shows the latest model interface implementing all previously described models. Section 7.2 subsequently shows a prototype of a new graphical user interface, followed by feedback results of this interface, described in section 7.3.

### 7.1 Latest model interface

Over time, the requirements identified in section 5.3 have been implemented more completely, and integrated into the model interface (Figure 7.1). Parameters have been split up more into sub sections in the interface, and for other parameters that were previously more laborious to enter and modify, a better solution has been found using a grid view. Also as more of the models and operation modes described in the modelling chapter have been implemented, the user interface has been adapted accordingly. In this interface, the different views can all easily be accessed via a single tab control, further making the work flow more intuitive.

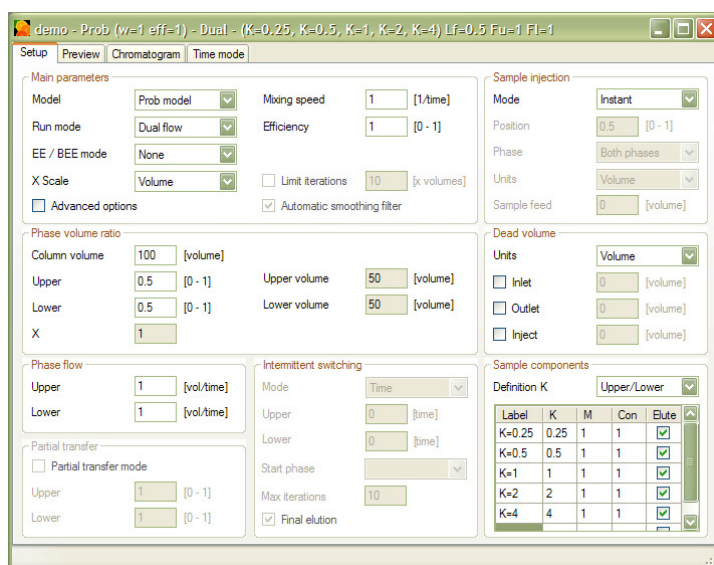


Figure 7.1 Interface accommodating an increased number of input parameters. Sample components can be entered and modified directly using a grid view (bottom right).

The interactive configuration explorer likewise evolved with the implemented models, showing relevant controls depending on the currently selected model (Figure 7.2). In this view, the graphical and numeric display improved showing more result detail.

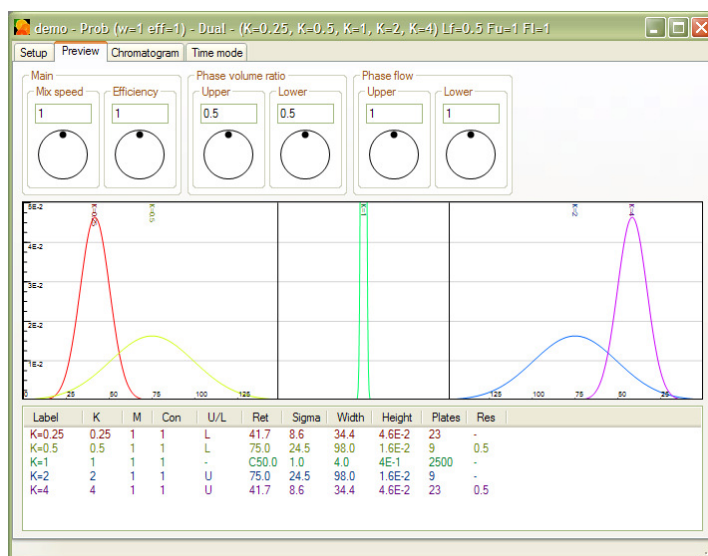


Figure 7.2 Screenshot of model: Real time interactive configuration explorer; with interactive controls relevant for currently selected model (top); chromatogram view (centre); key numerical results (bottom).

Additionally, the probabilistic units are visualised alternatively as unit density, shown in the chromatogram view (Figure 7.3), and in the time mode view (Figure 7.4). The 3D time trace view has been removed from the model interface, as the insight evaluation results revealed no added value.

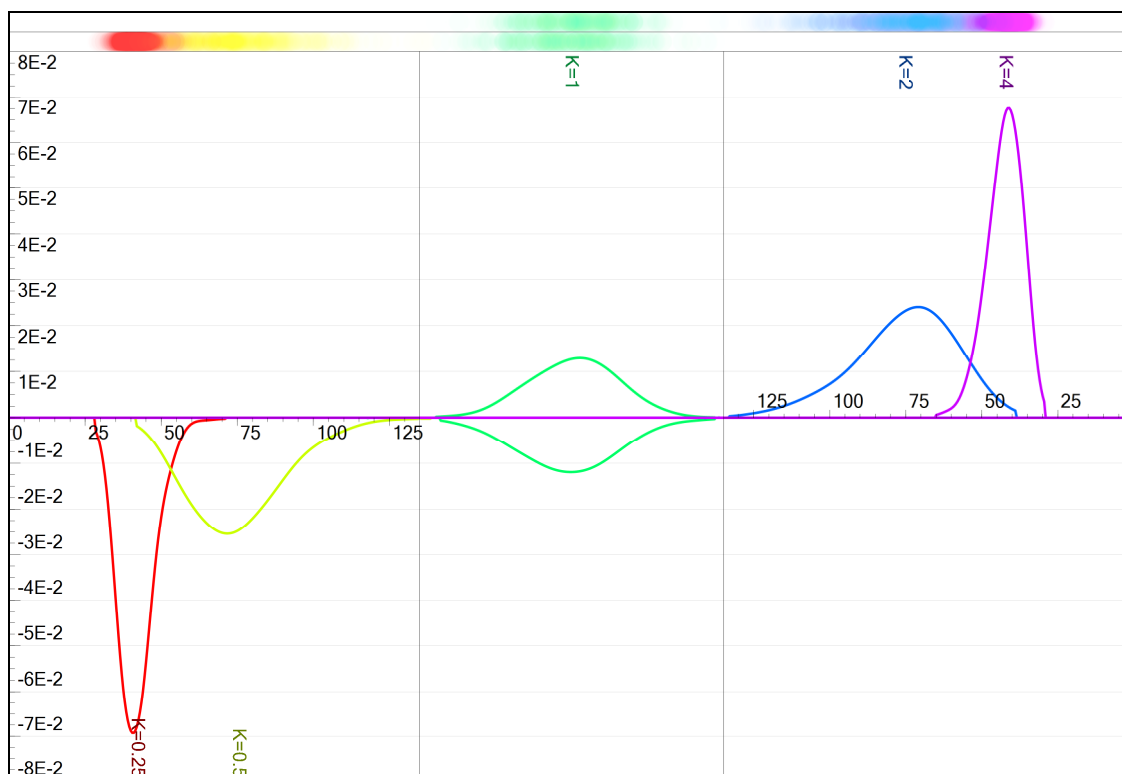
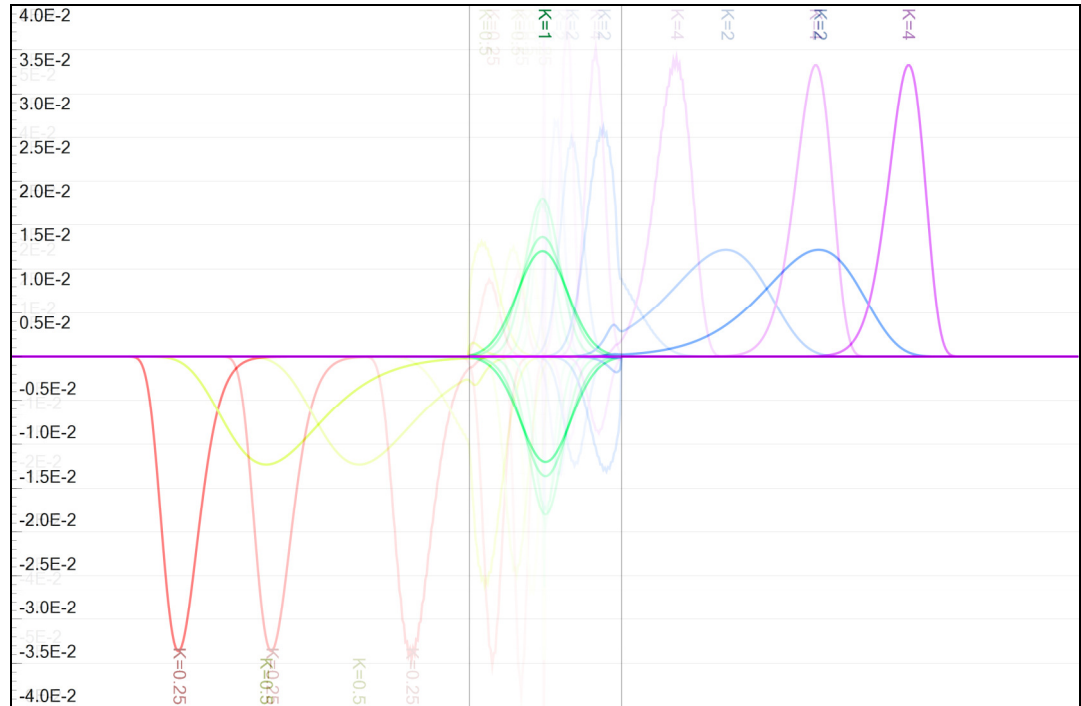


Figure 7.3 Chromatogram view, showing upper phase component in the upper half, and lower phase component in the lower half, visualising probabilistic units at the very top.

A



B

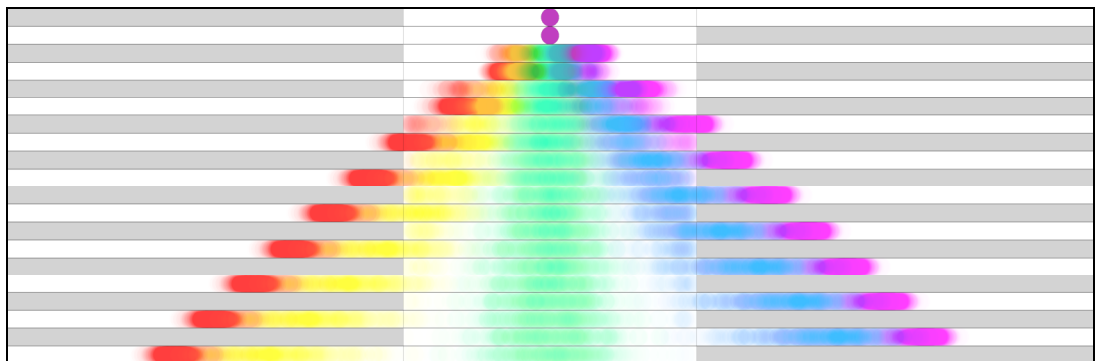


Figure 7.4 Superimposed screenshots of model: A: Time mode chromatogram where different views are shown in different opacity in this figure, illustrating the view at different points in time of the simulation process (at different positions of the slider control); B: The probabilistic units showing time from start to end (top to bottom).

## 7.2 Prototype graphical user interface

After receiving feedback on the computer model at an informal meeting of the current Brunel Institute for Bioengineering CCC research team at Brunel University on 11/3/2011, a new idea about a further improved user interface started forming. As more models were integrated into the user interface, three at this stage, and more model input parameters were added to the interface over time, the initial parameter setup window contained all these parameters. As mentioned before (section 5.3), a general comment at the main biennial CCC conferences was 'to keep it simple' [Berthod 2009]. It seemed a way should be found to reduce the apparent complexity of the user interface. Another main comment was 'to make [the model interface] more accessible to the CCC field; to enable them to use it'. Possible solutions considered for these issues, was to somehow partition the input parameters, only focussing on one particular category of parameters at one time. Then additionally a profile could be used, for example a CCC profile, where only parameters would be shown for that profile, or shown in the context of that profile. Another idea was to make a more visual user interface, incorporating a graphical representation of the chromatography system to increase understanding of the model and its configuration. This representation could then change according to the profile chosen. In this case the profile could be a chromatography method, such as CCC, CCD, CPC, etc., each showing a unique graphical representation.

This need was addressed by developing a completely new user interface. A Horizontal Prototype was made for this interface, combining the setup and preview screens into a single view (Figure 7.5). This interface incorporates a graphical representation of the chromatography system, which is different for each 'profile' chosen (i.e. CCC, CCD, CPC as shown in Figure 7.6), automatically selecting the most suitable model. The graphical interface is interactive, dynamically changing as key model parameters are changed. Different elements of the system can be selected, showing the model input parameters related to the selected element. The chromatogram view was also made more interactive (Figure 7.7).

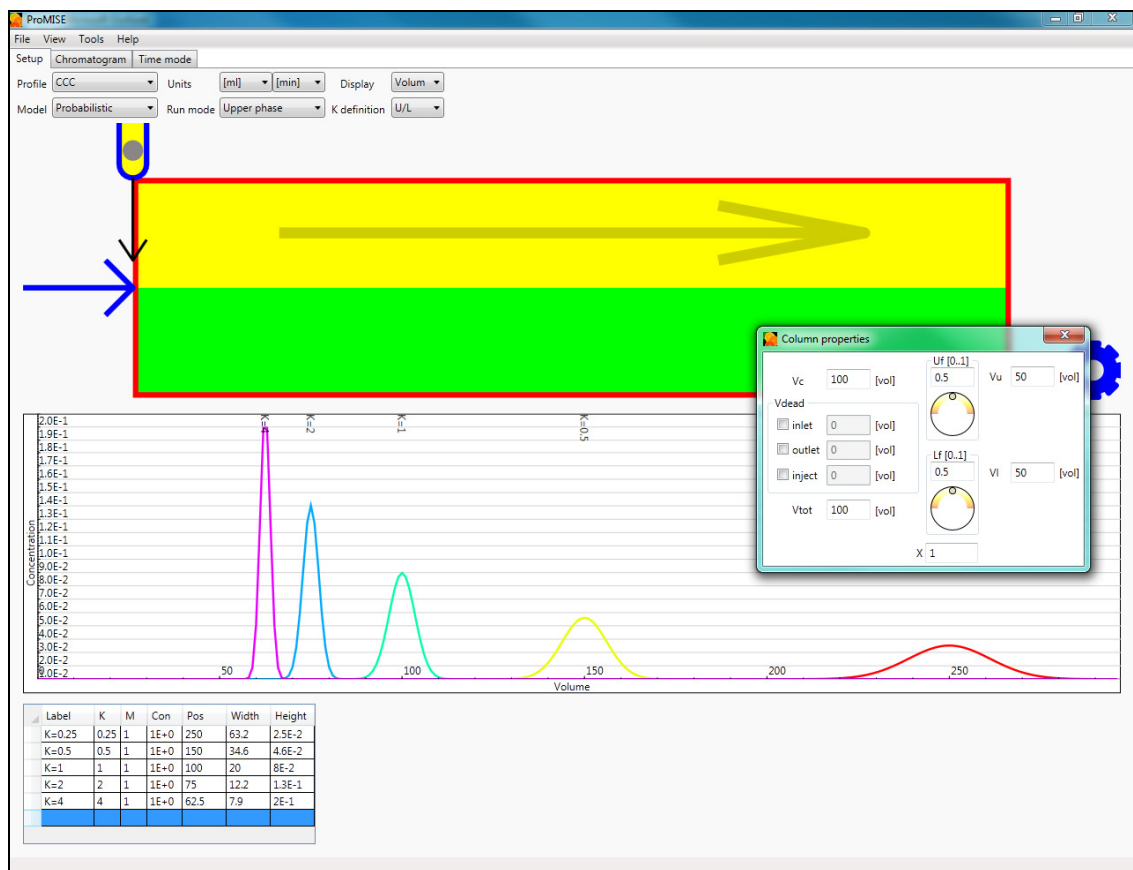


Figure 7.5 Prototype of combined graphical user interface; from top to bottom: general parameters, graphical representation of system according to profile, model input parameters for selected element (right), preview chromatogram, main chromatogram peak values. As the main input parameters are changed, the graphical representation dynamically visualises these changes.

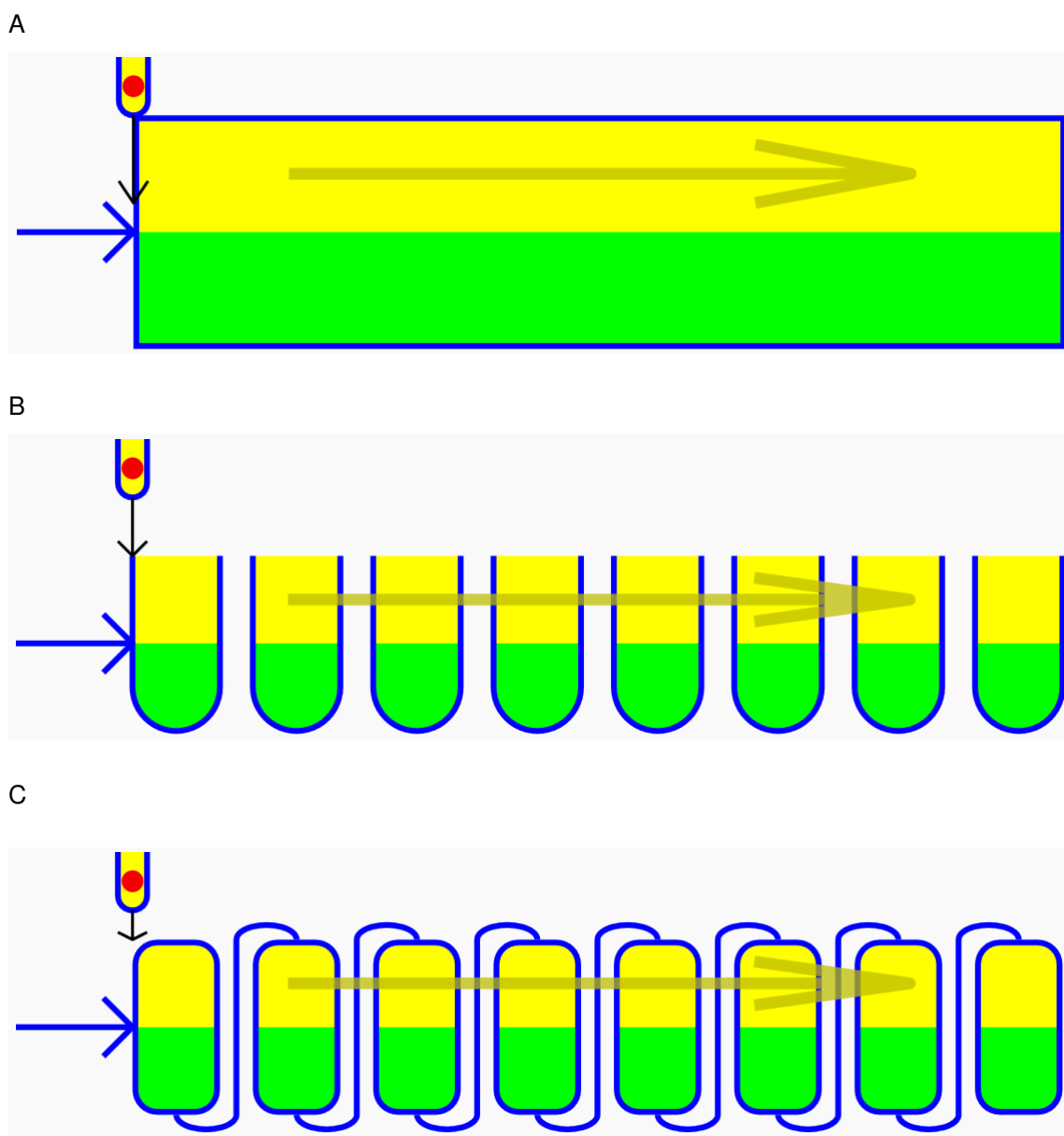


Figure 7.6 Visual representations of chromatography systems used in new graphical user interface A: CCC, B: CCD, C: CPC; The mobile phase arrows, phase distribution, point of injection etc. are visually represented, and change real-time as model parameters are changed.



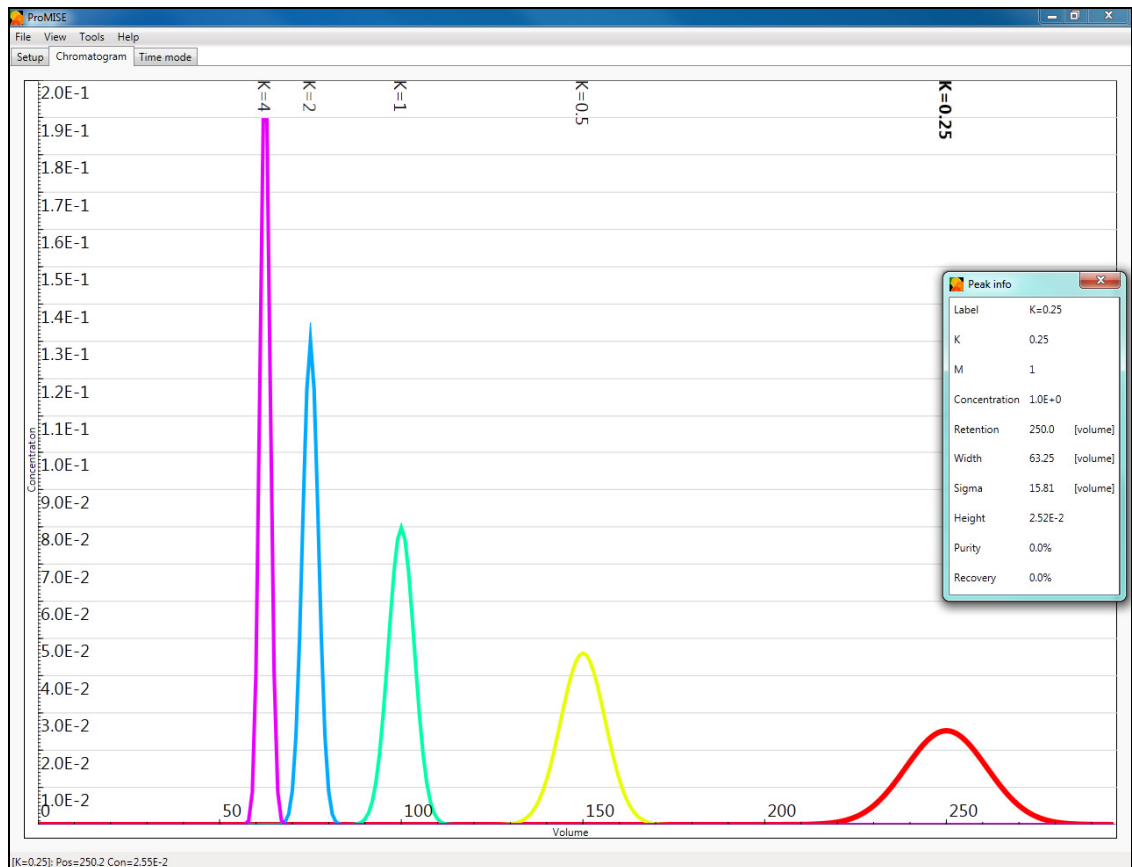


Figure 7.7 Prototype chromatogram view. Numerical values displayed by hovering over a peak, and main peak values displayed by selecting a peak.

User feedback collected on this prototype is described in the following section.

### 7.3 Prototype graphical user interface feedback

Summary feedback was collected using a focus group, using an unstructured group interview. The reason for choosing this feedback method was gaining consensus view of the system as opposed to personal feedback at this stage.

A prototype of this new graphical user interface was demonstrated, where the group interview was guided by a number of key questions (Appendix E). The main comments from the feedback on if and how the new interface has improved are summarised as follows. This new interface is indeed an improvement over the current model interface, the screen is not crowded, it is more modern and visual, it enables step by step modifying the model input parameters, and it shows the real time preview.

In response to the comment of elements being non-intuitive or difficult to understand, it was suggested to remedy this by clearer labelling in some sections. The areas on the graphical representation were highlighted while the mouse moved over them, but did not stay highlighted after being selected and the specific properties window appeared, therefore it was suggested to keep it highlighted. The units of the input parameters appeared unknown, so it was suggested adding units to them and additionally provide default units applicable to all parameters in a central location. Another comment was about the definition of the K value. When this definition was changed (e.g. from  $C_U/C_L$  to  $C_L/C_U$ ), the K values themselves were expected to be adapted accordingly. It was suggested to implement this, and make this automatic adaption optional.

Functionality to be added included: tooltips when moving over the selectable elements of the graphical representation, showing a short summary of all the parameters somewhere in the window, enabling the units to be chosen for all the parameters, and finally being able to print and export result data. Some of the functions to be added were actually already available in the current model software.

In summary, the visualisation development of the model interface was continued and further improvements were being implemented. As a result of an increasing amount of implemented model parameters, the interface has become more 'crowded'. This, and considering further feedback, in turn motivated development of a new, more integrated, completely graphical user interface addressing mentioned issues. A prototype of this interface has been realised and evaluated by collecting summary feedback using a focus group.

## 8 Educative visualisation

This chapter describes the development of an improved visualisation tool for the purpose of educative visualisation. Section 8.1 describes the tool and its development. Next, section 8.2 describes the evaluation method used to evaluate this improved visualisation. Section 8.3 discusses the results of this evaluation, and finally section 8.4 describes possible improvements to the visualisation resulting from the evaluation.

### 8.1 Improved visualisation tool

With the aim of educative visualisation, and simply to illustrate the concept of chromatography, a special visualisation tool was developed. This tool was based on the actual model, allowing the same model input parameters, but showing the column as a series of test tubes (Figure 8.1).

In the original visualisation (Figure 2.14), the component concentration was visualised as a discrete number of particles. However, it should be clear that only so many redistribution steps can be performed (usually only 2 steps), before a reasonable discrete number of particles would end up as a fraction. And this only worked for certain  $K$  values that resulted in a dividable number of particles. To be able to perform continued component redistribution even to the point of component elution and beyond, in the new visualisation the component concentration was instead represented by a single solid circle in each phase, where the area of the circle is calculated by the component equivalent mass. The old visualisation only enables showing 2 or perhaps 3 components maximum. To enable visualising more sample components, the phase area was split up in an optimal way (i.e. in horizontal and vertical direction showing 2 x 2, 3 x 3, etc. components). Above the CCD column representation, an additional test tube is shown for each sample component, indicating its  $K$  value and initial distribution over the phases according to the  $K$  value. Where the old visualisation showed the upper and lower phase each using a fixed colour, this has been removed and replaced by a composite colour representing the mixture of the different components in each phase / tube, providing more useful information and additionally giving a good visual overview of the general component separation along the chromatography process (Figure 8.1B). In the old visualisation, the component transfer was visualised by moving all the upper phase areas 'jumping' from one test tube to the next along an arched path. However, similarly visualising lower phase transfer is not really feasible. So in the new visualisation, the phase areas were simply 'sliding' from one test tube to the next in a straight line. An improved version of the animation (taking feedback from following evaluation into account) is currently available online <sup>4</sup>.

---

<sup>4</sup> <http://vimeo.com/joostdefolter/albums>

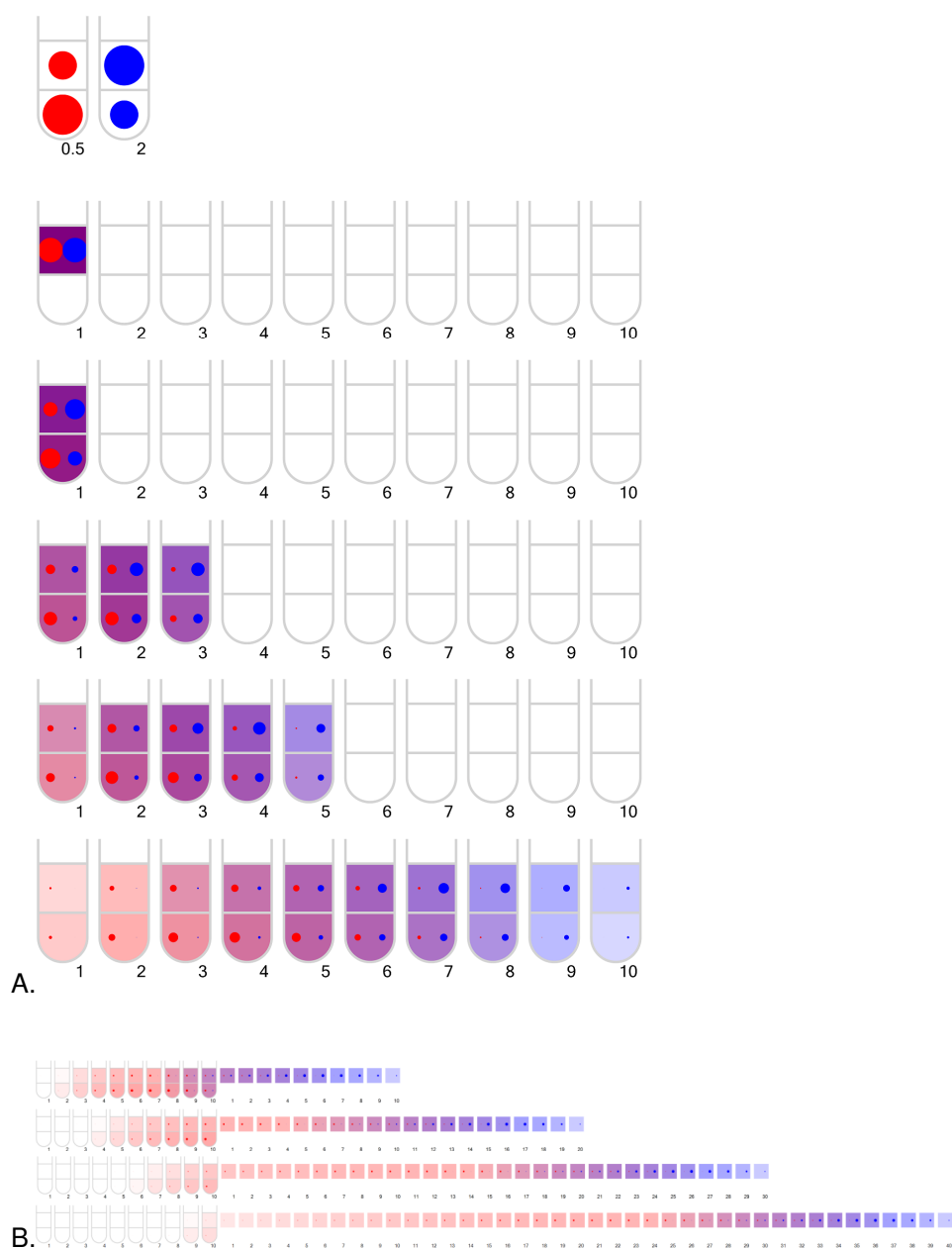


*Figure 8.1 Visualisation tool illustrating chromatography process: A. Sample components to be inserted (top left) are inserted into the first cell of the chromatography column representation. The column is represented by test tubes with the upper half showing the upper phase, and the lower half, the lower phase. Component mass is represented by coloured circles, and component concentration by the background colour of each cell; B. further showing component eluting from the column. Each horizontal column line represents a different point (in time) in the separation process.*

The animation tool was implemented using the same development environment used for the main model software. The tool actually incorporates a reduced implementation of the model, based on the CCD model. This means it can use the same model input parameter (files) used for the main model, incorporating the different modes of operation, such as normal mode, reversed mode, co-current mode, dual flow mode and intermittent flow mode. As the tool is used for visualisation, input parameters more suitable for this are used (i.e. a small number of system cells, more contrasting K-values).

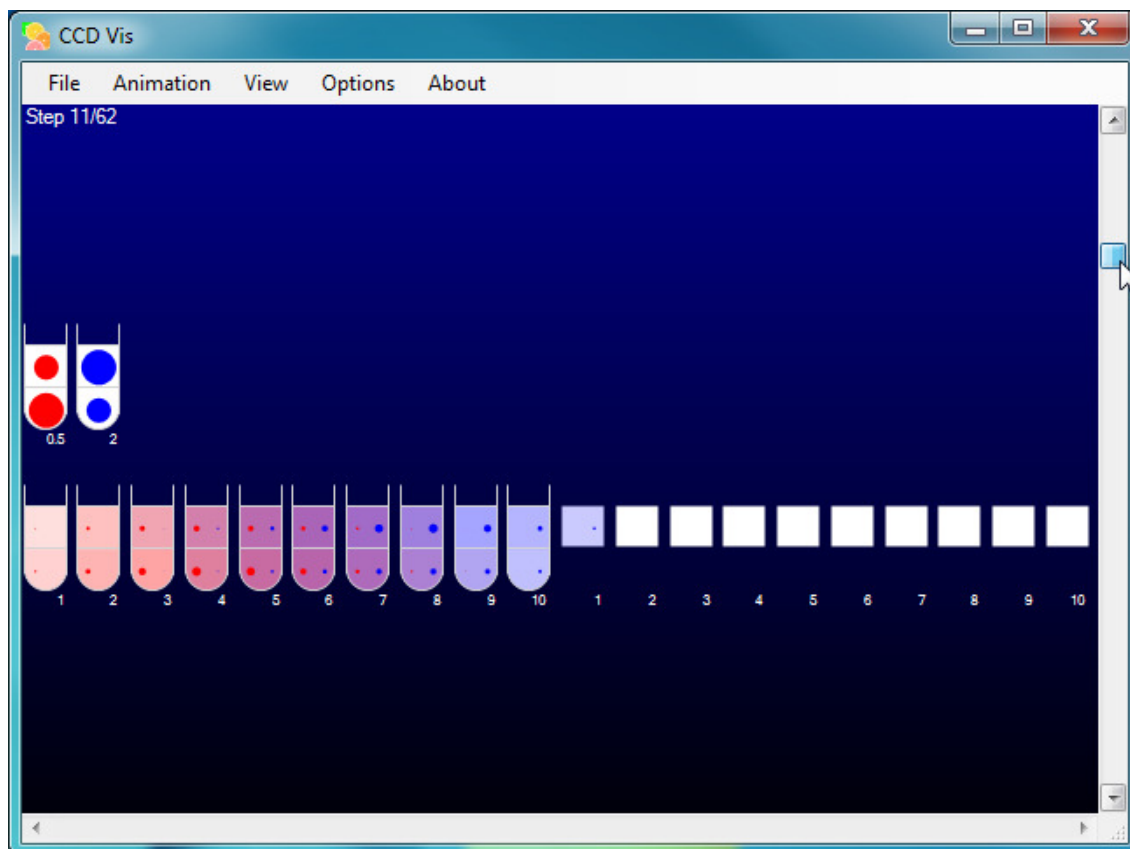


*Figure 8.2 Visualisation tool screenshot showing slider control manipulation to advance animation*

A slider control enables the user to move to any point in the simulation showing the component equivalent mass, and concentration of each cell (Figure 8.2). As the component concentration is shown by varying the background colour of the test tubes, this results in a gradient colour clearly visualising how the sample components resolve over time. As component is eluting from the column, mobile phase cell content is also shown. The display is highly customisable, and can be saved as images or a series of images that can easily be converted into a video file format. Although the tool incorporates the process to be automatically animated on the screen, the animation exported as video gives a more consistent playback quality and performance.

The next section describes an evaluation that was performed on how this improved visualisation compares to the 'old' visualisation (Figure 2.22).

## 8.2 Evaluation

Feedback was collected from colleagues with a varied experience with chromatography. First the old visualisation was shown (Figure 2.22), followed by the new one (Figure 8.1). At this point subjects were asked to fill out individual questionnaires, recording numerical values (ranging from 1 to 10) on the usefulness of the visualisation, whether it increased subjects' understanding, and how it compared to the old visualisation. Additionally there were some open questions; see Appendix F for the full questionnaire. After this, summary feedback was collected of the same subjects as a group, with guiding questions (see Appendix G). The results of this evaluation are shown in the following section.

## 8.3 Evaluation results

The quantitative results of the questionnaire are shown in Table 8.1. These results show most subjects consider this a useful tool for chromatography novices (average 7.5 out of 10), it increased most subjects' understanding of the chromatography process (average 7.9 out of 10), and the new improved visualisation was mostly considered better than the old visualisation (7.5 out of 10). Subjects that gave a low score (5 or less) in general commented in the open questions they particularly liked a visual element of the old visualisation, no longer present in the new one.

*Table 8.1 Feedback results*

Subject	Chromatography Experience	Experience [years]	Useful for novices	Increase understanding	New vs. Old
1	Yes	38	9	5	8
2	Yes	25	4	8	5
3	Yes	10	7	9	10
4	Yes	8	10	10	7
5	Yes	6	4	5	4
6	Yes	5	8	9	9
7	Yes	2	8	8	8
8	Yes	2	9	8	8
9	Yes		7	7	7
10	Yes		9	9	8
11	No		8	9	8
Average			7.5	7.9	7.5

The open questions on the questionnaire gave additional feedback. The general comment was that the new visualisation was better, as it showed more than 2 compounds, more steps, different modes of operation and considered to be more accurate. However, the old visualisation was considered good as it showed a discrete number of particles, slow, phase transfer and was 'zoomed in' showing large test tubes. At this point it should be noted that a number of the improvements in the new visualisation excluded certain elements that subjects appreciated in the old visualisation.

The subsequent summary feedback, collected after the subjects had completed the individual questionnaires reinforces earlier feedback, concentrating in more detail on these main points. The first guiding question in the group interview was, if the new visualisation was better than the old one, and if so, in what way. A general suggestion was to keep the old visualisation as first introduction, and next show the new visualisation. Alternatively, some of the elements of the old visualisation could be integrated into the new visualisation. Another comment was to possibly show the concentration graph (chromatogram) in the animation underneath the test tubes.

The second guiding question in the interview was about the purpose; what would the visualisation be used for. The main comment was to use the visualisation to demonstrate different modes of operation, as not only the classic isocratic flow modes, but also the dual flow, co-current and intermittent modes could be visualised. Another general comment was that the isocratic mode animation was considered useful for educational purposes as it showed the chromatography column, the components inside the column, and showed how the components eluted.

The third guiding question was if the visualisation could further be improved. The main proposal was to reduce the speed of the animation. An important suggestion was to visualise continuous chromatography instead of the test tubes (like in Figure 2.23). Another remark was about the  $K$  value definition, and whether this could be customised (i.e.  $K = C_S/C_M$  instead of  $K = C_U/C_L$ ). A suggestion was to run a PowerPoint presentation to manually advance through a set of still images. Finally, instead of showing the animation video, it was suggested to use the visualisation tool directly for improved control.

## 8.4 Improvements to visualisation

Looking at the user feedback obtained in the evaluation in more detail, it can be determined how a number of improvements could be made. The first and foremost of the comments was the animation speed. This could easily be adjusted, and in fact does not even rely on the visualisation tool, but rather on the frame rate set in the used stills-to-video conversion tool. As the original animation showed only 2 redistribution steps, and the new animation shows many steps, simply reducing the speed in the new animation would result in a very long animation. The solution for this would be a varying speed, starting slow and then speeding up as the sample components start to elute. Further elements subjects appreciated in the old visualisation were removed to enable visualising new modes of chromatography operation and other new elements subjects considered improvements over the old visualisation. This can therefore be considered a trade-off. Visualising other modes of operation, such as the co-current flow and intermittent mode are already possible, but were not included in the demonstration for the evaluation. Regarding the comment about the K value definition, this option is actually already available in the parameter configuration. About allowing users to manipulate the visualisation tool directly instead of showing a prepared video, although this is possible, in order to show the animation, the user would need to configure the visualisation tool which is not as easy as simply playing a video. Additionally, the mentioned improved level of control in terms of moving forward and backward in the chromatography process is arguable, as the same could be done with the video.

In summary, the basic chromatography visualisation showing the CCD test tube transfers has been widely used in the CCC field, in the form of an illustration showing a series of test tube sets, and in the form of animations. From the latter, a new animation was created enhanced with various different visual elements. For the purpose of customisation, for different flow modes and sample mixtures etc., a tool was developed that can create these custom animations. This new visualisation tool has been evaluated using individual questionnaires and a group interview. The evaluation showed the new animation tool has been an improvement on the previously created animations. Feedback and suggestions from the feedback have been taken into account, and from this, further improvements to the new visualisation have been identified.



## 9 Discussion

This chapter discusses the results for both modelling and visualisation and puts these into context. First, section 9.1 discusses modelling results. Next, the software implementation and the used methods are evaluated in section 9.2. The visualisation results are discussed in section 9.3. Section 9.4 finally discusses the integration of model and visualisation.

### 9.1 Modelling

Here the modelling results described in chapter 4 are considered. First, elution results are discussed (section 9.1.1), considering the various liquid-liquid separation techniques. Next, accurate sample injection results are discussed (section 9.1.2), followed by comparing results from an efficiency study (section 9.1.3). Finally the different models developed are discussed (section 9.1.4).

#### 9.1.1 Elution

This section discusses modelling elution results from section 4.1.

##### CCD

Model comparison with CCD as a classical chromatography technique was included for completeness (section 4.1.1).

As expected, the elution predicted by the CCD model concurs almost exactly with the experimental results. The model error in peak position and width, for peaks inside the column and eluted are small. Note that in this case no model calibration was necessary, as the model was simply set up using exactly the same parameters as the actual CCD experiment. Also as the model results match the experimental results very well, this confirms the mixing efficiency in this process is indeed 100%.

##### CPC

Two CPC cases were modelled (section 4.1.2). The efficiency of the mixing in each chamber is obtained by configuring the model as described in section 3.8. So the efficiency values used in the model to match experimental results are actually as much part of the model configuration as a valuable result.

Case 1 presents a model comparison of a single component (an antibody molecule) elution using a CPC instrument. The CCD model showed good correlation, with only a small error in model peak position (3.5%) and width (3.7%), using the configuration where the number of model cells matches the number of CPC chambers in the experiment. An efficiency of 40% was obtained to match experimental data. This is effectively a comparison of the CPC instrument considering each chamber a mixing / settling stage.

In the case reported in literature [Sutherland et al. 2008], the CCD model shows good correlation with the CPC experiment. The model comparison performed here as case 2 was set up similarly to CPC case 1 discussed previously. This study compares two CPC instruments. Modelling results show a similar correlation to the experimental data as the CCD model set up reported in literature (laboratory scale instrument: average error in peak position: 0.5% and width: 7.9%; pilot scale instrument: average error in peak position: 7.7% and width: 2.0%). However, the experiment was modelled more accurately in the current research, and additionally mixing / settling efficiencies are obtained. Opposed to the current research, the efficiency values reported in the literature [Sutherland et al. 2008] are not taking the efficiency value correction into account (as shown in Figure 3.8 and equation (3.29)). Without this correction, the mixing / settling efficiency is basically undervalued. Note that this is especially the case for low efficiency values (less than 10% efficiency) resulting in a difference of a factor of 2 approximately as can be observed in Figure 3.8A. For higher efficiency values (50% or more), this deviation is considerably less.

The mixing / settling efficiency is in the same order of magnitude for both instruments of case 2, and for both cases presented in the current research. The efficiency is lower than that of CPC case 1, which makes sense as the flow rate is higher than that of case 1. However, comparing the mixing efficiency of the two experimental setups reported here, the larger scale instrument shows a larger efficiency. However, the number of mixing chambers in both setups needs to be considered here. Compared to the smaller scale instrument, the mixing efficiency of the larger scale instrument is about 48% higher. The number of mixing chambers is interestingly about 48% lower in the larger scale instrument compared to the smaller scale one. This does not seem to be considered in the published research [Sutherland et al. 2008], and is interesting from a scaling point of view. Additionally it would be interesting to see if the different scale instruments could be modified so they have a matching number of mixing chambers, and perform more comparative experiments on these.

## CCC

The CCC modes isocratic, co-current, dual and intermittent mode were modelled (section 4.1.3).

Experimental data was compared to the theoretical, CCD, probabilistic, and transport models. The theoretical values are obtained using the theory as described in the simplified model (section 3.4). Note that the setup of the model parameters was different from that in previously published results [de Folter, Sutherland 2009], not only comparing peak position, but now also considering the peak widths. Each model used fixed specific model input parameters for all the experimental conditions, and therefore only total average errors are shown.

Starting with the isocratic mode, model results were compared to experimental data (Table 4.4) of a separation of two components with increased mobile phase flow rate. The modelled peak position for all the models shows very good correlation with the experimental data. However, the error in peak width shows a relatively large error compared to peak position. This is even the case for the theoretical model (15%). The reason for this is that the nature of the K-value theory and its definition result in an absolute value for the peak position, not relying on many experimental conditions. But the equation for the peak width is more empirically obtained, relying heavily on experimental conditions, with the mixing efficiency possibly introducing the largest variation. It is noted here that predicted values for more extreme values of K (in the order of 0.1 or smaller, or 10 or larger) show an increasing deviation from experimental data. Taking this into account regarding the peak width, looking at the CCD model, the modelled results show a reasonable correlation with the experimental data (average error of peak position: 0.3% and width: 14%). Modelled results using the probabilistic model show reasonable correlation with experimental data as well (average error of peak position: 0.7% and width: 15%). However, using fixed specific model input parameters for the transport model, modelled results show an increasing error in peak width for increased flow rate (average error of peak position: 0.3% and width: 29%). This suggests that for the transport model, different model input parameters are required for different experimental conditions, while for the CCD and probabilistic models, the same specific model parameters can be used for similar experimental conditions. More on this will be discussed in section 9.1.4 which compares the different models.

Next for the co-current mode, for each model, again the same specific model input parameters were used for the different experimental setups (Table 4.5). In general, except for very low and very high K values, the modelled peak width correlates well with experimental data using the different models, as can also be appreciated in Figure 4.3 and Figure 4.4.

Dual flow experiments match reasonably against experimental data, considering dual flow case 1 (Table 4.6). However there is a significant deviation of about 20% in peak position. The asymmetry of the peaks possibly account for some of this deviation. Another interesting observation can be made comparing the theoretical model to the CCD, probabilistic and transport model in terms of the peak position. In the case of asymmetric peaks, it appears the theoretical peak position, does not match the peak maximum, but rather, the peak average ( $\mu$ ). In dual flow case 2, a slow sample injection is modelled (Figure 4.5). For this type of injection, the peak width becomes less interesting, as it would correspond more to the injection time. As in this case peak position also is somewhat arbitrary, results were compared graphically instead of numerically. Considering the actual experiment, where there is a slow but constant sample injection, one would expect a smooth curve for the experimental data. The sudden jumps in the centre of the graph of the experimental data are therefore considered noise / inaccuracy or some experimental inconsistency. This could be caused (in part) by the reported manual back pressure control during the experiment [Ignatova et al. 2011]. However, apart from this the model results show reasonable match with the experimental data. Perhaps the shape of the peaks is of most interest here, which shows similarity across the different models.

Finally intermittent mode CCC was modelled, and compared to experimental data. This was done by graphically comparing the accumulated concentrations, which indeed show a reasonably good correlation for this experimental comparison. However, it must be noted that intermittent mode proved hard to model in general, as was attempted for various cases of the same publication [Hewitson et al. 2011] and from other publications [Hewitson et al. 2009] and [Ignatova et al. 2011]. There are a number of possible reasons for this, such as variable phase retention (phase ratio) in the columns during the switching, and non-homogeneous phase distribution, possibly similar to the one observed in dual flow mode by van den Heuvel [2008]. It appears the intermittent operation mode itself is still very novel and is expected to benefit from more research being done on it.

Considering how representative these comparisons with experimental data are, modelling isocratic experimental results which were not presented here, also show good consistency similar to the presented results. The same was observed for the co-current and dual flow mode data. However, for intermittent mode, this was not the case. As afore mentioned, intermittent mode data proved hard to model in general, and from 5 experimental data sets that were considered, only 1 could be modelled with reasonable correlation. Although the accuracy of the experimental data used for the model comparisons can't be commented on or validated, there are some observations to that effect. The most obvious and significant one is that in many cases the K-value and phase retention are reported with only 1 or 2 significant figures (e.g. a value of 0.3 implies a potential inaccuracy of up to  $\pm 16.7\%$ ).

### **Droplet CCC**

Droplet CCC is a somewhat historical separation technique, but was included for completeness (section 4.1.4). The model configuration was not as straight forward as for other techniques such as CCD, CPC and CCC.

First the CCD model was used, modelling each experimental tube as a CCD cell. This comparison (Table 4.7) showed quite poor results in terms of the peak width (average error 88%) compared to the experimental data. Next the CCD model was used again with the same number of cells, this time using a partial transfer. This showed very similar, poor results in peak width (average error 89%). Finally, the probabilistic model was used, showing reasonably good results (average error 16%). This shows Droplet CCC is better modelled with the probabilistic model and indicates this technique to be a more continuous behaviour. What is also interesting here is the mixing efficiency obtained (10%) is in similar order of magnitude as used for the other continuous technique CCC. So on the one hand there is no rigorous mixing like in CCC, but on the other hand, the mobile phase flow rate is extremely low, allowing the sample components more time to interact with the phases and separate. It appears the obtained efficiency value results from these two opposing effects.

### **Vortex CCC**

As a more discrete technique, Vortex CCC was modelled using the CCD model (section 4.1.5). The model results matched experimental data reasonably well (Table 4.8) (average error peak position: 10%, peak width: 24%). Comparing the high obtained mixing efficiency (80%) to CPC modelling results, it appears the Vortex mixing is a very efficient type of mixing.

### **Toroidal CCC**

The toroidal coil CCC experiments were modelled using the CCD model (section 4.1.6). Sutherland et al. [2011] describes Toroidal CCC as a discrete technique, suggesting each coil turn considered a discrete mixing chamber, so the model was set up accordingly. The CCD model was first set up using a partial transfer simulating the amount of volume transferred between each mixing / settling cycle caused by the planet motion centrifuge. This did not give good results in terms of peak width (average error 32%). Next, the same CCD model was used this time using the normal complete transfer, but using an efficiency value representing the mixing efficiency for each discrete step. The results of the CCD model using regular discrete transfer mode showed good results (average error of peak width: 9%), with a cell mixing efficiency of 22%.

## **Control-cycled pulsed liquid-liquid chromatography**

Control-cycled pulsed liquid-liquid chromatography is a very recent experimental technique developed by Kostanyan and colleagues [Kostanyan et al. 2011]. Literature mentioned the CCD model was used for comparison but no such results published. Modelled results of the CCD model were compared to experimental data here (section 4.1.7).

This technique is a discrete technique. Although CCD modelling results were reported matching published modelling method [Kostanyan 2011], this was only achieved by using different specific model input parameters. For different components, different efficiency values were used to successfully match to the experimental data. The mixing efficiency used to model the experimental data ranged from 29% to 59%, with an average of 41%. This is very unexpected, as peak broadening should be consistent for all components using a single efficiency value for a single experimental set up.

### **9.1.2 Sample injection**

This section discusses results from section 4.2.

Experimental CCC data with different concentrations was used for accurate sample injection modelling. The CCD, probabilistic and transport model were used. The model results showed a reasonable correlation with experimental data (Table 4.11) (average error of peak width for CCD model: 18%, probabilistic model: 21%, transport model: 15%). The peak positions could not be matched exactly (average error for CCD model: 17%, probabilistic model: 15%, transport model: 15%). An issue here was that the phase retention greatly varied during the experiment. Additionally, a time offset was applied to the experimental data, which may not have been corrected for accurately. However, the model results correlate quite well comparing the peaks of different concentrations which was the most important factor in this modelling experiment, and peak shapes look very similar to the experimental data qualitatively (Figure 4.7). What is also interesting to see is that all three models show very similar results, especially in peak shapes.

### **9.1.3 Efficiency**

This section discusses results from section 4.3.

Sutherland and colleagues recently performed research on stage efficiency of discrete chromatography techniques, using the CCD model [Sutherland et al. 2011]. In the current research an alternative efficiency study of continuous techniques was performed using the CCD and probabilistic models (Table 4.12). This experiment effectively calculates the mixing efficiency for various CCC setups. The CCD and probabilistic model show similar efficiency values. Interestingly these results show that for higher flow rates, in general higher efficiency values were obtained indicating better mixing.

### **9.1.4 Models in general**

#### **CCD model**

The CCD model gave good results for chromatography methods more discrete in nature such as CCD, CPC, Toroidal CCC and Vortex CCC. As to be expected, the CCD model very accurately matched the CCD experimental data. This was also the case for CPC and Vortex CCC, although their phase flow being of a more continuous nature, modelled very well using the CCD model. Therefore, for modelling discrete, hydrostatic type chromatography methods, the CCD model is recommended.

#### **Probabilistic model**

The probabilistic model accurately models the isocratic flow, co-current flow, dual flow and intermittent mode CCC. Although the CCD and transport model also give good results compared to experimental CCC data, the probabilistic model has the additional advantage of having more CCC related specific model input parameters, compared to the other models that have more theoretical model parameters. This model was considered ideal for modelling the continuous, hydrodynamic chromatography methods.

#### **Transport model**

The transport model showed good results for continuous types of liquid-liquid separations, including accurate sample injection. However, to further improve the accuracy of this model, the step size (for time  $\Delta\tau$  and distance  $\Delta Z$ ) needs to be decreased. This requires significantly more computational power in its current form. Additionally, the specific input parameters of this model are more theoretical in nature, making the model configuration and calibration to experimental data more complicated. The following section compares the transport and probabilistic models.

#### **Probabilistic model versus transport model**

As both the probabilistic and the transport model appear suitable for modelling continuous chromatography methods, it seems appropriate to compare their strengths and weaknesses, to determine which would be preferable to use (Table 9.1).

Table 9.1 Continuous model comparison

	<b>Probabilistic model</b>	<b>Transport model</b>
<b>Strengths</b>	Model parameters relate directly to experimental conditions	More traditional method
	Model results relate directly to physical parameters allowing direct conversion	
<b>Weaknesses</b>	Random element results in 'noise' when using low number of model units	Model parameters do not relate to experimental parameters
		Computationally very demanding to reach satisfactory accuracy

From this comparison it is clear the probabilistic model is preferred over the transport model (in its current form) to model continuous chromatography techniques. The most significant difference is in the nature of these models, where the probabilistic model relates directly to experimental conditions, and the opposite was observed in the transport model.



## 9.2 Software implementation

A User Centred Design (UCD) was followed in the design and development of the model user interface. Chapter 5 shows UCD is indeed an effective method of design with a lot of flexibility, contributing to developing a useful interface effectively taking user feedback into account. However in the UCD lifecycle model presented by Sharp and colleagues [Sharp et al. 2007], an important question is when, or if, the 'final product' stage is reached. Perhaps it would be better to call this a software / product 'release' step, where the iteration cycle can still continue after this, and can in turn produce another release, and so on.

The Evolutionary Prototyping [Sharp et al. 2007] approach was adopted, optimising continued development, reusing and enhancing the design across each feedback / modification iteration. This allows for more continuity of the interface, and is particularly helpful in case different versions of the software come in use along the development process, and users becoming accustomed to the interface, or if using the same subjects for successive evaluation iterations. However, it was found Evolutionary Prototyping is not always possible, when major modifications to the interface / behaviour are required, or when moving to another programming platform. This was the case in the development of the prototype of the graphical user interface (section 7.2).

The information visualisation reference model [Card et al. 1999] was used to implement the data flow from the model to the output view (section 3.7.2). This allowed an effective and optimised data flow, providing translation of the specific data format from each model to a common format, which could easily be exported to a spreadsheet program, and furthermore a speed optimised format enabling fast update of the interactive views.

The software implementation used Object Oriented Design and Design Patterns [Gamma et al. 1994]. The main design patterns used; Composition, the Observer pattern, Chain-of-responsibility and the Model-View-Controller combination, provided an efficient way of realising the software, maximising code reuse, resulting in well maintainable software. This is particularly important when developing continually changing software, due to different requirements specifications.

Using MS Visual C++ with the .NET library that provides an advanced and comprehensive collection of data types, mathematical functions, graphical functions and user interface controls, accelerated the implementation of the software. This furthermore allowed creating reusable custom controls; the 'jog' control and the interactive chromatogram views, which proved very useful. It also allowed developing speed optimised software resulting in very responsive model configuration and model output views.

## 9.3 Visualisation

Here the visualisation evaluation results described in chapters 6 and 7 are discussed. First the used visualisation techniques are considered (section 9.3.1). Subsequently, the insight evaluation results of the visualisation and interactive elements are discussed (section 9.3.2). Next, the prototype graphical user interface and its feedback is discussed (section 9.3.3). Finally, the improved visualisation tool and its evaluation are considered (section 9.3.4).

### 9.3.1 Visualisation techniques

The concept of model previews has been implemented resulting in an effective enhancement of the model interface (section 5.1). Adapting and extending concepts first used by Influence Explorer, model input parameters can be changed interactively, where the result complying with those conditions is shown in real time. In contrast to the developed model, the Influence Explorer [Tweedie et al. 1995; Spence et al. 1995] additionally enables determining suitable parameter spaces in respect to a desired model output. However, as mentioned before (section 2.8.3), this is only possible with a pre-computed data set. This appeared not feasible for the current model, which has a large number of independent parameters resulting in an equally large set of parameter permutations that full model results would need to be calculated for. However, the implementation of the interactive techniques shows how the user interface design contributed to the model configuration and interactive visualisation provided an additional tool for the modelling process. The initial evaluation of the model interface (section 5.2) indicated most of the implemented techniques were considered very useful. From the user feedback, new requirements were determined (section 5.3) and subsequently integrated into a model interface, optimising implementation of mentioned visualisation techniques (section 5.4). The evaluation of this interface will be discussed in detail in the next section.

### 9.3.2 Insight evaluation

This section discusses visualisation evaluation results described in chapter 6.

It can be seen that the proposed visualisations resulted in a relative increase in insights of 6.5 times over the basic chromatogram view. This proves the implemented visualisations give a major contribution to the understanding of the developed model and educational value.

The Interactive Chromatogram Explorer (ICE), implementing the interactive model configuration using the custom 'jog' controls, accounted for the majority (77%) of all significant insights achieved. The interactive time-mode chromatogram view accounting for 15% of the insights. Finally, the customizable chromatogram view accounting for the remaining 8% of the insights. The 3D time trace view did not account for any insights. The ICE mode furthermore generated five out of a total of six of the most important insights. It is apparent that most of these insights relate to what effect the input parameters have on the separation results, which are indeed very much domain related. This clearly proves the value of the insight evaluation method, providing valuable qualitative evaluation results desired for this model interface evaluation.

As mentioned in section 7.1, the 3D time trace view was removed from the model interface, as it indicated minimal to no contribution according to the evaluation results. The reason for this view not being considered useful, or not used much by subjects of the insight evaluation, is perhaps mainly due to the fact that sufficient information is already provided in the other interface views, and this 3D time trace view in turn doesn't contribute much over the other views. As concluded by Westerman and Cribbin [2000], the additional cognitive demands outweighed the extra information provided by 3D views, possibly another reason for this view not appearing useful from the evaluation results.

It is also interesting to see that the previously performed user feedback study showed similar tendencies to the insight evaluation results, to how the different elements of the user interface were valued.

The insight classification and scaled values (complexity and domain value) proved adequate for this study, and provided good detail and relevance. Although the general insight evaluation method was followed, subjects still seemed reluctant to be more explorative. Subjects possibly had an objective oriented mindset and/or had set a time limit in the context of the study. Another problem encountered was that some subjects tended to focus on the interface and its usability rather than the model itself, in spite of efforts made to encourage focusing on the behavior of the model. Overall, the number of recorded insights, whilst not as high as initially expected, was still sufficient to identify clear differences in the efficacy of each visual element.

Based on the success of the insight evaluation study, it was concluded that a longitudinal study of the same method could provide richer results [de Folter and Cribbin 2012]. This study was indeed started, by distributing the computer model amongst CCC experts, and explaining and encouraging them to submit insights as they occurred. The computer model incorporated an input screen, including insight classification, which could be easily filled out by subjects and automatically sent to the researcher. This method would allow users to fully familiarise themselves with the interface and to incorporate the interface into their natural work activity, overcoming a limitation of the supervised evaluation. Previous research [Saraiya et al. 2006] has shown that non-supervised recording of insights over a period of time provides subjects with significantly more freedom to achieve relevant and significant insights.

However, this study was unsupervised and relied on the users of the computer model voluntarily submit insights. Users were explicitly contacted and encouraged to take part in this study. Unfortunately no such results were actually received from users.

It seems that users were either not motivated, or unable to participate. The amount the users were actually using the model would also be an important factor. It is likely they were not constantly using the model, but more likely only for limited periods, to test the model in general or to compare and model a specific set of experimental data. Possibly there was reluctance to accepting modelling tools in general. Another cause may have been users not fully understanding or unable to relate to the task of explicitly recording insights.

Saraiya and colleagues [2005] found that subjects' motivation is an important factor on the number of insights reported. Perhaps users could have been encouraged more by providing a reward for participation. Secondly users could have been contacted repeatedly, reminding them of participation in the study. Another possibility would be to train participants in using the model, in particular how to record their insights. However by performing the latter, the study would then not be completely unsupervised, introducing bias.

### **9.3.3 Prototype graphical user interface**

The prototype graphical user interface feedback from section 7.3 is discussed here.

Summary feedback was collected using a focus group, using an unstructured group interview. The reason for choosing this feedback method was gaining consensus view of the system as opposed to personal feedback at this stage.

The prototype of the new graphical user interface was demonstrated, and summary feedback collected. Taken from the feedback, the main comments were that this new interface is an improvement as the screen is not crowded, it is more modern and visual, it enables step by step modifying the model input parameters, and it shows the real time preview. Although an in depth study has not been performed yet, based on initial feedback, it seems this new graphical user interface is a further contribution to the model interface.

### **9.3.4 Improved visualisation tool**

Scientific visualisation like shown in Figure 2.14 has been developed and widely used in the CCC field, proving a clear contribution of the educative visualisation.

The current section discusses the improved visualisation tool (chapter 8). The evaluation, consisting out of individual and group feedback, shows that in general the improved visualisation tool (Figure 8.1) is considered an improvement over the old visualisation tool (Figure 2.22). However, various elements of the old visualisation were considered of better educational value. Some of these elements were no longer present in the new visualisation, as they inhibited visualisation of the complete chromatography process and visualising advanced modes of operation. On the other hand, the main element considered of better education value, the movement being slower, would be very easy to implement, and actually depends more on the external conversion tool used to produce a movie from the exported still images. The evaluation showed most subjects considered the improved visualisation a useful tool for chromatography novices (average 7.5 out of 10), it increased most subjects' understanding of the chromatography process (average 7.9 out of 10), and the new improved visualisation was mostly considered better than the old visualisation (7.5 out of 10). This initial evaluation supports the contribution and educational value of the improved visualisation tool.

## 9.4 Integration

The integration of the chromatography model(s) with the visual and interactive elements (section 7.1) appears very useful. The visual / interactive enhancements are shown to directly contribute understanding and insight of the chromatography process being controlled by the interface.

The prototype of the new graphical user interface (section 7.2) attempts to take this integration even further, addressing all the newly identified issues of the user interface, resulting in an optimal environment for configuring the model.

The improved visualisation tool (chapter 8), using the model interface for parameter configuration and using the CCD model for subsequent visualisation, results in a valuable addition of the model with improved educational value.

The gap between visualisation researcher and domain expert that van Wijk reported [2006], has been bridged in the current research as both roles were in fact performed by the researcher. So this is effectively another way of bridging this gap, extending van Wijk's suggestion of "*domain experts to define visualizations themselves*" [van Wijk 2006].

## 10 Conclusion

This final chapter describes how the set objectives are met for modelling (section 10.1) and visualisation aspects (section 10.2), recommendations for future research (section 10.3), and ending with closing remarks (section 10.4).

### 10.1 Modelling

The models developed were demonstrated to model all main liquid-liquid chromatography techniques known to date (CCD, CCC, Toroidal CCC, CPC, Droplet CCC and Vortex CCC).

The models incorporated different modes of operation (normal phase mode, reversed phase mode, dual mode, co-current mode and intermittent mode).

The models are able to accurately model many sample components and complex sample injections and extended injections, such as used in high sample loading scenarios like in dual flow and intermittent mode injections.

The models show the sample components at the moment of injection, the final eluted results, and the chromatography process at any state in time, enabling appreciation of the entire chromatography process from injection to elution.

A new more elemental model was developed, the probabilistic model, which better models continuous liquid-liquid chromatography techniques. This model is not discrete in nature, and therefore does not have the number of model steps as an input parameter, and instead directly incorporates the mixing speed, which is a main liquid-liquid chromatography parameter. It also integrates an additional visualisation by showing the probabilistic units. This new model is considered a major contribution.

The CCD model is found most suitable for discrete chromatography techniques such as CCD, CPC, Toroidal CCC and Vortex CCC. The probabilistic model appears ideal for modelling continuous types of chromatography, such as CCC, including all its different modes of operation, such as isocratic flow, co-current flow, dual flow and intermittent mode. The transport model uses a more traditional theory and although it requires different input parameters, models continuous processes well. Note that the transport model is significantly more computationally intensive compared to the CCD and probabilistic models. The models are implemented in an accessible and readily usable computer application <sup>5</sup>.

---

<sup>5</sup> <http://theliquidphase.org/index.php?title=Modeling>

The developed models are based on well established chromatography theory, as described in section 2.2. This includes linear behaviour of the K value, which could be considered a limitation. The model therefore does not take any chemical or biological reactions into account. Another limitation is that the models assume homogeneous phase distribution (i.e. a constant  $S_F$ ) throughout the column.

The model software will be a valuable tool for industry for predicting, evaluating and validating experimental separations and production processes. It will also be a valuable tool for academia for teaching & training both staff and students on how to use the technology.

## 10.2 Visualisation

The developed model interface, combining the concept of dynamic querying and query previews as model previews, permits functional and effective model configuration, exploration and analysis.

A new visualisation method was developed that can accurately visualise different modes of operation (normal phase mode, reversed phase mode, dual flow mode, co-current mode and intermittent mode). This new visualisation helps understanding of the liquid-liquid chromatography process amongst CCC novices.

The described visualisation and interactivity enhancements have proven to contribute understanding and insight of the underlying chromatography process. It is clear the Interactive Chromatogram Explorer (Section 5.4.5; Figure 5.8) forms the largest contribution in this aspect.

The alternative visualisation of the probabilistic units in the form of the unit density (Section 7.1; Figure 7.4B), gives an additional method of visually interpreting modelling results.

The newly developed prototype graphical user interface (Section 7.2; Figure 7.5, Figure 7.6) showed great potential for combining model parameter input and exploring the liquid-liquid chromatography processes. It was developed with the aim of creating an optimal environment for configuring the model, and addressing issues newly identified in the conventional user interface. Although an in depth study has not been performed on this yet, it is clear this new graphical user interface is a further contribution to the model interface.

Various forms of visualisations that have been developed, have been widely used in the current research group and beyond, proving it is valuable and effective for educational purposes. Additionally an improved visualisation tool was developed showing improved educational value.

While effective models already existed, the use of interactive visualisation permits users to explore the relationship between parameters and performances in a simpler yet more powerful way. As mentioned, it will also be a valuable tool for academia for teaching & training both staff and students on how to use the technology. Prior to this work no such tool existed / existing tools were limited in their accessibility and educational value.

### **10.3 Future work**

The reasons for the recognised deviations noted in the comparisons of modelled and experimental values for more extreme values of  $K$  (in the order of 0.1 or smaller, or 10 or larger) will need further investigation.

The CCC dual flow and especially the intermittent flow modes would benefit from more theoretical research. However, there is also more understanding required of the experimental intermittent CCC process itself, which subsequently might enable improvement of the model.

Chromatographic regression could be included into the computer model, to extract peak values and even determine equivalent model input parameters. This would allow reproducing and experimenting with existing experimental runs. Theory on this was published [Vivó-Truyols et al. 2005a, 2005b], however the author has been unable to successfully reproduce said theory. It is suggested that more information is obtained, to apply this theory to liquid-liquid chromatography.

The prototype of the new graphical user interface (Section 7.2; Figure 7.5) showed great potential for combining the model input parameters view with the interactive chromatogram explorer view. Suggested for future work is to make improvements using collected feedback, and making this prototype fully functional. Subsequently, this could then be tested using the insight evaluation method to assert the contribution in more depth.

The improved visualisation tool could be further developed to, in addition to the discrete visualisation, implement a continuous form of visualisation, using the continuous probabilistic model. The visualisation could be further enhanced by showing the component concentration in a chromatogram style view underneath the main visualisation. One of the main suggestions from the evaluation showed that subjects considered showing the visualisation with slow movement better for educational purposes.



## **10.4 Closing remarks**

Although I did not consider doing a PhD my main goal in life, I felt called to do it and am glad the opportunity was given to me. And although I had a full time job during most of the study, even in an entirely different research area, being able to do a PhD in the UK while supporting my family was a very good opportunity. Doing the research part time makes it more stretched out over time I guess, but at the same time, helps give you more time to consider things and give you new ideas and inspiration. Although clearly I can't take all the credit for the latter as I attempted to relay in the acknowledgements. I consider being able to do this research to obtain a PhD a great blessing indeed.

## References

- Ahlberg, C. (1996) *Spotfire: an information exploration environment*. SIGMOD Rec., 25, 25-29.
- Ahlberg, C., Truvé, S. (1995) Tight coupling: guiding user actions in a direct manipulation retrieval system. *Proceedings of the HCI'95 conference on People and computers X*. Huddersfield, United Kingdom: Cambridge University Press.
- Ahlberg, C., Williamson, C., Shneiderman, B. (1992) Dynamic queries for information exploration: an implementation and evaluation. *Proceedings of the SIGCHI conference on Human factors in computing systems*. Monterey, California, United States: ACM.
- Bayes, Price (1763) *An Essay towards Solving a Problem in the Doctrine of Chances*. By the Late Rev. Mr. Bayes, F. R. S. Communicated by Mr. Price, in a Letter to John Canton, A. M. F. R. S. Philosophical Transactions, 53, 370-418.
- Beliv'06 (2006) *The BELIV Workshop, BEyond time and errors: novel evaluation methods for Visualization* [Online]. Available: <http://www.beliv.org/> [Accessed 1 October 2012].
- Bellot, J. C., Condoret, J. S. (1991) *Liquid chromatography modelling: a review*. Process Biochemistry, 26, 363-376.
- Berezkin, V. G. (1990) *Chromatographic Adsorption Analysis: Selected Works of M.S. Tswett*, New York, USA, Ellis Horwood Ltd.
- Berthod, A. (2002) *Counter-current chromatography - The support-free liquid stationary phase*, Amsterdam, The Netherlands, Elsevier.
- Berthod, A. (2006) *Band broadening inside the chromatographic column: The interest of a liquid stationary phase*. Journal of Chromatography A, 1126, 347-356.
- Berthod, A. (2009) Countercurrent Chromatography: From the Milligram to the Kilogram. In: Grushka, E., Grinberg, N. (eds.) *Advances in Chromatography Volume 47*. Boca Raton, USA: CRC Press.
- Berthod, A., Billardello, B. (2000) *Test to evaluate countercurrent chromatographs: Liquid stationary phase retention and chromatographic resolution*. Journal of Chromatography A, 902, 323-335.
- Berthod, A., Friesen, J. B., Inui, T., Pauli, G. F. (2007) *Elution-extrusion countercurrent chromatography: Theory and concepts in metabolic analysis*. Analytical Chemistry, 79, 3371-3382.
- Berthod, A., Hassoun, M. (2006) *Using the liquid nature of the stationary phase in countercurrent chromatography. IV. The cocurrent CCC method*. Journal of Chromatography A, 1116, 143-148.

- Berthod, A., Ruiz-Angel, M. J., Carda-Broch, S. (2003) *Elution–Extrusion Countercurrent Chromatography. Use of the Liquid Nature of the Stationary Phase To Extend the Hydrophobicity Window*. *Analytical Chemistry*, 75, 5886-5894.
- Bosch, R., Stolte, C., Stoll, G., Rosenblum, M., Hanrahan, P. (2000) *Performance analysis and visualization of parallel systems using SimOS and Rivet: a case study*. High-Performance Computer Architecture, 2000. HPCA-6. Proceedings. Sixth International Symposium on, 2000 Toulouse, France. IEEE, 360-371.
- Card, S. K., Mackinlay, J. D., Shneiderman, B. (1999) *Readings in information visualization: using vision to think*, San Diego, Academic Press.
- Clark, D. (2010) *Instructional System Design (ISD)* [Online]. Clark, D. Available: [http://www.nwlink.com/~donclark/hrd/isd/types\\_of\\_evaluations.html](http://www.nwlink.com/~donclark/hrd/isd/types_of_evaluations.html) [Accessed 1 November 2011].
- Clark, J. (2007) *Thin Layer Chromatography* [Online]. Jim Clark. Available: <http://www.chemguide.co.uk/analysis/chromatography/thinlayer.html> [Accessed 22 July 2011].
- Conway, W. D. (1990) *Countercurrent Chromatography - Apparatus, Theory & applications*, New York, VCH Publisher Inc.
- Courant, R., Friedrichs, K., Lewy, H. (1967) *On the Partial Difference Equations of Mathematical Physics*. *IBM Journal of Research and Development*, 11, 215-234.
- Craig, L. C. (1944) *Identification of small amounts of organic compounds by distribution studies*. *Anal. Chem.*, 20, 134-139.
- Craig, L. C. (1950) *Partition Chromatography and Countercurrent Distribution*. *Analytical Chemistry*, 22, 1346-1352.
- Craig, L. C., Craig, D. (1956) Laboratory extraction and countercurrent distribution. *In*: Weissberger, A. (ed.) *Separation and Purification*. New York, USA: Interscience Publishers.
- Craig, L. C., Hausmann, W., Ahrens, E. H., Harfenist, E. J. (1951) *Automatic Countercurrent Distribution Equipment*. *Analytical Chemistry*, 23, 1236-1244.
- Craig, L. C., Post, O. (1949) *Apparatus for Countercurrent Distribution*. *Anal. Chem.*, 21, 500-504.
- Cussler, E. L. (2007) *Diffusion; Mass Transfer in Fluid Systems*, Cambridge, UK, Cambridge University Press.
- de Folter, J. (1998a) *Countercurrent Chromatography Practical and Theoretical models*. Uxbridge, UK: Brunel Institute for Bioengineering, internal publication.

- de Folter, J. (1998b) *CCC Animations*, Animation. Directed by Sutherland, I., Hawes, D. UK: Brunel Institute for Bioengineering.
- de Folter, J., Cribbin, T. (2012) *Facilitating insight into a simulation model using visualization and dynamic model previews*. Journal of Visual Languages and Computing, 23, 344-353.
- de Folter, J., Sutherland, I. A. (2009) *Universal counter-current chromatography modelling based on counter-current distribution*. Journal of Chromatography A, 1216, 4218-4224.
- de Folter, J., Sutherland, I. A. (2011) *Probabilistic model for immiscible separations and extractions (ProMISE)*. Journal of Chromatography A, 1218, 6009-6014.
- Delannay, E., Toribio, A., Boudesocque, L., Nuzillard, J.-M., Zèches-Hanrot, M., Dardennes, E., Le Dour, G., Sapi, J., Renault, J.-H. (2006) *Multiple dual-mode centrifugal partition chromatography, a semi-continuous development mode for routine laboratory-scale purifications*. Journal of Chromatography A, 1127, 45-51.
- Dix, A., Ellis, G. (2002) by chance - enhancing interaction with large data sets through statistical sampling. *Proceedings of the Working Conference on Advanced Visual Interfaces*. Trento, Italy: ACM.
- Fernando, S. (2011) *Monoclonal antibody (mAb) purification by Counter Current Chromatography (CCC)*. PhD, Brunel University.
- Friesen, J. B., Pauli, G. F. (2005) *G.U.E.S.S.—A Generally Useful Estimate of Solvent Systems for CCC*. Journal of Liquid Chromatography & Related Technologies, 28, 2777-2806.
- Friesen, J. B., Pauli, G. F. (2007) *Reciprocal symmetry plots as a representation of countercurrent chromatograms*. Analytical Chemistry, 79, 2320-2324.
- Gamma, E., Helm, R., Johnson, R., Vlissides, J. (1994) *Design Patterns: Elements of Reusable Object-Oriented Software*, Addison-Wesley.
- Giddings, J. C. (1965) *Dynamics of Chromatography: Principles and Theory*, New York, USA, Marcel Dekker.
- Glueckauf, E. (1955) *Theory of chromatography: Part 10. - Formula for diffusion into spheres and their application to chromatography*. Transactions of the Faraday Society, 51, 1540-1551.
- Golshan-Shirazi, S., Guiochon, G. (1988) *Analytical solution for the ideal model of chromatography in the case of a langmuir isotherm*. Analytical Chemistry, 60, 2364-2374.
- Golshan-Shirazi, S., Guiochon, G. (1989) *Analytical solution for the ideal model of chromatography in the case of a pulse of a binary mixture with competitive langmuir isotherm*. Journal of Physical Chemistry®, 93, 4143-4157.

- Golshan-Shirazi, S., Guiochon, G. (1994) *Modeling of preparative liquid chromatography*. Journal of Chromatography A, 658, 149-171.
- Gu, T. (1995) *Mathematical Modeling and Scale-up of Liquid Chromatography*, Berlin, Germany, Springer.
- Guan, Y. H., Bourton, E. C., Hewitson, P., Sutherland, I. A., Fisher, D. (2009) *The importance of column design for protein separation using aqueous two-phase systems on J-type countercurrent chromatography*. Separation and Purification Technology, 65, 79-85.
- Guiochon, G., Felinger, A., Shirazi, D. G., Katti, A. M. (2006) *Fundamentals of preparative and nonlinear chromatography*, Amsterdam, The Netherlands, Elsevier.
- Guzlek, H., Baptista, I. I. R., Wood, P. L., Livingston, A. (2010) *A novel approach to modelling counter-current chromatography*. Journal of Chromatography A, 1217, 6230-6240.
- Hecker, E. (1955) *Verteilungsverfahren im Laboratorium*, Weinheim, Germany, Verlag Chemie.
- Herrod, S. A. (1998) *Using Complete Machine Simulation To Understand Computer System Behavior*. PhD, Stanford University.
- Hewitson, P., Ignatova, S., Sutherland, I. (2011) *Intermittent counter-current extraction-effect of the key operating parameters on selectivity and throughput*. Journal of Chromatography A, 1218, 6072-6078.
- Hewitson, P., Ignatova, S., Ye, H., Chen, L., Sutherland, I. (2009) *Intermittent counter-current extraction as an alternative approach to purification of Chinese herbal medicine*. Journal of Chromatography A, 1216, 4187-4192.
- Horváth, K., Fairchild, J. N., Kaczmarek, K., Guiochon, G. (2010) *Martin-Synge algorithm for the solution of equilibrium-dispersive model of liquid chromatography*. Journal of Chromatography A, 1217, 8127-8135.
- Hynninen, P. H. (1976) *Multiple liquid liquid partition. I. Theory of countercurrent distribution (CCD)*. Analytical Biochemistry, 74, 376-391.
- Ignatova, S., Hawes, D., van den Heuvel, R., Hewitson, P., Sutherland, I. A. (2010) *A new non-synchronous preparative counter-current centrifuge-the next generation of dynamic extraction/chromatography devices with independent mixing and settling control, which offer a step change in efficiency*. Journal of Chromatography A, 1217, 34-39.
- Ignatova, S., Hewitson, P. (2008) *Establishing the Key Operating Parameters for Continuous Counter-current Extraction*. 5th International Symposium on CounterCurrent Chromatography 2008, Rio de Janeiro, Brazil.

- Ignatova, S., Hewitson, P., Mathews, B., Sutherland, I. (2011) *Evaluation of dual flow counter-current chromatography and intermittent counter-current extraction*. Journal of Chromatography A, 1218, 6102-6106.
- Ito, Y. (1985) *Foam Countercurrent Chromatography Based on Dual Counter-Current System*. Journal of Liquid Chromatography, 8, 2131-2152.
- Ito, Y., Conway, W. D. (1995) *High-Speed Countercurrent Chromatography*, New York, USA, John Wiley & Sons, Ltd.
- Ito, Y., Ma, Z., Clary, R., Powell, J., Knight, M., Finn, T. M. (2011a) *Vortex counter-current chromatography*. Journal of Chromatography A, 1218, 6165-6172.
- Ito, Y., Ma, Z., Clary, R., Powell, J., Knight, M., Finn, T. M. (2011b) *Improved partition efficiency with threaded cylindrical column in vortex counter-current chromatography*. Journal of Chromatography A, 1218, 4065-4070.
- Ito, Y., Weinstein, M., Aoki, I., Harada, R., Kimura, E., Nunogaki, K. (1966) *The coil planet centrifuge*. Nature, 212, 985-987.
- James, A. T., Martin, J. P. (1952) *Gas-liquid Partition Chromatography: the Separation and Micro-estimation of Volatile Fatty Acids from Formic Acid to Dodecanoic Acid*. Biochem J., 50, 679-690.
- Keim, D., Andrienko, G., Fekete, J. D., Görg, C., Kohlhammer, J., Melançon, G. (2008) Visual Analytics: Definition, Process, and Challenges Information Visualization. In: Kerren, A., Stasko, J., Fekete, J. D., North, C. (eds.) *Information Visualization*. Springer Berlin / Heidelberg.
- Kolev, S. D. (1995) *Mathematical modelling of flow-injection systems*. Analytica Chimica Acta, 308, 36-66.
- Kostanian, A. E. (2002) *Modelling counter-current chromatography: A chemical engineering perspective*. Journal of Chromatography A, 973, 39-46.
- Kostanian, A. E., Berthod, A., Ignatova, S. N., Maryutina, T. A., Spivakov, B. Y., Sutherland, I. A. (2004) *Countercurrent chromatographic separation: A hydrodynamic approach developed for extraction columns*. Journal of Chromatography A, 1040, 63-72.
- Kostanyan, A. E. (2006) *General regularities of liquid chromatography and countercurrent extraction*. Theoretical Foundations of Chemical Engineering, 40, 587-593.
- Kostanyan, A. E., Belova, V. V., Kholkin, A. I. (2007) *Modelling counter-current and dual counter-current chromatography using longitudinal mixing cell and eluting counter-current distribution models*. Journal of Chromatography A, 1151, 142-147.

- Kostanyan, A. E., Voshkin, A. A., Kodin, N. V. (2011) *Controlled-cycle pulsed liquid-liquid chromatography. A modified version of Craig's counter-current distribution*. Journal of Chromatography A, 1218, 6135-6143.
- Linsen, L., Locherbach, J., Berth, M., Bernhardt, J., Becher, D. (2005) *Differential protein expression analysis via liquid-chromatography/mass-spectrometry data visualization*. Visualization, 2005. VIS 05. IEEE, 23-28 Oct. 2005. 447-454.
- Martin, A. J. P. (1964) Development of Partition Chromatography. *Nobel Lectures, Chemistry 1942-1962*. Amsterdam: Elsevier Publishing Company.
- Martin, J. P., Synge, R. L. M. (1941) *A new form of chromatogram employing two liquid phases. 1. A theory of chromatography 2. Application to the micro-determination of the higher monoamino-acids in proteins*. Biochem J., 35, 1358-1368.
- McClean, P., Johnson, C., Rogers, R., Daniels, L., Reber, J., Slator, B. M., Terpstra, J., White, A. (2004) *Molecular and Cellular Biology Animations: Development and Impact on Student Learning*. Cell Biology Education, 4, 169-179.
- Miyabe, K., Guiochon, G. (2000) *Kinetic study of the mass transfer of bovine serum albumin in anion-exchange chromatography*. Journal of Chromatography A, 866, 147-171.
- Miyabe, K., Guiochon, G. (2002) *New model of surface diffusion in reversed-phase liquid chromatography*. Journal of Chromatography A, 961, 23-33.
- Morris, C. J. O. R., Morris, P. (1976) *Separation methods in biochemistry*, New York, USA, Wiley.
- Nichols, P. L. (1950) *Useful Relations of Countercurrent Distribution Computations*. Analytical Chemistry, 22, 915-918.
- Nobelprize.org. (1952) *The Nobel Prize in Chemistry 1952* [Online]. Nobelprize.org. Available: [http://www.nobelprize.org/nobel\\_prizes/chemistry/laureates/1952/](http://www.nobelprize.org/nobel_prizes/chemistry/laureates/1952/) [Accessed 22 July 2011].
- North, C. (2006) *Toward Measuring Visualization Insight*. IEEE Comput. Graph. Appl., 26, 6-9.
- North, C., Chang, R., Endert, A., Dou, W., May, R., Pike, B., Fink, G. (2011) Analytic provenance: process+interaction+insight. *Proceedings of the 2011 annual conference extended abstracts on Human factors in computing systems*. Vancouver, BC, Canada: ACM.
- Patankar, S. V. (1980) *Numerical Heat Transfer and Fluid Flow*, New York, USA, Hemisphere Publishing Corporation.
- Plaisant, C., Venkatraman, M., Ngamkajornwiwat, K., Barth, R., Harberts, B., Feng, W. (1999) Refining Query Previews Techniques for Data with Multivalued Attributes: The Case of NASA EOSDIS. *Proceedings of the IEEE Forum on Research and Technology Advances in Digital Libraries*. IEEE Computer Society.

- Post, O., Craig, L. C. (1963) *A new type of stepwise countercurrent distribution train*. Analytical Chemistry, 35, 641-647.
- Roullier, C., Chollet-Krugler, M., Bernard, A., Boustie, J. (2009) *Multiple dual-mode centrifugal partition chromatography as an efficient method for the purification of a mycosporine from a crude methanolic extract of Lichina pygmaea*. Journal of Chromatography B: Analytical Technologies in the Biomedical and Life Sciences, 877, 2067-2073.
- Ruthven, D. M. (1984) *Principles of adsorption and adsorption processes*, Wiley-Interscience.
- Said, A. S. (1981) *The Rate Theory of Chromatography. Theory and mathematics of chromatography*. Heidelberg, Germany: Dr. Alfred Hüthig Verlag.
- Saraiya, P., North, C., Duca, K. (2004) *An Evaluation of Microarray Visualization Tools for Biological Insight. Proceedings of the IEEE Symposium on Information Visualization*. IEEE Computer Society.
- Saraiya, P., North, C., Lam, V., Duca, K. A. (2006) *An Insight-Based Longitudinal Study of Visual Analytics*. Visualization and Computer Graphics, IEEE Transactions on, 12, 1511-1522.
- Scriven, M. (1991) *Beyond formative and summative evaluation*. In: McLaughlin, M. W., Phillips, D. C. (eds.) *Evaluation and Education: A Quarter Century*. Chicago, USA: University of Chicago Press.
- Seo, J., Shneiderman, B. (2005) *A rank-by-feature framework for interactive exploration of multidimensional data*. Information Visualization, 4, 96-113.
- Sharp, H., Rogers, Y., Preece, J. (2007) *Interaction Design: Beyond Human-Computer Interaction*, Wiley.
- Shneiderman, B. (1994) *Dynamic Queries for Visual Information Seeking*. IEEE Softw., 11, 70-77.
- Snyder, L. R., Kirkland, J. J., Dolan, J. W. (2010) *Introduction to Modern Liquid Chromatography*, New Jersey, USA, John Wiley & Sons.
- Spence, B., Tweedie, L., Dawkes, H., Su, H. (1995) *Visualization for functional design. Proceedings of the 1995 IEEE Symposium on Information Visualization*. Atlanta, Georgia: IEEE Computer Society.
- Spence, R. (2001) *Information visualization*, Addison-Wesley.
- Staerk, D. U., Shitangkoon, A., Winchester, E., Vigh, G., Felinger, A., Guiochon, G. (1996) *Use of the equilibrium-dispersive model of nonlinear gas chromatography for the modelling of the elution band profiles in the preparative-scale gas chromatographic separation of enantiomers*. Journal of Chromatography A, 734, 289-296.



- Su, H., Nelder, J. A., Wolbert, P., Spence, R. (1996) *Application of generalized linear models to the design improvement of an engineering artefact*. *Quality and Reliability Engineering International*, 12, 101-112.
- Sutherland, I. A., de Folter, J., Wood, P. (2003) *Modelling CCC using an eluting countercurrent distribution model*. *Journal of Liquid Chromatography and Related Technologies*, 26, 1449-1474.
- Sutherland, I., Hewitson, P., de Folter, J. (2011) *Toroidal coil chromatography: The effect of scale-up and "g" field on stage efficiency*. *Journal of Chromatography A*, 1218, 6144-6147.
- Sutherland, I., Hewitson, P., Ignatova, S. (2009) *Scale-up of counter-current chromatography: Demonstration of predictable isocratic and quasi-continuous operating modes from the test tube to pilot/process scale*. *Journal of Chromatography A*, 1216, 8787-8792.
- Sutherland, I. A., Heywood-Waddington, D., Ito, Y. (1987) *Counter-current chromatography. Applications to the separation of biopolymers, organelles and cells using either aqueous-organic or aqueous-aqueous phase systems*. *Journal of Chromatography A*, 384, 197-207.
- Sutherland, I. A., Heywood-Waddington, D., Peters, T. J. (1984) *Toroidal Coil Countercurrent Chromatography: A Fast Simple Alternative To Countercurrent Distribution Using Aqueous Two Phase Partition*. *Journal of Liquid Chromatography*, 7, 363-384.
- Sutherland, I. A., Heywood-Waddington, D., Peters, T. J. (1985) *Countercurrent Chromatography Using A Toroidal Coil Planet-Centrifuge: A Comparative Study of The Separation Of Organelles Using Aqueous Two-Phase Partition*. *Journal of Liquid Chromatography*, 8, 2315-2335.
- Sutherland, I. A., Ito, Y. (1978) *Toroidal coil chromatography. A new high-speed, high-resolution method of separating cells and cell organelles on their distribution in two-phase polymer systems*. *Journal of High Resolution Chromatography*, 1, 171-172.
- Synge, R. L. M. (1964) *Applications of partition chromatography. Nobel Lectures, Chemistry 1942-1962*. Amsterdam: Elsevier Publishing Company.
- SYRED, P. A. *Light micrograph of HPLC packing* [Online]. Science Photo Library. Available: <http://www.sciencephoto.com/media/359391/view> [Accessed 22 July 2011].
- Tanimura, T., Pisano, J. J., Yoichiro, I., Bowman, R. L. (1970) *Droplet countercurrent chromatography*. *Science*, 169, 54-56.
- Tanin, E., Lotem, A., Haddadin, I., Shneiderman, B., Plaisant, C., Slaughter, L. (2000) *Facilitating data exploration with query previews: A study of user performance and preference*. *Behaviour & Information Technology*, 19, 393-403.

TIBCO. (2011) *Spotfire* [Online]. Available: <http://spotfire.tibco.com> [Accessed 25 February 2012].

Treffry, T. E., Sharpe, P. T., Walter, H., Brooks, D. E. (1985) Thin-layer countercurrent distribution and apparatus. *In*: Brooks, D. E., Fisher, D., Walter, H. (eds.) *Partitioning in Aqueous Two-Phase Systems*. Orlando, USA: Academic press.

Tweedie, L., Spence, B., Dawkes, H., Su, H. (1995) The influence explorer. *Conference companion on Human factors in computing systems*. Denver, Colorado, United States: ACM.

Tweedie, L., Spence, B., Dawkes, H., Su, H. (1996) The Influence Explorer (video) - a tool for design. *Conference companion on Human factors in computing systems: common ground*. Vancouver, British Columbia, Canada: ACM.

Tweedie, L. A. (1997) *Exploiting interactivity in graphical problem solving: From visual cues to insight*, London, UK, University of London.

van Buel, M. J., van Der Wielen, L. A. M., Luyben, K. C. A. M. (1997a) *Modelling gradient elution in centrifugal partition chromatography*. *Journal of Chromatography A*, 773, 13-22.

van Buel, M. J., van Der Wielen, L. A. M., Luyben, K. C. A. M. (1997b) *Effluent Concentration Profiles in Centrifugal Partition Chromatography*. *AIChE Journal*, 43, 693-701.

van Deemter, J. J., Zuiderweg, F. J., Klinkenberg, A. (1956) *Longitudinal diffusion and resistance to mass transfer as causes of nonideality in chromatography*. *Chemical Engineering Science*, 5, 271-289.

van den Heuvel, R. (2008) *Investigation into the mechanics and feasibility of continuous counter-current extraction*. PhD, Brunel University.

van den Heuvel, R., Siebers, R., Hewitson, P., Guan, Y. H., Sutherland, I. A. (2010) *J-type toroidal CCC for protein separations*. 6th International Symposium on CounterCurrent Chromatography 2010, Lyon, France.

van den Heuvel, R. N. A. M., König, C. S. (2011) *Improved g-level calculations for coil planet centrifuges*. *Journal of Chromatography A*, 1218, 6038-6043.

van Wijk, J. J. (2006) *Bridging the Gaps*. *Computer Graphics and Applications*, IEEE, 26, 6-9.

Vivó-Truyols, G., Torres-Lapasió, J. R., Van Nederkassel, A. M., Vander Heyden, Y., Massart, D. L. (2005a) *Automatic program for peak detection and deconvolution of multi-overlapped chromatographic signals: Part I: Peak detection*. *Journal of Chromatography A*, 1096, 133-145.

Vivó-Truyols, G., Torres-Lapasió, J. R., Van Nederkassel, A. M., Vander Heyden, Y., Massart, D. L. (2005b) *Automatic program for peak detection and deconvolution of multi-overlapped chromatographic signals: Part II: Peak model and deconvolution algorithms*. *Journal of Chromatography A*, 1096, 146-155.

Westerman, S., Cribbin, T. (2000) *Cognitive ability and information retrieval: When less is more*. Virtual Reality, 5, 1-7.

Wikipedia. (2011) *Thin layer chromatography* [Online]. Wikipedia. Available: [http://en.wikipedia.org/wiki/Thin\\_layer\\_chromatography](http://en.wikipedia.org/wiki/Thin_layer_chromatography) [Accessed 22 July 2011].

Williamson, B., Craig, L. C. (1947) *Identification of small amounts of organic compounds by distribution studies; calculation of theoretical curves*. J. Biol. Chem., 168, 687-697.

Williamson, C., Shneiderman, B. (1992) The dynamic HomeFinder: evaluating dynamic queries in a real-estate information exploration system. *Proceedings of the 15th annual international ACM SIGIR conference on Research and development in information retrieval*. Copenhagen, Denmark: ACM.

Wood, P. L. (2006) *The Hydrodynamics of Countercurrent Chromatography in J-type Centrifuges*. PhD, Brunel University.

Zhao, C.-X., Xu, Y.-L., He, C.-H. (2009) *Axial dispersion coefficient in high-speed counter-current chromatography*. Journal of Chromatography A, 1216, 4841-4846.

## **Appendix A : Software model user manual**

# ProMISE user manual

Probabilistic model for immiscible separations and extractions (ProMISE) developed by Joost de Folter, is freely available for non-commercial purposes (academic e-mail address required for free registration).

The model can be downloaded here:

<http://theliquidphase.org/index.php?title=Modeling>

## System requirements

Minimum requirements

- Operating system: Windows XP / Vista / 7

Recommended

- CPU: Multi core (e.g. dual core)
- RAM: 2 GB (or more)
- Internet connection

## Installation

If the model was downloaded, it is packaged as a compressed zip file.

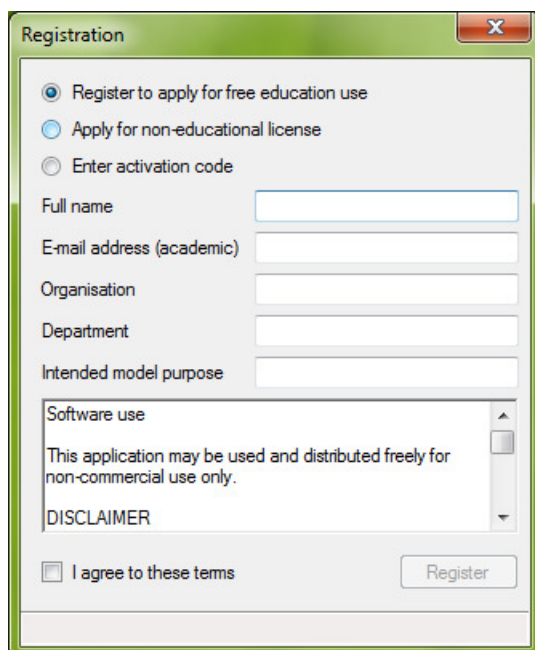
- Unzip the entire contents of the zip file into a folder
- Execute the installation wizard 'setup.exe', and follow its instructions
- This software requires .NET framework version 3.5 which will automatically be downloaded by the installation wizard (this needs to be done only once)

## Activation

Before the model can be used, ProMISE needs to be activated first. When ProMISE is executed, the about dialog will automatically open.

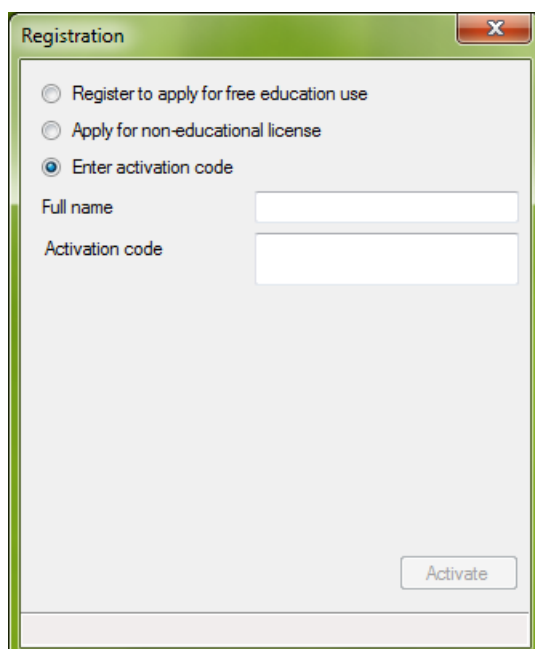


Select the Activate button to open the registration dialog. When ProMISE is executed for the first time, this dialog will also automatically open.



The Registration dialog box has a title bar with a close button (X). It contains three radio buttons: "Register to apply for free education use" (selected), "Apply for non-educational license", and "Enter activation code". Below these are five text input fields: "Full name", "E-mail address (academic)", "Organisation", "Department", and "Intended model purpose". A scrollable text area contains the text: "Software use", "This application may be used and distributed freely for non-commercial use only.", and "DISCLAIMER". At the bottom left is a checkbox labeled "I agree to these terms". At the bottom right is a button labeled "Register".

Enter the required details, read the software terms of use, and select the Register button. Normally an e-mail with the activation code will be sent within 24 hours. Execute ProMISE again, and copy the activation code from this e-mail, and paste it in the registration dialog in the field 'Activation code'.



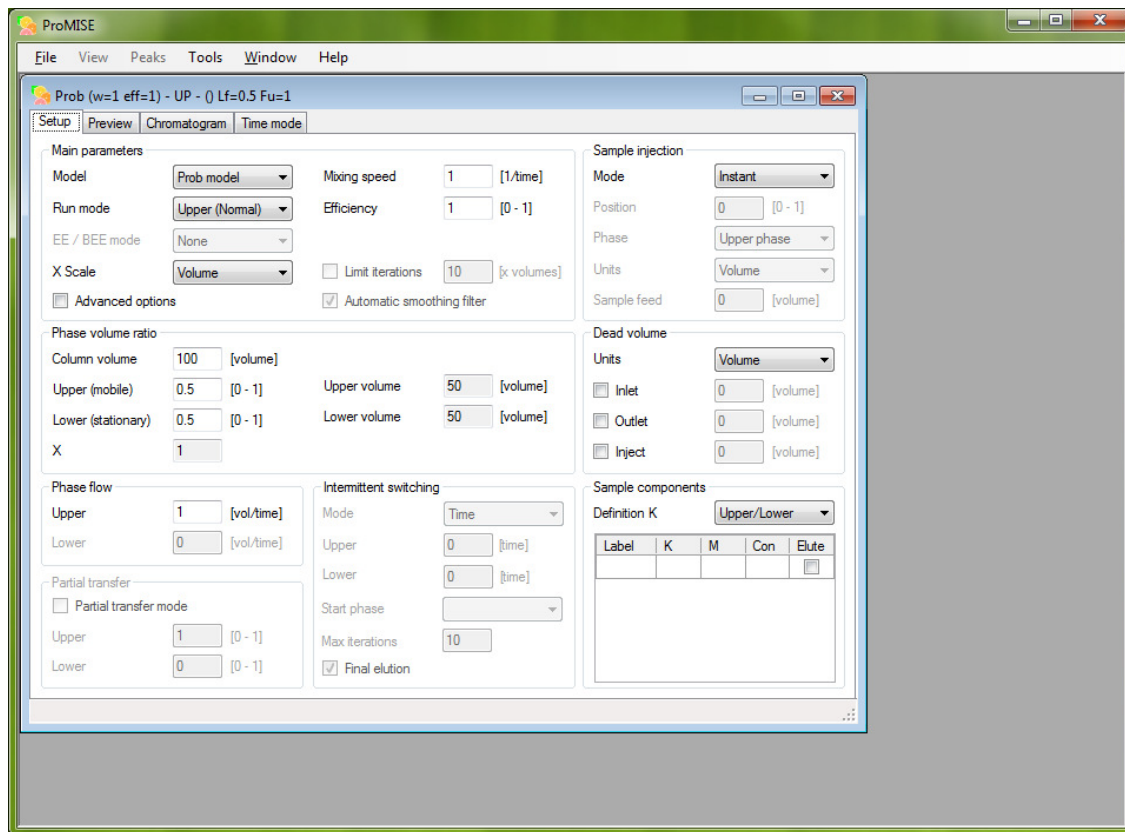
The Registration dialog box is shown with the "Enter activation code" radio button selected. The "Full name" and "Activation code" text input fields are visible. The "Register" button is no longer present, and an "Activate" button is located at the bottom right.

ProMISE will close to validate the activation code. Execute ProMISE again to access the model.

## Using ProMISE

### Model Setup

From the main menu, select File -> New to open a new model in the setup view.



The window has various tabs, accessible by direct mouse selection. Selecting the Chromatogram or Time mode views will run the model. Model execution can be aborted by returning to the setup or preview tab. Various instances of the model can be started concurrently.

The model setup view contains the input parameters for the model which are shown in a number of parameter groups. The input controls contain tool tips which are displayed by hovering the mouse over a particular control. The model window title shows a summary of the main input parameters currently selected.



## The main parameters group

Main parameters

Model	Prob model ▼	Mixing speed	1	[1/time]
Run mode	Upper (Normal) ▼	Efficiency	1	[0 - 1]
EE / BEE mode	None ▼			
X Scale	Volume ▼	<input type="checkbox"/> Limit iterations	10	[x volumes]
<input type="checkbox"/> Advanced options		<input checked="" type="checkbox"/> Automatic smoothing filter		

First, the model can be selected:

- CCD model: discrete model – recommended for modelling discrete type chromatography methods
- Probabilistic model ('Prob'): continuous model – recommended for modelling continuous type chromatography methods (default)
- Transport model ('Trans'): continuous model

Next the run mode is set:

- Normal phase: Upper phase is mobile (default)
- Reverse phase: Lower phase is mobile
- Dual flow: Both phases move in opposite direction
- Co-current flow: Both phases move in same direction
- Intermittent flow: Intermittently run Upper / Lower phase as mobile phase

EE / BEE mode (only enabled in advanced options mode; use in conjunction with limited number of iterations):

- None: Normal elution (default)
- EE: Elution – Extrusion
- BEE: Back Elution – Extrusion

X Scale: Sets the initial X-axis scale for the chromatogram view.

Advanced options: Enables modifying options for more expert users (default: disabled).

Limit iterations: limits number of model iterations to x times the column volume.

Automatic smoothing filter: enables automatic smoothing for appropriate run modes (default: enabled).

Most of the input parameters are the same for all models. However there are some model specific parameters, depending on which model is selected.

***CCD model specific parameters***

Transfer steps: Number of CCD system cells or (transfer) steps (default: 100).

Efficiency: Mixing efficiency (only enabled in advanced options mode) (default: 1):  $[0 < \text{efficiency} \leq 1]$

***Probabilistic model specific parameters***

Mixing speed: Rotational speed in CCC (or equivalent) (default: 1). [Suggested units: rotations / min]

Efficiency: Mixing efficiency (or equivalent) (default: 1):  $[0 < \text{efficiency} \leq 1]$

***Transport model specific parameters***

Transfer steps: Number of transport model steps (default: 100).

Mass transfer: the overall volumetric mass transfer coefficient ( $k_0a$ ) (default: 0.01) [units: 1/s]

## The phase volume ratio parameters

Phase volume ratio			
Column volume	<input type="text" value="100"/>	[volume]	
Upper (mobile)	<input type="text" value="0.5"/>	[0 - 1]	Upper volume <input type="text" value="50"/> [volume]
Lower (stationary)	<input type="text" value="0.5"/>	[0 - 1]	Lower volume <input type="text" value="50"/> [volume]
X	<input type="text" value="1"/>		

Column volume: active volume of the chromatography column. [Suggested units: ml]

Upper phase and lower phase ratio can be set (automatically updated), and in the case of a single mobile phase, this is automatically indicated.

The corresponding volumes are also displayed.

## Phase flow parameters

Phase flow	
Upper	<input type="text" value="1"/> [vol/time]
Lower	<input type="text" value="0"/> [vol/time]

The phase flow can be set here, depending on which phase(s) is/are mobile. [Suggested units: ml / min]

## Sample component parameters

Sample components

Definition K Upper/Lower ▼

Label	K	M	Con	Elute
K=0.5	0.5	1	1	<input checked="" type="checkbox"/>
K=1	1	1	1	<input checked="" type="checkbox"/>
K=2	2	1	1	<input checked="" type="checkbox"/>
				<input type="checkbox"/>

Definition K: Sets the definition for the K-values:

Upper/Lower means  $K = C_U / C_L$  (default)

Lower/Upper means  $K = C_L / C_U$

Sample components can be set by either entering a Label, or a K-value; remaining columns will be filled in automatically. A component can be removed by clearing its Label.

The columns are defined as follows:

- Label: Custom text, displayed in chromatogram at peak position (set by default when entering K-value)
- K: K-value of sample component. Note that setting K-value will only set label once. Subsequently changing K-value will not update label.
- M: Mass of sample component (can be left 1)
- Con: Concentration: this is automatically calculated
- Elute: Sample component has to elute. Can only be changed in advanced options mode (default: enabled)

## Sample injection parameters

Sample injection	
Mode	Batch
Position	0 [0 - 1]
Phase	Upper phase
Units	Volume
Sample feed	1 [volume]

Mode:

- Instant: instantaneous (ideal) sample injection in first model step (default)
- Batch: More realistic sample injection enabling specific sample feed amount
- Continuous: continuous sample feed (note: set limit iterations)

Position: Can only be changed in advanced options mode. The relative column position; from 0 (start of column) to 1 (end of column). (Default 0.5 for dual flow and intermittent modes, and otherwise 0).

Phase: Can only be changed in advanced options mode. Phase initially containing the sample components.

Units: set units for sample feed (default: volume).

Sample feed: feed amount for sample components. [Suggested units: Volume: ml, Time: min]

## Dead volume parameters

Dead volume	
Units	Volume
<input checked="" type="checkbox"/> Inlet	5 [volume]
<input checked="" type="checkbox"/> Outlet	5 [volume]
<input type="checkbox"/> Inject	0 [volume]

Units: units for dead volumes (default: volume).

Inlet / Outlet / Inject: Set dead volume for column inlet, outlet, and additional injection position in case sample is not injected at column inlet. [Suggested units: Volume: ml, Time: min]

## Intermittent switching parameters

Intermittent switching

Mode

Time

Upper

5

[time]

Lower

5

[time]

Start phase

Upper phase

Max iterations

10

☒ Final elution

These parameters are only enabled in the intermittent run mode.

Mode: units for switch amounts (default: time). Can also be set to 'Component', where a component can be selected that is allowed to elute (switching before other components elute).

Upper / Lower: switch amount for upper phase and lower phase flow. [Suggested units: Volume: ml, Time: min]

Start phase: The first phase used in the intermittent switch (default: upper phase).

Max iterations: The number of intermittent switches (for both phases) (default: 10).

Final elution: Can only be changed in advanced options mode. Enables final elution after intermittent switches have completed (default: enabled).

## Partial transfer parameters

Partial transfer

☒ Partial transfer mode

Upper

0.1

[0 - 1]

Lower

0

[0 - 1]

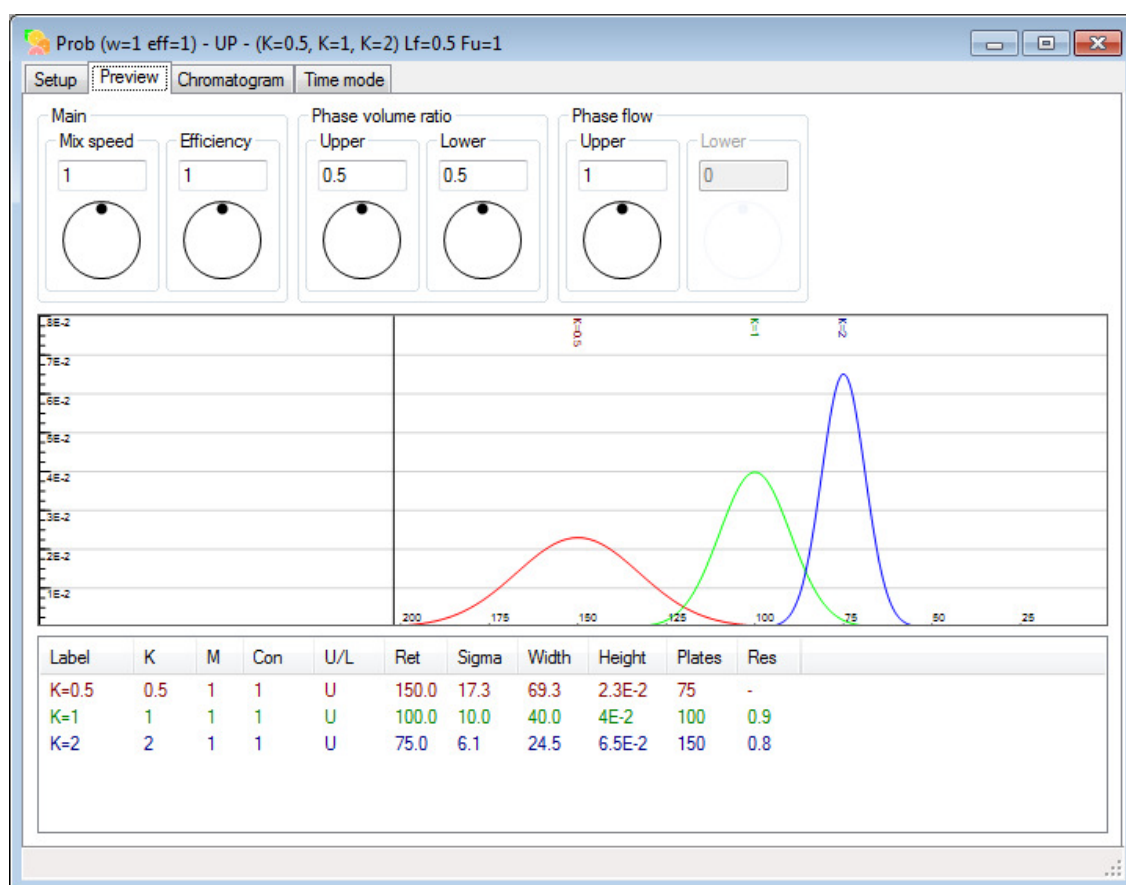
These parameters are only enabled when using the CCD model. This mode enables partial transfers of the cell content, as opposed to a normal transfer where the entire cell content is transferred between cells.

Partial transfer mode: Enable partial transfer mode (default: disabled).

Upper / Lower: The transfer factor for each respective phase; set to a value less than 1 (default: 1)

## Preview mode

This is an interactive view showing preview results of selected input parameters. Preview results are updated real time as the input parameters are modified.



The top of the screen shows springed jog wheel controls, enabling real time adjusting of a selected number of input parameters. The definition of these parameters is identical to that in the setup view described in the previous section.

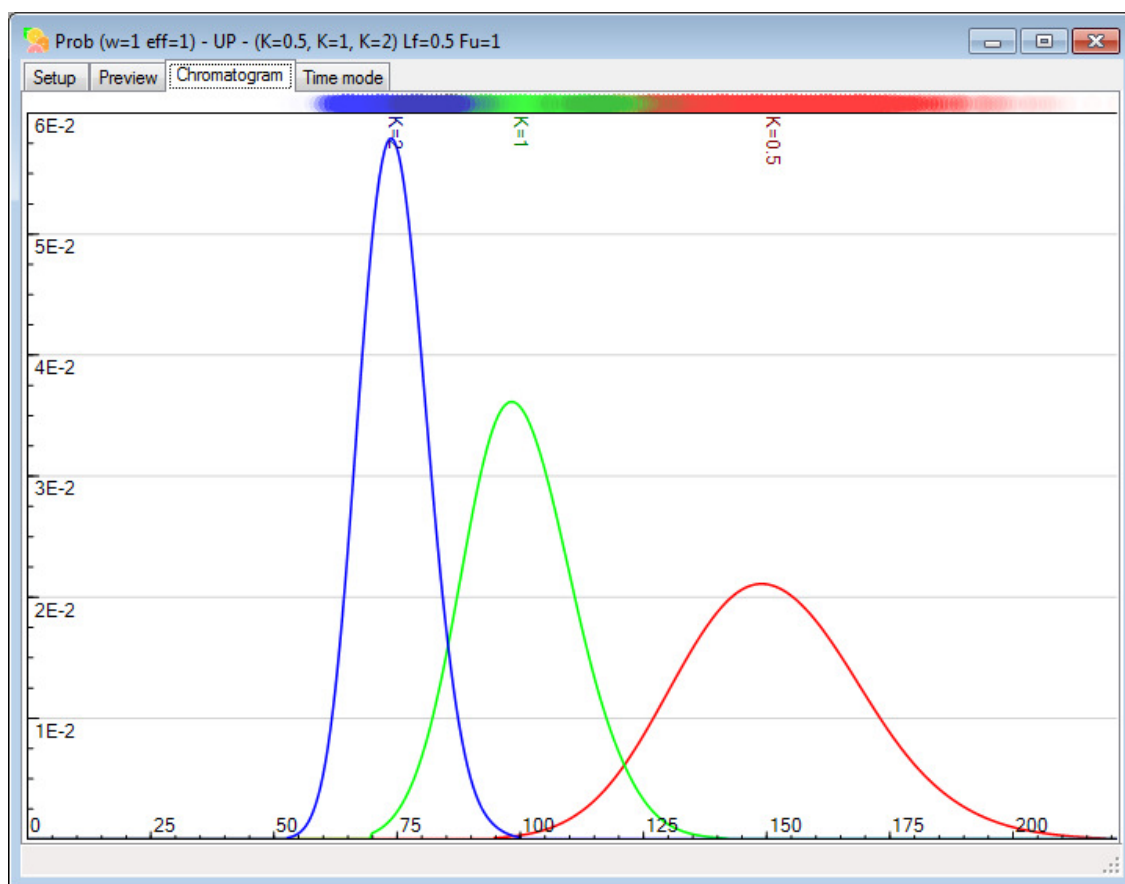
In the centre of the screen a preview chromatogram view is displayed. The X-axis units are as selected in the setup screen. The Y-axis units are component concentration with units used for input parameters.

At the bottom of the screen, a table containing numerical results is shown. Table columns:

- Label: Custom text, displayed in chromatogram at peak position
- K: K-value of sample component
- M: Mass of sample component
- Con: Concentration
- U/L: Eluted in Upper or Lower phase (a '-' symbol indicates component not eluted)
- Ret: Retention / elution time or peak position
- Sigma: The peak  $\sigma$  value (relates to peak width)
- Width: Peak width
- Height: Peak height or maximum concentration
- Plates: Number of theoretical plates
- Res: Resolution between previous and current peak in table (only calculated if peaks elute in same phase)

## Chromatogram view

Selecting the Chromatogram tab will run the model. Model execution can be aborted by returning to the setup or preview tab.



Model results are graphically displayed, showing the eluted upper phase content in this case. The X-axis units are as selected. The Y-axis units are component concentration with units used for input parameters. For the probabilistic model an additional unit / density graph is displayed at the top of the screen.

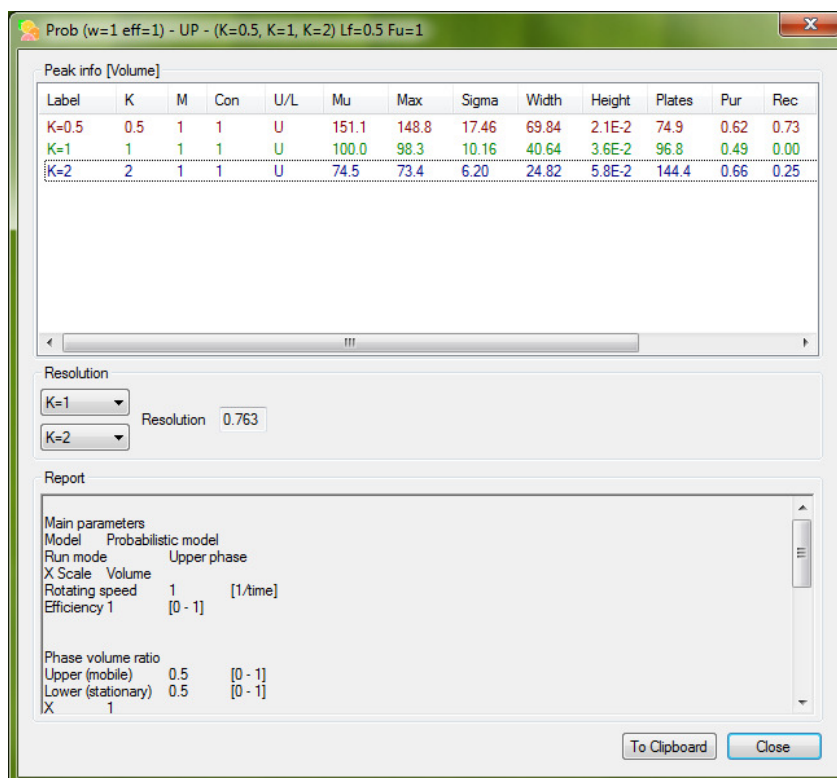
The chromatogram view is highly customisable, using the menu options (see the Menu section).

Peak information can be displayed by selecting Peaks -> Peak Info from the main menu.



## Peak information

The peak information window shows key properties of each component / peak.



A table at the top shows key results for each sample component. Mu and Max refer to different methods for obtaining the peak position (or retention time / volume). Table columns:

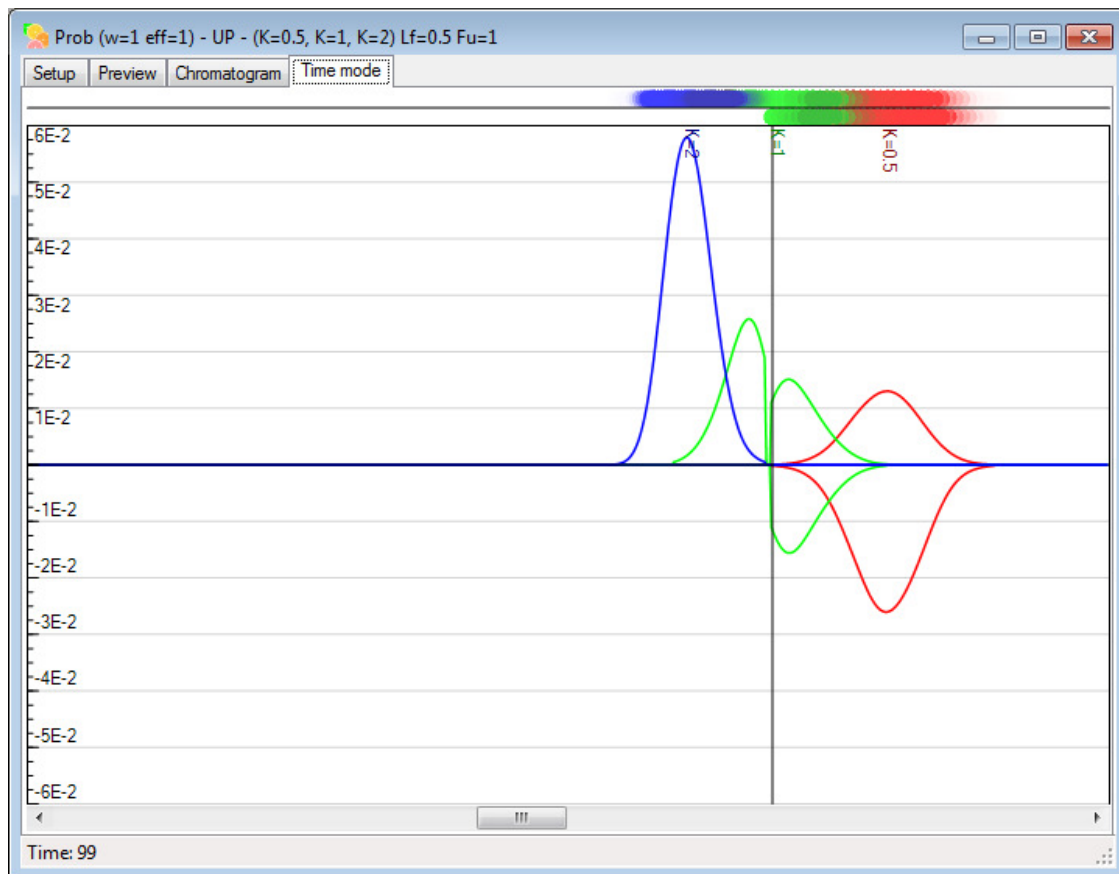
- Label: Custom text, displayed in chromatogram at peak position
- K: K-value of sample component
- M: Mass of sample component
- Con: Concentration
- U/L: Eluted in Upper or Lower phase (a '-' symbol indicates component not eluted)
- Mu: Retention / elution time or peak position (mathematical average)
- Max: Retention / elution time or peak position (position at maximum concentration)
- Sigma: The peak  $\sigma$  value (relates to peak width)
- Width: Peak width
- Height: Peak height or maximum concentration
- Plates: Number of theoretical plates
- Pur: Purity of eluted component (cut off at concentration = 0.1%)
- Rec: Recovery of eluted component (cut off at concentration = 0.1%)
- mUp: Component mass present in Upper phase
- mLp: Component mass present in Lower phase
- mTot: Total component mass
- Filter: Sigma ( $\sigma$ ) value of Gaussian filtering applied to component peak

At the centre of the screen, the resolution between two peaks can be calculated by selecting two different components.

At the bottom a report is displayed of selected input parameters.

## Time mode chromatogram view

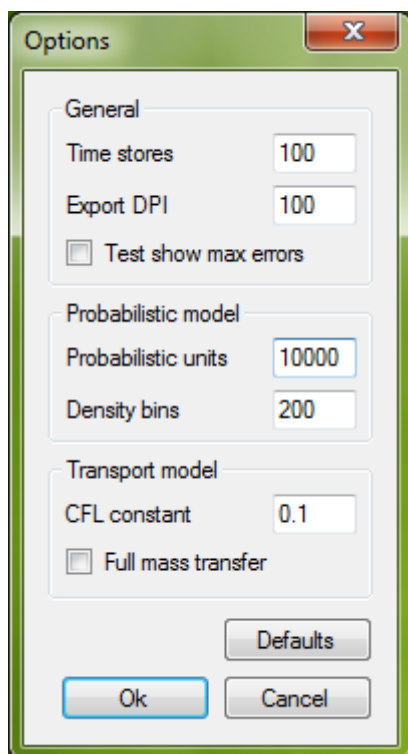
Selecting the Time mode tab will show the time mode chromatogram view. This is an interactive view, allowing appreciating the chromatography process as the components travel through the column and separate.



Using the scrollbar at the bottom of the screen, any point in the chromatography process between injection and elution can be viewed.

## Options dialog

The options dialog is accessed from the main menu: Tools -> Options. Various global setting can be set here and are stored. Use caution changing these. Use the Defaults button to restore default values.



### General

- Time stores: number of time store point for time mode chromatogram view (default: 100)
- Export DPI: DPI setting for image export (default: 100)
- Test show max errors: experimental setting for testing mode (default: disabled)

### Probabilistic model

- Probabilistic units: number of probabilistic units used (default: 10000)
- Density bins: base amount histogramical time stores for probabilistic mode (default: 200)

### Transport model

- CFL constant: stability condition constant (default: 0.1)
- Full mass transfer: use full mass transfer even for eluted component (default: disabled)

## Menu

- File
  - New : Open a new model window
  - Open : Open existing input parameters
  - Save As : Save input parameters
  - Export data : Export data in (text based) .CSV format (for spreadsheet applications)
  - Export image : Export chromatogram image
  - Print Preview : Open Print preview dialog to print chromatogram and report
  - Print : Open Print dialog to print chromatogram and report
  - Exit : Exit application closing all model windows
- View
  - Display phase : How sample concentrations in upper / lower phase are displayed
    - Upper/Lower Time : upper / lower phase on same scale
    - Upper/Lower : upper / lower phase separately
    - All : upper / lower phase combined
    - Upper : only upper phase
    - Lower : only lower phase
  - Display peaks
    - Peaks : component peaks separately
    - Peaks & Sum : component peaks + sum of all component peaks
    - Sum : sum of all component peaks
    - Show totals (int) : show accumulated totals (Intermittent mode only)
    - Units (prob) : show probabilistic units (probabilistic model only)
  - X Scale
    - Auto : automatically scale with window size
    - Zoom in : zoom in
    - Zoom out : zoom out
    - Reset zoom : reset zoom back to automatic scale
    - Steps : set units to steps
    - Volume : set units to volume
    - Time : set units to time
    - Norm : normalised to system volume
    - ReS : Reciprocal Symmetry Plots (K-value) scale
    - Sync scales : synchronise phase scales
  - Y Scale
    - Auto : automatic scale according to maximum concentration
    - Normalised : each component peak normalised
    - Absolute : absolute concentration scale with maximum 1
    - Logarithmic : use logarithmic scale
- Peaks
  - Peak info : open peak information window
- Tools
  - Options : open options dialog
- Window
  - [windows] : select individual currently opened model windows
- Help
  - Check for updates : check if a newer version of the software exists
  - Feedback : provide feedback
  - Stats : show model time statistics
  - About : open about dialog

## **Appendix B : Software versions**

Software build: CCD2

Date: 11/2007

Description: First implementation CCD model

Setup

Sim

Column size: 100

Insertion point: 50

Run condition: Dilute all

Dual flow mode: ☒

Dual phase move: ☒

Display mode: All

Phase distribution

Lower: 0.5

Upper: 0.5

X = L/U: 1

Run

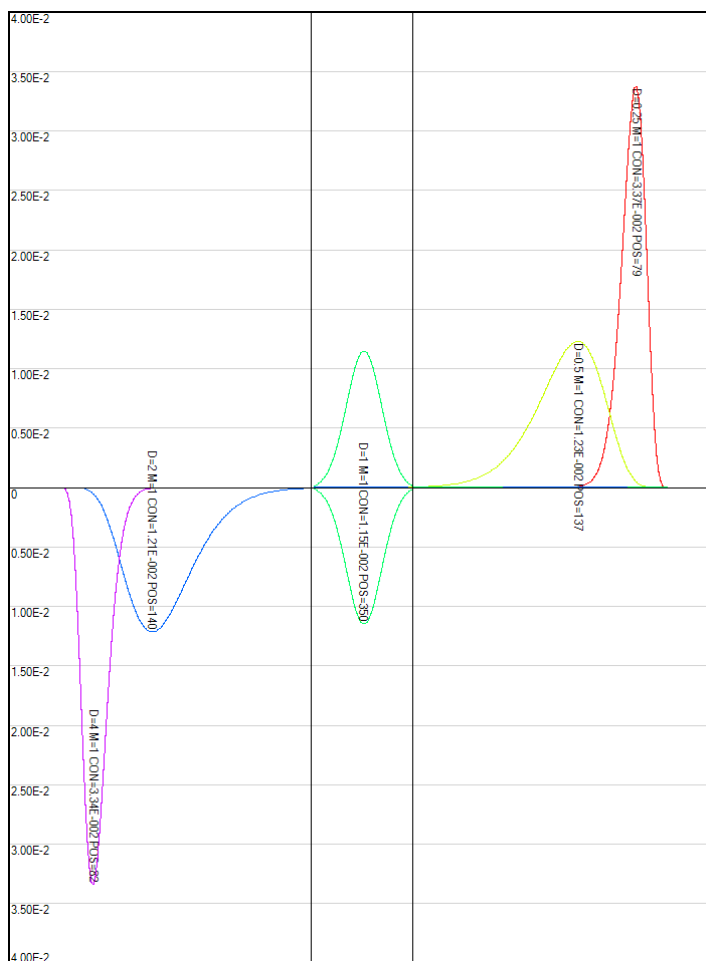
Cancel

Sample components

D=0.25	M=1
D=0.5	M=1
D=1	M=1
D=2	M=1
D=4	M=1

D value: 4 Mass: 1

Insert Remove



Software build: CCC2

Date: 4/2008

Description: Implemented model efficiency

Setup

Sim

Column size: 100

Insertion point: 50

Run mode: Dual flow

Run condition: Dilute all

Display mode: All

Efficiency: 1

Phase distribution

Lower: 0.5

Upper: 0.5

X = L/U: 1

Sample components

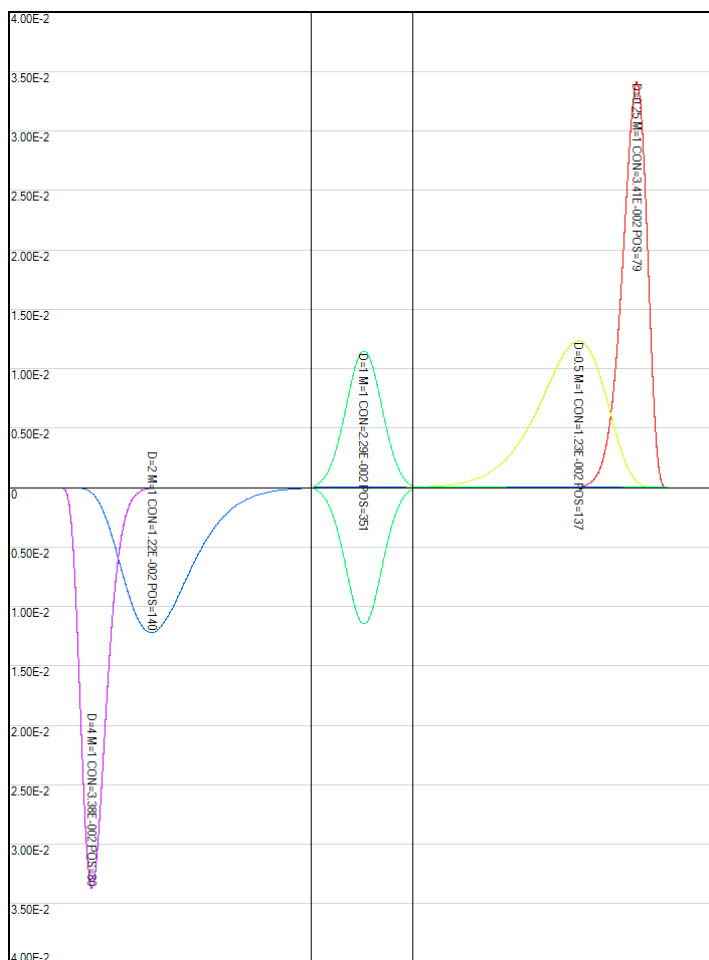
D=0.25	M=1
D=0.5	M=1
D=1	M=1
D=2	M=1
D=4	M=1

Sort

D value: Mass: 1

Insert Remove

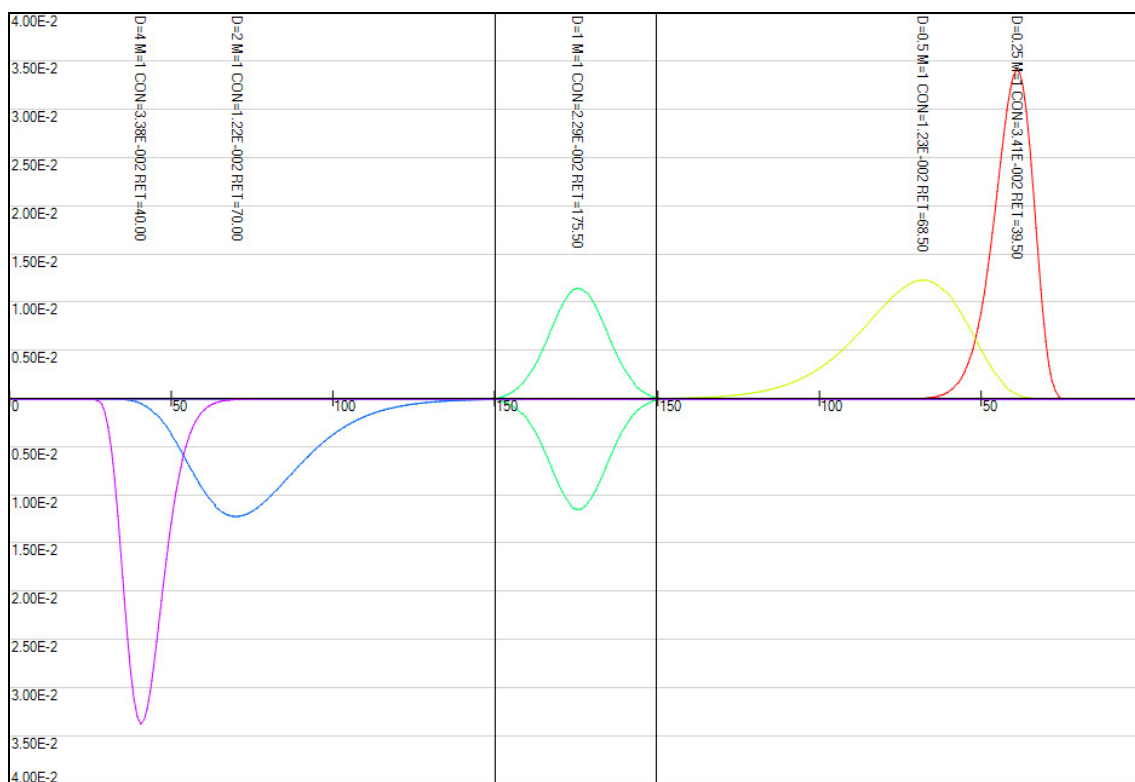
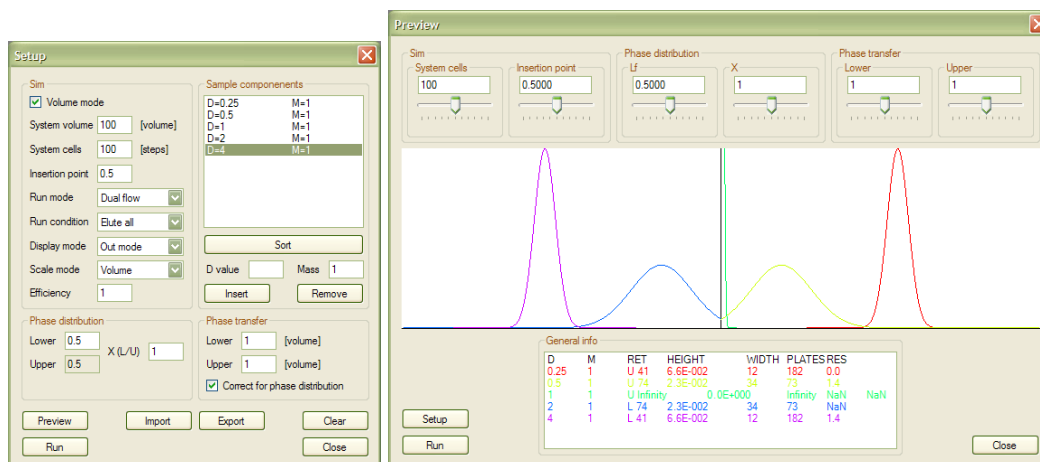
Run Import Export Cancel



Software build: CCC2 V1.0

Date: 7/2008

Description: Preview interface, implemented initial time mode chromatogram and 3D trace.  
First version to be evaluated.

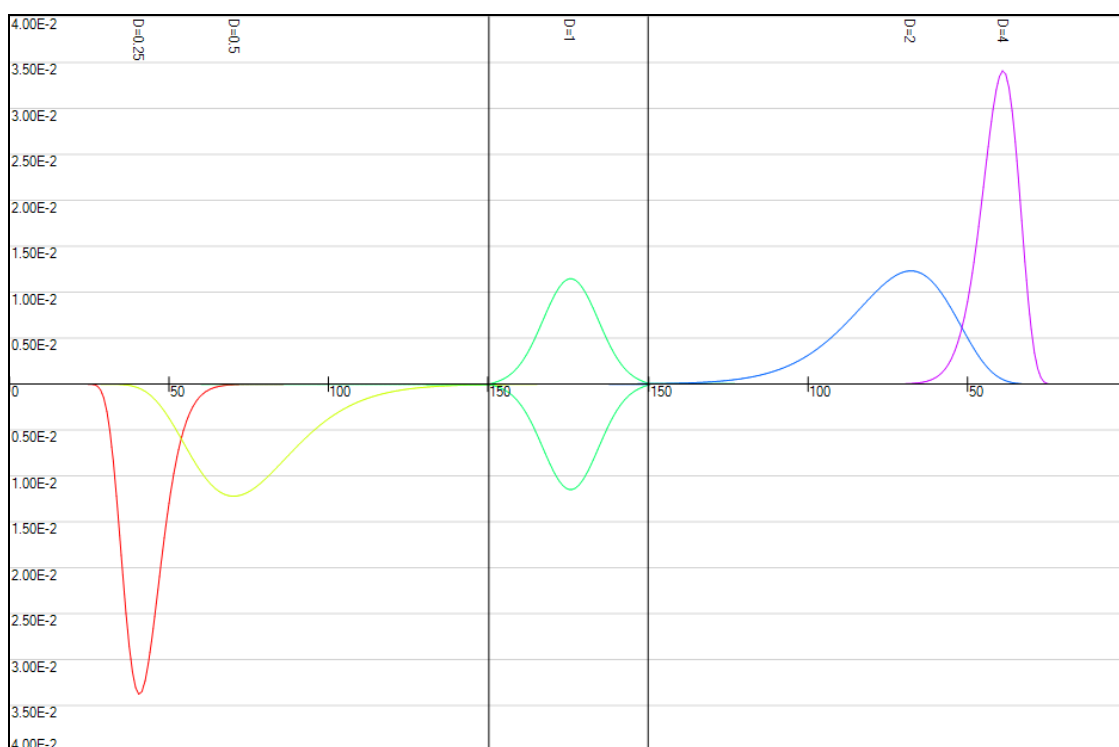
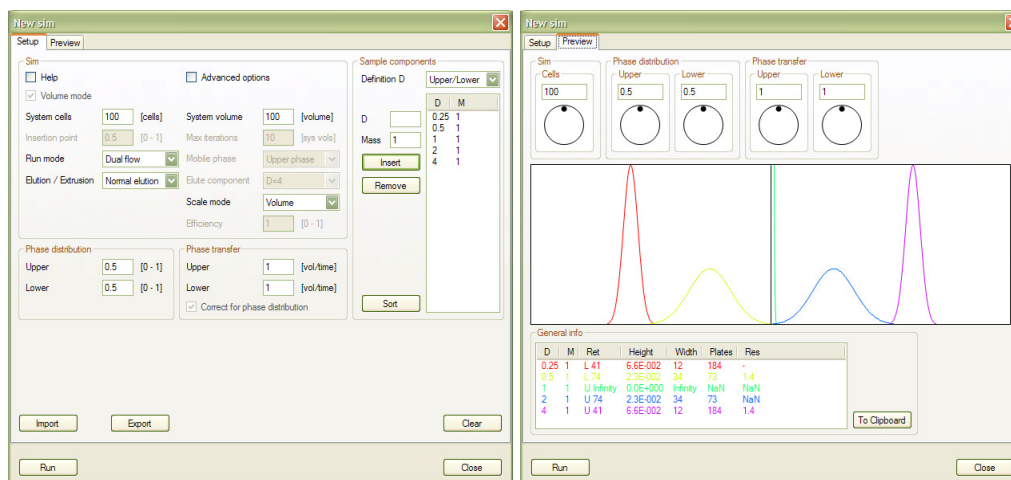




Software build: CCC2 V1.1

Date: 6/2009

Description: Setup / Preview combined into Tabs control, added Help mode, preview Jog wheel control. Integrated results from first evaluation. This version was subsequently used for the insight evaluation.



Software build: CCC2 V1.1 basic

Date: 6/2009

Description: Basic version of CCC2 V1.1: special version for insight evaluation study

**New sim**

Setup

Sim

System cells: 100 [cells] Insertion point: 0.5 [0 - 1]

Run mode: Dual flow Mobile phase: Upper phase

Phase distribution: Upper: 0.5 [0 - 1] Lower: 0.5 [0 - 1]

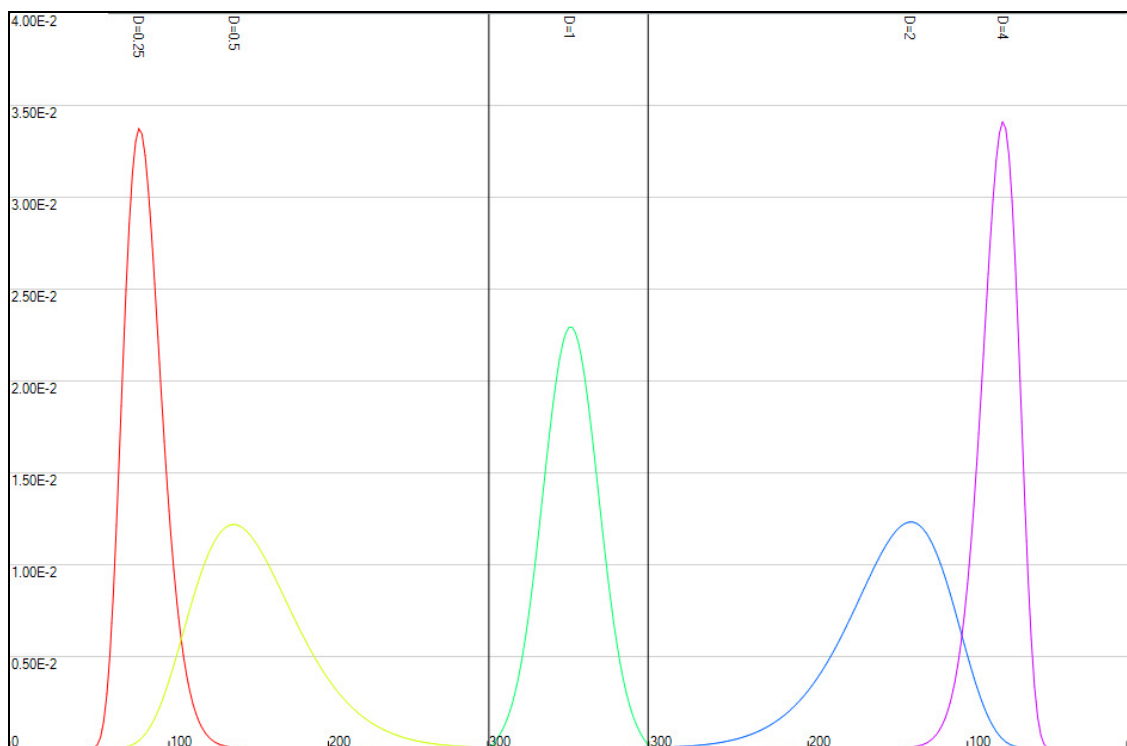
Phase transfer: Upper: 1 [cells/step] Lower: 1 [cells/step]

☒ Correct for phase distribution

Sample components

Definition D	Upper/Lower
D=0.25	M=1
D=0.5	M=1
D=1	M=1
D=2	M=1
D=4	M=1

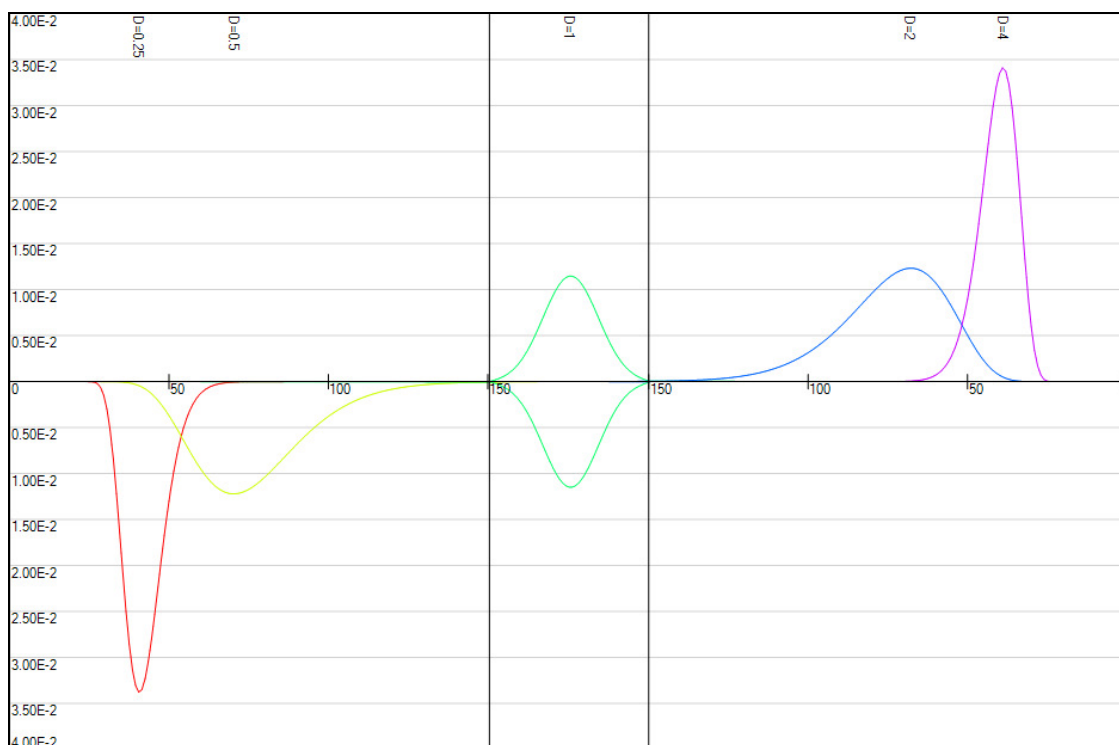
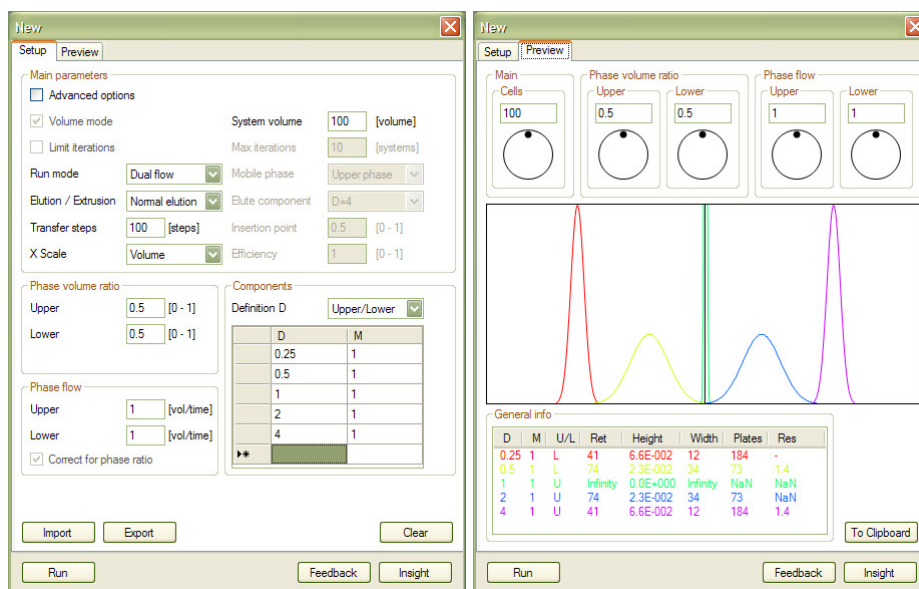
Buttons: Import, Export, Run, Clear, Close



Software build: CCC2 V1.2

Date: 2/2010

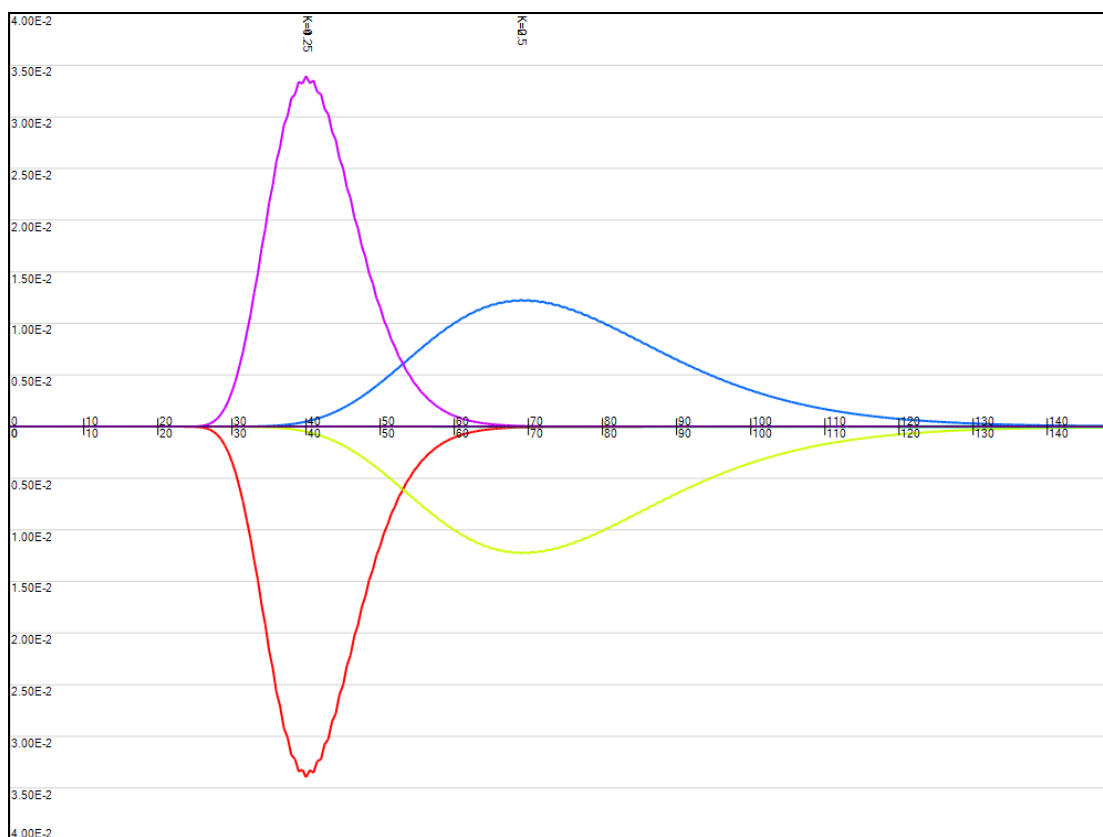
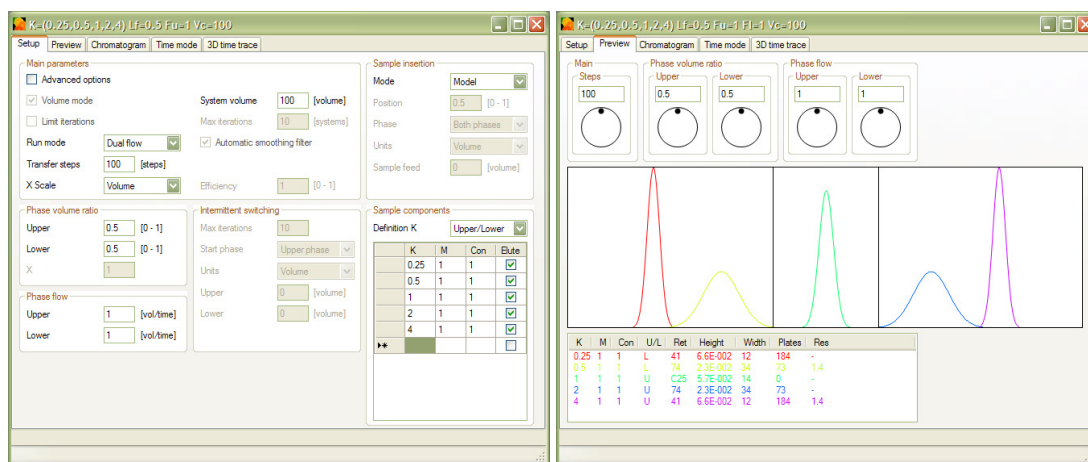
Description: Automatic Help mode, Insight (and feedback) submit functionality: special version for longitudinal insight evaluation study



Software build: CCC2 V1.3

Date: 4/2010

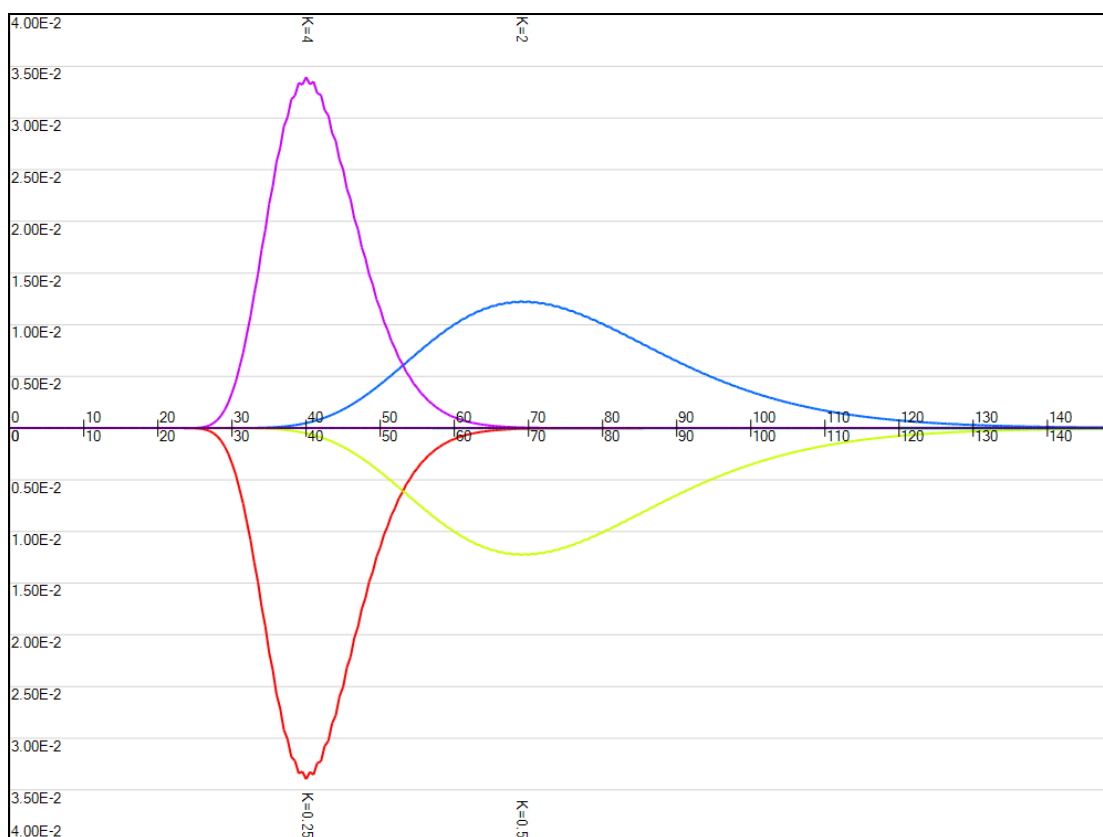
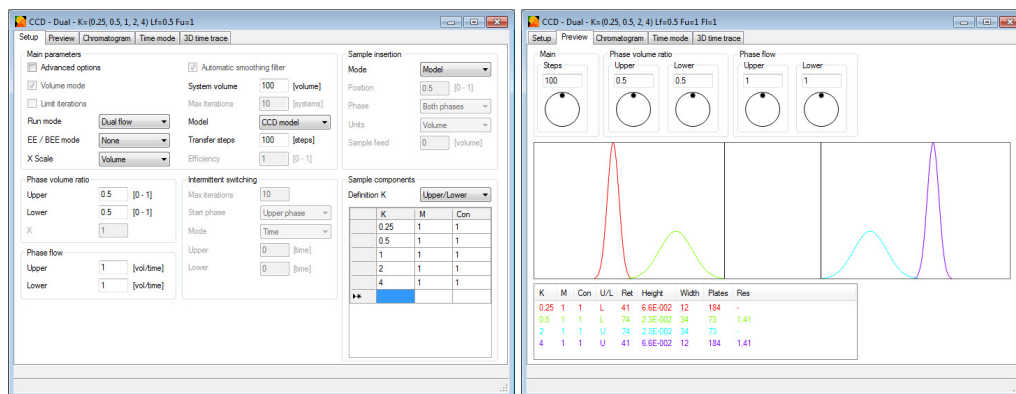
Description: All views combined into a single Tab control, dual phase view mode (for dual flow mode)



Software build: CCC3 V1.4 (CCD)

Date: 10/2010

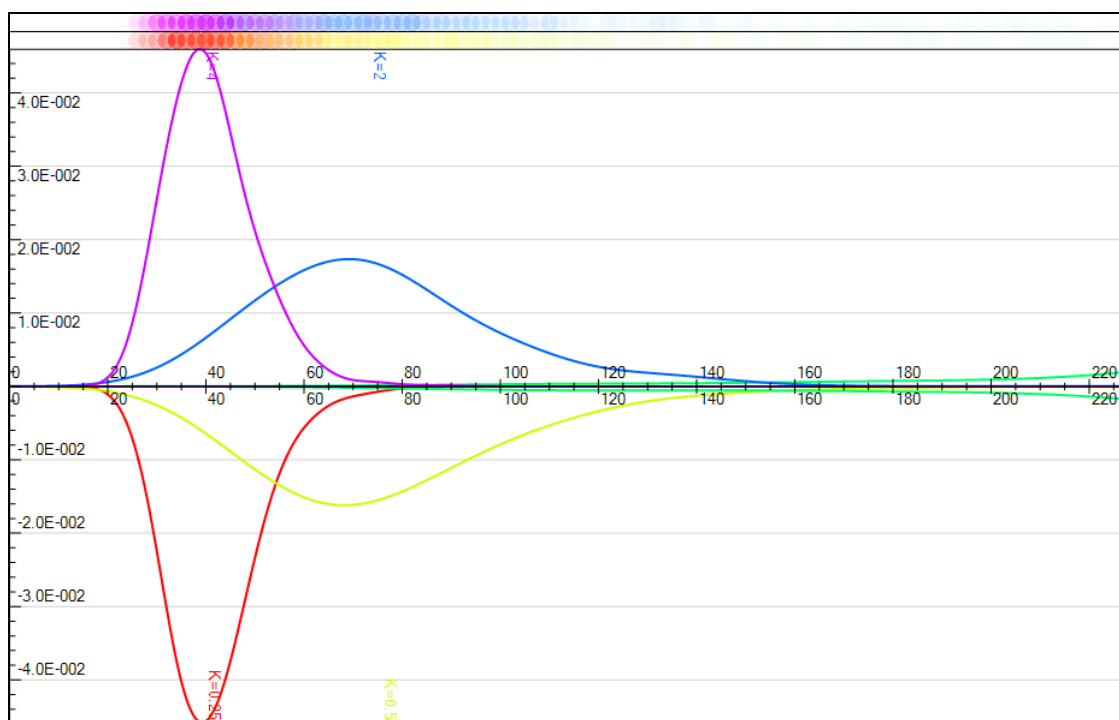
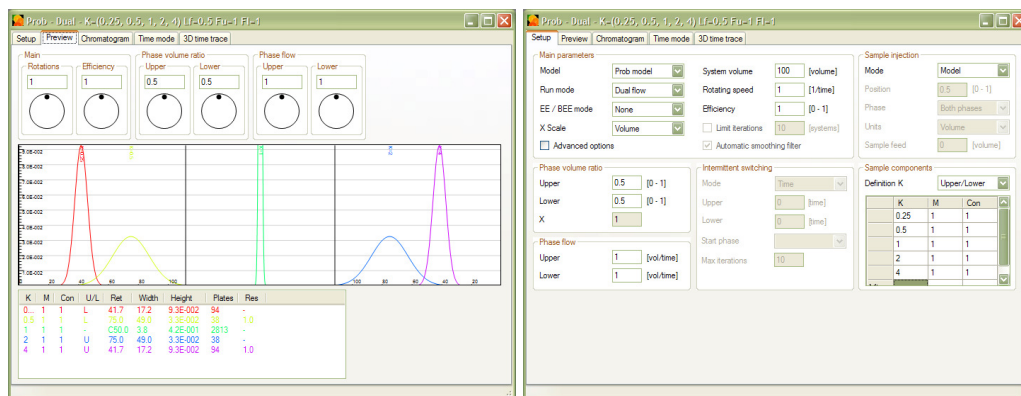
Description: Elution Extrusion mode



Software build: ProMISE V1.0

Date: 10/2010

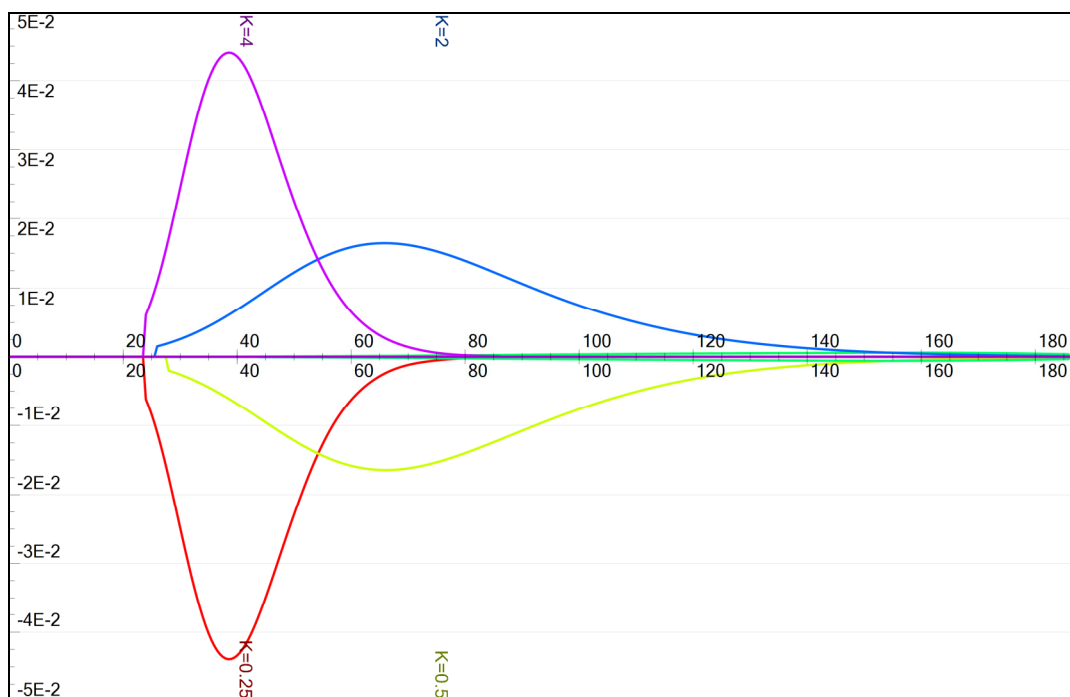
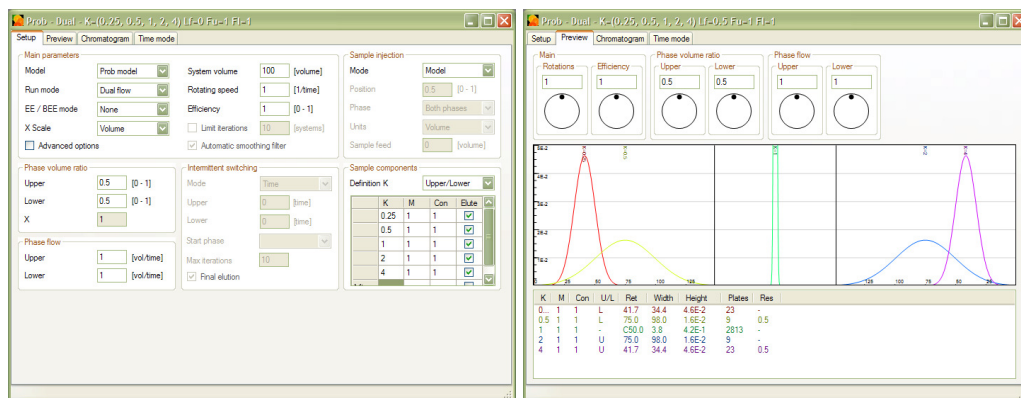
Description: Implemented probabilistic model



Software build: ProMISE V1.0

Date: 2/2011

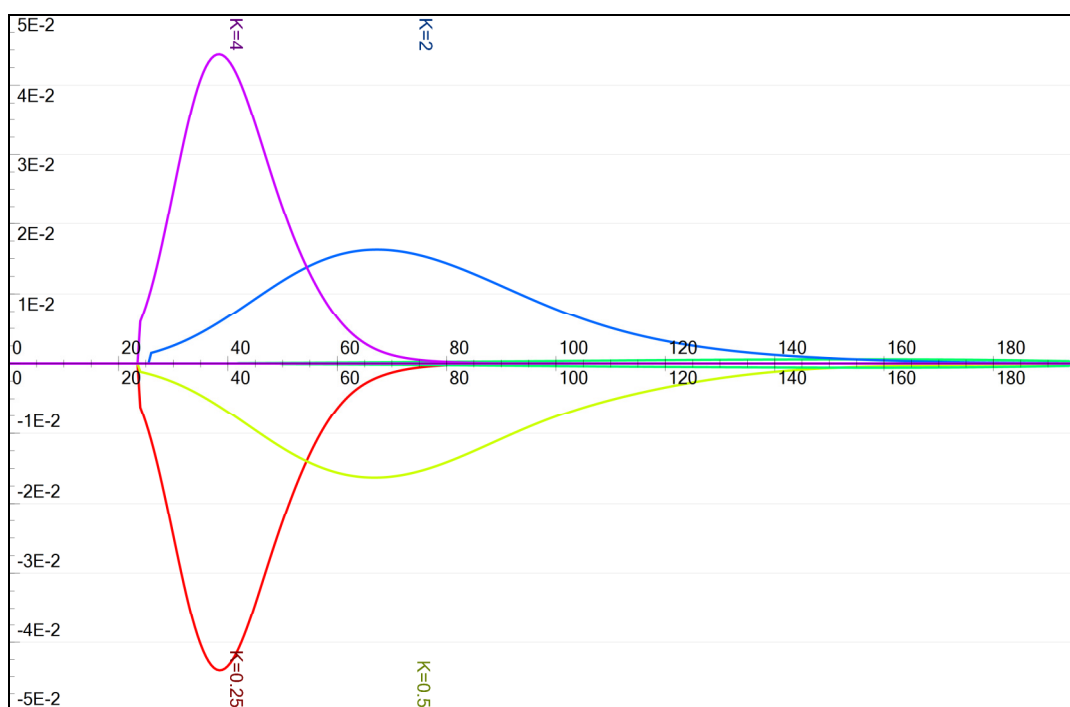
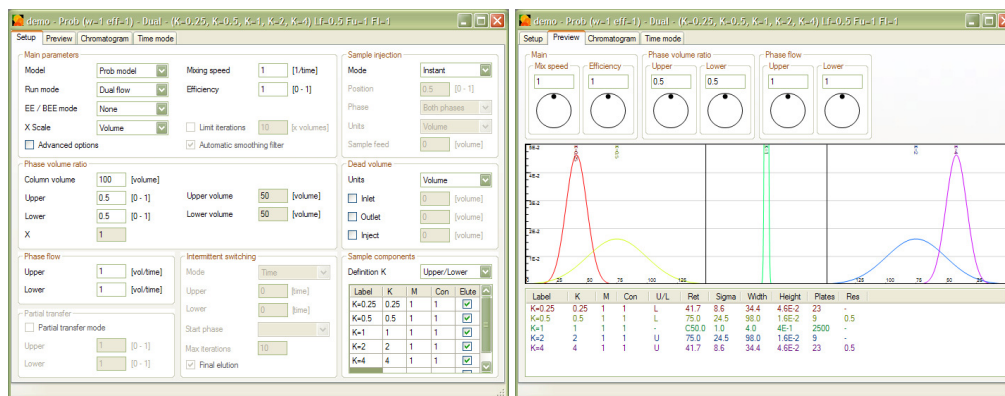
Description: Reimplemented CCD model



Software build: ProMISE V1.0

Date: 2/2012

Description: Implemented transport model, implemented dead volumes

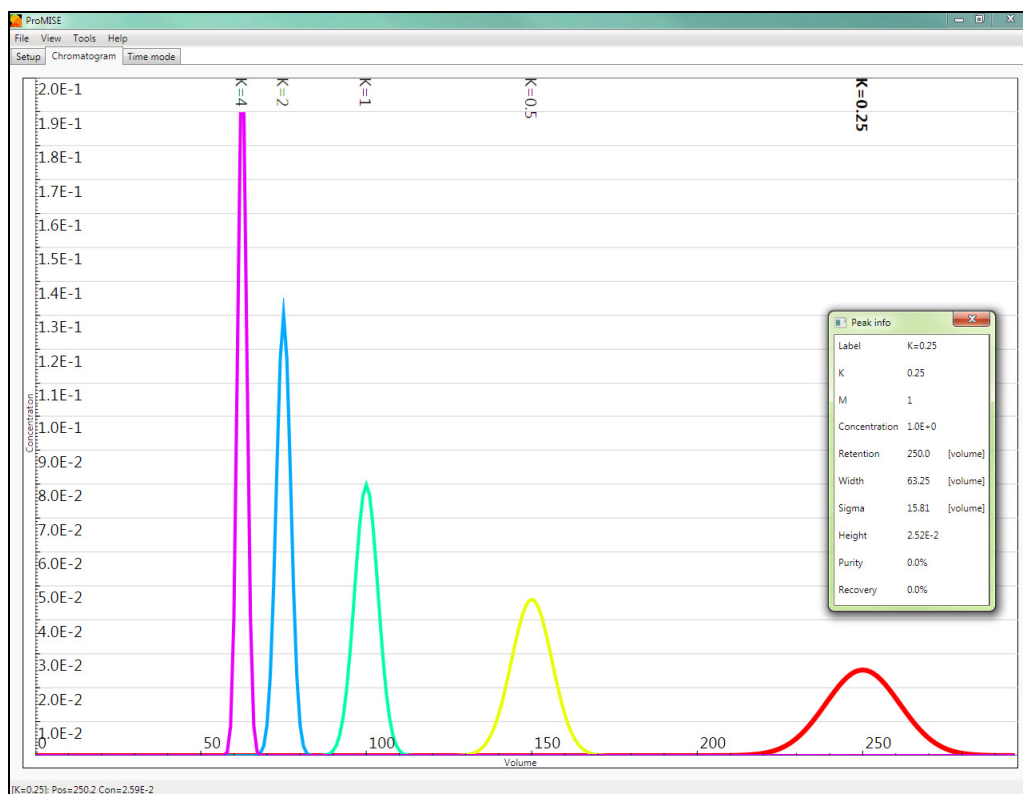
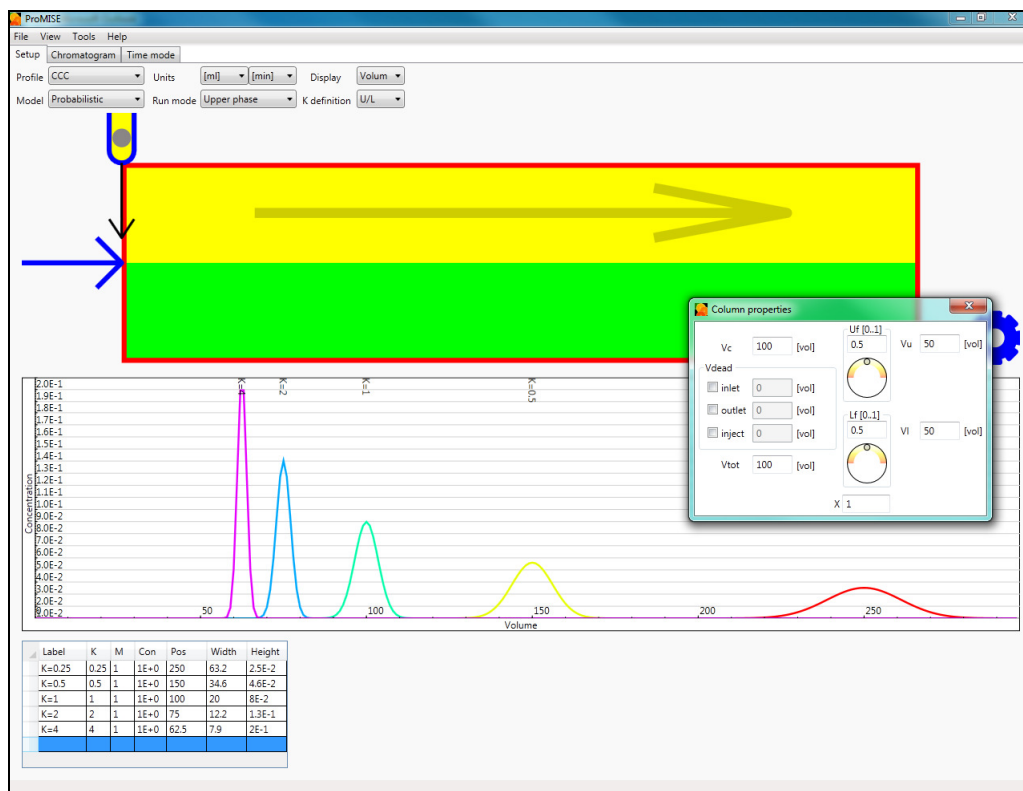




Software build: ProMISE2 prototype interface

Date: 9/2011

Description: Special prototype version of new graphical user interface



## **Appendix C : Model user feedback questionnaire**

# CCC visualisation Suggestions / Questionnaire

If you would like to see new features in the model, or if you have any comment about the existing model, please fill in this form and leave it here where I will collect regularly. By doing so you are helping make improvements for the next version of the model. Thank you!

What is your area of research?

---

Do you have any experience with CCC? ☐ No

☐ Yes, \_\_\_\_ Years

How useful do you think the model is?   Not very                      Slightly                      Very

- |                                    |                          |                          |                          |
|------------------------------------|--------------------------|--------------------------|--------------------------|
| – Configuration explorer           | <input type="checkbox"/> | <input type="checkbox"/> | <input type="checkbox"/> |
| – Chromatogram viewer              | <input type="checkbox"/> | <input type="checkbox"/> | <input type="checkbox"/> |
| – Time trace view (moving in time) | <input type="checkbox"/> | <input type="checkbox"/> | <input type="checkbox"/> |
| – Time trace view (3D view)        | <input type="checkbox"/> | <input type="checkbox"/> | <input type="checkbox"/> |
| – In general                       | <input type="checkbox"/> | <input type="checkbox"/> | <input type="checkbox"/> |

What do you like or dislike most about the model?

---

---

What would you use the model for?

---

---

Is there anything else you would like to see in the model?

---

---

If you would you like to be kept up to date about any progress, new versions, and how to obtain a copy of the model, please fill in your e-mail address:

## **Appendix D : Visual Walkthrough**

Task	Done	Explain	Problem	Notes
<b>Entering Setup mode</b>				
<b>Setup: Entering / changing parameters</b>				
Sim parameters				
Sim run/display modes				
Phase distribution				
Phase transfer				
Sample components				
<b>Clear all</b>				
<b>Importing / Exporting setup</b>				
<b>Entering Preview mode</b>				
<b>Preview: Entering / changing parameters</b>				
Sim				
Phase distribution				
Phase transfer				
<b>Running sim</b>				
<b>View (Out mode)</b>				
General navigating view				
Display mode (phases)				
X scale: zoom				
X scale: units				
Y scale				
<b>View (Time mode)</b>				
General navigating view				
Display mode (phases)				
X scale: units				
Y scale				
<b>View (Time trace 3D)</b>				
General navigating view				
Display mode (phases)				
X scale: zoom				
Y scale				
<b>Getting peak info</b>				
<b>Exporting sim</b>				
<b>Switching between sim windows</b>				

## **Appendix E : New graphical user interface group interview**

[1. Useful / Better]

Has it improved; In what way?

[2. Easy to understand / Intuitive]

Which elements are still difficult to understand?

[3. Complete]

What is missing?

[4. Other]

Other comments?

## **Appendix F : New visualisation feedback questionnaire**



# New test tube visualisation Suggestions / Questionnaire

By filling out this questionnaire you are helping make improvements to the new visualisation. Your feedback will be treated anonymously. Thank you!

- What is your area of research?

---

- Do you have any experience with chromatography?

☐ No                      ☐ Yes, \_\_\_\_ Years

- How useful do you think this visualisation is for chromatography novices?

Not useful                      Very useful

☐☐☐☐☐☐☐☐☐☐  
1 2 3 4 5 6 7 8 9 10

- Did this visualisation increase your understanding of the process?

Nothing                      A lot

☐☐☐☐☐☐☐☐☐☐  
1 2 3 4 5 6 7 8 9 10

- How do you feel the new visualisation compares to the old visualisation?

Worse                      Same                      Better

☐☐☐☐☐☐☐☐☐☐  
1 2 3 4 5 6 7 8 9 10

- What do you like or dislike most about the visualisation?

---

---

- Can you think of a way this visualisation could be improved?

---

---

## **Appendix G : New visualisation group interview**

[1. Useful / Better]

Has it improved; In what way?

[2. Purpose]

What would you use the visualisation for?

[3. Improve]

Can it be improved in any way?

[4. Other]

Other comments?